University of Alberta
Department of Civil &
Environmental Engineering

Structural Engineering Report No. 46

Prestressed Concrete I Beams Subjected to Combined Loadings

by

D.L.N. Rao

and

J. Warwaruk

November, 1973

ABSTRACT

Previous work and available theories concerning prestressed concrete members subjected to torsion, bending and shear are reviewed. The experimental study of this investigation consisted of tests on forty four eccentrically prestressed I section beams subjected to various proportions of torsion, bending and shear. All the beams had nominally the same length and cross sectional dimensions. The primary variables included two levels of average prestress, three eccentricities, three amounts of web reinforcement and various combinations of torsion, bending and shear. Only three beams did not have web reinforcement. Torque, transverse load, strains in the web reinforcement and the strands, angle of twist and flexural deflections at selected locations were measured during the tests.

Theoretical analyses were developed to predict the cracking and ultimate strength of prestressed I beams. Cracking strength was predicted by the following two methods.

1) Torsional shear stress distribution was assumed to be in accordance with plastic theory. The stresses due to other forces were considered to be elastic. Principal stress failure criteria was used coupled with a tensile strength of concrete equal to $6\sqrt{f'_c}$

2) A general three dimensional finite element analysis using hexahedrons was developed. Cracking was assumed to commence when the maximum principal tensile stress equalled the modulus of rupture es-

timated at $7.5\sqrt{f'_c}$. The out put of the program included maximum principal tensile stress, initial crack inclination, angle of twist, flexural deflections, for any given loading. This analysis was applied to several beams in the literature, in addition to the beams of the present investigation.

Tests showed that the I beams failed in skew bending either in a bending mode or a torsion mode. Expressions were developed based on a skew bending mechanism of failure for each of the modes to predict the ultimate strength of I beams of this investigation and other investigations.

Comparisons were presented for theoretical and test results both at cracking and ultimate and the agreement was generally found to be good.

TABLE OF CONTENTS

TABLE OF CONTENTS (continued)

TABLE OF CONTENTS (continued)

TABLE OF CONTENTS (continued)

TABLE OF CONTENTS (continued)

TABLE OF CONTENTS (continued)

LIST OF TABLES

LIST OF FIGURES

LIST OF FIGURES (continued)

LIST OF FIGURES (continued)

LIST OF PLATES

LIST OF SYMBOLS

Dimensions and Section Properties

A = cross sectional area of a beam

A_{ms} = area of longitudinal mild steel bar

A_{ps} = area of prestressing strand

A_t = cross sectional area of one leg of a closed stirrup

a_1, a_3 = bottom and top covers to strands

a_2 = bottom cover to strands at the second level

a_4, a_5 and a_6 = bottom, top, and side covers to stirrup

a_7 = side cover to strands

b = width of a rectangular section

b_f = width of the flange of I section

b_w = width of the web of I section

b_o = width between center of longitudinal corner bars

b_z = width of the section at any height of beam

e = eccentricity of prestress force with respect to centroid of cross-section

h = total depth of a beam

h_o = height between center of longitudinal corner bars

I = transformed-uncracked moment of inertia of a section

K_2x = depth of centroid of compressive force in concrete measured from the compression face of the beam

Q = statical moment of the cross-section area above (or below) that level (where shear stress is computed) about the centroidal axis

s = longitudinal spacing of web reinforcement

Vol = volume of plastic torsion surface

x = depth of neutral axis measured from the compression face of the beam

x_1 = smaller center-line dimension of a stirrup

x_{cr} = distance of initial crack from transverse load

x_u = distance of center of failure surface from transverse load

Y = distance from centroid of section to any point along height

Y_b = distance from centroid of section to extreme fiber in tension

Y_t = distance from centroid of section to extreme fiber in compression

Y_1 = larger center-line dimension of a stirrup

Material Properties

E_s = modulus of elasticity of prestressing reinforcement

E_t = modulus of elasticity of stirrup steel

E_c = modulus of elasticity of concrete

ε_u = ultimate strain in concrete in pure bending

ε_{ty} = yield strain of stirrup

f'_c = compressive strength of concrete cylinder

f_r = modulus of rupture of concrete

f'_t = tensile strength of concrete

f_{sp} = split cylinder tensile strength of concrete

f_{ty} = yield stress of stirrup

f_{my} = yield stress of longitudinal mild steel

f_{py} = yield stress of prestressing steel

Forces and Moments

C = compressive force in concrete

F = total effective prestress

M = bending moment

M_{cr} = bending moment at cracking

M_u = ultimate bending moment in combined loading

M_{uo} = ultimate shear-bending moment

M_{ub} = ultimate pure bending moment

P_{cr} = transverse load at cracking

P_u = transverse load at ultimate

T = twisting moment (torque)

T_b = bending component of applied torque

T_e = cracking torque based on elastic concept of concrete behavior

T_p = cracking torque based on plastic concept of concrete behavior

T_c = diagonal tension cracking torque in pure torsion

T_{cr} = diagonal tension cracking torque in combined loading

T_{up} = ultimate torque of plain concrete members

T_{uo} = ultimate strength in pure torsion

T_u = ultimate torque in combined loading

V = shear force

V_{cr} = shear force at cracking

V_u = ultimate shear in combined loading

V_{uo} = ultimate shear in the absence of torque

Stresses and Strains

Δ_{cr} = flexural deflection at cracking

Δ_u = flexural deflection at ultimate

ε = strain in concrete

ε_{cv} = ultimate strain perpendicular to the β plane

ε_{ce} = strain in concrete due to effective prestress

ε_i = strain induced parallel to strands due to load at the level of prestressing strand after the formation of the initial crack

ε_l = strain in longitudinal direction

ε_{se} = strain in prestressing strand due to effective prestress

$\varepsilon_{st\beta}$ = strain perpendicular to β plane at the level of the stirrups

ε_{th} = strain in horizontal leg of stirrup

ε_{tV} = strain in vertical leg of stirrup

f_b = stress at the extreme fibre due to bending moment

f_p = stress at any point due to prestress

σ_p = average stress due to prestress

σ_T = stress at top face of section due to prestress

σ_B = stress at bottom face of section due to prestress

ϕ_{cr} = angle of twist at cracking

ϕ_u = angle of twist at ultimate

τ_x, τ_y = torsional shear stress in two perpendicular directions

τ_t = torsional shear stress

τ_V = flexural shear stress

Miscellaneous

α = torsion factor in St. Venent theory

β = inclination of the compression zone to the longitudinal axis of the beam

β_1 = empirical constant used by ACI 318-71 Code to define compressive stress block

ζ = loading ratio defined as $T/V\ b_w$

ζ = loading ratio defined as T/M

θ = inclination of the tensile crack to the longitudinal axis of the beam

m = ratio of volume of longitudinal steel to volume of web reinforcement

p_t = web reinforcement percent based on total cross-sectional area

CHAPTER I

INTRODUCTION

1.1 General Remarks

Extensive research with respect to torsion in reinforced concrete has resulted in the formulation of a design criteria for such members. The ACI building code (ACI 318-71) for the first time, now contains provisions for designing reinforced concrete members to resist torsion combined with bending and shear. Though research has been in progress since the late 1960's similar design specifications for prestressed concrete members have not been formulated mainly because of inadequate test data. The majority of torsion investigations in prestressed concrete beams have been carried out for rectangular cross sections; only a limited amount of work has been done on practical shapes such as I, T and box sections.

Earlier studies of flanged sections of prestressed concrete (Gardner, 1960, Reeves, 1962) were of limited scope and dealt with I and T shaped sections without web reinforcement subjected to combined torsion and bending only. Zia (1961) conducted pure torsion tests of prestressed rectangular I and T beams with and without web reinforcement. The amount of web reinforcement was constant in his beams. Bishara (1969) described tests of prestressed rectangular, I, and T beams identical in cross-section to those of Zia (1961). These beams were tested in combined torsion bending and shear and no strength

predictions were proposed for the combined loading case. Gausel's (1970) investigation of prestressed I beams subject to torsion, bending and shear was limited to interaction studies. Wyss, Garland and Mattock (1969) made an experimental study of full scale I shaped bridge girders prestressed eccentrically with differing amounts of web reinforcement subject to pure torsion. More recently Wyss and Mattock (1971) conducted two series of tests on eccentrically stressed I girders for evaluating the interaction of torsion-bending and torsion-shear.

1.2 Object and Scope

Prestressed I beams used in bridges that are skew or curved in plan are subject to considerable amounts of torsion in addition to bending and shear. The test data and current knowledge about such beams under combined loading is very limited. The main objectives of this investigation were to obtain experimental data on the behavior and strength of prestressed I beams and to develop a simple, approximate but reasonably accurate method for predicting both the cracking and ultimate strengths of such beams. A total of forty four prestressed I beams were tested to failure to evaluate the effect of such variables as level of prestress (two levels of average prestress), eccentricity (three eccentricities), amount of web reinforcement (three amounts of web reinforcement) and loading combination (five T/Vb_w ratios). Measurements were made of torsional load, transverse load, strains in the web and prestressing reinforcements, angle of twist and flexual deflections at three locations in the test zone.

Cracking strength of these beams was predicted by a three dimensional finite element analysis and also by classical theories. Analytical expressions were developed based on skew bending mechanism of failure to predict the ultimate strength of prestressed I beams under combined loading. Comparisons were made of theoretical predictions and experimental results for beams of this investigation and several beams in the literature.

CHAPTER II

REVIEW OF PREVIOUS WORK AND AVAILABLE THEORIES

Long neglected in comparison with other forces, torsion in concrete members assumed increasing importance in the 1950's; previously torsional loads were considered to be secondary and were neglected as higher factors of safety of that time indirectly accounted for torsional effects. However, more recently, with reduced load factors and refined design methods it becomes mandatory to design for torsion explicitly. Further, in structural components such as edge beams, and girders curved in plan torsion is of primary consideration. This concern with torsion was reflected in the intensity of research work at various institutions resulting in significant contributions to the solution of the problem of torsion and its interaction with other forces. The accumulation of research findings to date is so vast that it is impossible to cover them all here and further, extensive reviews of the literature with emphasis on rectangular beams have been conducted by various authors (Kemp et al 1961, Zia 1968, Mukherjee and Warwaruk 1970, Gangarao and Zia 1970, Chander, Kemp, and Wilhelm 1970, Henny and Zia 1971, Woodhead and McMullen 1972).

In the sections that follow, first the cracking strength and the available solutions are discussed for concrete members presetressed or unprestressed under torsion alone or in combination with bending and shear. Later, research into the ultimate strength of prestressed rec-

tangular and flanged sections beams in torsion, bending, and shear is covered. Finally, the space truss theory for torsion is briefly reviewed.

2.1 Cracking Strength

2.1.1 General

Plain concrete beams under torsion alone or combined with other loadings fail abruptly at formation of the first crack. Providing reinforcement in such members in one direction alone does not yield any increase in strength beyond cracking. By providing reinforcement both longitudinally and transversely, the torsional strength can be increased substantially after cracking, however, the torsional stiffness reduces quite significantly once cracking occurs. In the case of prestressed concrete beams similar behavior is noted with respect to cracking. However, as the cracking strength is increased by the application of prestress for prestressed beams the level of cracking load is nearer the ultimate load. Hence, it is necessary to compute the strength of a beam at the onset of cracking, when torsional loads are applied alone, or in combination with other loads.

Computation of the torsional cracking strength of a concrete beam includes the following three different phases.

(a) Shear stress distribution across the section.

(b) Failure criteria for concrete cracking.

(c) Tensile strength of concrete.

In the following sections these three phases are discussed and used to calculate the cracking strength of beams subjected to combined loadings.

2.1.2 Available Theories

2.1.2.1 Classical Theories

In early torsion research on concrete, two classical theories have been used to predict the strength of plain concrete beams subjected to torsion. These were the elastic theory (Saint-Venant, 1856) and the plastic theory (Nadai, 1911). In the elastic theory, concrete is assumed to be ideally elastic. In the plastic theory concrete is treated as a fully plastic material; the shear stress distribution across the section is uniform.

Saint Venant's semi-inverse method of elastic solution of the torsion problem has limited application only to convex cross sections, without re-entrant angles as in the case of I, L, and T sections. However, for elastic shear stress distributions of more complicated shapes the soap film analogy by Prandtl (1903) may be used. The governing differential equation of the deflected shape of a soap film stretched by a small differential pressure over an opening of the same shape as the cross-section of the member under torsion, has the same form as the differential equation of the torsional stress function. The differential equation of the soap film can be solved numerically to arrive at the shear stresses at discrete intervals on a cross section.

A similar analogy, known as the Sand Heap analogy, was discovered by Nadai (1911) for the plastic torsion theory. If sand is piled on a plate having the same cross section of the member subjected to torsion the volume and slope of the sand heap are related to the applied torque and shear stress respectively.

Though the two theories adopt different assumptions regarding the material behavior, they use the same failure criteria, namely, principal stress-failure theory in which the member is considered to have failed when the maximum principal tensile stress becomes equal to the tensile strength of concrete. Most previous researchers observed that plain rectangular beams failed suddenly coincident with the appearance of first crack and the failure surface intersected all four sides in the form of helical cracks. The observed mechanism of failure was in line with Saint Venant's theory. The strength equations for a rectangular concrete beam take the following form:

Elastic Theory

$$T_e = \alpha b^2 h \, (\tau_y)_{max} \qquad (2.1)$$

Plastic Theory

$$T_p = \frac{1}{2} \left[1 - \frac{1}{3} \frac{b}{h}\right] b^2 h \, \tau_y \qquad (2.2)$$

Concrete however is known to have deformation properties intermediate between those corresponding to ideal elastic or ideal plastic materials. Hence neither of the two theories adequately reflects the behavior of concrete beams under torsion. For a given limiting tensile stress, the elastic theory underestimates the strength by as much as 50 percent while the plastic theory accounts for the excessive experimental strength, but fails to incorporate aspect ratio. The calculated elastic shear stresses are susceptible to the shape

of the cross section. Tests on concrete in torsion, of different cross sections as summarized by Marshall (1944) indicated that at failure plastic shear stresses were more consistent, less influenced by the cross-sectional shape, and, nearer to the so called tensile strength of concrete than the critical stresses computed on the basis of elastic theory.

Reeves (1962) pointed out that in these theories maximum stress was picked up and failure criteria applied without any regard for the stress gradient. He held that this method of approach was partly responsible for the general unsatisfactory results. Probably Hus (1968a) was the only investigator in torsion studies who took into account the strain gradient while deriving a relationship between the tensile strength and modulus of rupture, for his prediction equation of torsional strength.

The inelastic behavior of concrete was believed to be responsible for the increase in the strength over that obtained by the elastic theory. To account for this Miyamoto (1927), Turner and Davies (1934) and Marshall and Tembe (1941) using the non-linear stress-strain relationship of concrete in idealized forms, proposed torsion theories. These are called semiplastic theories as only partial plasticity of concrete was assumed. The strength computed by any of these theories should be intermediate between the predictions of elastic and plastic theories. However, the one advanced by Turner and Davies estimates torques higher than plastic torques whenever the height to breadth ratio exceeds 2.5 and thus becomes invalid.

In any case reasonable correlation with test results was ob-

tained by various researchers using any of the above mentioned classical theories coupled with appropriate values for the tensile strength of concrete.

2.1.2.2 Skew Bending Theory

Hsu (1968a) proposed a new skew bending theory for plain concrete beams, rejecting the classical theories on the ground that (i) the principal stress failure criterion might not be relevant to torsion problems and, (ii) the failure surface was not intersected on all the four faces of a rectangular cross section by a helical crack. Based on experimental observations, Hsu concluded that torsion failure is a bending phenomenon involving the development of a crack on three sides and a compression hinge adjacent and parallel to the long side of the section but inclined to the axis of twist. Hsu's torque equation is expressed as

$$T_{up} = \frac{b^2 h}{3} (0.85\ f_r) \qquad (2.3)$$

An examination of equation (2.1) and equation (2.2) reveals that Hsu's bending theory differs with classical theories in two aspects. First, his bending theory uses a constant of 1/3 for the torsion shape factor, while for the other theories, it is a function of aspect ratio (h/b). The 1/3 corresponds to the highest value of the shape factor in the elastic theory. Second, in the bending theory and the classical theories, the principal tensile stress should respectively exceed 0.85 times the modulus of rupture, and the tensile strength of concrete to cause failure. However, the difference between 0.85 f_r and f'_t becomes

negligible in beams of practical sizes since the strain gradient for them is reduced from that of test specimens. Equation (2.3) was modified by Hsu to involve the concrete compressive strength instead of modulus of rupture and is shown below.

$$T_{up} = 6\ (b^2+10)h\ \sqrt[3]{f'_c} \qquad (2.4)$$

In proposing his skewed bending theory, Hsu idealized the failure section as a plane, although it is actually a surface resembling a warped trapezium. Only the bending component of torque was considered in satisfying equilibrium, while the twisting component of torque on the failure surface was presumed only to cause a reduction in the modulus of rupture. He computed flexural tensile stress elastically at the ultimate stage. In spite of these defects, Hsu's skew bending theory, in using a torsional shape factor of 1/3 and modulus of rupture instead of other types of tensile stresses, improves on the classical elastic theory in that his strength predictions showed good correlation with experimental results.

2.1.2.3 Statistical Approach

All the preceding theories yield prediction equations of the same form shown below though in their specific assumptions they differ significantly.

$$T_{up} = Kb^2h\ f'_t \qquad (2.5)$$

where K = A dimensionless coefficient called shape factor which is a function of h/b in classical theories and a constant equal to 1/3 in bending theory

Mukherjee and Kemp (1967) attempted to generalize the different shape factors of the theories to yield one expression. They carried out a statistical regression analysis of available test results and determined the parameters of the shape function for concrete rectangular members under pure torsion. Their equation can be stated in the form:

$$T_u = 0.4124 \left[1-0.2333\frac{b}{h}\right] b^2 h\, f_t' \qquad (2.6)$$

where T_u = pure torsional strength of rectangular plain concrete beam

Shape factor $K = 0.4124 \left[1-0.2333 \frac{b}{h}\right]$

$$f_t' = 5\sqrt{f_c'}$$

Using equation (2.6), for slender beams the calculated torque capacity was closer to the elastic torque, but approached the plastic value at the height to width ratio equal to unity.

Subsequently, based on statistical observation of test results from different investigations Chander, Kemp, Wilhelm (1970) presented the following prediction equation.

$$T_c = b^2 h\, f_t' \left[0.4731 \left(1-0.5924 \frac{b}{h} + 0.2763 \frac{b^2}{h^2}\right)\right] \qquad (2.7)$$

where $f'_t = 5\sqrt{f'_c}$

This equation yields results much closer to those of the plastic theory rather than elastic and correlates well with test data. It shows that concrete though not capable of complete plasticity, need not be completely plastified as the contribution to torsional resistance is maximum from the outer fibres and only their plastification is necessary to yield results close to those obtained by the plastic theory.

2.1.3 Flanged Concrete Beams Under Pure Torsion

Comparatively little research work has been carried out on members of practical shape such as I, L and T sections subjected to pure torsion. Contributions to the knowledge of the behavior of the flanged concrete beams include those of Turner and Davies (1934), Marshall and Tembe (1941), Nylander (1945), Zia (1961), Arockiasamy (1964), and Ramakrishnan and Jayaraman (1968), Hsu (1968), Evans, Kemp, and Wilhelm (1970). Some of these investigators computed the strength of component rectangle sections and used Bach's (1911) approximation as detailed below to estimate the pure torque capacity of T and L sections. It may be recalled that the elastic shear stress distribution and the torsional strength can be obtained by membrane analogy. Torsional strength is proportional to the volume under the membrane . Bach's approximate method computes the volume, as the sum of the volumes of the individual component rectangles, treating the membrane of each rectangle as a uniform cylindrical surface. Thus, it neglects the end effect and junction effect which results in gain and loss of volume at the ends of each rectangle and junctions of any two rectangles,

respectively. For a section composed of narrow rectangles, the approximate method yields a volume close to that of the membrane analogy. But in concrete sections the component rectangles are not narrow and Bach's method underestimates the volume and hence the torque capacity. Depending on the relative dimensions of the cross-section this can be significant. Bach's equation for the maximum shear stress is

$$\tau_{max} = \frac{T\ t}{\sum \frac{1}{3} b^3 h} \qquad (2.8)$$

τ_{max} = maximum torsional shear stress

T = applied torque

t = largest thickness of component rectangles

b = width of each component rectangle

h = depth of each component rectangle

Plain concrete flanged beams (excluding the I sections) fail at the appearance of the first crack, thus the cracking and the ultimate torsional moments are the same. Recently Hsu (1968b) conducted tests on eight plain concrete T and L section beams subjected to pure torsion. He observed that non-rectangular beams under torsion fail by bending, and the calculation of failure torque based on his bending mechanism is difficult. Extending his equation (2.4) derived for rectangular beams, and using Bach's approximation, he presented the following equation for the strength of flanged beams.

$$T_{up} = \sum 6(b^2+10)h \sqrt[3]{f'_c} \qquad (2.9)$$

He stated that the outstanding flange width was ineffective if it exceeded about three times the flange thickness.

The skewed bending theory was applied to predict the strength of symmetric I sections tested and reported in this investigation and was found to be inadequate. While Bach's method used by Hsu to compute cracking of flanged beams does not consider the relative position of rectangles, the bending theory takes into account the position of an element on the section in terms of moment of inertia. This results in a disproportionate increase in moment of inertia, and hence a similar increase in failure torque, if the cross sectional area farthest from the bending axis increases slightly, and it may be concluded that his theory is of limited use in flanged beams.

In a recent study Evans, Kemp and Wilhelm (1970) investigated into the strength and behavior under pure torsion of 33 T-beams and 5 L-beams either plain or reinforced. The initial crack always occurred in the web (web was 6 in. thick, while flange thickness was either 3 in. or 4 in.) leading to immediate failure if the beams were plain or reinforced only in one direction. All the specimens having steel in both directions exhibited very large amounts of ductility and a concrete compression zone was observed only when a specimen was deformed well past its ultimate torsional strength.

Evans et al disputed with the rationality of the ACI's provision of associating flange effectiveness in resisting torsion to the ratio of the outstanding flange width to its thickness; and limiting such a ratio to three. Their test results showed that even at a ratio of five a limit had not been reached. However, they observed that if the

maximum tensile stress occurred in one of the component rectangles failure might occur before the other component rectangles developed their full capacity. It is generally believed that Bach's approximate method is adequate and yields conservative estimates of torsional strength for the flanged beams. Utilizing Bach's method, they computed the cracking strength of a flanged section on the premise that as the applied torque gradually increased each of the component rectangles undergoing the same rotation carried a portion of the total torque proportional to its torsional stiffness. The applied torque could increase until one of the component rectangles developed a crack while the others might not have been stressed to their capacity. The final cracking torque was then equal to the sum of the torques carried by each of the component rectangles at a rotation corresponding to the cracking rotation of that particular component in which the initial crack appeared. Additionally, junction effect had to be taken into account. This method of computation was similar to the moment distribution and considers the effectiveness of the component rectangles without restricting their size. They pointed out that the strength calculation by Bach's method for some large T beams in the literature was unsafe and the effective section concept yielded safe predictions. The equations derived by them are as follows:

$$T_c = 1.79 \sum (b^2 h)_{effective} \sqrt{f'_c} \qquad (2.10)$$

$$T_c = 7.3 \sum (\alpha b^2 h)_{effective} \sqrt{f'_c} \qquad (2.11)$$

However for design purposes, Evans et al stated that the ACI equation with its limitation of the flange width to depth ratio seemed adequate.

2.1.4 Prestressed Concrete Beams Under Pure Torsion

Nylander (1945) was the first to carry out an investigation into the torsion problem of prestressed concrete members. He tested a series of sixteen 8-inch square specimens under pure torsion. The prestress was applied in the form of axial compression. It was observed that the precompressed beams exhibited torsional strength about double that of their unprestressed counter parts at the first crack. The failure was similar to that observed in uncompressed beams. He concluded that the cracking torsional strength of his beams was adequately predicted by the plastic theory in conjunction with principal stress criteria of failure.

Cowan and Armstrong (1955) made tests on prestressed beams in pure torsion as well as in torsion and bending. Some beams had uniform prestress, while others had nominally triangular prestress distribution. They observed that the failure was sudden at the formation of the first crack in the case of beams subject to pure torsion or high torque/moment ratio. The addition of bending moment lessened the violence but increased the destructiveness of failure, and allowed an increase in load to be carried after the formation of the first crack. Their 6 x 8 in. eccentrically prestressed beams cracked on the top first in pure torsion. The equation proposed for the permissible strength of a rectangular prestressed concrete beam, M_T is

$$M_T = M_{TO} (1+f_p/f_t')^{1/2} \qquad (2.12)$$

where M_{TO} = maximum permissible twisting moment for a similar plain concrete section

f_p = magnitude of prestress

The experimental work reported by Humphreys (1957) related to the testing of 94 plain prestressed rectangular beams, four of which were eccentrically prestressed with zero stress at the top. Failure in the beams was so sudden that tensile cracking could not be detected. In the case of eccentrically prestressed 5 in-square and 10 in. x 5 in. rectangular beams the initial crack occurred on the top face.

Humphreys stated that, though the crack occurred at a location of zero prestress on the top in rectangular beams, the strength was governed by the same conditions as that for a concentrically stressed member, because of the higher torsional factor associated with the short side of the section. The square and rectangular beams developed a torsional strength 13 and 43 percent respectively in excess of their unprestressed counterparts. He approximated the principal tensile stress theory of failure by a regression equation which yields the following ultimate torsional stress.

$$\tau_{max} = f_t' + 0.307\ \sigma_p \qquad (2.13)$$

where τ_{max} = ultimate torsional shear stress.

His equation for the torsional strength prediction of a plain prestressed member is of the following form.

$$T = k(\tau+0.3\sigma_p)\, b^2 h \qquad (2.14)$$

where T = ultimate torsional strength

k = a function of depth to breadth ratio

τ = ultimate shear strength of a plain concrete member

Based on the tests in the literature, Hsu (1968c) extended his skew bending theory to concentrically prestressed rectangular beams without web reinforcement. The torsional strength of such a beam was obtained as the torsional strength of non-prestressed beams multiplied by a prestress factor which accounts for the effects of prestress. The equation is of the following form.

$$T_u = [6(b^2+10)h\, f_c'^{1/3}][1 + \frac{10\sigma_p}{f_c'}]^{1/2} \qquad (2.15)$$

where T_u = ultimate torque of plain prestressed beams

$(1 + \frac{10\sigma_p}{f_c'})^{1/2}$ = prestress factor

In establishing the prestress factor, the modulus of rupture was taken equal to $f_c'/8.5$. This prestress factor becomes identical to the factor that would be derived assuming a principal tensile stress failure criterion and a value of tensile strength equal to $f_c'/10$. From the test results of Humphreys (1957), Hsu concluded that a compression failure would occur if average prestress exceeded 70 percent of the

compressive strength. The applicability of equation (2.15) was limited to eccentrically prestressed sections which cracked on the wider face and in such cases the crack was assumed to occur at the centre of the wider face, neglecting the variation of prestress. This theory could not estimate the strength of nearly square beams which cracked first on the top face.

Mukherjee and Kemp (1967) extended their statistically derived prediction equation (2.6) for rectangular concrete members, to include the effect of concentric prestress. The torsion factor of this expression contains a term involving prestress which resulted in torques increasing slightly with the level of prestress. The enhancement of torsional shear resistance due to the presence of prestress was taken into account by using the maximum principal stress theory. The resulting expression is as follows.

$$T_c = [0.4124(1-0.2333\frac{b}{h}) + \frac{1}{6}\frac{\sigma_p}{f'_c}]\, b^2 h \tau_u \qquad (2.16)$$

where $\tau_u = \sqrt{(f'_t(f'_t + \sigma_p))}$

$f'_t = 5\sqrt{f'_c}$

Equation (2.7) was modified in a similar manner to account for the increased strength of plain concrete members due to prestress. This equation for a plain prestressed beam may be written as

$$T_c = [0.4731(1-0.5924\frac{b}{h} + 0.2763\frac{b^2}{h^2})]\, b^2 h \tau_u \qquad (2.17)$$

where $\tau_u = f'_t \sqrt{(1+\sigma_p/f'_t)}$

$f'_t = 5 \sqrt{f'_c}$

Chander et al observed from test results that the torsion factor was independent of degree of prestress. It was stated that tensile failure occurred if the average prestress did not exceed ten times the tensile strength of concrete. Equation (2.17) was checked by results of beam tests of several investigations in addition to their own and the correlation was found to be good.

In the case of eccentrically prestressed rectangular beams under pure torsion the initial crack was observed by Humphrey (1957) and Zia (1960) on the top face whereas Mukjerjee and Warwaruk (1970) and Gangarao and Zia (1970) observed it at the top of the longer side, and Chander et al (1970) and Woodhead (1972) at the centre of longer side. It was generally assumed that the principal tensile stress situation at the least compressed face determined the strength of such beams. Each of the above investigators observed experimental strengths in excess of that corresponding to a plain concrete beam. In some investigations, eccentrically prestressed beams exhibited the same strength as concentrically prestressed beams having the same average prestress.

With zero prestress at the top, Hsu's bending theory would predict a strength equal to that of a plain concrete beam if the first crack originates at the top of the vertical face. However, his theory cannot be applied if the top face cracks first.

Plastic theory cannot be applied in the usual form, as the shear stress would depend on the level of prestress at each point and it varies nonlinearly on the cross section.

For eccentrically prestressed beams only the elastic theory because of the higher torsion factor at the centre of the short face rather than on the long face predicts a higher strength than for a similar unprestressed beam. However, Chander et al (1970) observed that the elastic theory explained only a part of the increased strength and showed that a skewed sand heap analogy resulted in better strength predictions of such members. They assumed that failure occurred only when the complete section was plastic. The shear strength varied in accordance with the prestress. With no tensile stress at the top, the slope of the sand heap at the middle of the longer side controlled the failure. But for practical use they recommended the use of interaction diagrams as suggested by Mukherjee and Warwaruk (1970) for computing the torsional strength of eccentrically prestressed beams under torsion, treating the eccentricity of prestress as an external moment.

Zia carried out an extensive test program consisting of prestressed and unprestressed rectangular, T and I sections subjected to pure torsion. He believed that the elastic theory was more justified than the plastic theory because for short time loadings high strength concrete such as used in prestressed concrete structures exhibited very limited plasticity. Elastic shear stress distributions for rectangular, T and I sections were obtained using finite difference techniques. The increase in torsional shear stress due to prestress was computed uding modified Cowan's failure criteria developed by Zia.

Failure criteria in general require a knowledge of both compressive and torsional strength of concrete. Generally, a premise is made that the torsional strength is equal to the tensile strength of concrete. As for tensile strength the following relationship based on the test results of Gonnerman and Shuman was adopted by Zia.

$$f'_t = 0.68\ (f'_c)^{3/4} \qquad (2.18)$$

Rectangular and T section beams failed immediately after cracking. The agreement between the measured and theoretical cracking results of these beams was good. Zia observed in his testing that the cracking and ultimate strengths of plain, concentrically and eccentrically prestressed I sections without web reinforcement were quite different. For these beams he reported only test results at ultimate but not at cracking. Comparison was made between theoretical crackings strengths and experimental ultimate strengths. Thus it is not possible to determine how well the elastic theory compared with the first cracking load. But the fact was established that I beams of his investigations resisted substantial torques after cracking. This behavior of unstirruped I beams, different from rectangular and T beams, depends strongly on the relative proportions of the flanges and the web, and if prestressed also on the eccentricity of prestress. In a plain or concentrically prestressed beam, if the dimensions are such that first cracking occurs at the center of flanges then it spreads into the flanges and web and the beam collapses immediately. However, if the web is thicker than the flanges, the more highly stressed web picks up

the first crack and it progresses towards the flanges at a slower rate because of the presence of less stressed flanges on either side of the web. Zia stated that at this stage a redistribution of stress takes place in the flanges transforming the torsional shear in them to lateral bending shear. The external torque is resisted by the internal couple of the lateral shear forces developed in the flanges. In this case failure occurs when the lateral shear force equals the lateral shear strength of the flanges. Zia's beams fall in this category having a web thickness of 3-1/2 in. and a flange depth of only 2 in. Such behavior for example, was non existent in the plain I girders tested by Wyss et al (1969) although the first crack occurred in the web; here the web and flange thicknesses were equal and failure occurred at the formation of the first crack.

Irrespective of the thickness of the web relative to that of the flanges if the I beam is prestressed eccentrically Zia observed that the bottom flange became stronger than the top flange. When the top flange cracked first and the crack propagated towards the web the uncracked portion became a T section with the prestress more uniformly distributed on the uncracked portion. Such a section resisted torque in excess of the torque that caused top flange cracking. Unfortunately as pointed out earlier experimental cracking torques were not reported to assess the strength available between cracking and ultimate stages. If the experimental torques at the elastic limit in the I beams were assumed to be the test cracking torques, then the failure and cracking torques differ by about 11 to 40 percent depending on the eccentricity.

The cracking torques might have been greater than those at the elastic limit; then the difference between the strengths at cracking and ultimate would be less.

Though Zia did not draw any conclusions, his plain prestressed rectangular beams, and I beams showed essentially the same strength irrespective of the eccentricity. However in the case of plain prestressed T beams eccentricity of prestress had an adverse effect causing a decrease in strength.

A major test series consisting of 18 large concrete I girders and six rectangular beams under pure torsion was conducted by Wyss, Garland and Mattock (1969). Twelve of the I girders were eccentrically prestressed. In an attempt to estimate the cracking strength of these beams they applied a two dimensional finite element method. Triangular elements were used with nodes located at the intersections of a 1/2 x 1/2 in. mesh. The output from this program consisted of a shear stress distribution which is essentially elastic. Cracking was assumed to occur when the principal tensile stress at a critical location exceeded the measured split cylinder strength. For most of the I girders the measured torques were considerably larger while for the rectangular beams they were consistently smaller than the computed values.

In the case of web cracking, the calculated values compared well with the test results, if the high shear stress gradient in the vicinity of the web-flange juntion was neglected, and a smaller value of shear stress which existed at a distance 2 in. away from the top of the web and along the remainder of the web was adopted. With

regard to girders that cracked on the top, they stated that shallow cracks might have occurred at lower torques than those reported, but were not seen because of the rough trowelled top face. But no explanation was given for the opposite trend of lower test strengths than the computed ones in the case of rectangular beams.

2.1.5 Reinforced Concrete Beams Under Combined Loading

A beam under pure torsion develops equal tensile and compressive stresses on two perpendicular planes. The addition of a normal stress due to the application of any of the following loads prestress, bending, and direct tension or compression, further complicates the torsion problem. In such a case the maximum principal tensile stress is accompanied by normal stresses of varying degrees on orthogonal planes. Viewed differently, the shear stress distribution is to be obtained under the simultaneous action of a known direct stress. This does not seem to be possible. Assuming the stress situation is accurately known it remains to be determined when failure occurs. The strength of a material is dependent on the state of stress. Though several mathematical failure criteria were advanced in the past for the combined stress problem experimental verification is very difficult in the case of concrete.

The differences in the cracking analyses of various researchers are as follows.

First, elastic stresses due to bending moment, transverse shear, and prestress were separately obtained. The only difference related to the evaluation of the torsional shear stress distribution. For this purpose, any one of the following methods was used:

(a) Elastic theory

(b) Plastic theory

(c) Semiplastic theory

(d) Hsu's skew bending theory

(e) Statistical approach

Second, most of the investigators used a principal tensile stress criterion of failure. It was assumed that cracking would commence when the maximum principal stress due to the combined action of bending, shear, torsion, and prestress reached the tensile strength of concrete. However, very few used a failure criteria other than principal tensile stress.

Third, differences are considerable, as also noted earlier, in assuming a value for the tensile strength of concrete.

Most recently Barton and Kirk (1973) carried out a cracking analysis of their reinforced concrete T section beams subject to combined loadings assuming full plastic distribution of torsional shear stress and elastic distribution of bending and transverse shear stresses. They used the maximum principal stress failure criteria. The tensile strength of concrete was limited to $5\sqrt{f'_c}$. Two locations on the cross section, one at the neutral axis, the other either at the centre of top or bottom face, were examined for possible cracking. Ratios of test and analytical torques varied from 0.82 to 1.58 with a mean value of 1.13. It is to be noted that the moment used in the cracking strength equations referred to the centre of the test span.

2.1.6 Prestressed Concrete Beams Under Combined Loading

As a first part of an extensive test program, Gangarao and Zia (1970) reported the research findings of tests on prestressed rectangular beams (6"x12") under combined bending and torsion. Of the 42 specimens 28 were prestressed concentrically and the rest eccentrically. All beams had transverse reinforcement and some of them were provided with longitudinal mild steel while others were not. They presented a cracking analysis using the skewed bending theory. Bending was assumed to take place across a plane inclined at an angle to the longitudinal axis of the beam. The width of the failure plane was the length of the crack on the tension side of the beam. The initial crack was considered to occur when the internal stresses due to prestress, bending moment, and torque exceeded a reduced modulus of rupture. Stress due to flexural moment was computed elastically, and only the bending component of torque was considered to cause bending and contribute to the tensile stress. Two cracking modes, namely, bending mode and torsion mode were examined. In the former the tensile crack occurred in the bottom face while in the latter it appeared either at the top, bottom or centre of the wider face. Reduced modulus of rupture was approximated to $f'_c/10$. Finally, an equation was established involving torque and angle of cracking as unknowns. Minimization of torque with respect to crack angle provided a second equation for solving the cracking torque and angle. Gangarao and Zia stated that elastic torsion theory did not work well and proved to be highly conservative. Beams subjected to pure torsion developed an initial crack at the centre of the wider face if con-

centrically prestressed, at the top if eccentrically prestressed. Beams with eccentricity cracked at slightly lower torques than the beams without eccentricity.

Subsequently Henry and Zia (1971) investigated the behavior of 32 rectangular prestressed beams (6"x12") loaded in combined torsion, bending and shear. All the beams were provided with longitudinal mild steel and the same amount of web reinforcement. One half of the total beams had concentric prestress and the remaining one half had eccentric prestress. The cracking analysis presented was identical to that developed by Gangarao and Zia, but included the effect of transverse shear. In accordance with the elastic theory bending shear stress was assumed to be parabolic across the height of the section. They observed that the splitting tensile strength was an adequate measure of tensile stress as similar qualitative biaxial state of stress existed in the split test and the beam at initial cracking. Two cracking modes, bending and torsion, as in the earlier study, were identified. Two locations one at the centre and the other at the bottom of the side face on which shear and torsion stresses were additive, were checked for cracking in the torsion mode. The possibility of an initial crack at the top of the long side was not considered.

Flexural cracks were observed first near the bending load on the side at the bottom, even though the beam failed subsequently in a torsional mode. In some beams the initial crack formed at the centre of the side face. Henry and Zia observed that the cracking loads were very sensitive to loading combinations. The torque moment ratio used in the cracking analysis related to the failure section rather than the first crack section. This may then result

in computing a cracking strength at a section different from where the crack actually had formed.

More recently Johnston and Zia (1971) conducted a series of tests on 37, 12-in. square hollow eccentrically prestressed beams in various combinations of torsion, bending and shear. All beams except five contained web reinforcement. Stirrups were spaced either at 3 in. or 6 in. Two shear span to depth ratios were adopted.

Theoretical analyses were presented to predict cracking and ultimate strengths. They compared their test results at cracking with two methods of analyses. The first one based on skew bending theory, was presented by Gangarao and Zia; suitable modifications were applied to account for the hollow portion, presence of shear, and, the addition of the top cracking mode. The second one was elastic theory developed by themselves. A finite difference solution of the governing differential equation yielded torsional stresses which were combined with other stresses computed elastically. The initial crack was assumed to occur when the principal tensile stress exceeded the splitting tensile strength of concrete. The justification offered for the use of the splitting tensile strength was the insignificant strain gradient for a thin walled hollow beam as is the situation in the splitting test. Three cracking modes were analysed as the beams of this investigation cracked either on the bottom (Mode 1), or on top (Mode 3), or on the side (Mode 2).

Johnston and Zia showed that the bending theory failed to forecast the cracking strength of hollow beams adequately, yielding unconservative results for Mode 2 and Mode 3. But it gave good corre-

lation with test results for bending (Mode 1). This is not unexpected as cracking in Mode 1 is mainly due to bending. The elastic theory agreed well with test results though its predictions proved to be slightly unsafe for Mode 2.

To estimate the cracking strength of rectangular prestressed beams under combined loading Woodhead and McMullen (1972) used the elastic theory to compute the torsional, flexural shear, and bending stresses. Cracking was presumed to commence when the principal tensile stress equalled the tensile strength of concrete which was assigned a value of $7\sqrt{f'_c}$. Three critical locations, namely centres of the top, bottom and vertical faces, were examined. Several rectangular prestressed beams from different investigations were analysed and the correlation with the test results was good and ranged from 1.035 to 1.33. For flanged sections they suggested the same method but did not analyse any beams even though the strengths at first cracking in the case of prestressed I girders by Wyss et al (1969) were available.

Gardner (1960) reported tests on 16 plain I-beams nearly concentrically prestressed (eccentricity was only 0.2 in.) loaded under combined bending and torsion. He reported only the moments at the ultimate stage. Further, substantial bending moment was applied first, in some beams causing cracking, before any torque was applied. No beams were tested under pure torsion. He found that for the beams which did not develop tensile stresses on the application of bending moment, the limit of elastic behavior (defined as the limit of the linear part of the torque-twist curve) could be estimated using the

elastic theory. A finite difference method was used to determine the shear stress distribution.

The prestress used related to the centre of the web in spite of the eccentricity of the prestress. A value of 0.707 times the measured modulus of rupture was taken as the tensile strength of concrete. Another calculation assuming full plasticity at the ultimate stage, using a uniform prestress and shear stress distribution, principal tensile stress failure criteria, and tensile strength equal to that used in predicting the limit of elastic behavior yielded strengths very close to the ultimate torques.

Reeves (1962) described the testing of 42 plain prestressed concrete T section beams under combined bending and torsion. The prestress alone resulted in nominal stresses of 0 psi at the top and 2000 psi in the bottom. The load application was similar to that adopted by Gardner (1960). In some beams there were cracks due to the bending moment before the final torque was applied. Strengths were reported at the limit of elastic behavior and at the ultimate stage. He attempted to interpret the ultimate strength using the classical theories and concluded that the elastic and plastic theories could not adequately predict the torsional strength of his T sections at failure. If the section is cracked it is not possible to determine the torsion factor, the prestress distribution, and the critical shear strength.

Bishara reported tests on 24 prestressed rectangular, I and T beams subjected to combined torsion, bending and shear in various

combinations. Half of the beams were eccentrically prestressed. Rectangular beams developed initial cracks on the longer side where the torsional and flexural shear stresses were additive. These beams failed in a skew bending mode with the compression hinge on the side opposite to that where cracking started. In flanged beams cracking started randomly either on the web, or on the top face or at both the locations. It was observed that the flange(s) and the web appeared to behave as individual component rectangular members with regard to the extension of cracks to the adjacent sides implying discontinuity of cracks at the web flange junctions. However, failure finally took place by crushing of the concrete along a part of the web and the flange.

Bishara used the elastic theory and observed that it failed to predict the cracking strength of prestressed rectangular and flanged beams but did not suggest any alternate method. He obtained the stress distribution due to all the forces including the torque by the elastic theory. Principal tensile stress failure criteria was used. The principal tensile stresses at the critical locations varied from 400 psi to 1260 psi for rectangular beams and from 580 to 1600 psi for T beams. In the case of I beams the tension was from 900 to 1600 psi. These high stresses did not relate to any of the computed strengths such as 5 $\sqrt{f'_c}$ for the tensile strength and 7.5 $\sqrt{f'_c}$ for the modulus of rupture corresponding to his test specimens. He attributed this discrepancy to the inelastic behavior of concrete prior to cracking.

In accordance with the design philosophy of the ACI, Wyss and Mattock (1971) investigated the torsion-shear interaction

on diagonal tension cracking in a test series consisting of twenty full scale I section girders stressed eccentrically. The dimensions of the test section were identical to those adopted in their earlier study of pure torsion (1969). In the study of shear-torsion interaction, two cases, web cracking, and shear-flexure cracking were examined. Depending on the cross sectional dimensions and the eccentricity of prestress, initial cracking may occur either on the top or in the web when torque alone acts. Their study concerns the former case, while the latter case would prove to be more severe in combined loading, as the torsional and flexural shear stresses add on one vertical face. To establish the torque-shear interaction, stress distribution due to prestress, flexure and transverse shear was evaluated by the elastic theory and combined with the torsional shear stress computed by either elastic or plastic theory. Assuming the tensile strength as $6\sqrt{f'_c}$, tensile stress failure criteria was applied. Wyss et al noted that the computation of torsional stresses by the elastic theory was unrealistic and favoured the plastic theory. Three possible modes of diagonal tension cracking were recognized. In the case of cracking at the top, its center was examined. In the web the neutral axis was considered to be associated with the maximum principal tensile stress. However at a cross section higher tensile stresses may occur at the bottom junction with the flange if the rate of increase of tensile stresses due to flexural moment is more than that of prestress assuming both torsional and transverse shear stresses do not vary in the web.

In the development of their shear-flexure cracking strength Wyss and Mattock started with the ACI shear equation (1963).

$$V_{ci} = 0.6\, b'd\sqrt{f'_c} + \frac{M_{cr}}{\frac{M}{V} - \frac{d}{2}} + V_d \qquad (2.19)$$

where V_{ci} = diagonal tension cracking shear in a region of a beam cracked in flexure

b' = minimum width of a flanged member

d = effective depth of a beam

M/V = moment shear ratio due to applied loads

V_d = dead load shear

M_{cr} = net flexural cracking moment

The tensile stresses due to the second and third terms of the foregoing equation were combined with the plastic torsional shear stress (only in this case tensile strength was assumed equal to modulus of rupture estimated at $9\sqrt{f'_c}$). The first term of equation 2.19 was assumed to be affected by the presence of torque in the same way as the shear, torque interaction in the web cracking case. Their strength equations were not derived in general terms but certain known values were substituted and they are as follows:

Cracking on the top face

$$T_{cr} = 277\,(1.26 + \frac{V}{39.5})^{1/2} \qquad (2.20)$$

Web Cracking

$$T_{cr} = 492 - 5.95\ V_{cr} \qquad (2.21)$$

Shear flexure cracking

$$V_{ci} = 5.88\ (1 - \frac{T}{492}) + (29.52 - \frac{T^2}{20{,}600}) + 0.3 \qquad (2.22)$$

where T_{cr} = diagonal tension cracking torque in combined loading

T = torque applied to a section

V = shear applied to a section

V_{cr} = diagonal tension cracking shear in combined bending

V_{ci} = diagonal tension cracking shear in a region of a beam cracked in flexure

The predicted results were generally in good accord with the test results except in the case of some girders which had initial cracks in the web. They believed that the highly conservative predictions in the case of web cracking were due to either;

(i) the less stressed side of the web reinforcing the highly stressed side of the web delaying cracks, or

(ii) redistribution of stresses occurring which could not be taken into account by the elastic theory.

Probably the high stress gradient also might be responsible for this conservatism.

2.2 Ultimate Strength

2.2.1 General

The general methods developed in the literature for predicting the ultimate strength of reinforced concrete beams under pure torsion and combined torsion, bending and shear are indicated in the following sections. Reinforced concrete flanged beams analyzed by the skew bending theory are discussed. Usually the analyses available for reinforced concrete beams have been extended with certain modifications to evaluate the ultimate strength of prestressed members. The most recent investigations of prestressed rectangular beams under combined loading and prestressed flanged section beams are reviewed closely.

To achieve post cracking strength and ductility concrete members are provided with longitudinal and transverse reinforcement to resist torsion occurring alone or with other forces. These reinforced beams can be broadly divided into three categories, namely under-reinforced, over-reinforced and partially over-reinforced. In an under-reinforced beam both longitudinal steel and stirrups yield before the concrete crushes at ultimate. Strain compatibility need not be considered in such a beam. Most of the available analyses cover only this category of beams. A over-reinforced beam is one in which neither the longitudinal steel nor stirrups yield before the concrete fails. Over-reinforced beams are normally not permitted to be designed. A partially over-reinforced beam has an unbalanced ratio of longitudinal steel to stirrups. Only one reinforcement, either the longitudinal steel or the stirrups, yields while the other does not as the concrete crushes. For strength evaluation of such beams the strain in the steel which is not stressed

to yield at failure, must be known. Most of the prestressed concrete beams in the literature belong to this category.

To obtain an under-reinforced or a balanced failure, not only must the total amount of longitudinal and web steel not exceed a certain amount but also the distribution between the longitudinal steel and stirrups must be within certain limits. Though several investigators observed that the distribution ratio (ratio volume of longitudinal steel to web steel) can vary widely to produce balanced failures, the most often used value is unity. Knowledge about the variation of the distribution ratio is limited.

2.2.2 General Theories in Reinforced Concrete

Early investigators' and the ACI's approach for predicting the ultimate pure torsional strength of reinforced rectangular concrete beams can be related to an expression of the following form, based on the premise that the torsional strength is composed of the sum of strengths due to concrete and reinforcement

$$T_{uo} = kT_0 + \Omega\, x_1 y_1 \frac{A_t f_{ty}}{s} \qquad (2.23)$$

where T_0 = pure torsional strength of a plain concrete beam

Ω = a function of x_1 and y_1, and ratio of volumes of longitudinal steel and stirrups

k = a non dimensional factor

The first term accounts for the torsional resistance of the concrete and second term of the reinforcement. There were considerable differences

between estimates of these two torsional resistances cited in the literature.

Rausch (1929), proposing a truss analogy for the study of torsion of reinforced concrete beams, obtained a value of 2 for Ω, assuming uniform yield stress in the stirrups. Concrete strength contribution was considered to be zero. Anderson (1937) and Cowan (1950) disputed the uniform stress in the stirrups and based the stress distribution according to the elastic theory. Cowan's study resulted in a value of 1.6 for Ω and the concrete contribution equal to the torsional strength of a corresponding plain concrete member.

The first rational analysis for the ultimate torsional strength of reinforced concrete beams under combined loading was that of Lessig (1958,1959), who proposed that rectangular beams failed in one of two skew bending modes, namely bending mode and torsion mode. Using two of the six equilibrium conditions, one for forces and the other for moments, together with several assumptions she derived ultimate strength equations for each of the modes of failure. In her analysis the failure surface was idealized by a spiral crack at a constant inclination on the three sides of a beam, joined by a compression crack on the fourth. Inclination of this crack was determined by minimizing the torsional resistance of the member. Lessig's theory considers the combined resistance of concrete and reinforcement. However, it neglects the tensile strength of concrete.

Those who used Lessig's skew bending theory for reinforced concrete members with certain modifications and additions resulting

in refinements included Yudin (1962), Gesund et al (1964), McMullen and Warwaruk (1967), Collins et al (1968), Goode and Helmy (1968) Bradburn (1968), and Kirk and Lash (1971). Gangarao and Zia (1970) Henry and Zia (1971), Johnston and Zia (1971) and Woodhead and McMullen (1972) applied her theory in prestressed concrete. Yudin (1962) believed that it was accurate enough to assume the failure surface at an angle of 45 degrees with the longitudinal axis. He claimed it was more rational to consider moment equations about two axes, one about the axis parallel to the longitudinal axis and the other perpendicular to it; and one force equation. Gesund et al (1964a,1964b) considered the effect of dowel forces in their study of ultimate torsional strength. McMullen and Warwaruk (1967) observed that a beam having more longitudinal steel near the bottom face than the top failed developing a compression zone in the bottom face, and referred to this as a Mode three failure. Collins et al (1968) simplified Lessig's equations and also observed the Mode three failure. Goode and Helmy (1968) used a third equilibrium equation which furnished a condition to solve another unknown. They utilized this condition for estimating the steel stress in a partially over-reinforced case. Kirk and Lash (1971) applied the skew bending theory to T section beams, idealizing them as rectangular ones.

Observing that Lessig's theory did not account for certain experimental observations and did not numerically fit the test results, Hsu (1968d) proposed a theory for pure torsional strength of symmetrically reinforced rectangular beams based on his test program. Differing from that of Lessig he idealized the failure surface as a plane

inclined at 45 degrees to the axis of twist but perpendicular to the wider face. He stated that the inclination of the failure surface was constant irrespective of the cross-sectional dimensions and the ratio of longitudinal to web reinforcement. He believed that the failure surface should not cut the horizontal legs of the stirrups. The dowel forces in the longitudinal steel and the shear resistance of the shear-compression zone were taken into account. Establishing the equilibrium of moments about the longitudinal axis of the beam, the following expression was derived to predict the torsional strength of rectangular reinforced concrete beams:

$$T_{uo} = T_0 + \frac{\Omega\, x_1 y_1\, A_t f_{ty}}{s} \qquad (2.24)$$

where $T_0 = 2.4 b^2 h \sqrt{f'_c}/\sqrt{b}$

$\Omega = 0.66m + 0.33\, y_1/x_1$

m = ratio of volumes of longitudinal steel and stirrups

Hsu evaluated the term Ω experimentally. Thus the equation heavily depends on his test results. The first term of this equation is about 40 percent of pure torsional strength of a plain concrete beam which is also equal to the intercept on the T_{uo} axis of the experimental curve between T_{uo} versus reinforcement factor. However, Hsu obtained this term as the resistance of the shear compression zone.

An extensive continuing investigation of reinforced T and L section beams under combined loading has been reported by Ferguson and Farmer, Ersoy, Victor, Liao, Behara, and Rajagopalan (1967, 1967 and 1968, 1968a and 1968b, 1969, 1970a, 1970b, 1971 and 1972). The

equilibrium approach as proposed by [illegible] (1959) for rectangular beams was considered complex for a flanged beam and they analyzed their beams by interaction curves and surfaces.

Another intensive investigation by Mattock et al (1967, 1969) concerning rectangular and flanged beams was based on the interaction of torsion with other forces.

In a review paper based on the tests in the literature Zia (1970) indicated that I, T, and L sections also fail by skew bending and because of the complexity of the problem, one has to depend on the approximate approach using the summation procedure of component rectangles for computing the strength. Evans, Kemp and Wilhelm (1970) stated that the behavior and ultimate strength of such members depended on the degree to which the component rectangles act together. Based on their investigation referred to earlier, they proposed the following equation for predicting the ultimate strength of reinforced concrete T and L beams in which there were equal volumes of longitudinal and stirrup steel, were component rectangles reinforced transversely by closed stirrups and longitudinally at least at the corners, and the reinforcement from the component rectangles sufficiently overlapped to enable the flanged section to act as a unit.

$$T_{uo} = 0.45\, T_c + 2.0\Sigma\, x_1 y_1 \frac{A_t f_{ty}}{s} \qquad (2.25)$$

where T_c = cracking torque of a plain concrete beam.

The flanged sections tested by Hsu (1968b) at the PCA did not have any web reinforcement.

2.2.3 Flanged Reinforced Concrete Beams - Skew Bending Theory

Gvozdev, Lessig, and Rulle (1968) reported the test results of reinforced concrete I section beams under combined loading. The I beams had a flange width of 8.66 in., an overall depth from 15.75 in. to 18.11 in. and web thickness from 1.97 in. to 3.15 in. and were 11 feet long. The variables included the arrangement and amount of longitudinal and web reinforcements, cross-sectional dimensions and T/M ratios. The failure of under-reinforced I beams tested under combined torsion and bending was observed to be similar to that of rectangular beams. Two modes of failure namely bending mode and torsion mode were identified, which are shown in Fig. 2.1. The bending mode of failure was characterized by the development of a spiral crack on the bottom and the side faces, with the concrete failing in the compression flange along the line joining the ends of the spiral crack. In the torsion mode the failure crack was formed on the side, top and bottom faces. Splitting of concrete on the side faces of the top and bottom flanges took place, followed by the compression distress on the side of the web opposite to that on which the tensile cracks opened. The compression distress in the web was along a line connecting the ends of concrete split in the flanges. Gvozdev et al found from their tests that the crack inclination of the failure surface to the longitudinal axis was independent of torque/moment ratio and it followed the direction of principal tensile stresses due to torsion only, unlike in the case of rectangular beams. Hence they assumed a 45 degree inclined crack on all the three faces in the development of strength formulas irrespective of the relative proportions of the torque and

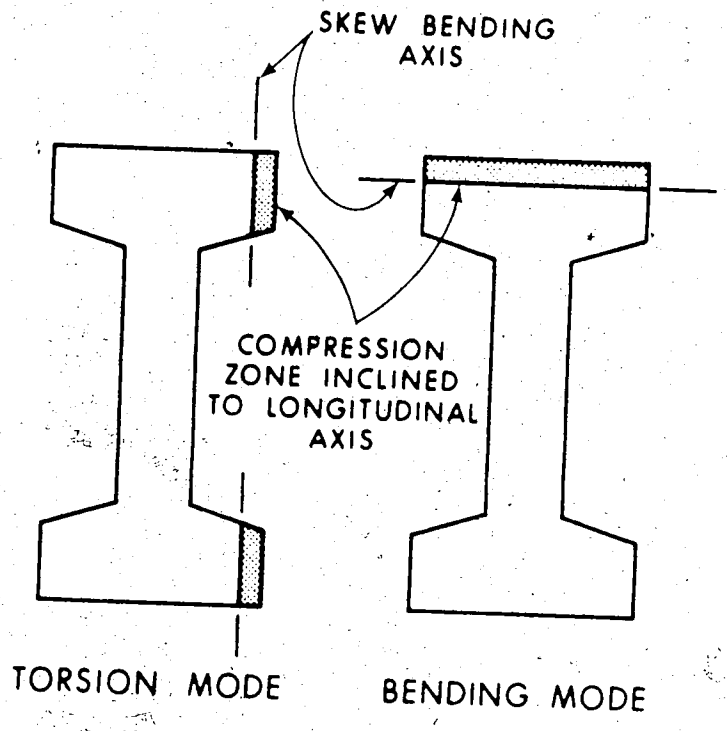

FIG. 2.1 SKEW-BENDING FAILURE ASSUMED BY GVOZDEV LESSIG, RULLE (1968) FOR COMBINED LOADING

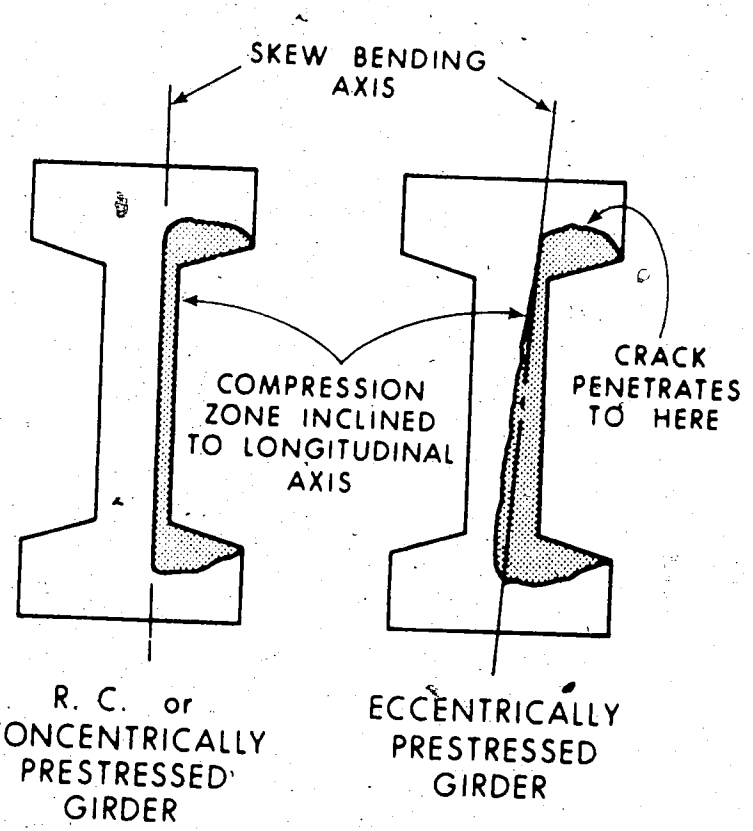

FIG. 2.2 PROBABLE SHEAR-COMPRESSION ZONE SUGGESTED BY WYSS, GARLAND AND MATTOCK (1969) FOR TORSION MODE

bending moment. Since the depth of the compression zone was small, it was taken equal to zero. The strength contribution of only those stirrups crossed by the tensile crack in the web portion was taken into account. With the foregoing assumptions, the same skew bending analysis (Lessig 1958, 1959) developed for the rectangular beams was applied to I section beams. The analytical strengths correlated well with the test results. However the strength prediction was slightly unconservative for beams tested in pure torsion. This is due mainly to the fact that Gvozdev et al chose to locate the skew bending axis in the torsion mode, close to one of the side faces of the flanges increasing the lever arm of the steel forces; though they observed compression distress in the web also. Gvozdev et al stated that the post cracking strength in pure torsion did not exceed 30 percent even for the highly reinforced I beams they tested and the torsional stiffness reduced sharply after cracking. They observed that the ultimate capacity of an open cross-section member such as an I beam, under torsion was limited by its deformation rather than by its strength.

Thirty seven reinforced concrete T beams were tested by Kirk and Lash (1971). Under combined bending and torsion all the beams were provided with a symmetric arrangement of top and bottom longitudinal reinforcement and most beams had web reinforcement. All beams were under-reinforced both longitudinally and transversely when torsion alone acted. The beams failed in a skew bending mode, bending taking place about an inclined axis on the flange connecting the spiral tensile crack on the remaining sides. The inclination of the failure surface varied from 45 degrees in the case of pure torsion to 90 degrees

in the pure bending. Considerable ductility was displayed by the reinforced beams at the ultimate stage. The compression zone in the flange was assumed to extend only in the web portion, neglecting the outstanding flanges. In essence it was treated as a rectangular beam for analysis. The ultimate strengths were computed by two methods, one proposed by Lessig (1959), and the other proposed by Collins (1968) for Mode 1 failure in the rectangular beams. Both methods gave good correlation with the test results, but Lessig's method correlated better.

In an extension of this investigation, Kirk and Loveland (1972) carried out tests on 18 T beams with an unsymmetrical arrangement of the longitudinal steel in the top and bottom of the T beams and all the beams had web reinforcement. At ultimate either the top or the bottom longitudinal steel yielded. The stirrups either yielded or approached yielding. The location of the compression zone depended on the relative amounts of the steel in the top and bottom and T/M ratio. The compression zone always formed in the flange for the beams with steel more at the top than the bottom, this is a Mode 1 failure. In the case of beams having more bottom steel, the compression zone formed in the flange for low torque to moment ratios, and in the bottom across the web for high torque to moment ratios, which is usually called a Mode 3 failure. The T section was assumed as a rectangular section and a Mode 3 Analysis similar to those of Lessig and Collins was proposed. For this series also, Lessig's method correlated better.

The formation of a compression zone on the side did not occur in T-beams reported in their investigation; as the transverse stiffness with respect to an axis perpendicular to the flange was much

larger than that parallel to the flange. In Mode 1., the over hanging portion of the flange was neglected in calculating the depth of compression zone. This assumption is not necessary as the failure loads are practically the same, whether the outstanding flanges are excluded or included for T beams tested in their investigation (Rao and Warwaruk, 1973).

2.2.4 Prestressed Rectangular Beams Under Combined Loading

As a first part of a continuing research program dealing with prestressed concrete members under combined loading at the University of Alberta, Mukherjee and Warwaruk (1970) reported the tests on fifty four rectangular (6 x 12 in) prestressed beams. One half of the beams were prestressed eccentrically and the other one half concentrically. Barring two, each beam had the same amounts of non-prestressed longitudinal and web reinforcement. Twenty-eight of the beams were tested under differing combinations of bending and torsion, and the remainder additionally had shear.

The inclination and the location of origination of the cracks depended on the level and eccentricity of prestress as well as T/M ratio. Initial cracking varied from the bottom side for the beams with high bending to the centre of side face for beams with high torque. In beams loaded under a medium range of T/M ratio cracks started simultaneously at the bottom and side faces. Eccentrically stressed beams cracked first at the top of vertical side. Presence of shear caused crowding of the flexural cracks in the vicinity of transverse load and the crowding of torsional cracks away from the bending load.

The torsional strength of the beams tested in their investigation

increased when bending was present in moderate amounts. This increase was greater in the case of eccentrically prestressed beams. Similarly the bending capacity was not increased with small amounts of torsion, but was not reduced significantly until the coexisting torque was about 40 percent of the pure torsional strength. The addition of flexural shear reduced the torsional strength regardless of the combination of torque and bending moment. They reported that the initial torsional stiffness was unaffected by the level of prestress, T/M ratio and the presence of shear. The rotational capacity reduced as the level of prestress increased and T/M ratio decreased. The reduction in torsional stiffness was more gradual when bending was predominant.

Mukherjee and Warwaruk indicated that most of the beams failed either in Mode 1 or Mode 2. However eccentrically stressed beams loaded under high T/M ratios showed upward deflections at failure. These beams may have failed in Mode 3 with the compression hinge in the bottom face. When transverse shear was present, as the T/M ratio increased, the failure zone shifted away from the bending load. The location of the failure zone could not be satisfactorily related, to any known parameters for a given T/M ratio. The failure surface is generally near the bending load in the bending mode (Mode 1), in the minimum moment region for Mode 3, and at any location in the pure torsion case. For Mode 2 it may partly depend on T/M ratio. However, it is to be noted that in this mode the influence of moment is not considerable. For correct computation of flexural moment, when it varies in the test zone, the knowledge of the location of the failure zone is necessary. No satisfactory solution is yet available to this end.

Mukherjee and Warwaruk observed that the interaction between bending and torsion was similar at the cracking and ultimate stages, and proposed a parabolic interaction curve involving the level of prestress and the eccentricity. This curve reflects the beneficial effect of increase in the torsional strength in the presence of moderate bending moments. The proposed interaction curve showed good correlation with their test results and those of Gangarao and Zia (1970) whose beams contained various amounts of web reinforcement. Further, Wyss and Mattock (1971) showed that this torque-moment interaction, though derived for rectangular sections, exhibited good agreement with their prestressed I girders tested in combined bending and torsion.

The effect of simultaneous action of torsion, bending and shear can be expressed in terms of an interaction surface. Mukherjee and Warwaruk proposed such a surface for the prestressed rectangular beams. On the torque-moment plane, the trace of the interaction surface was the fore-mentioned relationship proposed by them. For torsion-shear interaction a straight line relationship was utilized. In the past for reinforced concrete beams circular interaction was often proposed at cracking based on test results. As the web reinforcement amount increases this circular curve flattens and tends to a straight line as evidenced by the tests of Klus (1968). Thus a straight line is a lower bound in reinforced oncrete beams. Because of the paucity of test results it is safe to assume straight line interaction relationship between torque and shear. Assuming that full flexural capacity would be reached without a premature flexural shear failure due to

enough web reinforcement a rectangular trace was used on the bending-shear plane. This interaction surface predicted very well the ultimate strengths of their beams. Subsequently it has also been confirmed in tests of prestressed rectangular beams under combined loading by Woodhead and McMullen (1972) who reported very good correlation.

The study of prestressed beams under combined loading by Gangarao and Zia (1970), Henry and Zia (1971), and Johnston and Zia (1971) was introduced while discussing the cracking strength. Here a brief review of their ultimate strength analyses follows.

Gangarao and Zia observed from their tests that rectangular prestressed beams (6"x12") failed in either one of the two skew bending modes proposed by Lessig (1959), for reinforced concrete beams and derived prediction equations for ultimate strength. A bending mode was identified by the formation of an inclined compressive zone adjacent to the top face of the beam joining the two ends of the spiral crack on the remaining sides and by the yielding of either the prestressing strands or the horizontal legs of the stirrups near the tension face. In the torsion mode the compression hinge formed on the vertical side of a beam. This mode was considered to occur when the transverse reinforcement near the tension face just yielded. In both the modes the strain across the failure surface was assumed to be proportional to the distance from the neutral axis situated in a plane having the compression zone. This is an approximation only. The spiral crack inclination at failure, which is related to the inclination of the compression hinge, was based on cracking analysis. At ultimate, if either the stirrups or the longitudinal steel yielded and the other

did not, the strain in the steel that did not yield was obtained by Gangarao and Zia using the following assumption. The strain components parallel to the failure surface of both longitudinal and stirrup steel were equated assuming that the relative displacement along the direction of the failure surface was negligibly small for small rotations. However, the rotations at ultimate in general are not small. Strains in other steels in the beam were then assumed to be compatible with the yield strain of the steel which yielded. However, yield strain was assumed in the longitudinal mild steel on the tension face regardless of their assumption of compatibility.

Eccentrically stressed members developed slightly higher ultimate pure torsional strength than the concentrically stressed ones. Eccentricity of prestress increased the ultimate strength of a member under combined loading with a decrease in the T/M ratio. The addition of longitudinal mild steel did not result in a significant increase in the pure torsional strength, but it increased the ultimate strength of a beam under combined loading as T/M decreased. This is partly because torsional strength is usually limited by the transverse steel, while the flexural strength is limited by the longitudinal steels. Square and circular non-dimensional interaction relationships between torsion and bending were proposed conservatively, for beams with and without longitudinal mild steel respectively. Their theoretical predictions were consistent and in good agreement with the test results for high and low T/M ratios, but less reliable in the transition from the torsion mode to the bending mode which was characterized by the yielding of horizontal legs of stirrups in the bottom face.

For lack of sufficient data, limits for the amounts of steel were suggested only in the case of pure torsion to identify a balanced failure. The total volume of steel was not to exceed $3000\sqrt{f'_c}/f_{ty}$. Further, to ensure that both the longitudinal and the web steels yield the total steel needs to be distributed properly between the former and the latter. This ratio m, given by the following equation, was suggested to be 1.0 to 1.2,

$$m = \Sigma(A_{ms}f_{my}+A_{ps}f_{py})s/A_t f_{ty}(x_1+y_1)\cot^2\theta \qquad (2.26)$$

For beams under pure torsion, the torsional stiffness was unaffected by the spacing of the stirrups, but the ductility was much lower for beams with stirrup spacing at 4 in. than at 3 in. Eccentricity considerably increased the ductility. Presence of longitudinal mild steel resulted in little effect in the deformation prior to cracking, in great increase in ductility, negligible increase in pure torsional strength but considerable strength increase as T/M ratio decreased. The bending stiffness prior to cracking decreased with a decrease in T/M ratio, but the torsional stiffness changed only insignificantly. It was observed that for Mode 2 stirrups closer to the compression zone nearly yielded which indicated that the depth of the compression zone was negligibly small.

The study of Henry and Zia included the effect of shear. They observed that all the beams (6"x12") failed in either bending mode or torsion mode. The first cracks to form were generally flexural near the bending load, though a beam subsequently failed in a torsion mode.

Stirrups yielded when intersected by the failure surface at the ultimate stage. In the torsion mode the strands did not yield while in the bending mode they did. Yielding of horizontal legs of stirrups observed by Gangarao and Zia did not occur in these beams in bending mode failure. Contrary to the finding of Gangarao and Zia, Henry and Zia observed that the prestressing strands registered strain prior to cracking when T/M ratio was low. The strains recorded in the longitudinal mild steel were compressive, but they were assumed to have yielded in the analysis. The failure surface established by the cracks was less distinct in the bending mode than in the torsion mode. The location of the failure surface which is essential for computing the bending moment was found to be somewhat arbitrary.

Analytical expressions based on skew bending theory similar to those of Gangarao and Zia were presented to predict the ultimate strengths. The agreement between the test and theoretical results was good. The following conservative interaction relationships were proposed between torsion and bending and torsion and shear.

$$\left(\frac{T_u}{T_{uo}}\right)^2 + \left(\frac{M_u}{M_{uo}}\right)^2 = 1 \qquad (2.27)$$

$$\frac{T_u}{T_{uo}} = 1 - \frac{V_u}{V_{uo}} \qquad (2.28)$$

It was observed that the ultimate torsional strength of a beam could be increased up to about 30 percent of pure torsional strength whenever the amount of moment and shear was less than 20 percent.

The initial torsional stiffness was found to be nearly

independent of the loading ratio, prestressing force and its eccentricity, and span of beam. Post cracking behavior depended mainly on the loading ratio. There was little reduction in torsional stiffness between first flexural cracking and diagonal cracking. Increases in transverse shear decreased the torsional ductility of a beam under combined loads.

Johnston and Zia (1971) observed from their test results that prestressed hollow beams developed the skew bending mechanism of ultimate failure similar to solid reinforced and prestressed rectangular sections. Three modes of failure corresponding to a compression zone on either the top, vertical side or bottom face occurred. When transverse shear was high another mode having a compression zone in the top corner was identified, but was analyzed as mode 2. Theoretical analyses based on skew bending theory similar to those of Henry and Zia were presented. In mode 1, the failure was considered to occur when either the vertical legs of the stirrups yielded or, the longitudinal prestressing strands yielded. For mode 2 it was assumed that failure would occur when the horizontal stirrup legs first reached the yield stress. Generally but not always the cracking mode and the ultimate mode were the same. Theoretical predictions compared well with the test results.

The torsional stiffness was found to be independent of transverse shear, moment and web reinforcement, but increased with the concrete strength in the precracking stage. Post cracking torsional and flexural stiffnesses depended on the loading ratios and the amount of reinforcement. The necessity of more tests on beams with low torsion

and high shear was suggested.

Woodhead and McMullen (1972) carried out an investigation into the strength of thirty rectangular (6"x12") prestressed beams loaded in torsion, bending and shear. Two beams had concentric prestress and the rest eccentric prestress. Except for nine beams all had web reinforcement. Three of the web reinforced beams had longitudinal mild steel reinforcement. They presented analyses for cracking and ultimate strengths; the former analysis based on the elastic theory and the latter on the skew bending theory. The cracking analysis was discussed earlier. Ultimate strength analysis was proposed for each of the two modes, namely the bending mode and torsion mode observed in their tests and also for tests reported in the literature. Analysis of each mode covered prestressed beams with or without web reinforcement.

(a) Bending Mode: A pure flexural failure occurs with the formation of a rectangular compression zone adjacent to the compression side of the beam. With the addition of increasing torsion, this zone may become trapezoidal, triangular and may even extend partly on to the side before the torsion increases sufficiently to transform this mixed bending into a torsion mode. Though this was recognized by earlier investigators a rectangular compression zone was used in analyses, presumably for simplicity. Woodhead and McMullen took into account the changing shape of the compression zone by assuming that the neutral axis met one of the vertical faces at an angle which is given by the following expression:

$$\alpha = \tan^{-1} \frac{M_u}{T_u} \qquad (2.29)$$

They stated that this refinement resulted in little difference in the ultimate strength. Their equilibrium analysis was carried out similar to that for over reinforced beams in pure bending using the following empirical ultimate strain in concrete both for pure bending and combined loading as suggested by Evans and Khalil (1970).

$$\varepsilon_c = \varepsilon_{cu} \left(\frac{M_u}{M_{uo}}\right)^2 \qquad (2.30)$$

where ε_c = longitudinal compressive strain under combined loading

$\varepsilon_{cu} = 0.0034$

M_{uo} = ultimate bending capacity of beam in pure bending

If the beams were web reinforced the resistance of web steel was taken into account in establishing equilibrium. The strain in the longitudinal steel was known and the strain in the stirrups was obtained assuming the strain compatibility suggested by Gangarao and Zia (1970). Woodhead and McMullen showed good agreement of their bending mode analysis with several rectangular and flanged beams reported in the literature.

(b) Torsion Mode: Woodhead and McMullen applied their cracking analysis to compute the ultimate strength of prestressed beams without web reinforcement failing in torsion. For such beams cracking was regarded as constituting failure. The critical location for cracking was assumed at the centre of the vertical face for rectangular and I beams and centre of the top face for T beams regardless of eccentricity and T/M ratio. For web cracking in I beams their theory grossly under

estimated the test results as in the case of I beams of Wyss and Mattock (1971) ($T_{u(test)}/T_{u(theory)} = 1.62$).

For web reinforced beams Woodhead and McMullen considered two cases of torsion failure. The first case related to the beams longitudinally and transversely under reinforced and the analysis was similar to that proposed for reinforced concrete beams (Lessig 1959, McMullen and Warwaruk 1967, Collins et al 1968). Failure was assumed to occur with the yielding of longitudinal and transverse reinforcement away from the inclined compression face. The induced strains due to the loading were neglected in the reinforcement near the compression zone. The second case concerned beams transversely under-reinforced but longitudinally over-reinforced and failure was considered to take place when the vertical legs of the stirrups attained yield strain. The induced strains in the other reinforcements were related to the stirrup yield strain by a certain strain compatibility assumption. In both cases the two unknowns, the depth of compression zone and the torque, were obtained by solving the two equations established considering the equilibrium of forces and moments in a skewed plane. Prestressed beams of several other investigators were analyzed by both cases of the torsion mode and it was found that only a few beams were under-reinforced; many were under-reinforced only transversely but not longitudinally, some were over-reinforced. Empirical limits were proposed for the amounts of reinforcements to define what constituted under and over reinforced beams. Despite a variety of beams from different investigations, their strength predictions were in good agreement with test results.

Woodhead and McMullen extended the analysis of rsion mode to I beams with simplifying assumptions. They computed t. ultimate strength assuming the compression zone adjacent to the side faces of the flanges. The stirrups on the tension side were assumed to yield. The induced strain in the strands was arbitrarily taken equal to the yield strain of the web reinforcement. It was implied that the force in the leg of the stirrups adjacent to the compression zone was neglected, thus the strength was partly underestimated. This may be justified if the compression zone is very near to this vertical leg, but for I beams it is not. It was not indicated how the inclination of the compression hinge was arrived at. They tested the validity of the theory by applying it only to the test results of Gausel (1970).

In addition to several other conclusions, it was stated that the shear force reduced the ultimate strength in the torsion mode of failure. The theory was conservative near the torsion axis of the interaction diagrams as small amounts of bending moment increased the torsional strength above the pure torsional strength. The bending strength was equal to the ultimate flexural capacity until the coexisting torque was of the order of 30 percent of pure torsional strength. Circular interaction was conservative in both the torque-moment and torque-shear planes. The three dimensional interaction surface proposed by Mukherjee and Warwaruk (1970) predicted well the ultimate strengths of their beams.

2.2.5 Prestressed Flanged Beams

Gardner (1960) described the testing of 16 identical plain I beams, prestressed at a small eccentricity of 0.2 in., under combined bending and torsion. The beams were loaded initially with a predeter-

mined bending moment which varied from 10 to 80 percent of the pure bending capacity of the section, and then twisted to failure. None were tested under pure torsion. Within the range of flexural moments applied he observed nearly the same ultimate torsional strength for all the beams. The combined effect of prestress and the normal bending stress resulted in a moment with eccentric prestress before torsion was applied.

Gardner's beams seem to have failed in Mode 2, triggered by cracking in the web. Some I beams because of eccentric prestress might have developed initial cracking on the top face, but failed in Mode 2 as the stiffness about an axis parallel to the web was less than that about an axis perpendicular to the web. Mode 2 failure most probably is the reason for the uniform failure loads in all the beams. No new theory emerged from study of I beams but he computed the ultimate torque based on the plastic theory which was close to the ultimate torsional strengths.

Reeves (1962) described 42 tests carried out on three series of plain prestressed concrete T-beams subjected to combined bending and torsion. Beams within each series had identical properties and between the series only the breadth of the flange was varied. Prestress distribution in all the beams was triangular. Load application was similar to that used by Gardner (1960). The application of a predetermined bending moment caused in some beams initial cracking before the torsion was added.

The failure was abrupt and occurred by the development of a

tensile crack on one side of the web which passed through the section resulting in crushing on the opposite side of the web if the coexisting bending moment was between 0 to 70 percent of the pure bending capacity of the section. For larger moments a combination of bending and twisting failure occurred.

His beams exhibited considerable increase in torsional strength up to a certain increase in the bending moment. The optimum increase in the torsional strength, as much as 1.65 times the pure torque capacity depending on the geometry of the section, occurred when the flexural moment was of such magnitude as to cause a direct tensile stress in the bottom face equal to about the split cylinder strength. The torsional strength did not fall below the pure torque capacity until a bending moment equal to 80 percent of the pure flexural capacity was applied. Any increase in the moment above this value caused a rapid reduction in the torsional strength.

Reeves proposed a cubic polynomial interaction equation for each of his series based on a regression analysis of his test results. Other typical interaction curves available suggest that the torsion-bending interaction depends on geometry of section, distribution of prestress, and the reinforcement details. Reeve's interaction considers only geometry of the section. For estimating the ultimate strength of plain prestressed T beams under moment and torsion use of interaction curves was suggested. Reeve's compared three methods to obtain pure torsional strength.

(1) Plastic theory, with the direct stress at the critical location, using the failure criteria due to Bresler and Pister (1958).

(2) Plastic theory, with the direct stress at the critical location using principal tensile stress theory and the tensile strength equal to split cylinder strength.

(3) Elastic theory with the direct stress at the critical location, using principal tensile stress theory and the modulus of rupture. He recommended the third method as he found it statistically best.

Bishara's experimental investigation (1969) consisted of tests on prestressed concrete rectangular, I and T section beams with web and longitudinal mild steel reinforcement, under combined torsion bending and shear. For each type of cross section eight beams were tested. One half were concentrically stressed and the other half eccentrically stressed. These beams were similar to Zia's (1961).

The load deformation curves were observed to be linear up to about 90 percent of the cracking loads. Torsional stiffness as estimated by the elastic theory was close to the average measured values in the case of I and T beams but for the rectangular beams the correlation was poor. It was found that the initial torsional stiffness was independent of the T/M ratio and the eccentricity. His description of failure modes implied that the flanged beams generally failed in skew bending. On the average the ultimate load was higher than the cracking load only by about 15 percent.

Bishara found from his test results that the torsional strength of prestressed beams under combined loading could be increased from 1.3 to about 2.5 times the pure torque capacity, irrespective of the eccentricity, by the addition of bending moment. The

higher figure corresponded to flanged, members. It was further stated by Bishara, that the torsional strength was below the pure torsional capacity only if the moment and shear exceeded 80 percent of the strength of the beam when bending and shear acted alone.

Based on his limited test results Bishara presented the same form of parabolic interaction diagrams both for the torque-moment, and the torque-shear planes for each shape of the cross section. In establishing the interaction relationships there were no experimental values for pure torque and bending and shear capacities. The small span of 30 in. between the loading brackets might have (Pandit, 1970) influenced the test results. Woodhead (1969) showed that the torsional strength of a specimen significantly increased if the test length became small. Further the interaction relation will be influenced by the eccentricity of prestress; however the proposed curves were independent of eccentricity. Also the magnitude of the failure bending moment was taken as that relating to a section adjacent to the loading bracket in the test zone. Bishara used the following empirical expression to compute the pure torsional strength to establish his interaction curves

$$T_{uo} = 10\beta_1 V_p \sqrt{(f'_c + 12\sigma_p)} + 1.6\, x_1 y_1 A_t f_{ty}/s \qquad (2.31)$$

where T_{uo} = ultimate pure torsional strength of a prestressed concrete rectangular, I or T section member

V_p = volume of plastic membrane on section having unit slope

In the above expression the contribution of stirrups was added to the torsional resistance of plain prestressed concrete beam estimated by the plastic theory. The correlation between Zia's (1961) pure torsion test results and those computed by this equation was shown to be good. However, Henry and Zia (1971) showed that it grossly overestimated the pure torque capacity of Gangarao's (1970) beams.

Zia (1961) found that the ultimate strength of reinforced and prestressed concrete rectangular and T sections without web reinforcement under torsion was the same as the cracking strength, computed using the elastic theory of torsion, and the modified Cowan failure theory. However, for I section beams the ultimate strength was substantially different from the cracking strength; this was attributed to the redistribution of stress and transformation of the load resisting mechanism, discussed already. The ultimate strength of reinforced and prestressed members with web reinforcement was taken as the strength of that member without web reinforcement, to which the strength contribution of web reinforcement was added. The torsional strength of web reinforcement was estimated using the proposal of Cowan, referred to earlier in this section. In addition Zia tested three types of sections, which were non-prestressed. For such beams, the presence of web steel increased only the ductility but not the strength. He reasoned that this was due to the location of longi-

tudinal bars at the corners of narrow stirrups where stresses were low. Thus there was no longitudinal steel at highly stressed regions to resist the horizontal component of diagonal tension. His argument may not be completely valid as cracking terminates the elastic distribution of stress. However he reported that in prestressed beams, except for one series of T beams, the stirrups yielded resulting in their full contribution to the strength. He explained that though in prestressed beams the longitudinal bars were at the corners of the stirrups as in the non-prestressed specimens. the horizontal component of diagonal tension was resisted by the strands. In Zia's computation of ultimate strength of web reinforced specimens conrete contribution is equal to the cracking strength of the plain specimen, however, in the ACI method based on a similar hypothesis this contribution is only 40 percent of the cracking strength. His beams had web reinforcement equal to about 1.5 percent of the volume of core enclosed within the stirrup. It was observed that the web reinforcement did not influence the elastic torsional behavior of the member, but enabled the specimen to fail gradually developing a good amount of ductility. Spacing of stirrups was recommended at not more than 0.4 times the depth of the member.

Gausel (1970) described tests on 16 eccentrically prestressed I section beams. One half of each beam was provided with web reinforcement and the other half was not. Thus 32 tests were performed. The beams were subjected to differing transverse loads and then gradually increasing torque. Eight beams were tested under torsion and bending and the remainder had additionally shear. Only one beam was tested in pure torsion. In several of these beams, the amount of web rein-

forcement used was very small. In some beams the one half portions of the beam having web steel failed at a lower torque than the other half without web steel for which Gausel could not give any explanation. However, he observed that the web reinforcement used had no effect on the torsional strength of beams tested under torsion, bending and shear. Even a small amount of web reinforcement resulted in increases in ductility and prevented an explosive failure. It was noted that the sequence of loading did not have any effect on the ultimate strength, an observation [illegible] by Pandit and Warwaruk (1965).

Beams were divided into three groups for the purpose of analysis. The first group related to beams which developed little or no cracking under pure torsion or torsion and bending. The ultimate strength of these beams was calculated as the sum of the cracking strength and the contribution from stirrups; the former being estimated by the plastic theory and the latter by Hsu's equation.

$$T_{uo} = T_o + T_{stirrup} \qquad (2.32)$$

where $T_o = 2V f_t' \sqrt{(1 + \sigma_p/f_t')}$

$T_{stirrup} = (0.66m + 0.33\, y_1/x_1)\, A_t\, x_1 y_1\, f_{ty}/s$

$m = 1$

V = volume of sand heap with unit slope

f_t' = tensile strength taken equal to split tensile strength

Though the prestress was eccentric, σ_p was taken as the average prestress. In I beams Zia (1961) and Gausel considered the full contribution of concrete strength, while Wyss et al (1969) took into account

only a fraction of it (about 40 percent) and increased the lever arm of the stirrups, in estimating the ultimate strength. Gausel assumed that stirrups contributed only to the torsional strength but not to other strengths.

The second group consisted of beams under torsion, bending, and shear with minor cracking. Gausel found that the principal stress criteria gave poor correlation with test values and the following straight line interaction was suggested.

$$\frac{T_u}{T_{uo}} + 0.3 \frac{M_u}{M_{uo}} = 1 \qquad (2.33)$$

The third group consisted of beams subjected to torsion and bending or torsion, bending and shear with large flexure-shear cracking; the analysis was based on the shear failure theory of Walther, assuming uniform distribution of normal, and flexural stresses over the compression zone, and torsional shear stress over the whole cross-section. For torsion-bending a nearly rectangular interaction diagram and for torsion, bending and shear a circular interaction diagram were proposed. The rectangular interaction relationship was checked by Gardner's (1960) unstirruped beams.

In a study of torsional strength of eccentrically prestressed concrete bridge girders, Wyss, Garland and Mattock (1969) tested eighteen full scale I section girders and six rectangular section members with web reinforcement. The principal variables were level of prestress (average prestress 0, 530, 1150 psi) and amount of web reinforcement. I section girders were divided into three groups.

One group did not have any prestress and the other two had two levels of prestress. Within each group the level of prestress was constant and the girders were provided with varying amounts of web reinforcements ranging from 2 in spacing of stirrups to no stirrups. Rectangular members had the same height, width of web, and web reinforcement as the I-section girders and served the purpose of comparison. For a given amount of web steel, longitudinal reinforcement in the form of straight deformed bars was designed by the following equation suggested by Hsu (1967).

$$A_\ell = 2 \frac{(x_1+y_1)}{s} A_t - \frac{F}{f_{ty}} \qquad (2.34)$$

where F = effective prestress

A_ℓ = total area of longitudinal reinforcement to resist torsion

This equation implies equal volumes of longitudinal and transverse reinforcements and that the initial prestress in the tendons provided the force that would otherwise have been supplied by the longitudinal torsional reinforcement. By this scheme some girders did not require any longitudinal torsional reinforcement. For I sections the web reinforcement was made up of two separate vertical legs and two horizontal bars across the full width of the flanges.

They observed that the initial torsional stiffness up to torques less than 80 percent of cracking torques was linear. It was taken as the average slope of the linear part of the torque-twist curve and was found to be in reasonable agreement with that calcu-

lated using elastic theory. They further observed that the initial torsional stiffness increased with the level of prestress but it was unaffected by the amount of web reinforcement. The eccentricity of prestress resulted in progressive cracking and because of this the reduction in torsional stiffness at torques slightly above the cracking torque was not as abrupt as in the case of reinforced girders. However further slight increases in torque caused large reductions in stiffness. As the level of prestress increased, the torsional ductility reduced.

The basic mode of failure for all the I girders was observed to be skew bending. They stated that the skew bending axis was probably inside the web, close to one of its faces. But the Russian investigators Gvozdev, Lessig, and Rulle (1968) proposed that the skew bending axis was close to one of the side faces of the flanges. Wyss et al ruled out the possibility of location of the neutral axis as suggested by Gvozdev et al. They asserted:

(a) The critical crack in the web did not penetrate the full thickness of the web and was not visible on the compression side of the girder as shown in Fig. 2.2.

(b) Shear compression forces developed near the inside faces of the flanges but the compression distress in flanges was never oriented as postulated by Gvozdev et al.

(c) If the neutral axis were located as hypothesized by Gvozdev et al, the internal lever arm of the stirrup forces increased very much resulting in gross over estimates of strengths.

Hsu (1967) proposed the following equation for calculating

ultimate torsional strength of concentrically prestressed rectangular section beams.

$$T_{uo} = T_c + \Omega \frac{A_t x_1 y_1 f_{ty}}{s} \qquad (2.35)$$

where $$T_c = \frac{x^2 y}{\sqrt{x}} 2.4\sqrt{f'_c} \left[2.5\sqrt{\left(1 + \frac{10\sigma_p}{f'_c}\right)} - 1.5\right]$$

$$\Omega = 0.66 + 0.33\, y_1/x_1 \leq 1.5$$

where x = width of a rectangular section

y = depth of a rectangular section

Hsu's equation (2.35) was found consistently to underestimate the strength of eccentrically prestressed I section members. Wyss et al modified this equation by increasing the lever arm of stirrup forces from x_1 to $(x_1+b_w)/2$ and arrived at the following equation.

$$T_{uo} = T_c + \frac{(x_1+b_w)}{2} \frac{y_1}{s} f_{ty} \qquad (2.36)$$

where $$T_c = \frac{x^2 y}{\sqrt{x}} 2.4\sqrt{f'_c} \left(2.5\sqrt{\left(1 + \frac{10\sigma_p}{f'_c}\right)} - 1.5\right)$$

x = width of a rectangular section

y = depth of a rectangular section

The ultimate capacity was limited to

$$T_{uo(max)} = 14\sqrt{f'_c}\, \frac{x^2 y}{3}$$

In deriving the equation (2.36), the prestress was assumed to affect only the contribution of concrete to torque, T_c. As in reinforced concrete, the value of T_c was less than the cracking torque. But Chander, Kemp, and Wilhelm (1970) observed that the level of prestress influenced the reinforcement factor. However the equation was very well substantiated by test results of their girders.

The minimum reinforcement necessary to develop strengths greater than cracking torque, for the girders was obtained using the equation shown below derived for rectangular concrete beams.

$$\frac{A_t}{s} = \frac{125\ xy}{f_{ty}(x_1+y_1)} \qquad (2.37)$$

where x = width of a rectangular section

y = depth of a rectangular section

It was stated that the presence of prestress or the flanges in these beams did not appear to change the minimum reinforcement requirement The maximum stirrup spacing was not found to be controlled by the web thickness. To limit crack widths it was recommended that stirrup spacing should be less than one-half of the flange width or one and one-half times the web width, whichever was greater. The form of web reinforcement used in their I section girders was found to be adequate in lieu of closed rectangular stirrups.

A beam of given dimensions can be provided with flexural reinforcement as specified by ACI to resist a given moment. A beam of identical dimensions can be designed in an under-reinforced way

with certain transverse reinforcement and corresponding longitudinal torsional reinforcement to resist a particular pure torque. If the beam is provided with a total reinforcement corresponding to pure moment and pure torque, it is reasonable to expect the beam to fail in an under-reinforced way developing simultaneously a bending moment equal to pure moment capacity and a torque equal to pure torsional capacity. This was possible in reinforced concrete beams (Osburn et al 1969). ACI permits this approach and the longitudinal reinforcement can be designed independently for bending and torsion and added in a combined loading case resulting in a nearly rectangular interaction relationship.

In the second part of the investigation consisting of eleven girders divided into three series Wyss and Mattock (1971) examined the possibility of a rectangular interaction relationship between torsion and bending, of eccentrically prestressed I girders. The six specimens of the first series were provided with #4 stirrups at 9 in. centers and the four specimens of the second series at 6 in. centers. The eleventh girder together with two others constituted the third series and contained only longitudinal reinforcement without transverse and unprestressed reinforcement. Girders within each series differed only in the unprestressed longitudinal steel. One in each series was tested to obtain the pure torsional strength. One girder furnished the pure flexural strength for all the series. The remaining girders of the three series were subjected to combined torsion and bending in a ratio of approximately that of pure torsional strength to pure flexural strength.

The girders under combined loading failed in a over-reinforced manner without developing either the pure torsional strength or the pure flexural strength. Thus the rectangular interaction could not be obtained. They observed that the torsionally induced cracking tended to split off the overhanging parts of the flange restricting the effective compression zone to web only and sufficient compression could not be mobi ed to produce the yield force in the reinforcement. However it may be pointed out here that the prestressed beams of Gangarao and Zia when augmented with unprestressed longitudinal reinforcement developed rectangular interaction between bending and torsion. The test specimens of Wyss and Mattock were concentrated in one region of an interaction diagram and were very closely represented by the interaction relationship proposed by Mukherjee and Warwaruk (1970).

2.2.6 Space Truss Theory

The behavior of reinforced concrete beams under torsion differs considerably before and after cracking. Hsu (1968d, 1968e) and Lampert and Thurlimann (1968) showed experimentally that hollow beams developed initial cracks at a smaller torque than the corresponding solid beams of the same size and concrete strength. This can be easily explained by the contribution of the concrete in the core to the cracking torque. Their tests also showed that the ultimate torques were the same for hollow and solid beams. This is probably due to the fact that at failure the concrete core is penetrated by cracks. Lampert and Thurlimann found that in the advanced post cracking stage solid and hollow beams had the same deformations and the same stresses. Hence Lampert et al concluded that due to the elongation of the stirrups an outer

comparatively thin concrete supporting shell was formed which alone carried the load i.e. the strength depended only on the reinforcing cage. The remaining core did not contribute materially to the ultimate strength. Because of this, in their theoretical study of the space truss, equally reinforced solid rectangular sections were considered equivalent to fictitious thin walled box sections .

Based on their tests carried out on beams with square cross-section of 20 x 20 in., Lampert and Thurlimann confirmed the general validity of simple truss theory of Rausch and improved upon it. Their space truss model consists of longitudinal reinforcement which is assumed to be concentrated into stringers at the corners and intermediate shear walls. Stirrups act as posts in these shear walls and the concrete between the inclined cracks provides the compression diagonals. All the reinforcement is assumed to yield at ultimate. The concrete compression diagonals are necessary for equilibrium only; concrete does not provide any additional contribution to the torsional resistance. Lampert et al found from tests that the crack angle, θ, depended on the ratio of transverse to longitudinal reinforcement amounts. The inclination of the inclined cracks and hence the inclination of the concrete compression diagonals changed in spite of existing cracks to accommodate a redistribution of the forces between the longitudinal and transverse reinforcements especially after yielding of one part of reinforcement unlike in simple truss theory. It is interesting to note here that Hsu's surface of failure does not depend on the amounts of reinforcement but is a plane perpendicular to the wider face and inclined at 45° to the axis of the beam. In reinforced concrete investi-

gators using the Lessig-type skew bending theory obtained the crack angle by minimizing the expression for torque which was a function of amount of stirrups and of longitudinal steel. Others working with prestressed concrete arrived at this angle from the stress situation at cracking.

Lampert et al used the location of longitudinal bars to determine the cross-sectional dimensions of the failure model because they observed that the diagonal forces in the shear walls were deflected into the adjacent wall by the longitudinal corner bars. The lengths of the moment lever arms corresponded to the distances between the longitudinal bars in their theory. Other theories assumed the centerlines of the stirrups, x_1, Y_1, as the lengths of the moment lever arms. In fact these lever arms depend on the depth of the compression zone. The former assumption is more conservative. However Elfgren (1972), and Kuyt (1971) working with the truss model used the latter assumption. This difference is significant for the small cross-sections commonly used in testing. Rational determination of the cross-sectional dimensions of the failure model is difficult because of the complex situation existing at the corners of the beam.

For solid sections Lampert et al suggested a wall thickness, t, for the corresponding hollow beam to be h/6 or $h_o/5$ whichever was smaller. In space truss theory the strength of under-reinforced beams is independent of the wall thickness and a nominal wall thickness is needed only to check the possibility of an over-reinforced failure. Some investigators and codes such as the ACI 318-71 have assumed that the concrete contributes to the torsional strength due to the fact that torsion is

considered similar to shear. However Leonhardt (1970) has argued that in torsion there are no favourable effects such as the shear carrying capacity of the compression zone or the flat inclination of the compression struts. The aggregate interlock does not come into play as the torsional cracks open perpendicular to the crack inclination. In this respect torsion is more analogous to flexure rather than shear. For flexure no theory is proposed for the independent contribution of concrete to the strength of the beam.

The function of the longitudinal reinforcement is mainly to the horizontal component of the diagonal tension i.e. to satisfy ilibrium. For this purpose the longitudinal steel need not be t the corners. The longitudinal steel located in the center of ion such as prestressing steel is suggested by Lampert et be effective. However to anchor the concrete diagonals and to prevent a push-out of the diagonals (Mitchell et al, 1971) longitudinal reinforcement in the corners is stated necessary. But based on certain test observations concerning ductility and brittleness of failure McGee and Zia (1973) have recommended that the prestressing tendons may not be considered effective as longitudinal torsion reinforcement.

The space truss model for rectangular hollow cross-section is shown in Fig. 2.3. The following expression was obtained for the pure torsional strength of a symmetrically reinforced beam.

$$T_{uo} = 2b_o h_o \sqrt{\frac{A_L f_{my} A_t f_{ty}}{2(b_o+h_o)s}} \qquad (2.38)$$

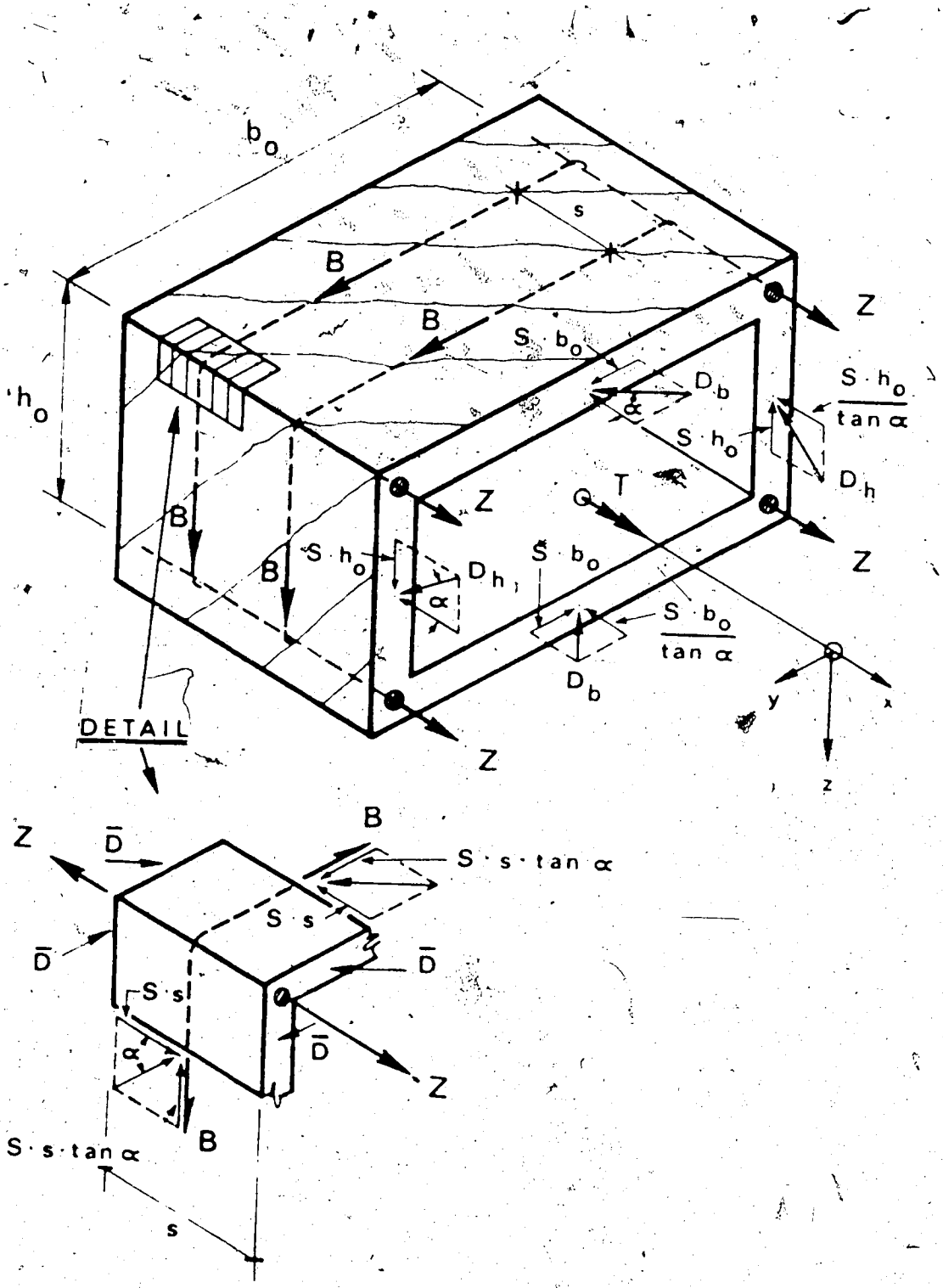

FIG. 2.3 SPACE TRUSS MODEL FOR PURE TORSION

where A_L = area of one longitudinal mild steel bar

f_{my} = yield force of longitudinal mild steel bar

The angle between the concrete diagonal and the beam axis, α, was given by

$$\tan^2\alpha = \frac{A_t f_{ty}\, 2\,(b_o+h_o)}{s\Sigma\, A_L\, f_{my}} \qquad (2.39)$$

An unsymmetrically reinforced section could be replaced by a symmetrically reinforced section having the longitudinal steel with the lowest yield force on all sides since failure was governed by yielding of the weakest longitudinal bar.

The space truss model for pure torsion was extended to beams subjected to torsion and bending taking into account the differing forces in the top and bottom longitudinal reinforcement. Lampert and Thurlimann (1969) used the same torsion lever arm, h_o, for the pure bending capacity of a section instead of the flexural lever arm. However recently Collins and Lampert (1971) suggested that the skew bending theory developed by Collins (1969) be used for computing the pure bending capacity of a section since it contains flexural lever arm, Jd.

Leonhardt (1970) observed that if the longitudinal reinforcements required individually for torsion and bending were superimposed, the resulting interaction diagram between torsion and bending was rectangular apart from a small section in the outer corner.

Tests aimed at web compression failure showed that the concrete compression struts failed at a lower nominal torsional shear stress

than in flexural shear. Lampert and Thurlimann attributed this to the warping of the initially plane walls of the hollow box beams into hyperbolic paraboloids. This caused eccentric stressing of compression struts forcing failure sooner than in flexural shear where the web remained plane. Hence in torsion and torsion and shear lower values are to be permitted for the upper limit of shear stress than in flexural shear.

Kuyt (1971) showed that the space truss theory and Lessig's skew bending theory (Ultimate Equilibrium Method) were not each others antipoles but on the contrary would yield the same results if certain assumptions were made. He pointed out that the skew bending theory considered the equilibrium in a possible failure surface, provided no information with respect to failure surface or steel stresses in the several parts of the reinforcement crossing the failure surface. Kuyt preferred the space truss theory because it was on a more definite basis with regard to the internal equilibrium of the beam as a whole. He differentiated between beams with longitudinal bars concentrated in the corners and beams with these bars distributed along the four sides and stated that the assumption that all the steel crossing the failure crack was valid only in the latter kind of beams. It was also pointed out by him that for the beams with the longitudinal bars at the corners only, the assumptions that the inclination of the failure crack was the same on each side of the beam and that the stresses in the stirrups crossing the failure surface were of the same magnitude, were invalid.

Based on a truss model for combined torsion, bending and shear Kuyt (1972) established equilibrium for each one of the sides of

the beam; but this results in the violation of compatibility of the failure mechanism.

Lampert, Luchinger and Thurlimann (1971) extended the space truss theory to cover prestressed beams. They carried out tests on two 20 in. square, pretensioned beams with stirrups. Of the two, one beam was solid, concentrically stressed and tested in pure torsion while the other was hollow eccentrically stressed and tested in combined torsion and bending. They found that there was no basic difference between reinforced and prestressed beams with regard to ultimate strength and concluded that the space truss theory was applicable to prestressed beams if the initial prestress in the tendons was at the usual level and the strands yielded after a load-induced stress nearly equal to the yield stress of the mild steel. It was shown by them that a prestressed and an unprestressed beam of about equal longitudinal yield force subjected to torsion and bending exhibited the same ultimate moment and angle of twist at yield. The strands are to be bonded to the concrete for the space truss theory to apply.

Woodhead and McMullen (1972) found from their test results that the truss theory was far more conservative than a design procedure based on the ACI code (318-71) requirements for reinforced conrete since the truss theory neglected the concrete contribution to the torsional strength.

Lampert (1971) stated that the space truss theory was valid for solid and hollow reinforced and prestressed concrete beams of general shape subjected to torsion, bending and axial force, provided the longitudinal and transverse reinforcement yielded at failure and the St. Venant

torsion was predominant. From his study of a general cross-section he found that in the collapse mechanism of such a section except the two longitudinal bars defining the compression hinge at failure, all transverse and longitudinal reinforcement should yield.

In a recent paper Lampert and Collins (1972) have contended that the problem of torsion and bending is basically solved. They suggest that space truss theory furnishes a rational accurate and well verified model to predict the pure torsional strength. The second step necessary for the design of torsion and bending is the interaction relationship between torsion and bending. It has been shown by them that both skew bending and space truss theories are in close agreement and predict the same parabolic interaction between the torsional and flexural strengths. If torsion is predominant there is a truss-like behavior up to failure as in pure torsion. If bending dominates the behavior is similar to that in pure bending except that the compression zone is inclined. When space truss theory is extended to combined torsion and bending the flexural capacity predicted by the space truss theory deviates from the conventional flexural strength of the beam as this theory uses the torsional lever arm, b_o, in the whole range of torsion-bending interaction. Similarly skew bending theory uses the flexural lever arm, though in space truss theory it should change to torsional lever arm for strength predictions near the torsion axis of the interaction diagram. Lampert and Collins for design suggested equal volume of longitudinal and stirrup steel as has been suggested and used by others. The longitudinal reinforcements required individually for torsion and bending are to be superimposed. Lampert and Collins allowed

for a reduction in the torsional longitudinal reinforcement in the flexural compression zone due to the presence of flexural compression. In the case of continuous beams reduction of longitudinal reinforcement as a result of presence of flexural compression may be only slight since reinforcement for anchorage in the vicinity of inflection points must still be provided and would exist in the compression regions.

CHAPTER III

ANALYSIS OF CRACKING STRENGTH

3.1 Introduction

This chapter deals with the development of equations for the cracking strength of prestressed Concrete I beams subjected to combined torsion bending and shear. Two methods of cracking analysis are presented here. The first is based on the classical theories and the second is concerned with the finite element method using three dimensional hexahedron elements. The inclination of the initial crack obtained from the cracking strength analysis by Method 1 is used in the ultimate strength analysis in defining the symmetric skewed failure surface. The experimental cracking strength is defined to correspond to that load which causes initial visible cracks on the surface of the beam.

3.2 Method 1

3.2.1 Assumptions of Analysis

The following assumptions are made in developing the equations for predicting the cracking torque of prestressed concrete I beams.

1. The torsional shear stresses are distributed on the cross section according to plastic theory.

2. The flexural shear stresses and the flexural normal stresses are distributed according to elastic theory.

3. Cracking initiates when the maximum principal tensile stress equals the tensile strength of concrete.

4. The transformed area of steel is taken into account in the calculation of section properties.

5. The stresses in the steel due to the applied loads are negligible prior to the formation of the initial crack.

Nylander (1945) was probably the first to recognize that the maximum principal tensile stresses computed using the elastic theory in the case of beams subjected to torsion, were much different from the usual tensile strength of the concrete. He proposed that the torsional shear stresses be assumed in accordance with the plastic theory. This approach has been preferred by Kemp, Wyss and Mattock.

According to assumption 1, the torsional shear stress is computed considering full plastification of the section. On the cross section of a bar under torsion, as the shear stress reaches the yield strength of the material at any point, there the two orthogonal components of the shear stress τ_x and τ_y have to satisfy the condition of plasticity and equilibrium (Nadai, 1950).

$$\tau_x^2 + \tau_y^2 = K^2 \tag{3.1}$$

where K is a constant

$$\frac{\partial \tau_x}{\partial x} + \frac{\partial \tau_y}{\partial y} = 0 \tag{3.2}$$

Expressing the shear stress components in terms of a stress function F(x,y)

$$\tau_x = \frac{\partial F}{\partial y} \text{ and } \tau_y = -\frac{\partial F}{\partial x}$$

the condition of plasticity can be given as

$$\left(\frac{\partial F}{\partial x}\right)^2 + \left(\frac{\partial F}{\partial y}\right)^2 = K^2 \qquad (3.3)$$

The plastic stress function F(x,y) represents the sloping plastic stress area and K is the steepest slope of this area. From Nadai's sand heap analogy, the plastic stress function at any point is proportional to the height of the sand heap at the corresponding point and the uniform plastic shear stress is proportional to the slope of the sand heap. The applied plastic torque is proportional to the volume of the sand heap. The ideal sand heap covering the plastified section of the I beams tested in the present investigation is shown in Fig. 3.1. Using unit slope the volume of this sand heap varied from 34 to 35.5 in^3 for various nominally identical beams.

The stress distribution due to all other forces acting on the beam is determined using elastic theory.

3.2.2 Theories of Failure for Concrete

Cracking of concrete under combined loadings will occur under a complex state of stress. This of course is the case with crushing also under such loading. Quite often the stress condition

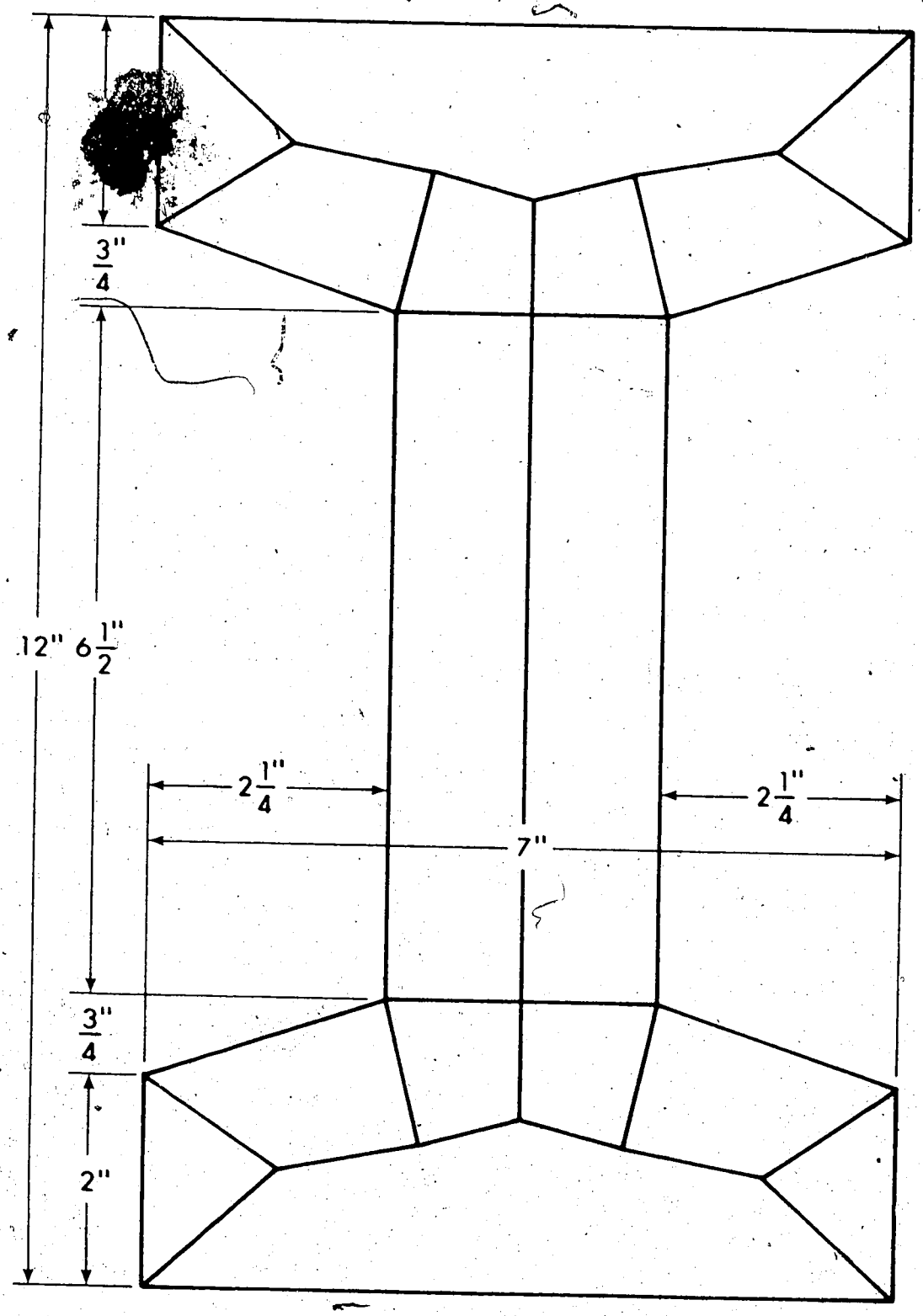

FIG. 3.1 IDEAL SAND HEAP COVERING PLASTIFIED SECTION

in a structural member is idealized to a biaxial state of stress assuming the stress in the third direction equal to zero. Various strength theories have been proposed in the past to determine the failure of structural materials. Of these, Mohr's theory of failure is the most appropriate for a brittle material like concrete. Various stress conditions in a concrete differential element can be represented by Mohr's circles. A failure envelope can then be obtained by joining all those Mohr's circles that represent failure conditions. Such a failure envelope has to be established for given material based on tests under combined stress conditions but this is not easy. Because of this, different theoretical shapes of this failure envelope have been proposed using simplifying assumptions.

The commonly used failure hypothesis in torsion studies are shown in Fig. 3.2. Rankine's principal stress theory assumes that failure is attained as soon as the magnitude of the principal stress reaches the strength of concrete in uniaxial compression or tension. The failure envelope on the Mohr's diagram consists of a pair of straight lines parallel to the shear stress axis. Coulomb's internal friction theory implies that failure occurs by sliding along a certain plane and the resistance to failure is composed of a constant shearing strength and an internal friction proportional to the normal stress on the sliding plane. The failure envelope consists of a pair of straight lines tangent to the pure shear and compression circles. Mohr generalized Coulomb's internal friction theory and assumed that the resistance to sliding is a function of the normal stress on the sliding plane.

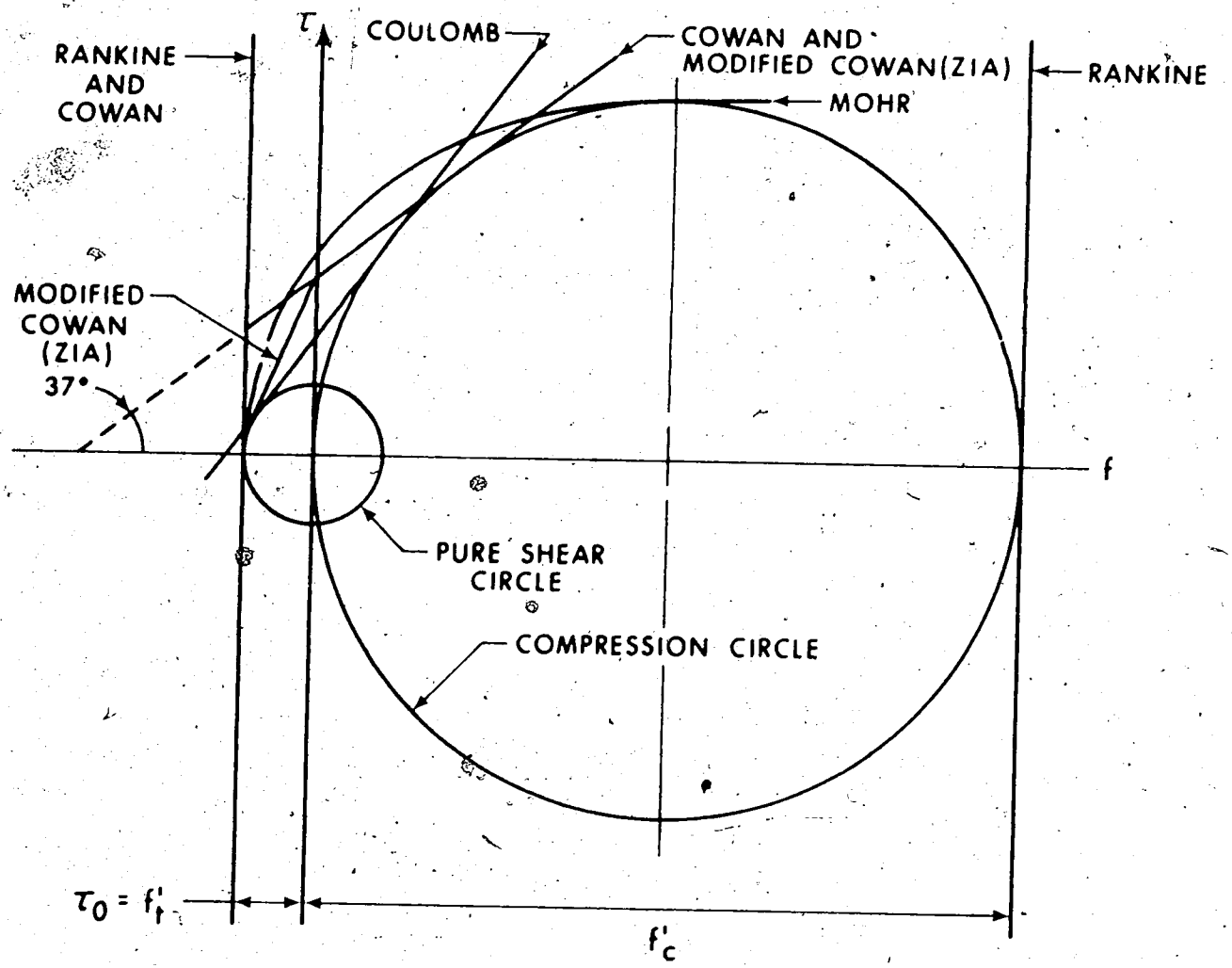

FIG. 3.2 FAILURE THEORIES OF CONCRETE UNDER BIAXIAL STRESSES

The resulting failure envelope is curvilinear, the shape of which is to be determined by tests. Cowan's theory is based on a dual criterion of failure. He combined Rankine's maximum stress theory and Coulomb's internal friction theory; the former for cleavage failure and the later for shear fracture. Zia's modification to Cowan's failure theory is aimed at a closer approximation to the Mohr's generalized internal friction theory. The modification predicts the failure of concrete transitional from tension failure to shear compression failure. Failure theories for concrete subjected to combined stresses have been discussed in the literature (Bresler and Pister 1955, Zia 1961 and 1968). It is to be noted that the difference between these theories is greater when the compression (prestress) is high in which case failure is likely to be governed by principal compressive stress rather than the principal tensile stress. But when the prestress is of the order of 0.5 f'_c which is more practical and about the maximum permitted by the ACI the theories due to Rankine and Cowan are identical and modified Cowan theory differs by a maximum of only about 12 percent.

None of the above mentioned theories consider the effect of the intermediate principal stress and the strain gradient. It has been suggested by several investigators that the effect of the intermediate principal stress is significant in failure theories for concrete subjected to complex three dimensional states of stress. Bresler and Pister (1958), Seth (1958) McHenry and Karni (1958) have proposed failure theories taking into account all the principal stresses. In many cases such as in relatively slender beams, it is

considered accurate enough to use a failure criteria based on biaxial stress condition. It is interesting to note that in the three dimensional finite element analysis of cracking strength presented later in this dissertation, the intermediate principal stress under combined loading was negligibly small. Hence it can be concluded that the intermediate principal stress can be safely neglected in such studies.

Further, the above theories do not consider the effect of strain gradient. For example, in the thin web of an I section the strain gradient is very high. However, it is small in a hollow concrete beam.

Recently Kupfer, Hilsdorf, and Rusch (1969) investigated experimentally the biaxial strength concrete over the entire range of biaxial stress combinations. They used square concrete plates (7.9 x 7.9 x 2 in.) subjected to an in-plane loading. Historically in tests on concrete under biaxial tension and compression hollow cylinders subjected to either torsion and axial compression or to internal hydraulic pressure and axial compression were used. For such stress states the test data from various investigations do not deviate from each other considerably. However, in biaxial compression tests the friction between the bearing platens and the specimens was sufficiently large to yield strengths of unusal magnitudes; for the case of equal compressive stresses in both principal directions the resulting strengths reported were in the range of 80 to 350 percent of the uniaxial compression strength for identical test specimens. Kupfer et al replaced the usual solid bearing platens by "brush bearing platens"

which were flexible enough to follow the concrete deformations without causing appreciable restraint of the test specimens. They concluded contrary to the previous investigations that the maximum strength increase under biaxial compression was only 27 percent in excess of the uniaxial compression strength. Their tests in the region of combined compression and tension corroborate the findings of other investigators; i.e. stress at failure decreases as the simultaneously acting tensile stress is increased. The strength of concrete under biaxial tension is approximately equal to its uniaxial tensile strength.

3.2.3 Tensile Strength of Concrete

It is evident from the literature review that the tensile strengths used in torsion research by various investigators deviate from each other significantly for the following reasons.

The tensile strength of concrete depends mainly on the state of stress at a point and also on the strain gradient. Beams acted on by combined loadings are subject to widely varying combined stress conditions; and different strain gradient Further, concrete is not a perfectly elastic material.

Each method of test available for evaluating the tensile strength of concrete has a certain stress situation associated with it. For example in the direct tensile test, there is a uniform stress along only one axis without any strain gradient. This is the only test which does not use any assumptions of elasticity or plasti-

city to calculate tensile stress. In the flexure test, tensile stresses are along one axis only with no stresses on the orthogonal planes; but there is a strain gradient. The splitting tensile strength test is characterized by a stress system which varies from biaxial compression immediately beneath the packing material to compression-tension over the most part of the diameter. The magnitude of the compressive stress varies and is about three times the magnitude of the tensile stress. The magnitude and sign of the third principal stress along the longitudinal axis is unknown. The measured strength may correspond to a complex function of the strength under the multiaxial stress system.

Each investigator presumably chose a tensile test having a stress distribution which was nearer to the stress condition in his test beams under combined loading though it may not necessarily be satisfactory for all combinations of loadings.

To predict cracking strength by method 1, the tensile strength of concrete taken in the present investigation, is equal to splitting tensile strength. It is believed that this tensile strength represents qualitatively the biaxial stress condition of compression-tension encountered in beams subject to combined loading. The relationship between splitting tensile and compressive strengths for each beam is shown in Fig. 3.3. For each beam the concrete compressive strength is obtained as the average of three cylinder tests and the tensile strength as the average of two split cylinder tests. The visually best fit line through the data yields a value of $6\sqrt{f'_c}$ for the splitting tensile strength of concrete; this value is adopted in the cracking analysis of method 1.

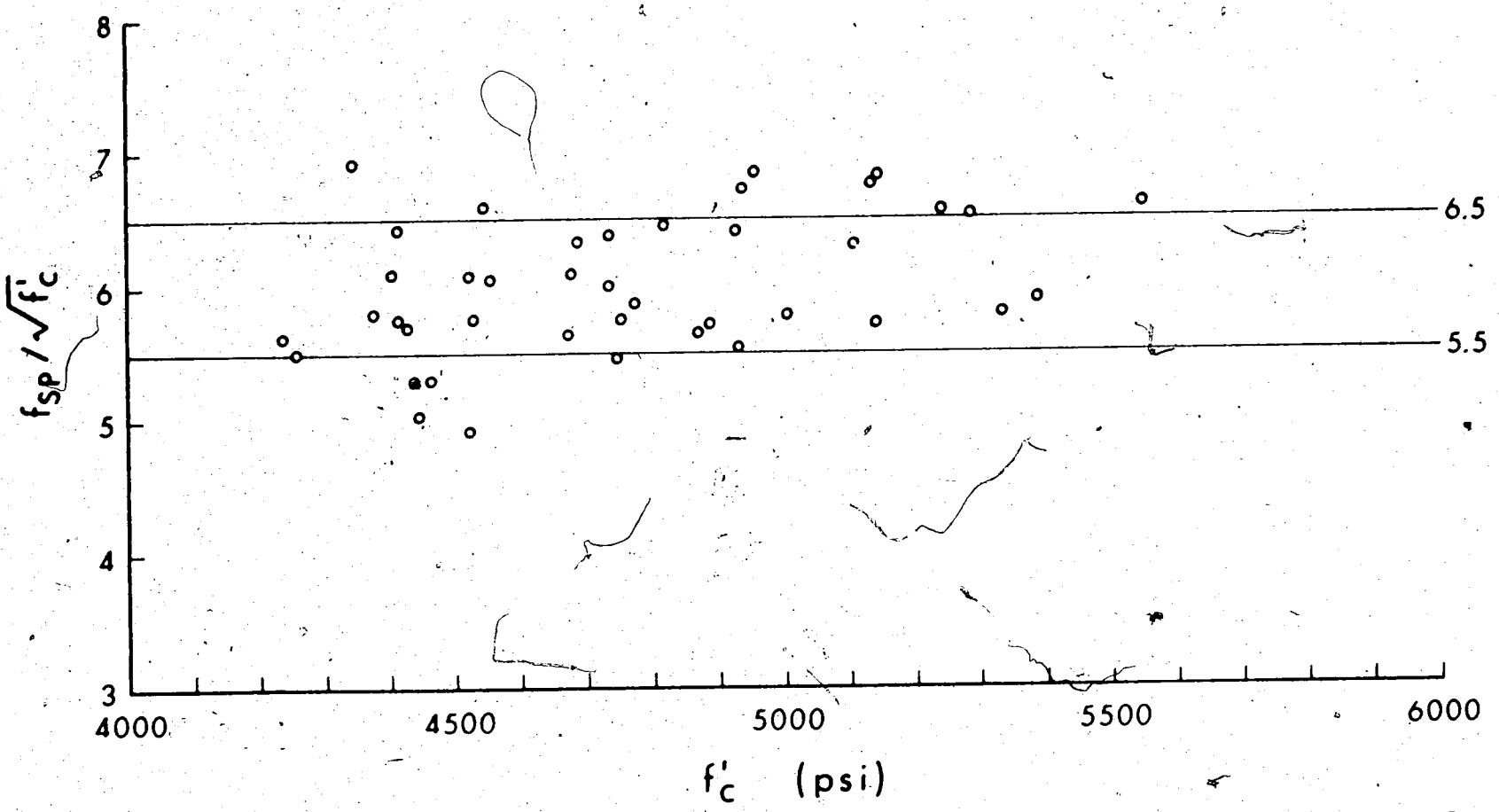

FIG. 3.3 RELATION BETWEEN SPLITTING TENSILE STRENGTH AND COMPRESSIVE STRENGTH OF CONCRETE CYLINDERS

3.2.4 Analysis

The stress components causing the initial crack at any location can be calculated as follows. Tensile stresses are considered positive. The distributions of these stresses are shown in Fig. 3.4.

1. Shear stress due to torque

$$\tau_t = \frac{T}{2\ Vol} \tag{3.4}$$

2. Shear stress due to flexural shear

$$\tau_v = \frac{VQ}{Ib_z} \tag{3.5}$$

3. Normal stress due to prestress

At top face,

$$f_p = -\frac{F}{A} + \frac{FeY_t}{I} \tag{3.6}$$

At neutral axis,

$$f_p = -\frac{F}{A} \tag{3.7}$$

At bottom face,

$$f_p = -\frac{F}{A} - \frac{FeY_b}{I} \tag{3.8}$$

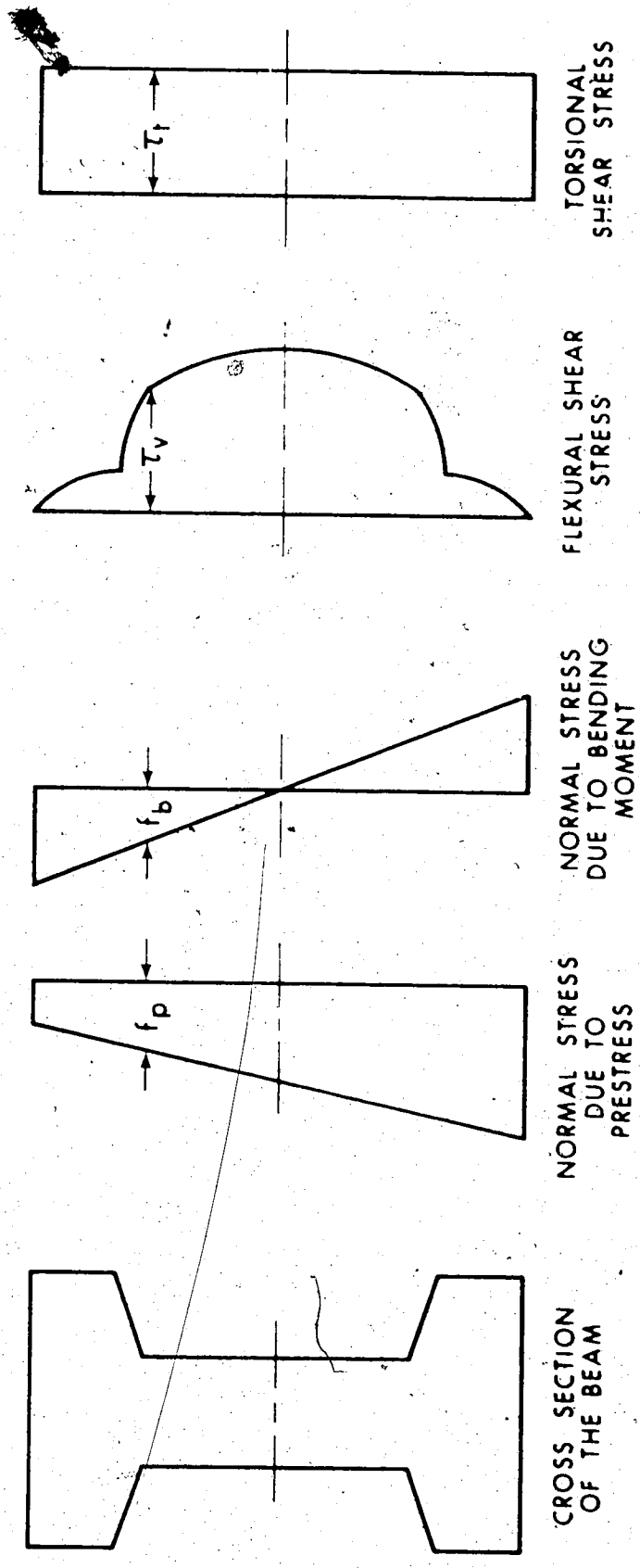

FIG. 3.4 STRESS DISTRIBUTION IN PRESTRESSED CONCRETE SECTION PRIOR TO CRACKING DUE TO VARIOUS FORCES

4. Normal stress due to flexural moment

At top face,

$$f_b = - \frac{MY_t}{I} \tag{3.9}$$

At neutral axis,

$$f_b = 0 \tag{3.10}$$

At bottom face,

$$f_b = \frac{MY_b}{I} \tag{3.11}$$

At diagonal tension cracking, the stress components are related as follows:

$$\tau_t + \tau_v = f'_t \sqrt{1 - \frac{(f_p + f_b)}{f'_t}} \tag{3.12}$$

where f'_t is the tensile strength of concrete equal to $6\sqrt{f'_c}$. Expressing equation (3.12) in terms of forces and ratios $\phi(= T/M)$, and $\delta(= T/Vb_w)$ yields

$$T_{cr}^2 \left[\frac{1}{2} N\phi l + \frac{Q}{\delta I b_z b_w}\right]^2 + \frac{f'_t y}{I} T_{cr} - f'_t (f'_t - f_p) = 0 \tag{3.13}$$

Solution of this quadratic equation yields the cracking

torque. The equation can be specialized for each of the following three critical locations.

1. Cracking at the top face,

$$T_{cr}^2\left[\frac{1}{2}/Vol\right]^2 - \frac{f_t' Y_t T_{cr}}{\psi I} - f_t'\left(f_t' + \frac{F}{A} - \frac{FeY_t}{I}\right] = 0 \qquad (3.14)$$

2. Cracking at neutral axis

$$T_{cr} = \frac{\overline{f_t'\,(f_t' + F/A)}}{\left(\frac{1}{2}/Vol + \frac{Q}{\delta I b_w^2}\right)} \qquad (3.15)$$

3. Cracking at bottom face

$$T_{cr}^2\left[\frac{1}{2}/Vol\right]^2 + \frac{f_t' Y_b T_{cr}}{\psi I} - f_t'\left(f_t' + \frac{F}{A} + \frac{FeY_b}{I}\right) = 0 \qquad (3.16)$$

Any other critical locations can be examined by substituting appropriate quantities in the equation (3.13).

The inclination of the initial tensile crack θ, with respect to the longitudinal axis can be obtained by the following equation

$$\tan(180-2\theta) = \frac{(\tau_t + \tau_v)}{(f_p + f_b)/2} \qquad (3.17)$$

solution of equations (3.14), (3.15) and (3.16) furnish three different values of torques and the cracking torque is chosen as the smallest of these three values.

3.3 Method 2

3.3.1 General Remarks

The finite element method has proved to be a convenient and versatile tool to aid in understanding the behavior of structural systems. It has been demonstrated in the past that this method can be applied with considerable success to various static and dynamic problems. Recently the method has been extended to include both material and geometric nonlinearities.

3.3.2 Finite Element Method

An attempt is made herein to predict by the finite element method, the cracking strength of reinforced and prestressed concrete beams under combined loading. Torsional cracking is a three dimensional phenomenon; accordingly the finite element model for such a study should be three dimensional. Clough (1969) compared various three dimensional elements in terms of their structural performance and computational efficiency, and recommended an eight node isoparametric hexahedron with 24 degrees of freedom for the analysis of elastic solids. These isoparametric elements are completely isotropic and can be fitted to quadrilaterally curved boundaries and were shown to be very effective finite elements. If the finite element system is analyzed by a displacement method of analysis to yield nodal point displacements and internal stresses, the models are stiffer in general. It was shown by him for this element, that any possible modification of the assumed interpolation functions would change the flexibility characteristics only to a small extent. Clough further showed that for structural

systems in which shear stresses are predominant the 8 node element is preferable to a 20 node refined element, but it is not very effective in representing plate bending behavior where shear stresses are low.

The three dimensional eight node solid element used in the program in this dissertation is based on the element developed by Irons and Zienkiewicz. In analyzing beams of usual proportions, the bending characteristics of this element are observed to be poor even at aspect ratios of the order of 2.5. Hence the element has been modified here by adding incompatible deformation modes as suggested by Wilson (1966); this improved the bending behavior of the element significantly. These deformation modes are eliminated at the element level by static condensation. The necessary integration for the element stiffness formulation cannot be done explicitly for this element and hence numerical integration is generally used. Two point Gauss quadrature is used in the present investigation. This gives exact values for rectangular prisms. Element stiffness formulation is skipped for identical elements. The structure stiffness matrix is generated in blocks and solved in blocks by direct Gaussian elimination. For solving the system of simultaneous equations an equation solver developed by Gopalakrishnayya (1973) is used in this program. The program developed herein can solve various load conditions with the stiffness matrix inversion made only once; which results in considerable economy of computation time. The facility of automatic nodal and element data generation has considerably reduced the input data.

The theoretical background, essential features and listing of the finite element program developed herein are presented in Appendix B. The analysis developed is an elastic analysis, and the basic assumption made is that concrete is homogeneous and perfectly elastic until the formation of an initial crack. Before crack formation the stresses in the steel induced by the applied loads are neglected. Cracking is considered to commence when the principal tensile stress equals the tensile strength of the concrete.

3.3.3 Elastic Constants and Tensile Strength of Concrete

For forming the modulus matrix, knowledge of the basic elastic constants of modulus of elasticity E_c and Poissons ratio ν of concrete is necessary. The modulus of elasticity of concrete is taken as $57{,}000 \sqrt{f'_c}$ in accordance with ACI 318-71. Poissons ratio is assumed as 0.15 or 0.16. It is to be noted that an error in the assumption for the values of E_c and ν affect only the deformations, not the stresses; in statically determinate structures such as the beams analyzed herein.

The tensile strength of concrete is taken as $7.5 \sqrt{f'_c}$ for the reasons listed below.

1. The finite element analysis at best is an elastic analysis. However the torsional shear stresses are distributed at least semi-plastically. Hence a higher value of tensile strength than the one assumed in method 1 is appropriate.

2. ACI 318-71 specifies modulus of rupture to be equal to $7.5 \sqrt{f'_c}$.

3. CEB suggests modulus of rupture as $9.5\sqrt{f'_c}$.

4. Woodhead and McMullen (1972) in their elastic analysis of prestressed rectangular beams for cracking used a value of $7\sqrt{f'_c}$. This value consistutes a lower bound to the values that would result from the equation (2.17) of Chander et al (1970) if the elastic theory and their equation were to give the same torque.

3.3.4 Finite Element Layout

Unfortunately three dimensional analyses demands very large computational effort, even for problems of very small size. Hence it is not surprising that a compromise must be achieved between the desirable accuracy and the computational time. The selection of the present finite element layout for rectangular beams in the literature and author's I beams was based on the experience gained by testing the program on similar smaller problems. It is believed that the mesh size in terms of bandwidth and number of equations used produces an adequate degree of accuracy without further increasing the already excessive computational effort. For the rectangular beams analyzed the maximum aspect ratio of the element varied from about 3 to 6, while in the case of I section beams it was 4. Outside the test zone slightly higher aspect ratios were used. The number of equations did not exceed 2500. With the usual solution techniques the computation effort is roughly proportional to the number of equations and to the square of the band width. The computations are performed in single precision for reasons of economy of memory and computational time. With large systems of equations round off starts to play an important role. This can be remedied significantly by doing the computations in double precision.

But this roughly doubles the core storage requirement. Another alternative is to keep the number of equations to the minimum possible which is adopted in the present case.

The general layout and discretization of the beams and the boundary conditions at either support are shown in Fig. B.2 and Fig. B.3. The beams were simply supported in the tests and the analysis was carried out accordingly. The right hand side support is torsionally restrained, allowing flexural rotation, and longitudinal translation. To achieve this all the nodes in the bottom face have displacements in all except the longitudinal direction equal to zero. All other nodes at this support have sideway displacements equal to zero because the cross section is torsionally restrained. The torsional load is applied at the left hand support and the nodes on this cross section are allowed to displace except the node at the centre of the cross section which is fixed in all directions. Both end sections of the test I beams of this investigation were made rectangular to facilitate easy gripping in the torsional heads. In the finite element analysis these were idealized as I section beams throughout the length for simplicity.

The boundary forces must be distributed exactly in the same fashion as the calculated stresses if the exact stress distribution is to be obtained throughout the member. If the distribution of these forces does not conform to the exact solution but still has the same statically equivalent system of forces, then the resulting stresses are significantly different only in the vicinity of the applied forces. Inspite of these local perturbations, the exact stress distribution

develops a short distance from the areas where the forces are applied. To have the correct stress distribution as near as possible to the loaded ends, the transverse, prestress, and torsional loads are applied at the nodes to reflect the exact stress distribution reasonably. Prestress was applied as external load. In the present case the stresses are in good agreement with the exact stresses at distances about one and one half times the depth of a beam or beyond the third cross-section from the ends of the beam. However, in each beam the end regions where the perturbations distort the stress distribution correspond to non-test zones which are of little interest in analysis.

3.3.5 Procedure of Analysis

In this method of analysis the input consists of a set of forces and the output in stress and strain distribution at every node and element face. As the cracking loads are known from tests before hand these loads are applied to obtain the stresses. This is not necessary in that any arbitrary set of loads in the same torque-shear proportion used in the test could be applied. The output consists of nodal deformations, the six components of stress and strain at the centers of element faces and average values at the nodes. It also includes, principal stresses, strains and their directions. From this the resulting stress and strain distributions associated with the applied cracking loads are obtained.

The loading combination for each beam test corresponds to a load vector consisting of transverse, prestress and torsional loads. If the beam geometry, material properties, and the boundary conditions

do not change and only the load vector changes, solutions for 10 to 12 load vectors or load combinations are obtained by inverting the stiffness matrix just once. It took 2132 seconds to get solution for the first problem, while for the remaining nine problems, the time required was 3946 seconds when ten problems with a band width of 150 and number of equations of 2340 were solved at a time.

3.3.6 Stresses

Once the stress distribution at the cracking loads is known, the maximum principal tensile stress is located in the test zone either at a node or centre of an element. Cracking is assumed to initiate at that point. The maximum principal tensile stress occurred in the bottom face if the bending moment was predominant, and in the web or in the top face if the amount of torsion was high. The location of this principal tensile stress agreed with the test location in most of the beams. The cracking starts when the maximum principal tensile stress occurring in the test zone equals the tensile strength of concrete. These principal stresses are presented for each beam in Table 7.1 and 7.3. From the nodal deformations, the flexural deflections, and the angle of twist in a certain span length are obtained.

The beams analyzed were subjected to various possible combinations of moments and forces. Of the resulting three principal stresses, the third was the tensile stress and related to the tensile strength of concrete. The first principal stress was usually compressive having varying degrees of magnitude. The intermediate principal stress was either compressive or tensile and had a magnitude of the order of 10 psi or less in all the beams.

This study has thus reinforced the possibility of neglecting the intermediate principal stress in determining the failure criteria of concrete for slender beams; because its magnitude is very small.

Cracking is assumed to occur when the maximum principal tensile stress equals the assumed tensile strength of the concrete. However in the theoretical computations the test cracking load may produce a tensile stress different from the assumed tensile strength. In such a case a different load will produce a tensile stress equal to the assumed tensile strength, which is taken to be the theoretical cracking load. This theoretical cracking load is computed eliminating the effect of prestress from the stress distribution obtained by the finite element analysis associated with the test load at cracking. In making this calculation it is assumed that the principle of superposition holds good and the location of the maximum principal tensile stress does not change. The equations used are given in Appendix B.

CHAPTER IV

ANALYSIS OF ULTIMATE STRENGTH

4.1 General Remarks

In this chapter equations are developed based on skew bending theory to predict the ultimate strength of prestressed concrete I section members subjected to torsion, bending and shear. The I section members tested by the author in the experimental phase of the program, failed generally in skew bending about an axis inclined to the longitudinal axis, either in Mode 1 or Mode 2. In mode 1 the compression zone formed on the top face while in Mode 2 it was observed inside the web close to one of its faces. Previously in Chapter II Mode 1 and Mode 2 were referred to as bending mode and torsion mode respectively. It is evident from the literature review that flanged beams failed mainly in the skew bending mode. To date no adequate theory is generally available to compute the ultimate strength of prestressed I beams under combined loadings. The strength of such beams depends considerably on the degree with which the component rectangles act together, in other words, it depends on the reinforcement detail. In the sections that follow, the skew bending theory is extended and applied to I section members.

4.2 Analysis of Bending Mode of Failure

4.2.1 Assumptions of Analysis

The following assumptions are made in the analysis:

1. The compression zone is rectangular; it is adjacent and parallel to one of the flange widths of the beam.

2. The failure surface is defined by continuous tensile cracks, at a constant inclination with respect to the longitudinal axis, on the three sides of beam and joined on the fourth side by a compression zone. The crack inclination at failure is same as the initial crack angle.

3. The strain across the failure crack is proportional to its projected distance from the neutral axis measured in the vertical plane, referred as the plane, containing the compression zone.

4. The concrete compressive strain, ε_u, at the extreme fibre in the direction of the longitudinal axis at ultimate is given by a limiting value 0.0035.

5. The stress-strain relationship of concrete in compression is given by

$$\sigma = \frac{E\varepsilon}{1 + \left[\frac{\varepsilon}{\varepsilon_o}\right]^2} \qquad (4.1)$$

where σ = stress

ε = strain

$E = 2\sigma_{max}/\varepsilon_o$

$k_3 = (1.2-0.05 f'_c) \leq 1$ and f'_c in ksi

$$\varepsilon_o = (0.25\, k_3 f'_c + 500)10^{-6}$$

6. The shear force in the compression zone is neglected.

7. A premature shear failure does not occur.

8. The dowel forces in both the longitudinal reinforcement and the stirrups are neglected.

9. The mild steel reinforcement has a well defined yield plateau.

10. The tensile force resisted by the concrete is neglected.

11. The failure zone contains no external loads.

4.2.2 Discussion of Assumptions

Assumption 1 states that the compression zone is rectangular. This is true only when flexural moment and transverse shear act. Presence of torsion makes it either trapezoidal, triangular, or part of the compression zone may extend onto one of the vertical sides depending on the relative proportions of the torque. Rectangular compression zone was used by Lessig (1958) and others for reinforced concrete beams and by Henry and Zia for prestressed concrete beams. Woodhead and McMullen (1972) used an inclined neutral axis, the inclination depending on the relative magnitudes of torque and moment and found that this refinement resulted in little difference to the theoretical ultimate strength. It is therefore considered adequate to assume a rectangular compression zone.

Assumption 2 defines the failure surface. The three lines composing the spatial crack are assumed for simplicity to be straight and at the same inclination. The crack inclinations on the south and north faces differed mainly as the torsional and flexural shear stresses were additive on the former and subtractive on the latter. Crack inclinations computed based on the uncracked section, are assumed to hold

good at ultimate. This is an approximation, however, a slight change in the inclination has not significantly affected the calculated ultimate strength.

Assumption 3 is approximate and has been used by Henry and Zia (1971) and Woodhead and McMullen (1972).

Assumption 4 relates to the useful limit of strain for concrete in compression under combined loading. This magnitude under bending only also depends on several factors. A limiting strain value of 0.0038 was assumed by Hognestad, 0.004 by Warwaruk, and 0.0034 by Lin. As a lower bound the ACI suggests 0.003. Evans and Khalil (1970) observed that the longitudinal strains in the compressed concrete were essentially the same under pure bending and under combined bending and torsion for equal bending moments. Hence the same ultimate strain in concrete was used by them both in pure bending and combined loading. However they did not specify which value they adopted. Woodhead and McMullen (1972) used a value of 0.0034. In the analysis developed herein a value of 0.0035 is used as an average between 0.004 and 0.003.

In assumption 5 equation (4.1) expresses the stress-strain relationship of concrete in compression; this is due to Desai and Krishnan (1964).

It is to be noted that in this analysis of the six equations of equilibrium, two equations are satisfied. This has been the usual approach followed by the previous investigators. Of these two, one is the equilibrium of forces perpendicular to the β plane, and the other is the equilibrium of moments about an axis in the β plane which is parallel to the top face. As the β plane is vertical, the transverse

shear acting vertically on the plane does not enter in either of the Mode 1 equations. The transverse shear is resisted in part by the compression zone and the dowel action of the reinforcement. The sixth and the eighth assumptions concerning the neglect of this shear resistance are introduced to simplify the analysis. Since the failure section is assumed symmetric the forces in the two legs of the stirrups on either side of the web must be equal and opposite. It can be seen that torque is partly carried by the two legs of a stirrup developing equal but opposite forces. Also transverse shear is in part carried by the same two legs of a stirrup with the development of equal forces. Thus the transverse shear does not enter into the theoretical expression as, the equilibrium of the vertical forces is identically satisfied. In essence no attempt is made to satisfy the vertical equilibrium of forces.

Assumption 7 is introduced to exclude the possibility of a premature shear failure. If a beam acted on by only bending and shear fails in shear, such a beam probably develops a shear mode of failure when acted on by torsion, bending and shear. To date the question of shear strength alone is far from settled. Consequently the problem of combined torsion and shear is even further from solution as this is a much more complex problem. The effect of transverse shear is discussed later in Chapter VII.

Assumptions 9 through 11 are used to simplify the analysis.

4.2.3 Scope and Steps of Analysis

The analysis can be applied to under-reinforced as well as over-reinforced beams. From the assumptions it is clear that failure is considered to occur when the concrete crushes on a plane inclined at

an angle β to the longitudinal axis due to the attainment of a limiting strain along this axis. The flanged beams in which the torsional cracking splits off the outstanding parts of the compression flange are analyzed assuming that the width of the beam in the compression zone is equal to the web width. For others full flange width may be used. The analysis details are similar to those used for computing the ultimate flexural strength of an over-reinforced prestressed beam. The equilibrium equations are established with reference to the β-plane which is vertical and inclined to the longitudinal axis at an angle β, containing the compression zone and the neutral axis. The strain distribution in the β plane is shown in Fig. 4.1. Components of internal and external forces perpendicular to the β-plane are equated to zero. Moments of the forces are taken in β-plane about an axis parallel to the top face and passing through the point of action of concrete compressive force. With the maximum compressive strain obtained from equation (4.3), a depth of neutral axis is assumed in the β-plane. The induced strains in all the reinforcements are then compatible with the maximum concrete compressive strain and the assumed depth of the neutral axis. The compressive forces in the concrete and in any steel present in the compression zone, and the tensile forces are determined perpendicular to the β-plane and equilibrium checked. Different values of the depth of neutral axis are tried until the forces equilibrate. After finding the neutral axis, moments of all the forces internal and external are taken about the axis mentioned above and equated to zero. Solution of the moment equation yields the ultimate torque.

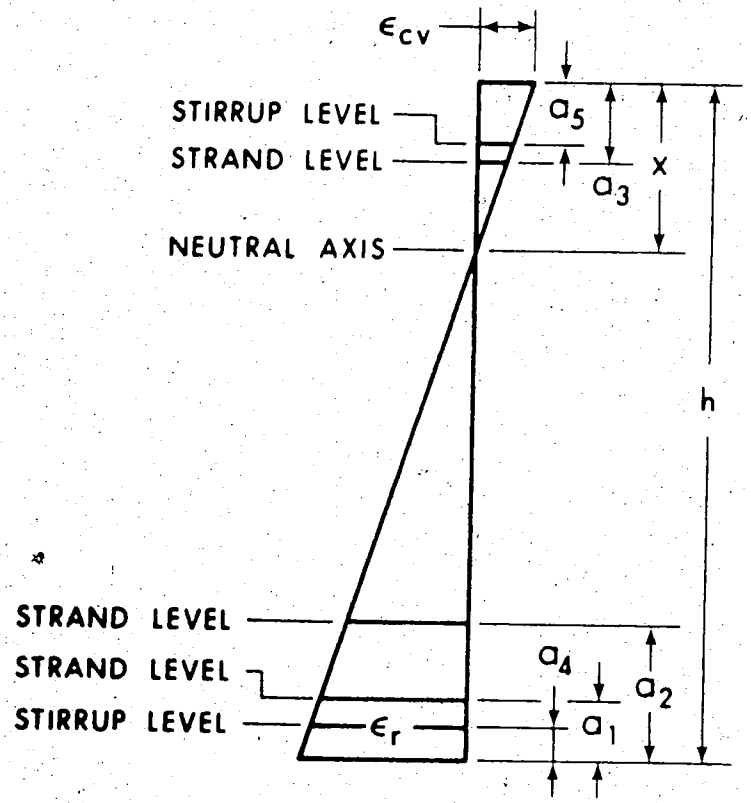

FIG. 4.1 STRAIN DISTRIBUTION ACROSS PLANE IN BENDING MODE (Mode 1)

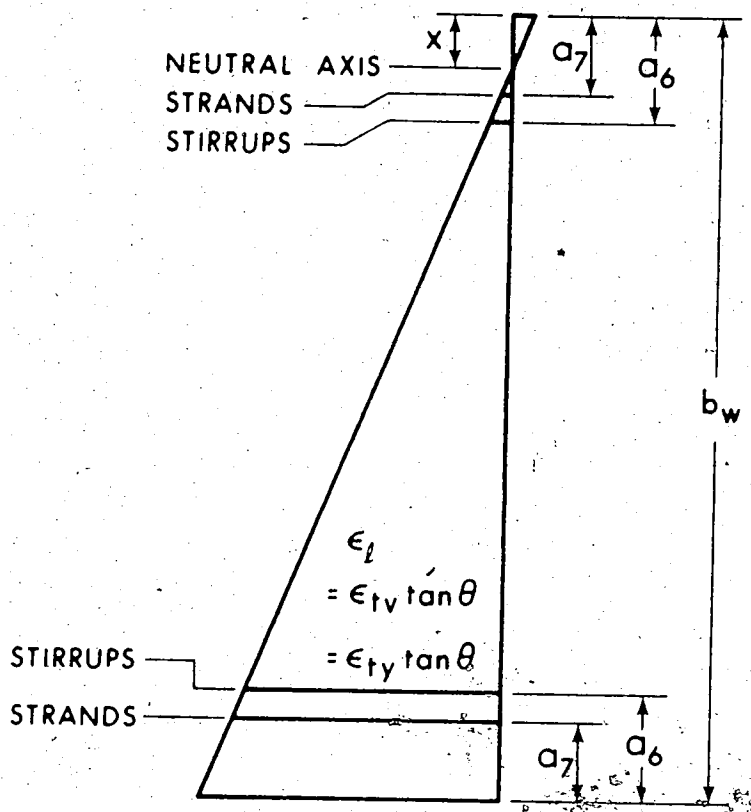

Note: Strain in longitudinal direction induced by loads

FIG. 4.2 STRAIN DISTRIBUTION ACROSS PLANE IN TORSION MODE (Mode 2)

4.2.4 Inclination of Failure Surface

At failure the beam sections adjacent to the failure crack rotate about a neutral axis inclined at an angle β to the longitudinal axis. The developed failure surface for the bending mode is shown in Fig. 4.3 from which the inclinations of the tensile crack and the compression hinge can be related by equation (4.2). The tensile crack inclination θ at ultimate is same as that at the instant of initial cracking and is obtained from the cracking analysis using equation (3.17).

$$\tan\theta = \frac{(b_f+2h)}{b_f} \tan\beta \qquad (4.2)$$

4.2.5 Compressive Force in the Concrete

It is recognized that the equations of equilibrium can be established with reference to any plane. In the present analysis the β plane is used instead of a plane perpendicular to the longitudinal axis as the torque cannot be involved in either of the equations of equilibrium if the latter plane is used.

In Mode 1, the concrete on the top face of the flange is subjected to longitudinal compressive stresses and shear stresses due to flexural and torsional moments, respectively, and this state may be resolved into that of principal compression and tension. At failure the beam rotated about an axis in the β plane with crushing taking place across the β plane accompanied by an orthogonal tensile strain. Because there is tensile strain on the orthogonal plane the ultimate compressive strain perpendicular to the β plane is considerably less than the strain at which concrete fails under pure compression. Kupfer,

Hilsdrof and Rusch (1969) showed that in biaxial compression-tension of concrete when the tensile stress was about 20 percent of the compressive stress failure occurred at a compressive strain less than 0.0005. This is almost an order of magnitude less than the uniaxial compressive crushing strain which is of the order of 0.0035. It can also be noted from their tests that even when the orthogonal tensile stress was only 5 percent the failure compressive strain was less than 0.0015.

Experimentally Evans and Khalil (1970) measured the longitudinal concrete strains on the vertical face along the depth of the beam, for the beams tested under pure bending and for other beams tested in combined bending and torsion. They stated that the presence of torsion had no significant effect on the distribution of the longitudinal strains, and on the depth of the compressed concrete for equal flexural moments. Having recognized that the concrete was crushing in a combined stress state at strains far less than the pure compression strain, Evans and Khalil introduced an empirical relationship given by equation (2.30) i.e. $\varepsilon_c = \varepsilon_{cu} (M_u/M_{ub})^2$

where ε_c = compressive strain in concrete in combined stress,

ε_{cu} = longitudinal compressive strain in pure bending,

M_u = ultimate bending moment in combined loading,

M_{ub} = ultimate pure bending capacity.

For example if $M_u = 0.7\ M_{ub}$ and ε_{cu} is assumed as 0.0035, then the failure strain ε_c will be 0.0017 from equation (2.30).

Woodhead and McMullen also noted a drastic reduction of the compressive failure strain across the β plane. They obtained this strain by starting with the longitudinal compressive strain and resolving it across the β plane. i.e. ε_β = strain perpendicular to the plane = $\varepsilon_c \sin^2\beta$. The longitudinal compressive strain, ε_c, was obtained by the empirical relationship suggested by Evans and Khalil i.e. equation (2.30).

In light of the previous research and the appearance of the tensile cracks on the top flange just before failure in the beams of this investigation failing in Mode 1, the ultimate compressive strain perpendicular to the β plane is obtained by the following equation:

$$\varepsilon_{cv} = \varepsilon_u \sin^2\beta \qquad (4.3)$$

For the assumed depth of neutral axis, this compressive force can be computed knowing the stress-strain relationship of concrete in compression given by equation (4.1). By numerical integration the compression force and its centre of action can be determined. The steps are shown in Fig. 4.4.

4.2.6 Forces in the Longitudinal Reinforcement

The prestress results in a compressive strain in the concrete. As the load is applied the strain in the reinforcement

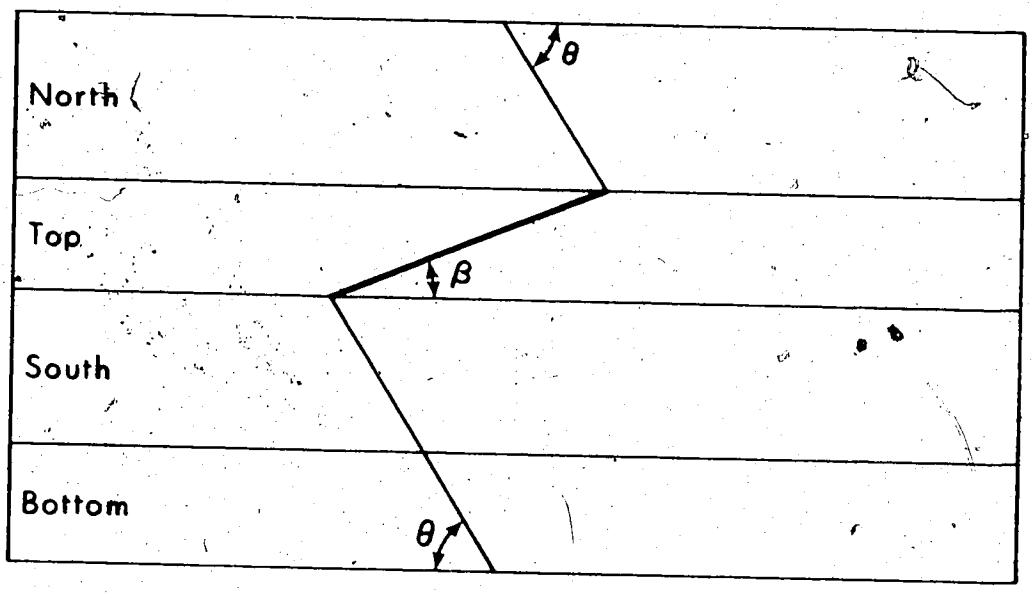

MODE 1

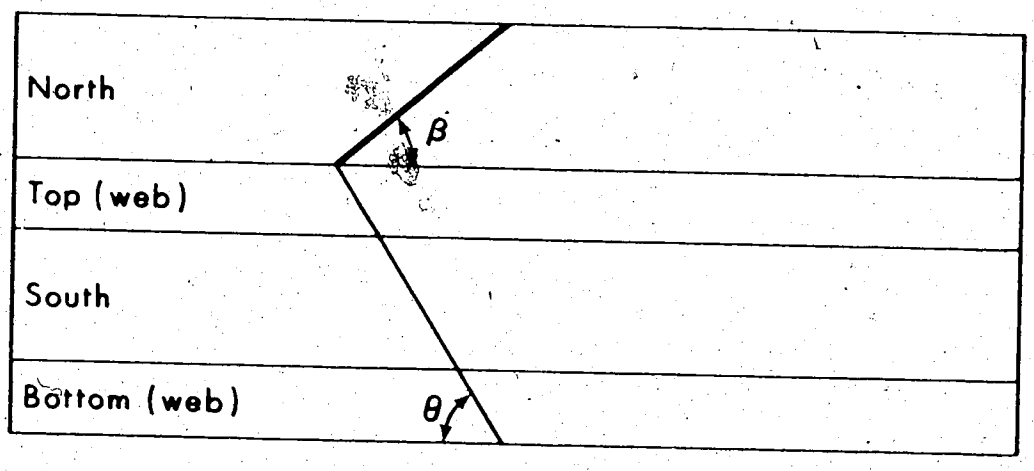

MODE 2

Note :

North side - Side on which shear stresses due to torsion and shear are subtractive

South side - Side on which shear stresses due to torsion and shear are additive

FIG. 4.3 DEVELOPED FAILURE SURFACES

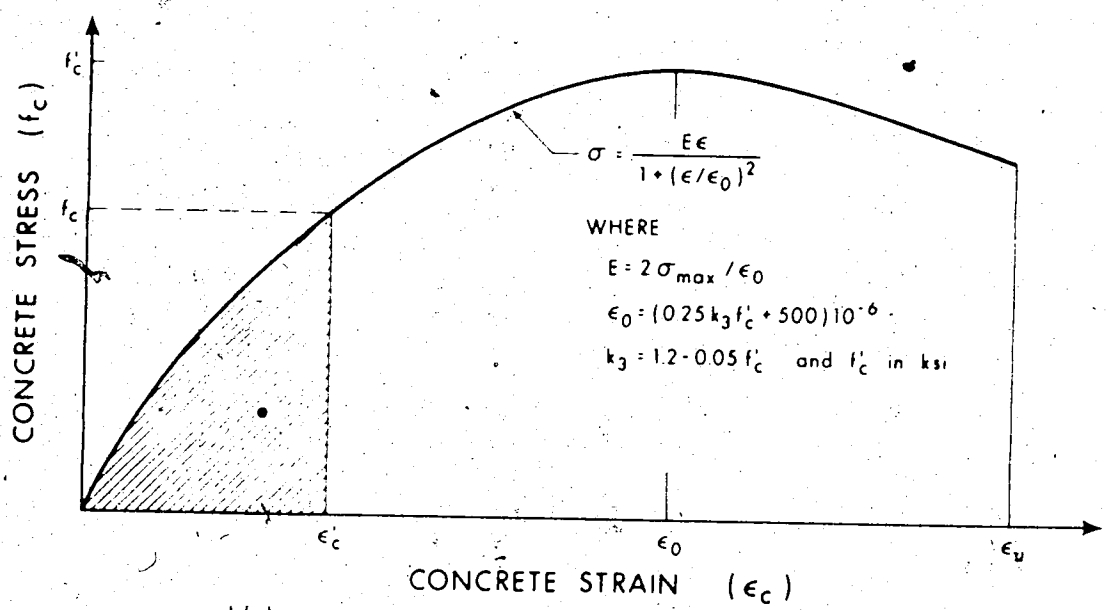

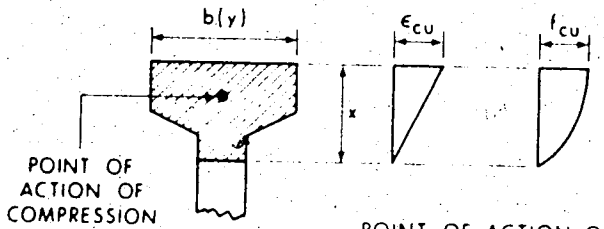

COMPRESSION IN CONCRETE

$$C = \int_{y=0}^{y=x} f_c(y)\, b(y)\, dy$$

POINT OF ACTION OF COMPRESSION FROM NEUTRAL AXIS

$$= \frac{\int_{y=0}^{y=x} f_c(y)\, b(y)\, y\, dy}{\int_{y=0}^{y=x} f_c(y)\, b(y)\, dy}$$

FIG. 4.4 CONCRETE COMPRESSION AND ITS CENTROID

increases first an amount equal ε_{ce} and later a small quantity of strain sufficient to cause cracking in the unstressed concrete. However the strain necessary to induce cracking in the unstressed concrete is of the order of 0.0001 and is neglected. Further increase in the strain in the reinforcement is defined as induced strain ε_i and is related to the useful limit of strain in the concrete by the strain compatibility. The total strain thus is equal to $\varepsilon_s + \varepsilon_{ce} + \varepsilon_i$. The induced strain can be determined by knowing the depth of neutral axis and the concrete strain at the extreme fibre. The maximum force in the strands is assumed not to exceed the force corresponding to a strain of one percent.

4.2.7 Forces in the Transverse Reinforcement

The number of stirrups intersected by the tensile crack on the bottom face can be obtained from Fig. 4.5. As the crack inclination near the compression zone is approximately equal to β, in estimating the number of horizontal legs intersected by the crack, θ is replaced by β. The strain in the horizontal legs can be obtained as $\varepsilon_{st\beta}/\cos\beta$ where $\varepsilon_{st\beta}$ is the strain perpendicular to the β plane at the level of the stirrups. The forces in the vertical legs of the stirrups do not enter the force equation. However, their moment contribution is to be taken into account. Hence, the force in the vertical legs of stirrups is to be estimated. The maximum strain in these branches of the stirrups is obtained by equating the components of the strains in the longitudinal direction and in the vertical legs of the stirrup in the direction of the failure surface, assuming no relative displacement along the failure surface for small rotations (Gangarao and

Zia, 1970). This is shown in Fig. 4.6. The number of vertical legs of stirrups intersected by the tensile crack is obtained from $(h-a_4-a_5)\cot\theta/s$. The force in the vertical legs is assumed to vary triangularly with the maximum force at the bottom and the minimum at the neutral axis. The force is considered not to exceed the yield force in any part of the stirrup. Hence, if the strain exceeds the yield strain, the stirrup carries a force equal to yield force.

4.2.8 Analysis

Figure 4.7 shows the freebody diagram with the forces on it in mode 1 failure. Components of all the internal forces perpendicular to the β-plane are as follows:

Compressive force in the concrete

$$= \frac{C}{\sin\beta} \tag{4.4}$$

Tensile force in the strands near the tension face

$$= \Sigma A_{ps} E_s [\varepsilon_{se}+\varepsilon_{ce}+\varepsilon_i] \sin\beta \tag{4.5}$$

Tensile force in the strand at the second level

$$= A_{ps} E_s [\varepsilon_{se}+\varepsilon_{ce}+\varepsilon_i] \sin\beta \tag{4.6}$$

Tensile force in the strands near the compression face

$$= \Sigma A_{ps} E_s [\varepsilon_{se}+\varepsilon_{ce}+\varepsilon_i] \sin\beta \tag{4.7}$$

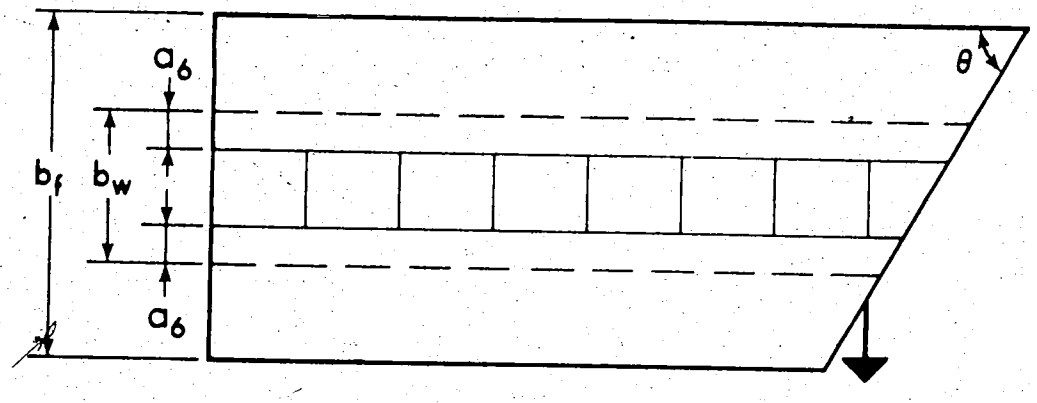

NUMBER OF STIRRUPS INTERSECTED BY TENSILE CRACK

$$= (b_w - 2a_6)\frac{\cot\theta}{S}$$

FIG. 4.5 HORIZONTAL LEGS OF STIRRUPS INTERSECTED IN THE BOTTOM FACE

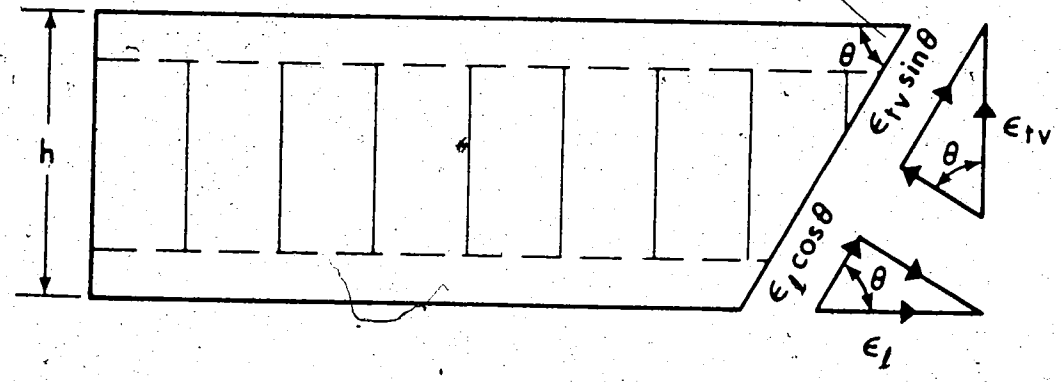

$$\epsilon_l \cos\theta = \epsilon_{tv} \sin\theta$$

NUMBER OF STIRRUPS INTERSECTED BY TENSILE CRACK

$$= (h - a_4 - a_5)\frac{\cot\theta}{S}$$

$$\epsilon_l = \frac{\epsilon_{st\beta}}{\sin\beta}$$

WHERE $\epsilon_{st\beta}$ IS THE STRAIN PERPENDICULAR TO THE β PLANE AT THE LEVEL OF STIRRUPS

FIG. 4.6 RELATION BETWEEN LONGITUDINAL AND TRANSVERSE STRAINS

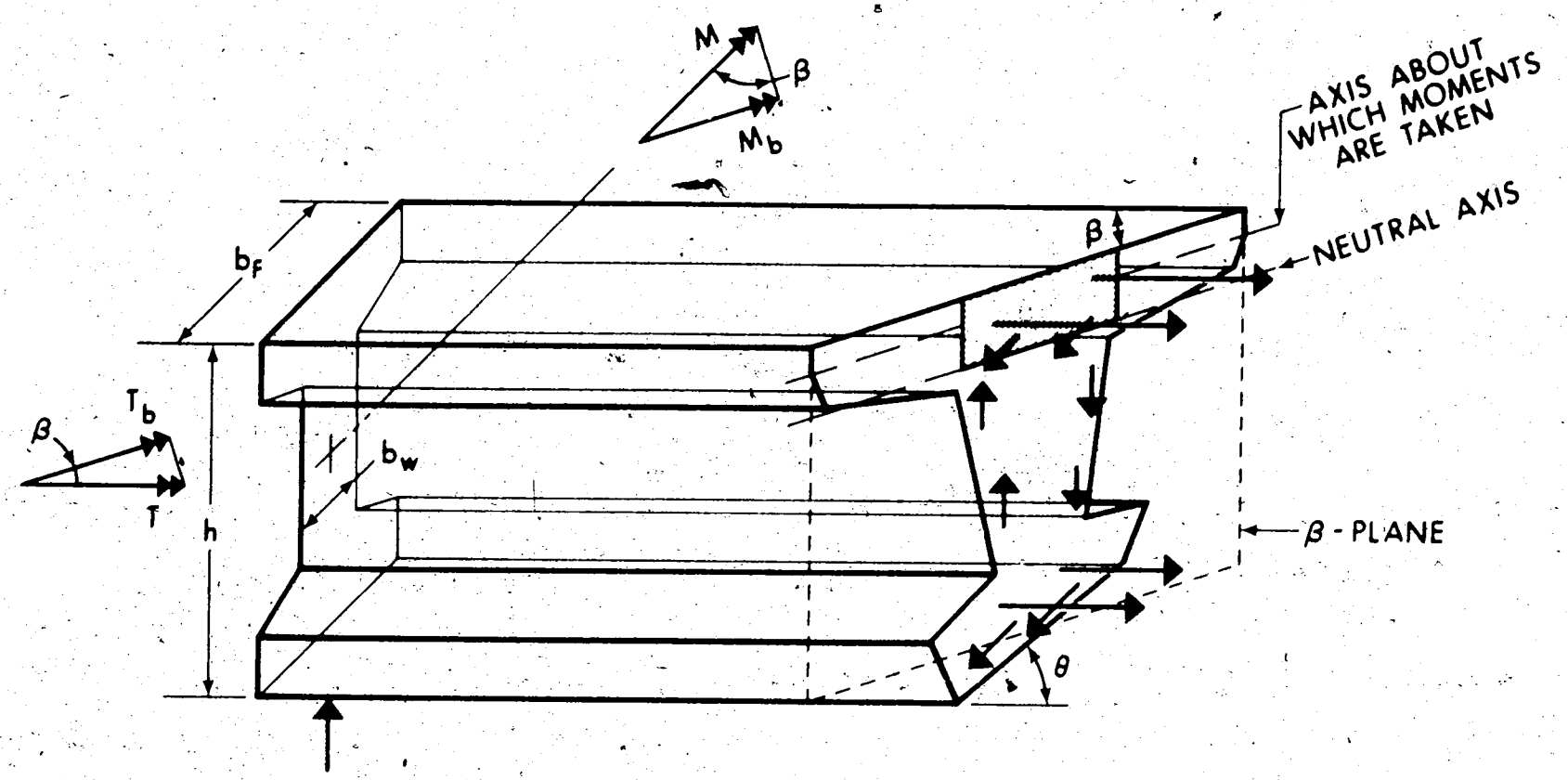

FIG. 4.7 BENDING MODE FAILURE SURFACE (MODE 1)

Tensile force in the horizontal legs of the stirrups near the tension face

$$= A_t\, E_t (b_w - 2a_6) \frac{\cot\theta}{s} \left| \frac{\varepsilon_{cv}}{\cos\beta} \frac{h-x-a_4}{x} \right| \cos\beta \qquad (4.8)$$

Tensile force in the horizontal legs of the stirrups near the compression face

$$= A_t\, E_t (b_w - 2a_6) \left| \frac{\cot\beta}{s} \frac{\varepsilon_{cv}}{\cos\beta} \frac{(a_5-x)}{x} \right| \cos\beta \qquad (4.9)$$

There are no components of external forces perpendicular to the β-plane.

Summation of forces of equations (4.4) through (4.9) furnishes an equation which can be solved by an iteration procedure to evaluate the depth of the compression zone.

The moments of all the forces are taken about an axis in the β-plane which is parallel to the top face and passes through the point of application of the concrete compressive force. External moments include:
Component due to torsional moment

$$= T \times \cos\beta \qquad (4.10)$$

Component due to bending moment

$$= M \times \sin\beta \qquad (4.11)$$

Internal moments include:

Moment contributions due to prestressing strands on the tension face

$$= \Sigma A_{ps} E_s [\varepsilon_{se}+\varepsilon_{ce}+\varepsilon_i]\sin\beta [h-a_1-k_2x] \qquad (4.12)$$

Moment contribution due to force in prestressing strand at the second level

$$= A_{ps} E_s [\varepsilon_{se}+\varepsilon_{ce}+\varepsilon_i]\sin\beta [h-a_2-k_2x] \qquad (4.13)$$

Moment contribution due to force in prestressing strands near the compression face

$$= \Sigma A_{ps} E_s [\varepsilon_{se}+\varepsilon_{ce}+\varepsilon_i]\sin\beta [a_3-k_2x] \qquad (4.14)$$

Moment contribution due to force in horizontal legs of the stirrups near the tension face:

$$= A_t E_t (b_w-2a_6) \varepsilon_{cv} \frac{(h-x-a_4)}{sx} \cot\theta (h-a_4-k_2x) \qquad (4.15)$$

Moment contribution due to force in horizontal legs of the stirrups near the compression face:

$$= A_t E_t (b_w-2a_6) \varepsilon_{cv} \frac{(a_5-x)}{sx} \cot\theta (a_5-k_2x) \qquad (4.16)$$

Moment contribution due to force in vertical legs of stirrups

$$= 2\left(\frac{1}{2} A_t E_t \frac{\cot\theta}{\sin\beta} \varepsilon_{cv} \frac{h-x-a_4}{x}\right) \frac{(h-a_4-a_5)}{s} \cot\theta \frac{2}{3}(h-x-a_4) \cot\theta\sin\beta \qquad (4.17)$$

In equation (4.17) $(h-a_4-a_5)\cot\theta/s$ gives the number of vertical legs of stirrups intersected by the crack. As the strain and hence force varies linearly with a maximum value at the level of the horizontal legs of the stirrups in the bottom face and a zero value at the neutral axis, the strain in the stirrups intersected at different levels along the height is taken as the mean of the forementioned maximum and zero strains. The factor 1/2 accounts for this. The moment contribution due to the vertical legs on both sides of the web is same and is taken care of by the factor 2. The stirrup forces are distributed triangularly and the lever arm of the resultant of these forces from the neutral axis is to be accordingly calculated. This explains the presence of the factor 2/3.

The external moments of equations (4.10) and equation (4.11) are equated to the equation (4.12) through (4.17) to establish the equation of moment equilibrium. The flexural moment can be expressed in terms of the torque and the only unknown, the ultimate torque can be solved.

4.3 Analysis of Torsion Mode of Failure

4.3.1 General Remarks

In rectangular beams failing in torsion mode, the inclined compression zone forms close to one of the vertical sides and the two parts of the beam at failure rotate about the compression hinge. But for I beams, the literature review reveals that each investigator considered such a compression zone was either closest to the vertical sides of the flanges or in the web close to one of its sides. The

author noted the following observations during his I beam tests with reference to the location of the skew bending axis. The tensile cracks on one side of web did not penetrate completely to the other side i.e. tensile cracks on either side of the web were oriented in opposite directions. Shear-compression distress was observed clearly on the sloping portion of the flanges and faintly in the web. The vertical legs of the stirrups away from the tension face of the web recorded tensile strains. The compression distress on the vertical sides of the flanges was not evident as suggested by Gvozdev et al (1968) and Woodhead and McMullen (1972) though it was clearly visible in the flanges of most of the beams tested. From these observations it was concluded that the shear-compression zone is along the sloping portion of the flanges and near the vertical face of the web, the magnitude and the centre of action of corresponding forces is very difficult to establish precisely. It is equally difficult to establish the axis about which the rotation at failure takes place. However to develop a simple, approximate, reasonably satisfactory method for estimating the ultimate strength in the torsion mode, it is assumed in the following analysis that the inclined skew bending axis is inside the web parallel and close to one of its faces. The presence of the outstanding flange on the compression side is neglected. Failure is considered to occur when the strain in the vertical legs of the stirrups on the tension side reaches yield strain. The strain in other reinforcements is assumed compatible with this yield strain of the stirrup leg. In addition to assumptions 3 and 6 through 11 of section 4.2.1 the following

assumptions are made.

4.3.2 Assumptions of Analysis

1. The rectangular compression zone is parallel and adjacent to one of the vertical sides of the web extending throughout the height of the beam.

2. The depth of the compression zone $\beta_1 x$ computed according to the ACI equivalent rectangular stress block is very small.

3. The failure surface is symmetric skewed and is defined by continuous tensile cracks at a constant inclination θ with respect to the longitudinal axis on the three sides of beam and joined on the fourth side by a compression zone. The compression zone makes an angle ξ with the longitudinal axis. The crack inclination θ at failure is same as the initial crack angle assuming that the initial crack occurs in the web.

4. The transverse reinforcement is uniformly distributed along the length of the beam.

4.3.3 Analysis

The free body diagram for the torsion mode showing the failure surface and the forces acting on it, is shown in Fig. 4.8. The β plane is perpendicular to the sides and is inclined at an angle β with respect to the longitudinal axis. It contains the compression zone and the neutral axis and serves as a reference plane for establishing force and moment equilibrium equations.

The assumed developed surface for the torsion mode is shown in Fig. 4.3. The relationship between the inclination of the tensile

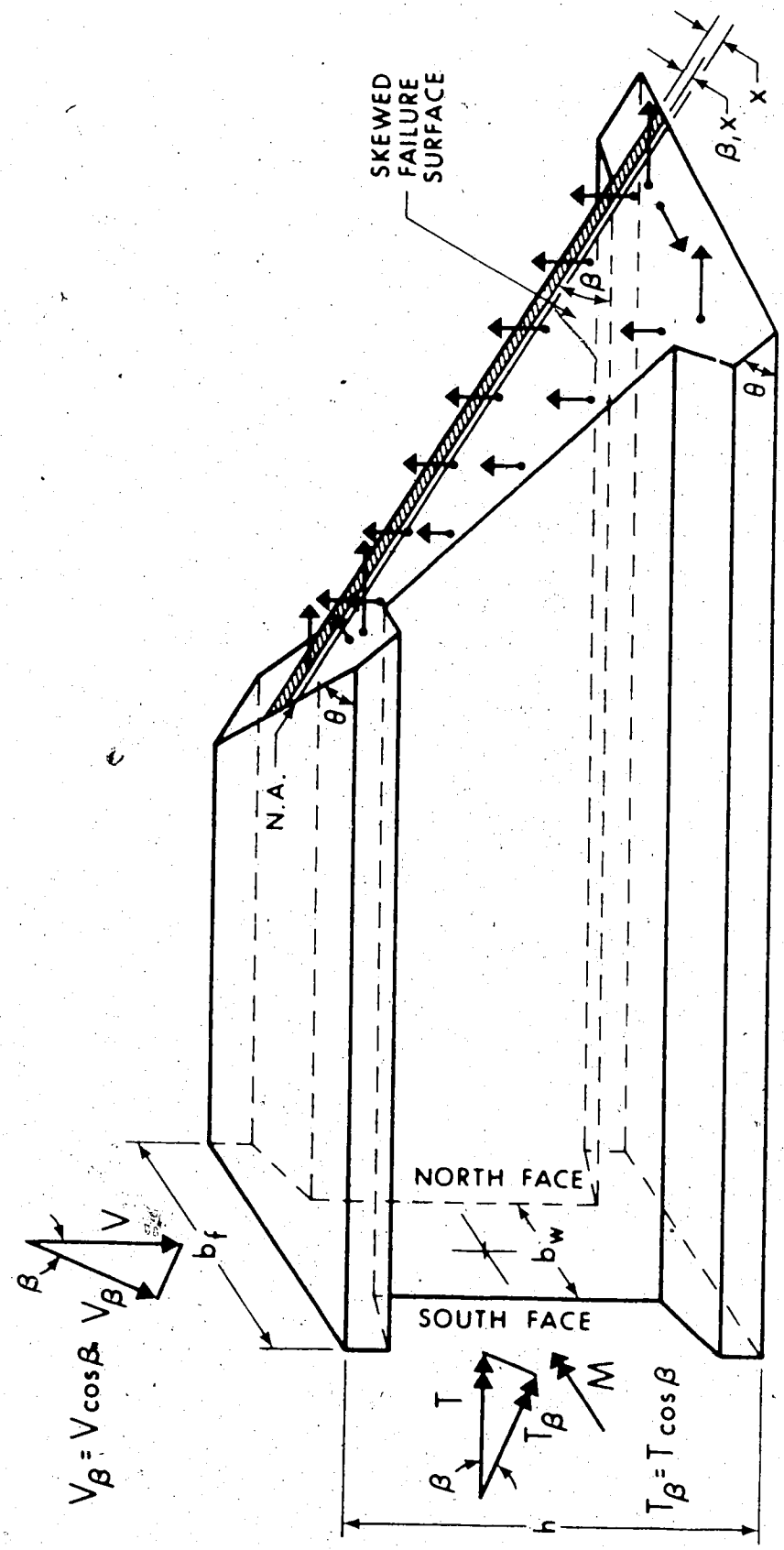

FIG. 4.8 TORSION MODE FAILURE SURFACE (MODE 2)

crack and the compression hinge obtained from Fig. 4.3 can be written as

$$\tan\theta = \left(\frac{h+2b_w}{h}\right) \tan\beta \qquad (4.18)$$

As the compression zone is assumed rectangular and the bending moment vector is orthogonal to the neutral axis, the bending moment does not enter the equations developed here for the torsion mode. Since the moment equilibrium about one axis is considered, only the bending component of the torque is taken into account.

According to assumption 2, a concrete stress of $0.85 f'_c$ is assumed uniformly distributed over an equivalent rectangular compression zone. The depth of compression is $\beta_1 x$ as defined by ACI 318-71.

All the beams of this investigation failing in the torsion mode were under reinforced transversely and over-reinforced longitudinally. As noted before, failure is defined to occur when the transverse steel first reaches its yield strain and the strains in other reinforcements at that instant were assumed to be related to the yield strain of the transverse steel by the same strain compatibility noted earlier for Mode 1. The strain distribution in the β plane along the web is given in Fig. 4.2. The strain in the longitudinal direction at the level of the stirrups can be related to the strain in the vertical legs of the stirrups by the following expression (Gangarao and Zia, 1970)

$$\varepsilon_{\ell} = \varepsilon_{tv} \tan\theta = \varepsilon_{ty} \tan\theta \qquad (4.19)$$

This relationship is obtained from Fig. 4.6, similarly the strain in the horizontal legs of the stirrups and the longitudinal strain are related

$$\varepsilon_{\ell} = \varepsilon_{th} \tan\theta \qquad (4.20)$$

For the torsion mode in the following analysis two equations of equilibrium, equilibrium of forces perpendicular to the β plane and equilibrium of moments about an axis of the θ plane, are satisfied. The two equations allow the two unknowns namely the depth of neutral axis and the ultimate torque to be determined. Summing the forces perpendicular to the β plane on the free body:

$$\text{compressive force in the concrete} = 0.85 f'_c \beta_1 xh/\sin\beta \qquad (4.21)$$

Tensile force in the strands near the tension face

$$= \sum A_{ps} E_s \left[\varepsilon_{se} + \varepsilon_{ce} + \varepsilon_{ty} \tan\theta \left(\frac{b_w - a_7 - x}{b_w - a_6 - x}\right)\right] \sin\beta \qquad (4.22)$$

If the longitudinal reinforcement is outside the web near the tension face then a_7 is taken equal to zero. Tensile force in the strands near the compression face

$$= \sum A_{ps} E_s \left[\varepsilon_{se} + \varepsilon_{ce} + \varepsilon_{ty} \tan\beta \left(\frac{a_7 - x}{b_w - a_6 - x}\right)\right] \sin\beta \qquad (4.23)$$

If the longitudinal reinforcement is outside the web near the compression face then a_7 is taken equal to zero. If nonprestressed steel is provided, its contribution can be obtained by substituting ε_{se} and ε_{ce} equal to zero in the equations (4.22) and (4.23). Tensile force in the vertical legs of the stirrups near the tension face

$$= A_t E_t \varepsilon_{ty} \left[\left(\frac{h-a_1-a_3}{s}\right) \cot\theta\right] \cos\beta \qquad (4.24)$$

Tensile force in the vertical legs of the stirrups near the compression face

$$A_t E_t \left[\varepsilon_{ty}\left(\frac{a_6-x}{b_w-a_6-x}\right)\right]\left[\left(\frac{h-a_1-a_3}{s}\right)\cot\beta\right] \cos\beta \qquad (4.25)$$

Of the external forces only the flexural shear has a component perpendicular to the β plane

$$= V \cos\beta \qquad (4.26)$$

Using the relation between torque and shear $\delta = T/Vb_w$ and assuming approximately one-half of stirrup steel cover to be equal to the depth of neutral axis in the equations (4.22) through equations (4.25), the expression for the depth of neutral axis may be written as follows:

$$x = \frac{\sin^2\beta}{0.85 f'_c \beta_1 h}\left\{-\frac{T}{b_w \delta}\cot\beta + \Sigma A_{ps} E_s\left[\varepsilon_{se}+\varepsilon_{ce}+\varepsilon_{ty}\tan\theta\left(\frac{b_w-a_7-a_6/2}{b_w-a_6/2}\right)\right]\right.$$

$$+ \Sigma A_{ps}E_s[\varepsilon_{se}+\varepsilon_{ce}+\varepsilon_{ty}\tan\beta(\frac{a_7-a_6/2}{b_w-a_6/2})]$$

$$+ A_tE_t\varepsilon_{ty}[\frac{(h-a_1-a_3)}{s}\cot\theta]\cot\beta$$

$$+ A_tE_t[\varepsilon_{ty}(\frac{a_6/2}{b_w-a_6/2})][\frac{(h-a_1-a_3)}{s}\cot\beta]\cot\beta\} \qquad (4.27)$$

Equilibrium of moments is established by taking moments of all the forces about an axis in the β plane at the level of the vertical legs of the stirrups close to the tension face of the web.

Internal moments include:

Moment contribution due to force on concrete

$$= 0.85\ f'_c\ \frac{\beta_1 xh}{\sin\beta}\ [b_w-a_6-\frac{1}{2}\beta_1 x] \qquad (4.28)$$

Moment contribution due to force in prestressing strands on the tension face and compression face of the web

$$= -\Sigma A_{ps}E_s[\varepsilon_{se}+\varepsilon_{ce}+\varepsilon_{ty}\tan\theta(\frac{b_w-a_7-x}{b_w-a_6-x})]\ \sin\beta\ .\ (a_7-a_6) \qquad (4.29)$$

$$= -\Sigma A_{ps}E_s[\varepsilon_{se}+\varepsilon_{ce}+\varepsilon_{ty}\tan\beta(\frac{a_7-x}{b_w-a_6-x})]s \qquad (b_w-a_6-a_7) \quad (4.30)$$

Moment contribution due to force in the vertical legs of stirrups near the compression face of the web

$$= -A_tE_t[\varepsilon_{ty}(\frac{a_6-x}{b_w-a_6-x})][\frac{(h-a_1-a_3)}{s}\cot\beta]\cos\beta\ (b_w-2a_6) \qquad (4.31)$$

Moment contribution due to force in the horizontal legs of stirrups at top and bottom

$$+ 2\left(\frac{1}{2} A_t E_t \varepsilon_{ty}\right) \left(\frac{b_w - 2a_6}{s} \cot\theta\right) \left(\frac{1}{3} [b_w - a_6 - x]\cot\theta \sin\beta\right) \qquad (4.32)$$

The term $(b_w - 2a_6)\cot\theta/s$ gives the number of stirrups intercepted by the crack. The factor 2 accounts for the top and bottom legs of the stirrups, while the factor 1/2 averages the strain as it varies from a maximum value of ε_{ty} on the tension side to zero on the compression side. The term $1/3[b_w - a_6 - x]\cot\theta\sin\beta$ gives the lever arm of the triangularly varying force in the stirrups. The external moments are shown in Fig. 4.8 and include:

Due to the bending component of torsional moment

$$= T \cos\beta$$

Due to the flexural shear assuming that it acts at the centre of the web

$$= - V \cos\beta \left(\frac{b_w}{2} - a_6\right)$$

Using the relation between the torque and shear, $\delta = T/Vb_w$ and equating the internal and external moments an expression for the ultimate torque

T_u is:

$$T_u = \frac{1}{\cos\beta\left(1 - \frac{1}{2\delta} + \frac{a_6}{b_w \delta}\right)} \{0.85 f'_c \beta_1 \frac{xh}{\sin\beta} (b_w - a_6 - \frac{1}{2}\beta_1 x)$$

$$- \Sigma A_{ps} E_s [\varepsilon_{se} + \varepsilon_{ce} + \varepsilon_{ty} \tan\theta (\frac{b_w - a_7 - x}{b_w - a_6 - x})] \sin\beta (a_7 - a_6)$$

$$- \Sigma A_{ps} E_s [\varepsilon_{se} + \varepsilon_{ce} + \varepsilon_{ty} \tan\beta (\frac{a_7 - x}{b_w - a_6 - x}] \sin\beta (b_w - a_6 - a_7)$$

$$- A_t E_t [\varepsilon_{ty} (\frac{a_6 - x}{b_w - a_6 - x})(\frac{h - a_1 - a_3}{s})\cot\beta] \cos\beta (b_w - 2a_6)$$

$$+ 2(\frac{1}{2} A_t E_t \varepsilon_{ty})(\frac{b_w - 2a_6}{s})\cot\theta(\frac{1}{3}[b_w - a_6 - x]\cot\theta\sin\beta)\} \qquad (4.33)$$

Equations (4.27) and (4.33) contain both x and T_u and hence have to be solved either simultaneously or by trial and error to determine the ultimate torque.

CHAPTER V

EXPERIMENTAL INVESTIGATION

5.1 Test Specimens

The experimental program involved tests on forty four prestressed I section beams, which were subjected to various combinations of torsion,bending and shear. The beams were divided into four series. All the beams in each series nominally had identical properties and differed only in the amount of transverse reinforcement. Among the series either the prestress, or its eccentricity, or both, were varied. The beams are designated by a system consisting of one letter followed by two numbers. The letter refers to the series, while the first and second numbers indicate the spacing of #2 stirrups, and an index of loading combination as shown in Table 7.1, respectively. For example, Beam A-3-2 related to A-series, had a stirrup spacing of 3 in and was tested at loading combination 2. For loading combination 2 the torque-shear ratio (T/Vb_w) is equal to 5.2.

The nominal details of the beam cross sections are shown in Fig.5.1. The arrangement of #2 stirrups used for web reinforcement is shown in Fig. 5.2. Actual beam dimensions were measured before test at three locations in the test zone, along the length of the beam. The positions of strands were similarly measured before casting and after testing. For calculation purposes dimensions at the measured location nearest to the failure section were chosen and are furnished

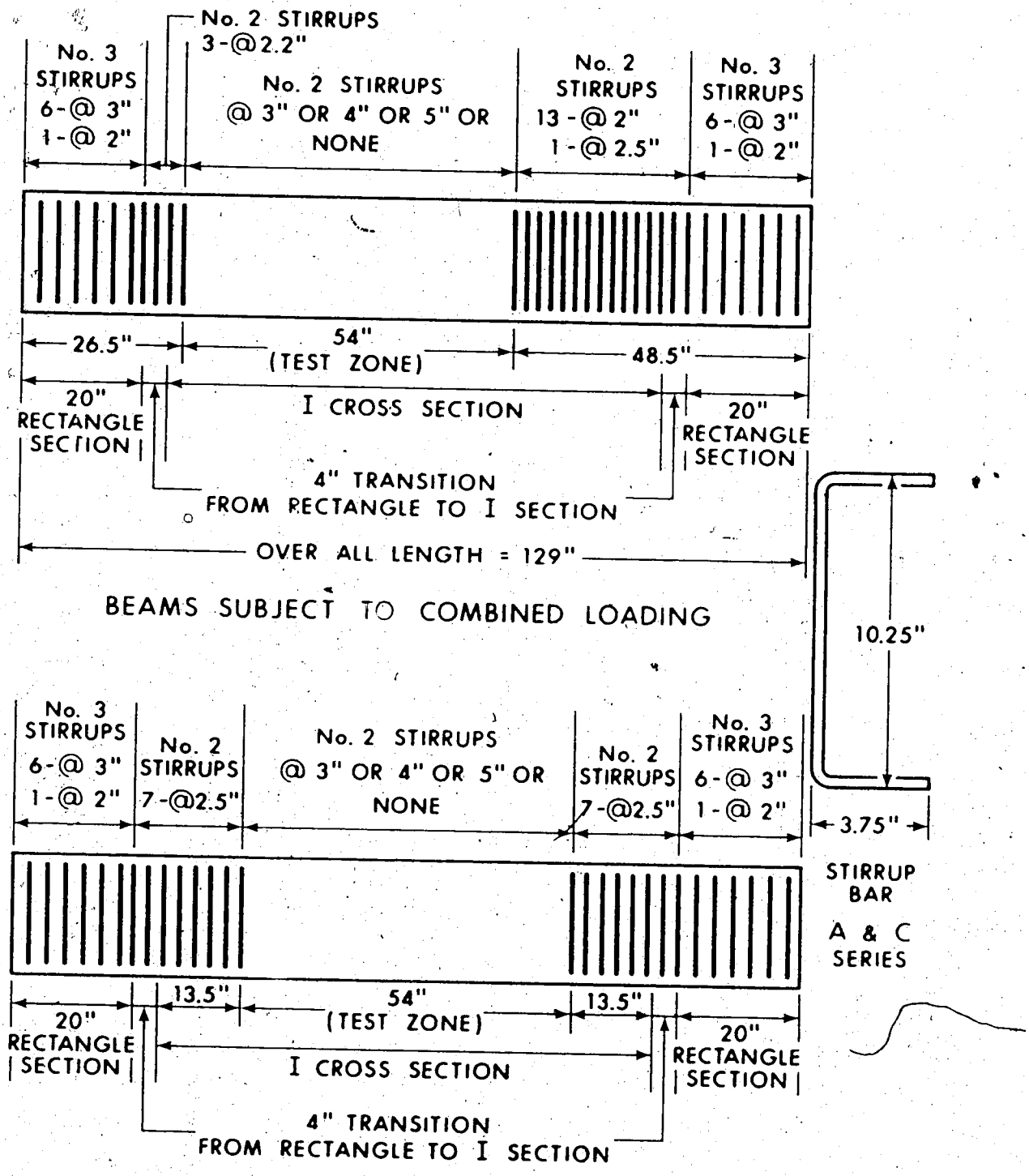

FIG. 5.2 ARRANGEMENT OF STIRRUPS

in Table 5.1. The properties of all beams are summarized in Table 5.2.

5.2 Materials

Three sizes of prestressing strand were used in the test beams. Series A and C beams had two 1/2-in. and two 3/8-in. diameter strands while Series B had six 3/8-in. diameter strands. Series D beams were provided with four 5/16-in. and one 3/8-in. diameter strands. All were seven wire stress-relieved strands meeting the specifications of ASTM A-416 with a minimum guaranteed ultimate strength of 250 ksi. The physical properties of typical strands are shown in Fig. 5.3.

In practice such as used by the Highway Department of the State of Washington each two legged stirrup for prestressed I section beams subjected to torsion, bending and shear consists of four pieces involving two vertical legs and two horizontal pieces, for ease of fabrication of torsion stirrups around the tensioned strands. However, this may lead to difficulties in anchorage. Torsion specifications normally require a continuous stirrup as tensile stresses are developed on all faces of the beam. In I girders because of the narrow web, the aspect ratio of the stirrup is such that the vertical legs would develop most of the torsional strength and short legs would be stressed less. Wyss et al (1969) used a 4 piece stirrup similar to that noted above and showed that it was not necessary to use closed rectangular stirrups for torsion web reinforcement in I section beams as the main contribution to the strength in torsion came from the vertical legs. Nevertheless in the present investigation, the two

	250k GRADE STRANDS		
	$\frac{1}{2}$" DIA.	$\frac{3}{8}$" DIA.	$\frac{5}{16}$" DIA.
ULTIMATE TENSILE STRENGTH (kips)	39.800	22.050	16.050
ULTIMATE TENSILE STRESS (ksi)	276.389	275.625	276.800
LOAD AT 1% ELONGATION (kips)	35.200	19.900	14.225
MODULUS OF ELASTICITY (ksi)	27500	28900	27700
AREA (sq. in.)	0.1438	0.0799	0.0578
YIELD STRAIN	0.01	0.01	0.01

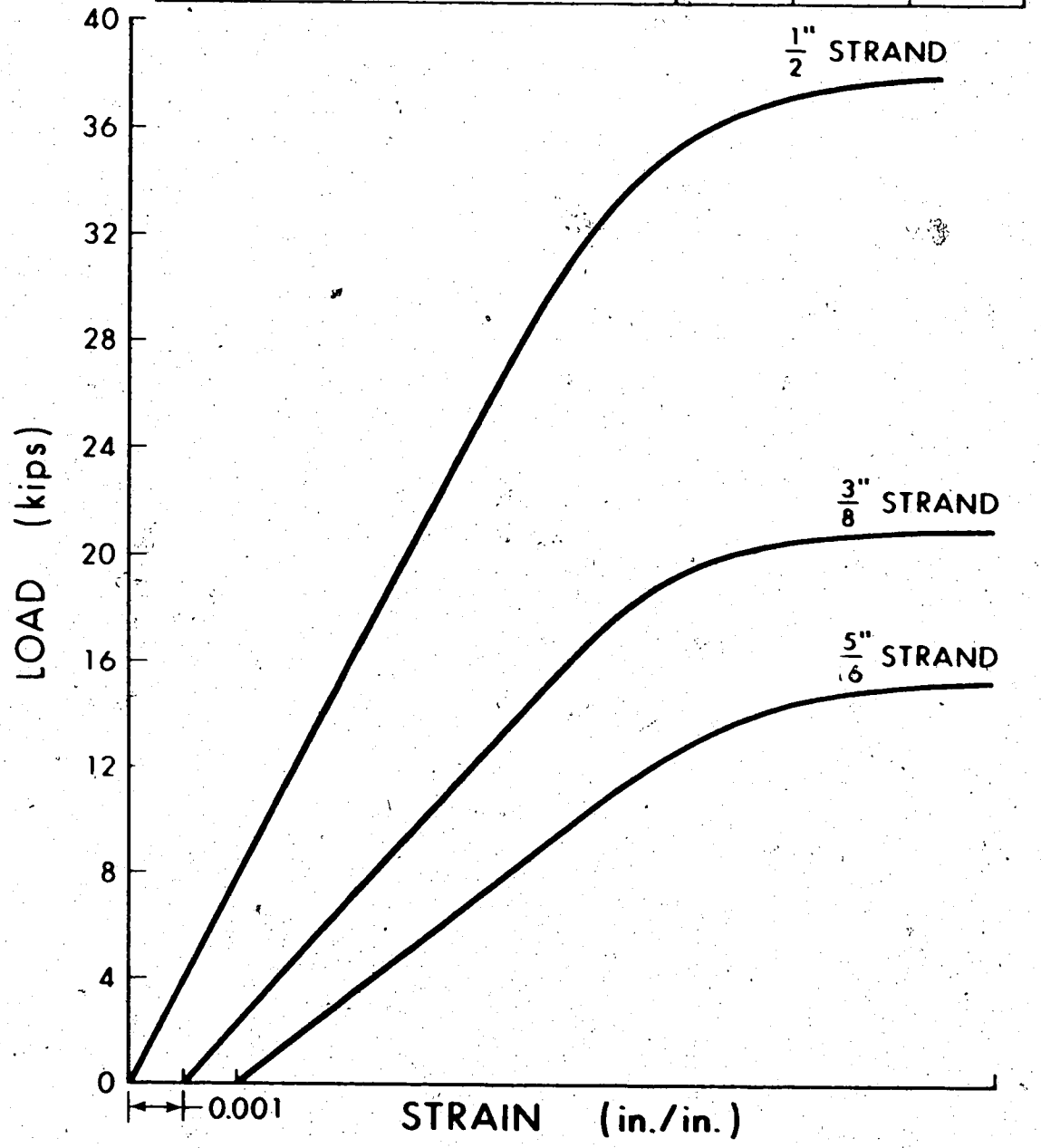

FIG. 5.3 LOAD-STRAIN CURVES AND PROPERTIES OF PRESTRESSING STRAND

TABLE 5.1
DIMENSIONS OF TEST SPECIMENS

Beam No.	Overall Depth	Top Flange			Bottom Flange			Web		Strand Cover	
		Depth at end	Depth at junction with web	Width	Depth at end	Depth at junction with web	Width	Depth	Thickness	Top	Bottom
A-0-4	12.12	2.19	2.94	7.06	2.03	2.78	7.10	6.40	2.56	1.66	0.97
A-5-4	12.12	2.22	2.97	7.03	2.06	2.81	7.09	6.34	2.56	1.73	1.06
A-4-4	12.12	2.24	2.99	7.12	2.02	2.77	7.28	6.36	2.60	1.69	0.03
A-3-4	12.12	2.27	3.02	7.0	2.05	2.75	7.43	6.35	2.59	1.67	1.06
A-5-3	12.12	2.25	3.00	7.06	1.94	2.69	7.40	6.43	2.63	1.81	1.12
A-4-3	12.12	2.22	2.97	7.00	2.02	2.77	7.37	6.35	2.59	1.81	1.03
A-3-3	12.12	2.26	3.01	7.00	1.98	2.66	7.40	6.43	2.60	1.80	1.00
A-5-2	12.12	2.20	2.95	7.00	2.00	2.75	7.31	6.42	2.64	1.72	1.01
A-4-2	12.12	2.22	2.97	7.06	2.02	2.77	7.37	6.34	2.56	1.81	1.12
A-3-2	12.12	2.22	2.97	7.05	2.03	2.77	7.37	6.36	2.56	1.81	1.03
A-0-1	12.12	2.23	2.98	7.00	1.98	2.73	7.37	6.41	2.63	1.81	1.03
A-5-1	12.12	2.19	2.94	7.06	2.00	2.75	7.37	6.43	2.59	1.69	1.01
A-4-1	12.12	2.22	2.97	7.06	1.97	2.72	7.37	6.47	2.63	1.81	1.00
A-3-1	12.12	2.19	2.94	7.00	2.05	2.80	7.42	6.39	2.56	1.72	1.07
A-3-0	12.12	2.25	3.00	7.06	1.98	2.73	7.37	6.39	2.63	1.66	1.12
B-3-4	12.12	2.22	2.97	7.03	2.07	2.82	7.31	6.33	2.56	1.72	1.12
B-5-3	12.12	2.25	3.00	7.00	1.96	2.71	7.37	6.41	2.63	1.75	1.03
B-4-3	12.12	2.19	2.94	7.12	2.07	2.82	7.31	6.36	2.63	1.72	1.12
B-3-3	12.12	2.17	2.92	7.00	2.03	2.78	7.37	6.42	2.44	1.75	1.03
B-5-2	12.12	2.25	3.00	7.12	2.01	2.77	7.28	6.36	2.56	1.69	1.12
B-4-2	12.12	2.22	2.97	7.01	2.00	2.75	7.37	6.40	2.62	1.75	1.03
B-3-2	12.12	2.24	2.99	7.00	1.98	2.73	7.37	6.42	2.62	1.78	1.03
B-5-1	12.12	2.21	2.96	7.10	2.05	2.80	7.37	6.33	2.63	1.81	1.12
B-4-1	12.12	2.24	2.99	7.00	2.05	2.80	7.37	6.33	2.63	1.75	1.03
B-3-1	12.12	2.22	2.97	7.00	2.06	2.83	7.37	6.42	2.63	1.81	1.03
B-0-1	12.12	2.25	3.00	7.03	2.03	2.76	7.37	6.36	2.63	1.78	1.12
C-0-4	12.12	2.22	2.97	7.04	1.98	2.71	7.40	6.44	2.63	1.72	1.00
C-5-4	12.12	2.25	3.00	7.00	1.94	2.67	7.40	6.46	2.67	1.81	1.06
C-3-4	12.12	2.24	2.99	7.03	2.01	2.76	7.37	6.39	2.63	1.75	1.03
C-5-3	12.12	2.22	2.97	7.00	1.96	2.71	7.40	6.46	2.67	1.81	1.03
C-4-3	12.12	2.20	2.95	7.00	1.96	2.71	7.40	6.46	2.67	1.84	0.98
C-3-3	12.12	2.20	2.95	7.00	1.96	2.71	7.40	6.46	2.67	1.84	0.98
C-5-2	12.12	2.25	3.00	7.05	1.93	2.68	7.46	6.44	2.63	1.75	1.00
C-4-2	12.12	2.26	3.01	7.00	1.95	2.73	7.40	6.47	2.44	1.81	0.94
C-3-2	12.12	2.25	3.00	7.04	1.95	2.70	7.19	6.42	2.47	1.81	1.00
D-3-4	12.12	2.16	2.91	7.06	2.08	2.83	7.32	6.38	2.56	1.75	1.05 2.96
D-3-4A	12.12	2.22	2.97	7.03	2.04	2.79	7.25	6.38	2.56	1.69	1.09 2.56
D-3-3	12.12	2.22	2.97	7.00	2.06	2.81	7.12	6.34	2.53	1.75	1.05 2.56
D-3-2	12.12	2.22	2.97	7.03	2.03	2.78	7.16	6.37	2.50	1.75	1.09 2.56
D-3-1	12.12	2.25	3.00	7.12	2.00	2.75	7.22	6.37	2.56	1.66	1.01 2.59
D-3-0	12.12	2.26	3.01	7.03	2.00	2.75	7.25	6.37	2.44	1.66	1.03 2.59

*All dimensions in inches

TABLE 5.2
PROPERTIES OF TEST SPECIMENS

Beam No.	Concrete Strength f'_{cy} (psi)	Concrete Strength f_{sp} (psi)	Prestressing Reinforcement Top No.	Top Strand (dia)	Bottom No.	Bottom Strand (dia)	Transverse Reinforcement Spacing of #2 Stirrups in.	P_t (%)	f_{ty} (ksi)	Effective Prestress (kips)	e (in)	T (psi)	B (psi)	p/f'_c	Age at test (days)
A-0-4	4425	380	2	3/8	2	1/2	-	-	-	39.[illegible]	2.039	200	1209	0.168	64
A-5-4	5480	464	2	3/8	2	1/2	5	0.62	39	55.59	2.067	214	1376	0.154	10
A-4-4	4708	433	2	3/8	2	1/2	4	0.78	39	43.43	2.036	213	1296	0.169	11
A-3-4	4254	362	2	3/8	2	1/2	3	1.04	39	37.84	1.920	209	1099	0.163	73
A-5-3	4372	389	2	3/8	2	1/2	5	0.62	39	40.77	1.941	229	1204	0.173	113
A-4-3	5140	486	2	3/8	2	1/2	4	0.78	39	43.45	2.129	184	1322	0.156	35
A-3-3	4460	354	2	3/8	2	1/2	3	1.04	39	34.33	1.872	210	1004	0.144	107
A-5-2	4549	409	2	3/8	2	1/2	5	0.62	39	42.29	2.116	187	1295	0.173	36
A-4-2	4737	376	2	3/8	2	1/2	4	0.78	39	39.72	1.917	224	1158	0.155	63
A-3-2	4390	464	2	3/8	2	1/2	3	1.04	39	48.22	2.266	167	1508	0.203	12
A-0-1	5383	433	2	3/8	2	1/2	-	-	-	39.[illegible]	2.036	194	1176	0.135	106
A-5-1	4896	398	2	3/8	2	1/2	5	0.62	39	41.64	2.169	169	1278	0.157	37
A-4-1	4407	425	2	3/8	2	1/2	4	0.78	39	42.39	2.063	206	1263	0.179	59
A-3-1	5686	495	2	3/8	2	1/2	3	1.04	39	[illegible]	2.11[illegible]	201	1398	0.149	[illegible]
A-3-0	4706	449	2	3/8	2	1/2	3	1.04	39	42.63	1.964	233	1262	0.168	10
B-3-4	4932	415	[illegible]	3/8	4	3/8	3	1.04	39	64.42	1.3[illegible]	603	1653	0.242	10
B-5-3	4401	404	2	3/8	4	3/8	5	0.62	39	62.20	1.279	601	1576	0.262	13
B-4-3	5135	407	2	3/8	4	3/8	4	0.78	39	65.58	1.568	506	1765	0.235	11
B-3-3	4731	438	2	3/8	4	3/8	3	1.04	39	61.55	1.290	624	1639	0.255	12
B-5-2	5109	451	2	3/8	4	3/8	5	0.62	39	67.27	1.617	507	1830	0.242	10
B-4-2	4431	350	2	3/8	4	3/8	4	0.78	39	62.01	1.044	694	1489	0.261	20
B-3-2	4670	387	2	3/8	4	3/8	3	1.04	39	63.94	1.301	614	1636	0.256	32
B-5-1	4930	470	2	3/8	4	3/8	5	0.62	39	65.69	1.360	586	1669	0.243	34
B-4-1	4684	433	2	3/8	4	3/8	4	0.78	39	66.07	1.231	655	1653	0.261	21
B-3-1	5279	473	2	3/8	4	3/8	3	1.04	39	65.63	1.366	591	1687	0.230	29
B-3-0	4384	444	2	3/8	4	3/8	3	1.04	39	65.03	1.312	615	1662	0.275	12
C-0-4	4237	367	2	3/8	2	1/2	-	-	-	36.80	0.689	496	809	0.162	110
C-5-4	4516	329	2	3/8	2	1/2	5	0.62	39	40.56	0.829	512	925	0.168	62
C-3-4	5132	484	2	3/8	2	1/2	3	1.04	39	41.53	0.927	500	976	0.152	81
C-5-3	4440	336	2	3/8	2	1/2	5	0.62	39	35.53	[illegible].731	454	800	0.149	99
C-4-3	5330	42[illegible]	2	3/8	[illegible]	[illegible]	4	0.78	39	[illegible].59	0.708	503	[illegible]	[illegible]	108
[illegible]	[illegible]	49[illegible]	2	[illegible]	[illegible]	[illegible]	[illegible]	1.04	39	[illegible]	0.771	498	[illegible]	[illegible]	87
[illegible]	[illegible]	[illegible]	[illegible]	[illegible]	[illegible]	[illegible]	[illegible]	[illegible]	[illegible]	[illegible].44	0.730	46[illegible]	[illegible]	0.14[illegible]	84
[illegible]	[illegible]	[illegible]	[illegible]	[illegible]	[illegible]	[illegible]	[illegible]	0.78	[illegible]	[illegible]	0.963	44[illegible]	891	[illegible]	104
[illegible]	[illegible]	[illegible]	[illegible]	[illegible]	[illegible]	[illegible]	[illegible]	1.04	[illegible]	[illegible]	[illegible]	514	[illegible]	[illegible]	[illegible]
[illegible]	[illegible]	[illegible]	[illegible]	[illegible]	[illegible]	[illegible]	[illegible]	[illegible]	[illegible]	[illegible]	[illegible]	49[illegible]	[illegible]	[illegible]	[illegible]
[illegible]	[illegible]	[illegible]	[illegible]	[illegible]	[illegible]	[illegible]	4	[illegible]	[illegible]	[illegible]	[illegible]	46[illegible]	[illegible]	[illegible]	[illegible]
[illegible]	45[illegible]	4[illegible]	[illegible]	[illegible]	[illegible]	[illegible]	[illegible]	1.04	39	[illegible]	[illegible]	478	891	[illegible]	[illegible]
D-3-4	[illegible]	[illegible]	2	5/16	2+1	2-5/16 & 1-3/8	[illegible]	1.04	39	[illegible]	1.4[illegible]	361	116[illegible]	0.16[illegible]	[illegible]
D-3-4A	4407	38[illegible]	2	5/16	2+1	2-5/16 & 1-3/8	3	1.04	39	41.5[illegible]	1.419	369	1116	0.175	9
D-3-3	5236	475	2	5/16	2+1	2-5/16 & 1-3/8	3	1.04	39	4[illegible].31	1.522	360	1203	0.155	[illegible]
D-3-2	4767	407	2	5/16	2+1	2-5/16 & 1-3/8	3	1.04	39	42.87	1.493	367	1185	0.169	8
D-3-1	4955	484	2	5/16	2+1	2-5/16 & 1-3/8	3	1.04	39	40.21	1.541	329	1111	0.150	10
D-3-0	4820	449	2	5/16	2+1	2-5/16 & 1-3/8	3	1.04	39	40.67	1.427	370	1109	0.159	9

horizontal pieces were dispensed with and the vertical leg was bent and extended as a horizontal portion of the stirrup. The two legged stirrups for the beams were formed by two separate bars bent as shown in Fig. 5.2. The horizontal portion of the bent bars extended to the end of the flange width allowing for cover. The stress-strain curve and general properties of the #2 smooth bars used for web reinforcement are presented in Fig. 5.4.

The concrete mix was designed to yield a nominal 28 day compressive strength of 5000 psi; Type III high early strength cement was used to facilitate early transfer of prestress. The coarse aggregate was 1/2-in. maximum size crushed gravel. For each beam and its control cylinders the concrete was mixed in one batch of five cubic feet. Each batch consisted of the following mix proportions:

Cement - Type III	135 lbs.
Sand	279 lbs.
Coarse aggregate	450 lbs.
Water	76 lbs.

As the moisture content of the aggregates varied slightly the amount of water was adjusted in each batch to obtain a slump of the order of three inches.

5.3 Fabrication of Specimens

All the I beams were nominally 12 in. deep, 7 in. wide and 10 ft.9 in. long. The depth of both top and bottom flanges was 2 in. at the outside edge and increased to 2.75 in. at the junction with the web. The thickness of the web was 2.5 inches. These beams were

BAR SIZE	#2
AREA (sq in)	0.05
YIELD STRESS (ksi)	39
YIELD STRAIN	0.0013
MODULUS OF ELASTICITY (ksi)	30000

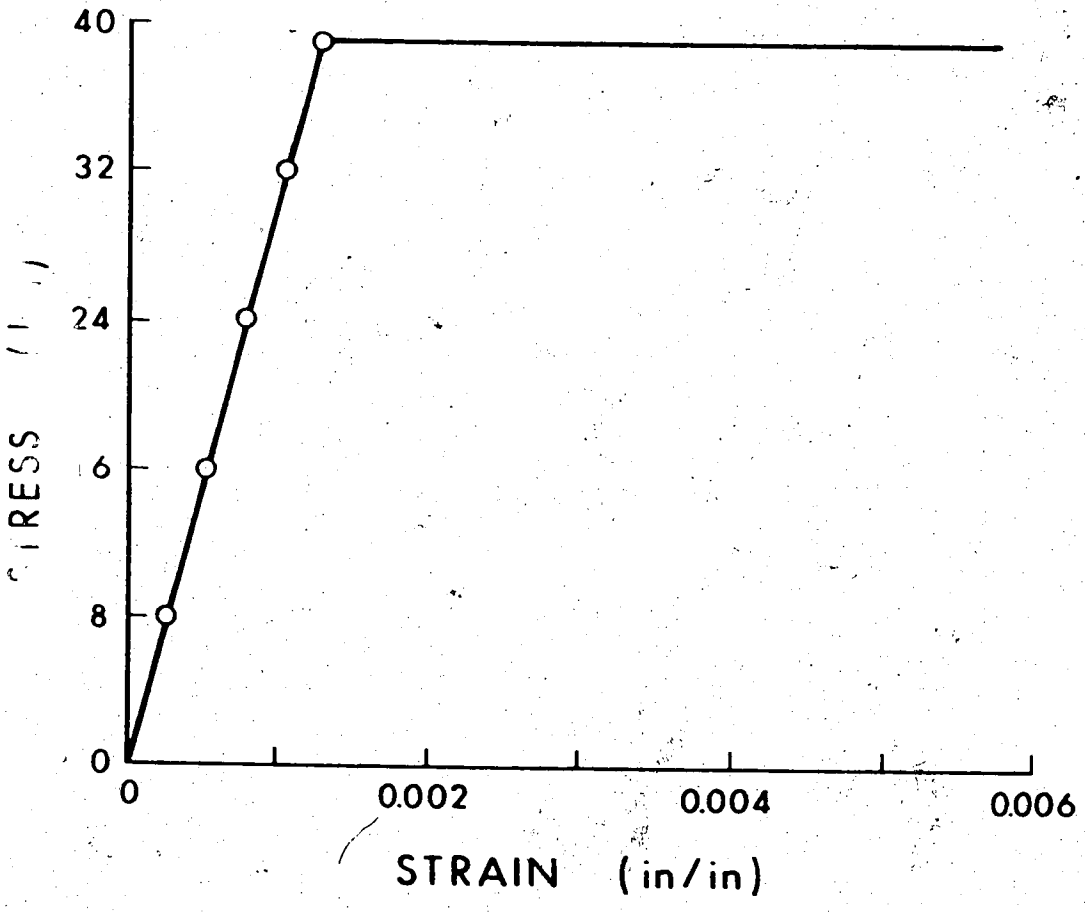

FIG. 5.4 STRESS-STRAIN CURVE OF NO. 2 BAR

dimensioned to have approximately half the size of full scale girders tested s et al (1969). Both end sections were made rectangular to faci. e easy gripping in the torsional heads. To force the failure in the test zone, the portions of the beam beyond test zone were reinforced with additional mild steel bars, consisting of #3 stirrups in the rectangular section portions and #2 stirrups in the transition and I section parts as shown in Fig. 5.2. Additionally the non-test zones were provided with inclined bars on both vertical sides of each beam in the probable direction of the principal tensile stresses, and four #2 longitudinal bars. The longitudinal bars extended into the test zone for about 9 in. and terminated in a staggered manner to avoid a plane of weakness.

The 26 ft. long prestressing bed in the laboratory, permitted fabrication of beams in pairs. The strands were individually tensioned by a 30 ton electrically-operated hydraulic jack; the force in each strand being measured by a load cel.. Each strand was stressed in excess by an estimated amount to account for losses and finally to yield the required tension at the time of test. After all the strands were tensioned, the mild steel cage was assembled. Stirrups instrumented with KYOWA electrical resistance strain gages of 5 mm length (Type KFC-5-C1-11, Resistance = 120.0, Gage Factor = 2.12) were positioned at estimated locations of failure in the test zone. Budd GA-1 cement and a catalyst were used to mount each strain gage on the prepared surface of the stirrup. The gages were waterproofed with three coats of Budd GW-2 compound followed by two layers of insulating tape. Finally a coating of epoxilite compound was applied. For in-

strumenting strands, small cavities were created in the bottom and top flanges at two or three locations of probable failure, by inserting styrofoam plugs between the strand and the form before casting. After casting the plug holes were cleaned and foil gages of 1 mm and Type KFC-1-C1-11 (Resistance = 119.6, and Gage factor = 2.13) were instal d on the strands using Budd GA-1 cement and catalyst.

The mould consisted of two steel channels with wood inserts to form the I section and the transition portion to the rectangular section on either end of test zone. The steel channels were bolted to a heavy steel base. At each end of the form a mild steel plate was used as an end stop.

Prior to casting the side forms were oiled and positioned. Concrete was mixed in the laboratory and each beam together with its control cylinders were cast from the same batch of concrete. One day after casting, the beams and the test cylinders were demoulded and subsequently cured for six days by wrapping with wet burlap and plastic sheets.

Prestress was transferred one week after casting. The strands exposed between the two beams were cut by heating them gradually over a length using an oxy-acetylene torch. The beams were then stored in the laboratory until time of test. To measure the prestress losses, a series of Demec gage points were glued to the surface of the two vertical faces and top face at the middle of the beam. Demec gage readings were taken immediately before and after the release of prestress in order to obtain the prestress loss due to elastic shortening. Before the test another set of readings were taken to determine loss of

prestress due to creep, shrinkage and relaxation. The difference in the readings taken before the application of prestress and before the test gave the total losses and hence the effective prestress.

5.4 Instrumentation of Specimens

The test specimens were instrumented to obtain the measurement of angle of twist, vertical deflections, and reinforcement strains.

(a) Angle of Twist

Two twist meters were mounted at each end of the gage length over which the total angle of twist was to be measured. Each twist meter was fabricated by two pieces of 1-1/2 in. x 1 in. aluminum channel sections. On the top channel a level bubble was mounted. The base and top channels were pin jointed at one end, and at the other end, a micrometer screw was mounted between them, for measurement of their relative movement. A spring forced contact between micrometer screw needle and top channel. The whole assembly was mounted on the beam. The pin joint and the micrometer screw needle were 15 inches apart and the micrometer least count was 0.001-in. The spirit bubbles were initially levelled by the micrometer screws, and as the beam twisted one bubble was more displaced than the other. Micrometer screws were adjusted until they were level again. The difference between the initial and current readings of a twist meter furnished the angle of twist of the section. The difference between the angles of twist of each twist meter was the total twist over the gage length. Rotations were measured over a gage length of 48 inches. Locations of twist meters are shown in Fig. 5.5.

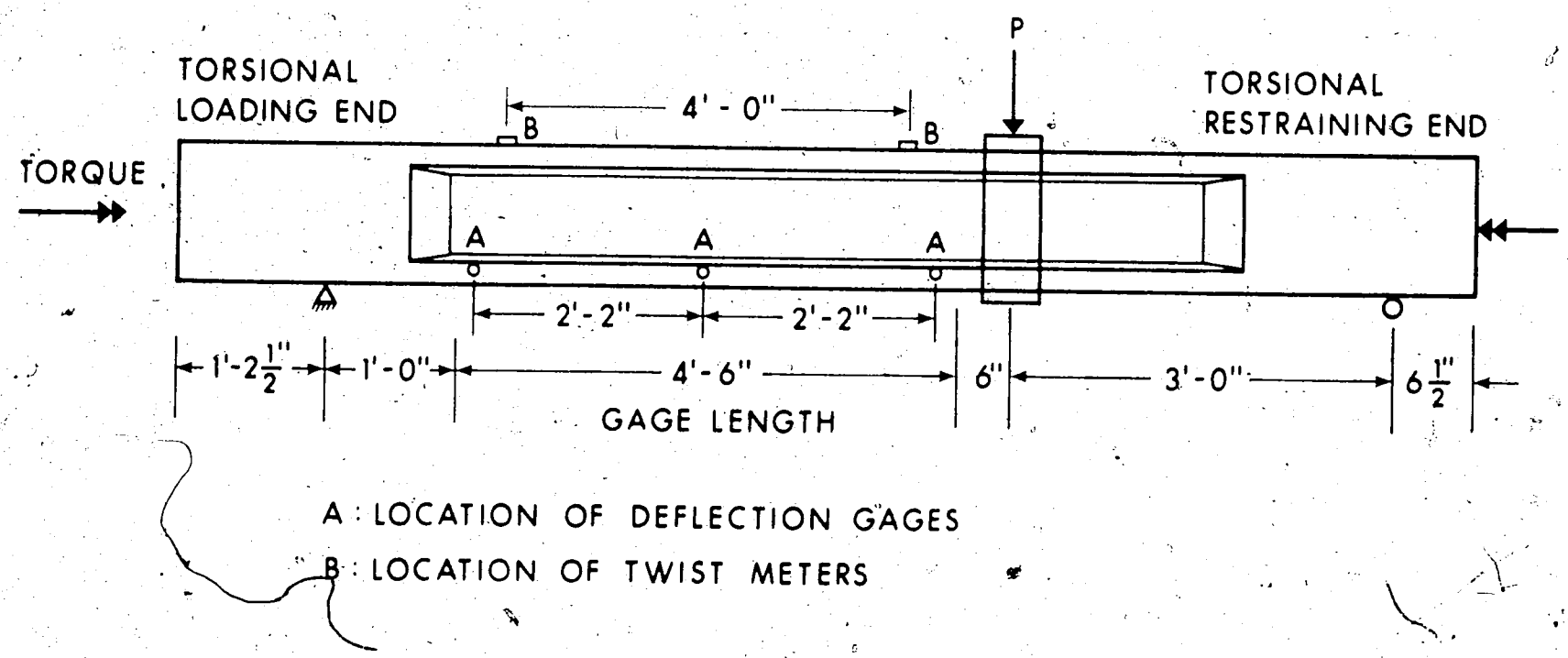

FIG. 5.5 BEAM LOADING ARRANGEMENT

(b) Deflections

The vertical deflections for each of the beams were measured at three locations in the gage length as shown in Fig. 5.5. At each of the three locations two small curved nails were glued on the two vertical sides of bottom flange and from these nails two scales were freely suspended equidistant from the centre of twist of the uncracked beam. The least count of the scales was 0.01 inch. The six scales were read using two precise levels located on either side of the beam. The average of readings of the two scales at each location was taken as the deflection of the centre of the cross section.

(c) Reinforcement Strain Measurement

SR-4 electrical resistance strain gages were used to measure the strain in the vertical legs and occasionally in the horizontal portions of the stirrups. Three stirrups having gages were provided in each beam at probable locations of failure. Both on bottom and top strands on the south side of the beam, foil gages were used at two locations. The output from all these gages was monitored by SS-24R switching and balancing box and SM-60 AT strain indicator.

5.5 Test Setup and Procedure

A general view of the test setup is shown in Plate 5.1 and a schematic diagram is shown in Fig. 5.5. The torsion test rig allowed the twisting and shear-flexural loads to be applied separately by means of two independent loading systems.

The transverse load was applied by an Amsler Jack of 44 kip capacity, hung from the top girder of the loading frame. An electrically

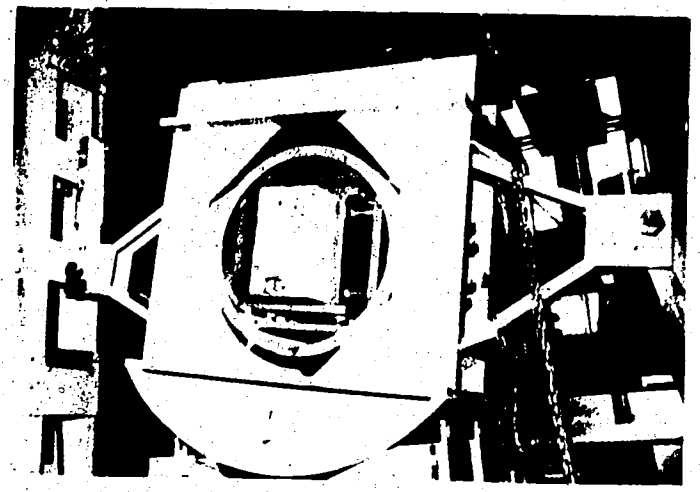

(a) TWISTING HEAD

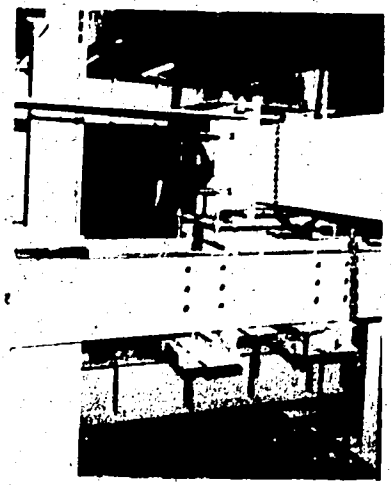

(b) RESTRAINING HEAD

(c) GENERAL VIEW OF TEST SETUP

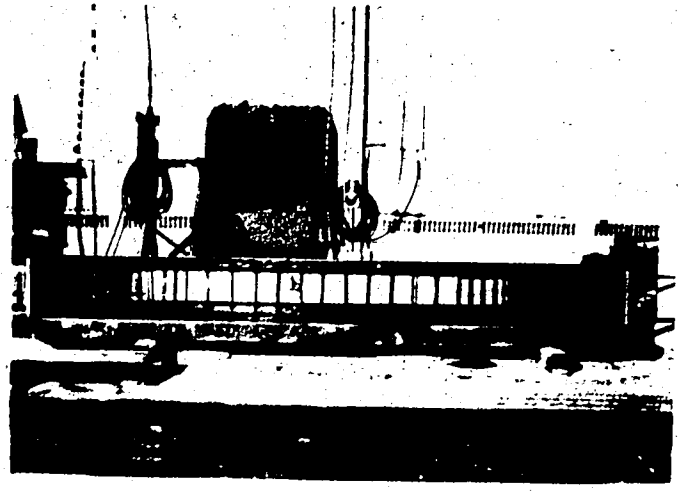

(d) BEAM BEFORE CASTING IN THE PRESTRESSING BED

PLATE 5.1 TEST SETUP AND PRESTRESSING BED

operated Amsler pump fitted with a load indicator, was connected to the jack. The pump with its load maintaining device, maintained flexural load steadily at any desired level during the test. The Amsler jack transferred the load to the beam through a roller assembly and a pipe collar. The roller assembly was supported on the pipe collar which in turn was clamped to the test beam coaxially. The pipe collar provided free rotation of the test beam maintaining the roller assembly without any transverse displacement. Further, four horizontal tie bars, two on each side of the beam were used to keep the roller assembly in position.

The east end of the specimen was supported by a twisting head, and the west end by a restraining head. The effective span of the beam was 9 feet. The twisting head permitted the specimen to rotate freely about its three principal axes while the restraining head allowed flexural rotation and translation, but prevented any torsional rotation of the specimen. For the twisting head the twisting couple was produced by two equal and opposite forces in two cables spaced 72 inches apart. The cables were connected between the torsion arms of the twisting head and the ends of a cross beam located below the load bed. The cross beam was designed to move freely within guides as it was loaded at its center by two 20 kip hydraulic jacks coupled in series. The jacks, operated by a manual pump, were coupled in order to increase the travel to 16 inches, which enabled the twisting head to develop a rotation of approximately 26°. The maximum rotation the twisting head is capable of is slightly greater than 26°. As the forces in the cables were essentially the same, only one of these was

measured using a load cell and an indicator during the tests. Reports by McMullen and Warwaruk (1967) and Mukherjee and Warwaruk (1970) present detailed illustrations of the torsion testing rig.

The Amsler load indicator was preset at a reading appropriate to the self weight of the roller assembly and the pipe collar, as these were supported by the test specimen. Similarly, the weight of the cross beam had to be taken into account in reading the torsional load. Initially the cables hung freely as the cross beam rested on a support. The zero reading on the torque load cell indicator was adjusted, to correspond to a no tension situation in the cables, before the cross beam support was removed. The first torsional load applied to a specimen was the weight of cross beam.

Each beam was tested to failure by applying loads in a series of increment which consisted of increasing to a predetermined level both the transverse load and the torsional load by a definite proportion, simultaneously. As the beam was subjected to a moment gradient, in the presence of transverse shear, the predetermined proportion was chosen in terms of torque-shear ratio which was constant in the test zone throughout the test. It took about one minute, for increasing the loads, after which, they were held constant, while steel strains, deflections, and rotations were measured and cracks marked. The holding period after each increment varied from two to four minutes. Smaller increments of loads were used as cracking and failure loads were approached. In certain beams, concrete surface strains were measured by Demec gage readings to relate to the strains recorded by strain gages mounted on the strands. In all instances,

load application was continued well beyond the stage at which peak values were observed. The location of the first crack and the ultimate failure plane were noted. Usually 20 to 25 increments were used prior to failure and the entire test took about 1-1/2 hours. Photographs of the crack patterns were taken at the end of each test.

CHAPTER VI

PRESENTATION OF TEST RESULTS

6.1 Introduction

The principal test results and the observed behavior of the beams are presented in this chapter. Additional experimental details consisting of torque-twist, and load-deformation curves for the whole range of loading, photographs of two side views of each beam and sketches of typical developed failure surfaces are furnished in Appendix A.

In Table 6.1 principal test results such as transverse load, torsional moment, bending moment, flexural shear both at cracking and ultimate are recorded. The location of the initial crack and the centre of the failure surface with reference to the position of the transverse load are also listed. The flexural deflections and the torsional rotations at cracking and ultimate conditions are tabulated in Table 6.2. Figure 5.5 shows the locations where these deformations were measured.

Beams of each series were tested at one of the five nominal load ratios of $T/Vb_w = \delta$ of ∞, 10.4, 5.2, 2.229 and 0.0. One beam in series D was tested at a ratio of δ equal to 20.8. In the beam designations, the last numeral is the load combination corresponding to a particular load ratio. These nominal ratios did not include the dead load shear. However in presenting the load ratios ψ and δ in Table 6.1 dead load moment and shear were included. For any one of the

TABLE 6.1

PRINCIPAL TEST RESULTS

Beam No.	f'_c (psi)	$\frac{T_u}{M_u}$	$\frac{T_u}{V_u b_w}$	ℓ_{cr}[a] (in)	ℓ_u[b] (in)	P_u (kips)	Cracking Loads: T_{cr} (in-kips)	M_{cr}[c] (in-kips)	V_{cr}[c] (kips)	Ultimate Loads: T_u (in-kips)	M_u[d] (in-kips)	V_u (kips)	Location of First Crack	Observed Mode of Failure
A-0-4	4425	-	-	34	[illegible]	[illegible]	36.[illegible]	6.[illegible]	0.0[illegible]	37.[illegible]	[illegible]	[illegible]	TF	Mode 2
A-5-4	5460	-	-	[illegible]	28	[illegible]	47.94	6.3	0.05	54.95	6.[illegible]	[illegible]	TF	Mode 2
A-4-4	4708		-	14	[illegible]	[illegible]	46.59	6.[illegible]	0.02	56.[illegible]	6.[illegible]	[illegible]	TF	Mode 2
A-3-4	4254	-	-	29	[illegible]	[illegible]	38.64	[illegible]	0.05	5[illegible]	[illegible]	0.[illegible]	TF	Mode 2
A-5-3	4372	0.649	9.9[illegible]	3[illegible]	44	[illegible]	44.2[illegible]	[illegible]	[illegible]	5[illegible]	5[illegible]	[illegible]	web	Mode 2
A-4-3	5140	0.[illegible]	10.15[illegible]	42	[illegible]	[illegible]	[illegible]	[illegible]	[illegible]	54.[illegible]	[illegible]	[illegible]	web	Mode 2
A-3-3	4460	0.77[illegible]	9.91[illegible]	28	41	[illegible]	4[illegible].34	[illegible]	[illegible]	[illegible]	[illegible]	[illegible]	web	Mode 2
A-5-2	4549	0.26[illegible]	5.036	1[illegible]	2[illegible]	[illegible]	39.[illegible]	192.4	3.04	44.[illegible]	[illegible]	[illegible]	web	Mode 2
A-4-2	473[illegible]	0.272	5.626	12	[illegible]	[illegible]	38.[illegible]	166.5	2.69	4[illegible]	16[illegible]	3.24	web	Mode 2
A-3-2	4390	0.243	5.189	15	20	[illegible]	4[illegible].6[illegible]	215.5	[illegible]	5[illegible]	240.6	4.[illegible]	web	Mode 2
A-0-1	5383	0.085	2.219	14	[illegible]	39.[illegible]	[illegible].04	267.5	4.52	36.23	42[illegible]	6.55	BF	Mode 1
A-5-1	4896	0.089	2.219	12	[illegible]	24.0	[illegible]	[illegible]	4.[illegible]	44.[illegible]	5[illegible].4	[illegible]	BF	Mode 1
A-4-1	440[illegible]	0.094	2.437	6	[illegible]	19.5	[illegible]	292.[illegible]	4.29	39.9	4[illegible]	[illegible]	BF	Mode 1
A-3-1	5686	0.087	2.220	10.5	9	[illegible]	[illegible]	291.4	[illegible]	43.9	5[illegible]	[illegible]	BF	Mode 1
A-3-0	4708	0	0	5.5	5.5	26.5	[illegible]	[illegible]	4.[illegible]	-	[illegible]	[illegible]	BF	No torsion
B-3-4	4932	-	-	30	[illegible]	[illegible]	[illegible]	[illegible]	[illegible]	6[illegible].9	[illegible]	[illegible]	TF web	Mode 2
B-5-3	447[illegible]	0.59[illegible]	10.4[illegible]	30.5	[illegible]	[illegible]	[illegible]	[illegible]	[illegible]	4[illegible].55	[illegible]	2.[illegible]	web	Mode 2
B-4-3	5135	0.628	10.135	[illegible]	[illegible]	[illegible]	[illegible]	[illegible]	[illegible]	4[illegible].44	[illegible]	[illegible]	web	Mode 3
B-3-3	473[illegible]	0.59[illegible]	10.29	[illegible]	[illegible]	[illegible]	[illegible]	[illegible]	[illegible]	[illegible]	[illegible]	2.5[illegible]	web	Mode 2
B-5-2	5109	0.274	5.153	2[illegible]	[illegible]	14.5	[illegible]	[illegible]	4.46	[illegible]	[illegible]	4.[illegible]	web BF	Mode 2
B-4-2	4431	0.259	5.05	30	26	14.[illegible]	[illegible]	[illegible]	4.3[illegible]	[illegible]	[illegible]	4.[illegible]	web	Mode 2
B-3-2	4670	0.281	5.161	2[illegible]	[illegible]	[illegible]	[illegible]	[illegible]	4.[illegible]	65.2[illegible]	[illegible]	5.[illegible]	web	Mode 2
B-5-1	4930	0.08[illegible]	2.204	[illegible]	[illegible]	[illegible]	27.[illegible]	3[illegible]	[illegible]	3[illegible]	4[illegible]	6.[illegible]	BF	Mode 1
B-4-1	4684	0.087	2.219	[illegible]	[illegible]	[illegible]	33.44	[illegible]	[illegible]	43.[illegible]	[illegible]	[illegible]	BF	Mode 1
B-3-1	5279	0.09[illegible]	2.325	[illegible]	[illegible]	[illegible]	[illegible]	[illegible]	[illegible]	4[illegible]	4[illegible]	[illegible]	BF	Mode 1
B-3-0	4354	0	0	6.5	6.5	[illegible]	[illegible]	35[illegible]	6.39	[illegible]	[illegible]	[illegible]	BF	No torsion
C-0-4	423[illegible]	[illegible]	[illegible]	[illegible]	[illegible]	[illegible]	4[illegible]	[illegible]	[illegible]	[illegible]	[illegible]	[illegible]	TF	Mode 2
C-5-4	4516			[illegible]	[illegible]	[illegible]	4[illegible]	[illegible]	[illegible]	[illegible]	[illegible]	[illegible]	TF	Mode 2
C-4-4	[illegible]			[illegible]	[illegible]	[illegible]	4[illegible]	[illegible]	[illegible]	[illegible]	[illegible]	[illegible]	TF	Mode 2
C-5-3	4440	0.[illegible]	9.96[illegible]	[illegible]	[illegible]	[illegible]	[illegible]	[illegible]	[illegible]	[illegible]	[illegible]	[illegible]	web	Mode 2
C-4-3	[illegible]	0.[illegible]	9.[illegible]	[illegible]	[illegible]	[illegible]	[illegible]	[illegible]	[illegible]	[illegible]	[illegible]	[illegible]	web	Mode 2
C-3-3	5139	0.48[illegible]	10.[illegible]	40	[illegible]	[illegible]	[illegible]	[illegible]	[illegible]	[illegible]	[illegible]	[illegible]	web	Mode 2
C-5-2	4930	[illegible]	[illegible]	[illegible]	[illegible]	[illegible]	[illegible]	[illegible]	[illegible]	[illegible]	[illegible]	[illegible]	web	Mode 2
C-4-2	[illegible]	[illegible]	[illegible]	[illegible]	[illegible]	[illegible]	[illegible]	[illegible]	[illegible]	[illegible]	[illegible]	[illegible]	TF [illegible]	Mode 2
[illegible]	412[illegible]	0.[illegible]	[illegible].124	[illegible]	[illegible]	[illegible]	[illegible]	[illegible]	[illegible]	[illegible]	[illegible]	[illegible]	[illegible]	Mode 2
[illegible]	[illegible]	[illegible]	[illegible]	[illegible]	[illegible]	[illegible]	[illegible]	[illegible]	[illegible]	[illegible]	[illegible]	[illegible]	[illegible]	Mode 1
C-4-1	5003	0.085	2.236	13.75	[illegible]	[illegible]	[illegible]	[illegible]	[illegible]	[illegible].58	[illegible]	[illegible]	BF	Mode 1
C-3-1	4519	0.08[illegible]	2.214	[illegible]	[illegible]	[illegible]	[illegible]	214.[illegible]	[illegible]	[illegible]	[illegible]	[illegible]	BF	Mode 1
D-3-4	4879				16	[illegible]	45.24	[illegible]	[illegible]	[illegible]	[illegible]	[illegible]	TF	Mode 2
D-3-4A	440[illegible]	[illegible]	19.597	40	[illegible]	[illegible]	5[illegible].29	[illegible]	[illegible]	[illegible]	[illegible]	[illegible]	TF	Mode 2
D-3-3	5238	0.607	9.79	29	33	[illegible]	5[illegible]	[illegible].9	[illegible]	62.8	[illegible].6	2.5[illegible]	TF web	Mode 2
D-3-2	476[illegible]	0.278	5.120	43.5	2[illegible]	14.0	49.85	[illegible]4.4	3.95	60.24	2[illegible].4	4.[illegible]	web BF	Mode 2
D-3-1	4955	0.083	2.214	5.5	[illegible]	2[illegible].5	[illegible]	2[illegible].9	[illegible].39	4[illegible]	50[illegible]	[illegible].55	BF	Mode 1
D-3-0	4820	0	0	[illegible]	6	24.0	[illegible]	[illegible]	3.82	[illegible]	534.2	[illegible].05	BF	No torsion

[a] Distance of initial crack from transverse load.
[b] Distance of center of failure surface from transverse load.
[c] Calculated by statics at the location of initial crack.
[d] Calculated by statics at the center of failure surface.

TF - Top Face;
BF - Bottom Face.

TABLE 6.2

EXPERIMENTAL DEFORMATIONS

	At cracking		At ultimate				
	ϕ_{cr}[a] (10^{-6} Rad/in)	Δ_{cr}[b] (in)	ϕ_u[a] (10^{-6} Rad/in)	Δ_u[b] (in)	$(T_{cr})_{Test}$	$(\frac{T_{cr}}{T_u})_{Test}$	$\frac{T_{cr}/\phi_{cr}}{\text{k-in}^2/\text{rad} \times 10^{-4}}$
A-0-4	309.7	--	506	--	36.02	0.96	11.6
A-5-4	302.8	--	842	--	47.94	0.87	15.8
A-4-4	331.9	--	1233	--	46.59	0.83	14.0
A-3-4	290.3	--	2108	--	38.64	0.76	13.3
A-5-3	276.4	0.050	731	0.075	44.21	0.88	16.0
A-4-3	336.1	0.035	721	0.040	50.28	0.89	14.96
A-3-3	284.7	0.050	1704*	0.140	43.34	0.77	15.22
A-5-2	260.8	0.080	647	0.125	39.01	0.84	14.96
A-4-2	291.7	0.085	624	0.125	38.33	0.83	13.14
A-3-2	356.9	0.105	961	0.175	47.68	0.82	13.36
A-0-1	116.7	0.155	271	0.510	25.04	--	21.46
A-5-1	127.2	0.115	524	0.630	25.08	0.56	19.72
A-4-1	144.4	0.125	438	0.565	27.84	0.70	19.28
A-3-1	143.1	0.128	541	0.530	25.99	0.59	18.16
A-3-0	0	0.115	0	0.670*	0	--	--
B-3-4	450	--	1916*	--	53.33	0.86	11.85
B-5-3	417	0.055	628	0.070	58.08	0.94	13.93
B-4-3	445.8	0.055	1966	0.070	60.68	0.92	13.61
B-3-3	431	0.060	1703	0.100	57.21	0.87	13.27
B-5-2	434.7	0.123	622	0.140	57.43	0.92	13.21
B-4-2	393.1	0.110	603	0.140	56.35	0.90	14.3
B-3-2	331.9	0.100	722	0.185	54.18	0.83	16.3
B-5-1	140.3	0.115	328*	0.21*	27.86	0.74	19.86
B-4-1	173.6	0.160	343	0.32	33.44	0.77	19.26
B-3-1	158.3	0.120	439*	0.35	29.72	0.68	18.77
B-3-0	0	0.150	0	0.690	0	--	--
C-0-4	266	--	403	--	41.26	0.92	15.51
C-5-4	320.5	--	1775	--	45.24	0.91	14.10
C-3-4	298.6	--	2017	--	45.25	0.77	15.15
C-5-3	336.1	0.050	1462	0.105	41.61	0.89	12.38
C-4-3	313.0	0.050	1875	--	48.95	0.87	15.51
C-3-3	361.1	0.045	2014	0.17	49.41	0.88	13.68
C-5-2	294.4	0.085	519	0.095	39.27	0.94	13.34
C-4-2	327.8	0.115	842	0.145	44.75	0.94	13.65
C-3-2	236	0.090	850	0.225	36.84	0.79	15.61
C-5-1	79.2	0.105	435	0.98	20.07	0.50	25.34
C-4-1	69.4	0.120	393*	0.62*	20.43	0.52	29.44
C-3-1	81.9	0.120	556	1.29	19.43	0.49	23.72
D-3-4	347	--	950	--	45.24	0.80	13.04
D-3-4A	387.5	0.010	904*	0.03	50.29	0.84	12.98
D-3-3	388.9	0.065	1369	0.125	57.27	0.91	14.73
D-3-2	334.7	0.110	761	0.145	49.85	0.83	14.89
D-3-1	87.5	0.115	510	0.69	48.58	0.44	21.23
D-3-0	0	0.115	0	0.72*	0	--	--

[a]Rotation measured over a gage length of 48 inches

[b]Deflection measured at a distance of 7 inches from the transverse load

*Deformations at one load stage prior to the ultimate stage

following two reasons the actual magnitude of δ deviated slightly from the nominal value. Firstly in each beam test torque and shear were applied simultaneously maintaining the same predetermined load ratio at the end of each increment throughout the whole loading range. However in some beams failure occurred while the torque was still being applied. Secondly, for some beams in applying the increment leading to failure, a very large rotation was necessary to reach the predetermined torque. In this process of twisting the failure torque sometimes slightly exceeded the predetermined torque corresponding to the load increment. The ultimate loads presented in Table 6.1 relate to the centre of the failure surface.

6.2 Behavior Under Test

In all the nine beams tested under pure torsion, the initial cracks formed in the middle of the top face at torques ranging from 76 to 96 percent of the ultimate torques. In the case of B-3-4 initial cracks occurred simultaneously in the top face and in the web at its junction with the top flange. The inclination of the initial cracks with respect to the axis of the beam was 37, 36, 31 and 36 degrees in series A, B, C and D respectively. As the torsional load was increased, these cracks extended across the width of the top flange and down the vertical faces. At about the same load, cracks occurred independently in the web. Web cracks extended down to the bottom of the web. Generally the web cracks joined the wider cracks on the flange sides, but in some cases they were slightly apart. In other cases they were bridged by a horizontal crack along the web-flange junction.

When the web cracks spread downwards, beams A-0-4 and C-(-4 without web reinforcement failed suddenly. As the beam approached failure load one major web crack opened with the appearance of web crushing on the opposite face of the web in a skew bending mode. These beams without stirrups developed only one crack.

In beams with stirrups further increases in torque caused more cracks to appear on the top face and the web. As the stirrup spacing reduced the cracks were more numerous. In the later stages of loading several diagonal tension cracks formed in the bottom flange spreading continuously up the vertical sides of the bottom flange. As the failure was approached the diagonal tensile cracks on the top face, and the side faces of both flanges were quite wide, and the torsional displacements between concrete on either side of these cracks were clearly visible. Failure was triggered by yielding of the stirrups accompanied by compression distress in the top flange, together with web crushing and shear compression failure of the bottom flange. The shear compressive distress was more extensive in the bottom flange if the eccentricity was high as in the case of A-4-4, A-5-4, and D-3-4 or if prestress was high as in the case of B.3.4. If the level and eccentricity of prestress was less this distress was also less as evidenced in the pure torsion beams of series C. Yielding of stirrups occurred only one or two load increments prior to failure. Beams in pure torsion failed in skew bending Mode 2; in some beams the line of web crushing was somewhat arbitrary and it was either on the south or on the north side of the web. Beams with stirrups ex-

hibited increased strength and ductility as compared to those without.

The type of web reinforcement used in the present test beams has adequately resisted the torsional load without any anchorage failure; the vertical legs developing yield strain. This can be found by comparing two beams with and without stirrups. A-0-4 without stirrups cracked initially on the top face and the failure followed immediately. In the case of all beams with stirrups redistribution of stresses occurred after cracking; stirrups carried the tensile forces formerly held by the concrete. Further increases of load caused the stirrups to yield and the gain in strength beyond cracking was as much as 25 percent for pure torsion beams, depending on the amount of stirrups.

Beams tested at load combination 3 had high torsion, low bending moment and shear force. The initial diagonal tension cracks in these beams originated on the south face of the web. On this face the torsional and flexural shear stresses were additive while they were subtractive on the north face of the web. Cracks on the north face were comparatively fewer in number than on the opposite face. The first cracks were sloped to the axis of the beam at 33, 38 and 36 degrees respectively for series A, B and C. A further one or two increments of load developed cracks on the top face which extended over the top flange sides. On the south face of the web numerous diagonal cracks appeared fairly evenly propagating throughout the web; the closer the spacing of the stirrups the closer the spacing of the cracks. The bottom flange face developed cracks independently which linked up to the cracks on its sides occurring at about the same time.

Further increase of load caused opening up of one major crack and subsequently failure resulted from yielding of the stirrups followed by a shear compression failure of both the flanges and compression distress on the north face of the web in Mode 2; these were readily noticeable in the case of highly prestressed beams of Series B, but not clear in the case of other beams. These failures were highly ductile. In the range of large rotation, beams with stirrup spacing at 3 inches exhibited increasing resistance to load as the rotation increased. For beams with larger stirrup spacing increasing rotation resulted in decreasing strength as in Series A and B, and increasing strength in Series C. This rate of increase or decrease of strength as rotation increased depended on the level and eccentricity of prestress, as can be found in Fig. 6.1 through Fig. 6.3.

Beams loaded at load combination 2 developed initial cracks mainly in the web and occasionally in the bottom flange at 83 to 88 percent of the ultimate load. The inclination of these cracks to the axis of the beam was 27, 33 and 26 degrees for series A, B and C beams. Crack propagation was similar to that described for load combination 3. All beams appeared to fail in a torsion mode accompanied by a shear compression failure of the flanges for most beams; however the line of web compression was not clear in several beams.

The beams tested at load combination 1 had a high proportion of flexural moment and shear. Except in series D, the T/M ratio is approximately equal to the ratio of the ultimate torsional and bending capacities. The first cracks to form were flexural either on the

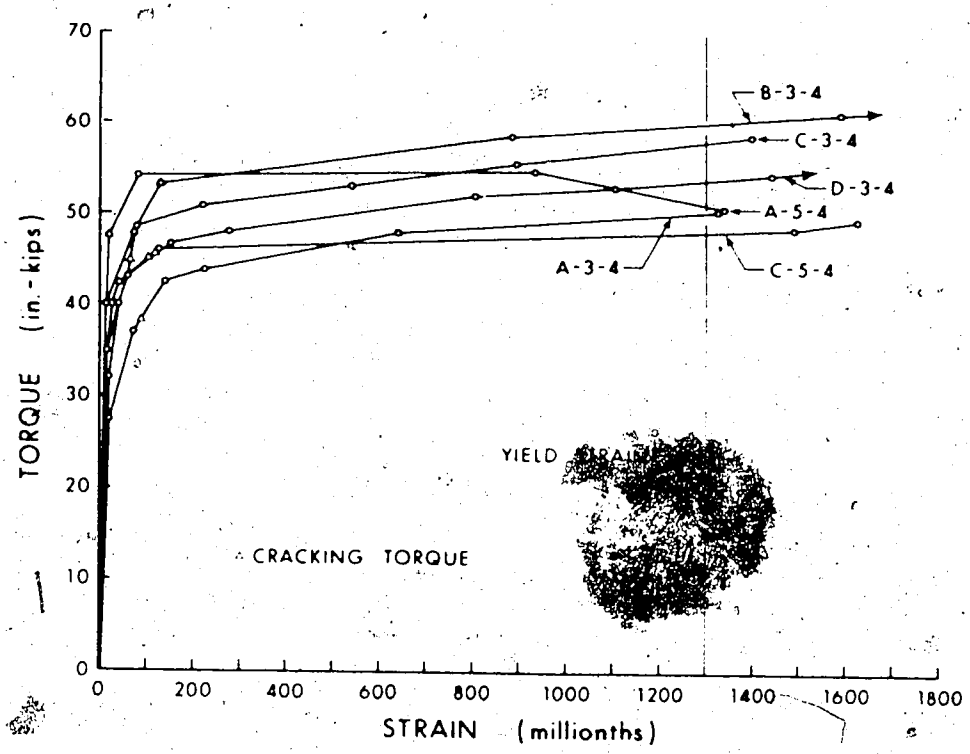

FIG. 6.1 TORQUE-MAXIMUM WEB REINFORCEMENT STRAIN CURVES OF BEAMS UNDER PURE TORSION

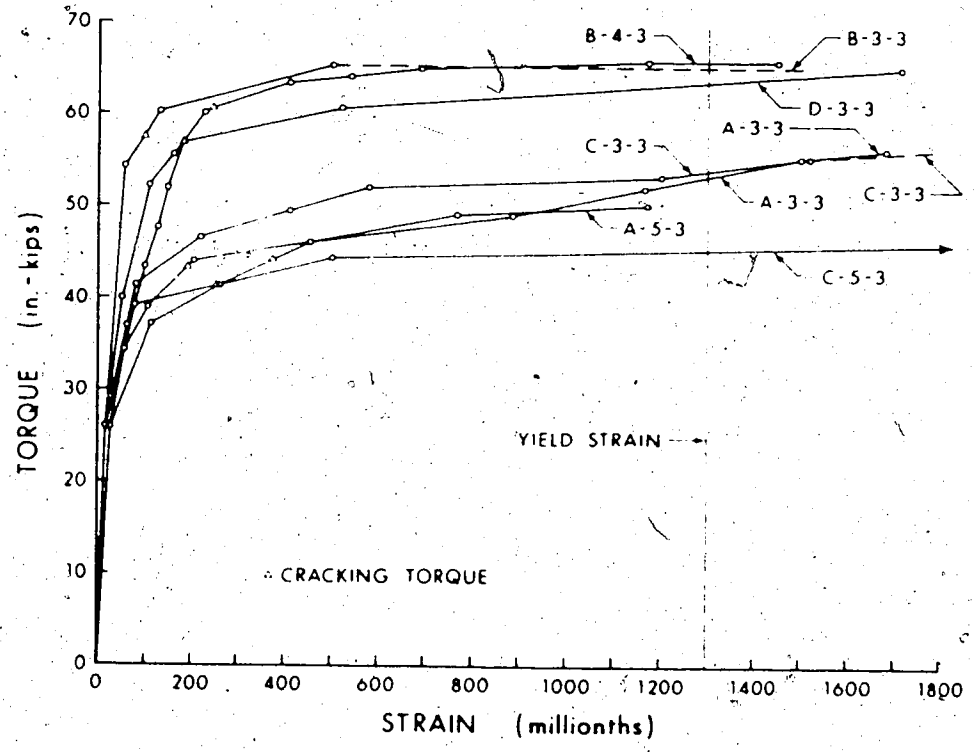

FIG. 6.2 TORQUE-MAXIMUM WEB REINFORCEMENT STRAIN CURVES OF BEAMS AT LOAD COMBINATION 3

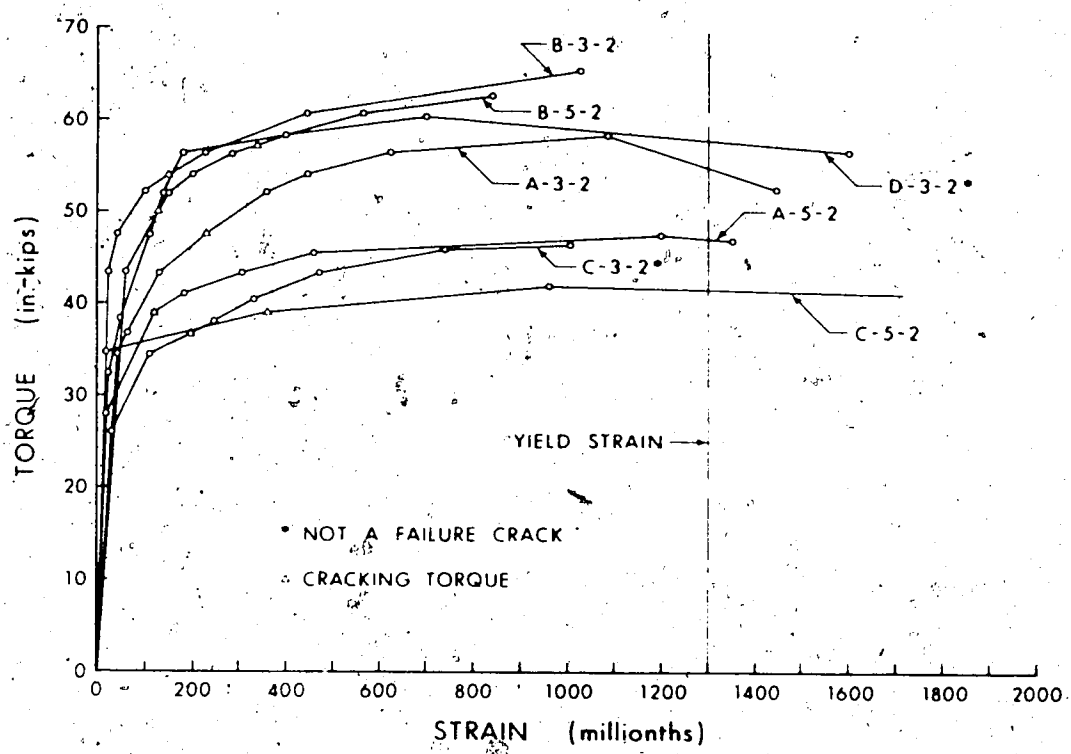

FIG. 6.3 TORQUE-MAXIMUM WEB REINFORCEMENT STRAIN CURVES OF BEAMS AT LOAD COMBINATION 2

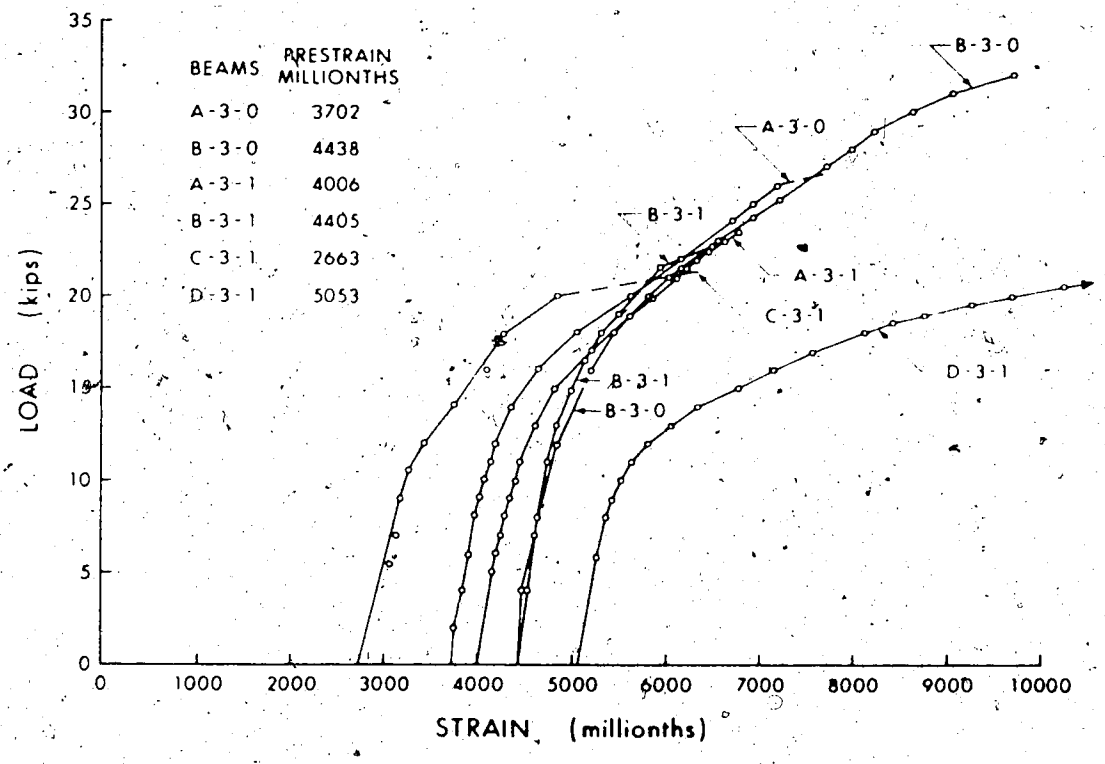

FIG. 6.4 LOAD-MAXIMUM STRAND STRAIN CURVES OF BEAMS AT LOAD COMBINATION 1

bottom or on the south vertical side of the bottom flange. Depending on the magnitude and level of prestress the cracking torque was between 50 and 73 percent of the ultimate load. The initial cracks sloped at 50 to 75 degrees to the axis of the beam. The cracks on the bottom flange sides were nearly vertical and linked up those on the bottom face. As the load increased cracks formed in the lower parts of the web and extended upwards with further increase of load, travelling towards the load point. Cracks on the north side of the web were fewer than on the south side and occasionally there were none. If they were present they could not propagate as far as top flange except in the case of Series C beams. The cracks on this side were inclined as on the south side, towards the flexural load because of the greater influence of flexural shear stresses. On the south side, the diagonal cracks reached the top flange-web junction and after travelling along this junction extended into flange side at a smaller inclination to the horizontal than in the web. At higher loads, cracks formed independently in the middle of the top face and these joined the cracks on the side faces. At this point the outstanding parts of the top flange started to split away from the web, reducing the available area resisting the compressive force. Consequently failure occurred immediately in a skew bending mode since the middle of top face crushed and the compression distress extended into the web. This was the general behavior observed for all these beams with slight variations among the different series. Beam A-4-1, tested at a slightly higher T/M ratio, exhibited more torsional cracking. In beam

D-3-1 the bottom strands fractured at failure, developing nearly the flexural capacity and the torque associated with its T/M ratio. Irrespective of the magnitude and eccentricity of prestress and variation of amounts of longitudinal and stirrup reinforcements, these beams failed approximately at the same loads. The likely reason for this is the reduced compressed area of the top flange due to torsional cracking. When the torsional cracks reached the top flange-web junction, these tended to split off the outstanding flanges. The effective compression zone then decreased significantly and the compressive force required to balance the yield forces of the tensile reinforcement could not be developed; hence the failure was sudden and violent. Such a behavior will probably be nonexistent in rectangular beams, and is applicable to I beams.

Beams A-3-0, B-3-0 and D-3-0 were subjected to bending and shear only. D-3-0 having least longitudinal steel of the above three beams, failed in bending in an under-reinforced manner. The initial tensile cracks appeared at about 50 percent of the ultimate load in the bottom flange and spread to the side faces of the flange almost vertically. As the load increased, these cracks extended into the web and propagated towards the transverse load point. They reached the web-top flange junction at about 90 percent of the failure load. At the same time tensile cracks in the bottom flange were quite wide. When inelastic strand strains were reached large deflections occurred with little increase in load, finally leading to crushing of the concrete. This was followed by fracture of the bottom strands. The

beam thus developed its full flexural capacity.

Beam B-3-0 had a higher prestress than D-3-0 and A-3-0 and was slightly over-reinforced. The initial cracks originated in the bottom flange at approximately 50 percent of the ultimate load. The cracks curved towards the load point in the web as in the case of D-3-0, but the number of cracks were fewer in this case and extended to only about 75 percent of web depth at 90 percent of ultimate load. They did not seem to penetrate further. Failure occurred suddenly and violently in that the crushing extended into the web fully and it was completely destroyed. The strands in the compression zone buckled.

Beam A-3-0 was designed to exhibit approximately a balanced failure, but failed in a slightly over-reinforced way. First cracks appeared in the bottom flange at about 45 percent of the ultimate load and the behavior was nearly same as that of B-3-0 except that the cracks which curved towards the load point extended higher in the web than in the case of B-3-0, almost reaching web-top flange junction. In this beam also at failure the compression zone was completely destroyed, the compression distress was evident in most of the web and the top strands also buckled.

Generally for all beams failure occurred in skew bending either in a bending mode or a torsion mode. However in a few cases, particularly in some beams tested using load combination 2, the failure mode was not clear. They might have failed in a mode transitional between bending mode and torsion mode. In some cases it was difficult to establish the failure section, because of discontinuous

cracks, and absence of a line of compression distress.

6.3 Deformations

6.3.1 Torsional Stiffness

The torque-twist curves for all beams are presented in Appendix A. In Table 6.2 the test secant torsional stiffness at cracking is tabulated for each beam. The torque-twist curves are essentially linear in the initial portion up to about 70 percent of the cracking load. A study of the initial torsional stiffness reveals that it is apparently little affected by the amount of transverse reinforcement, loading combination, level and eccentricity of prestress and the amount of flexural shear. When the cracking torque is approached the torque-twist relationship becomes nonlinear, more so in the case of beams with high cracking torques. The secant torsional stiffness at cracking as shown in Table 6.2 is approximately the same for all the beams except for those tested with loading combination 1, that is, with predominant bending moment where it was slightly larger. This is probably due to the following reason: Beams exhibiting higher torsional stiffness cracked in the bottom face in bending mode at considerably smaller torques than other beams which failed in torsion mode. At higher torque the torsional stiffness was smaller due to microcracking and smaller shear modulus. It can be seen from Table 6.2 that the beams in C series tested at load combination 1 and cracking at the lowest torques, have the highest torsional stiffnesses.

Post cracking torsional stiffness depended on several factors, primarily on the level of prestress, eccentricity of prestress, T/M

ratio, and amount of steel.

The torque-twist diagrams indicate that as the magnitude of the flexural [illegible] increased the torsional ductility decreased. This can be clearly observed when beams tested at loading combination 1 and others are compared. A decrease in T/M ratio caused a decrease in the rotation capacity. When T/M ratio was low the loss in torsional stiffness after cracking occurred very slowly and gradually. This is because the progress of flexural cracking is less extensive than that of torsional cracking. For a beam under pure torsion, addition of small amounts of flexural moment and shear delayed cracking, changed the mode of cracking and enabled the beam to retain the precracking stiffness up to torques greater than pure torque capacity. However subsequent decline in post cracking stiffness was faster. This behavior is readily noted in B-3-4, B-3-3, and B-3-3 and applies equally well to other series. Beams with less eccentricity exhibited a less gradual reduction in torsional stiffness than beams with higher eccentricity in the vicinity of the cracking load since cracking is more gradual in the latter case. It can be seen in Table 6.2 and also in the torque-twist curves for series B beams that the angle of twist at failure was generally less than for corresponding beams in other series. Stated otherwise, prestress reduced torsional ductility. It is observed from the torque-twist curves that the stiffness of all beams was reduced nearly to zero at ultimate load.

6.3.2. Flexural Stiffness

Load deflection curves for all beams are presented in Appendix A. The initial portions of the load-deflection curves are generally

straight. The flexural stiffnesses of the uncracked beams corresponding to the earlier stages of the load-deflection diagrams are about the same. These curves are similar in shape to torque-twist curves in the uncracked range. After cracking, the flexural stiffness reduced, gradually, and also flexural ductility increased as T/M ratio decreased after cracking.

6.4 Reinforcement Strains

Data obtained from the strain gages is generally qualitative because of several uncertainities. However from the measured strains several behavioral trends can be observed. The strain gages in the present test program were not monitored continuously. Measurements were made at the end of each load increment. In the case of abrupt failures the readings may correspond to a load slightly less than the ultimate load. In a few beams the gages were intersected only by minor cracks but not by failure cracks.

Prior to cracking the stirrups were virtually unstressed. It can be seen in Fig. 6.1 through Fig. 6.3 that the maximum stirrup strain at cracking was about 0.0001 for beams under pure torsion and about 0.0003 to 0.00035 for beams cracking in the web. For most beams these strains did not increase significantly immediately upon cracking. The strains increased rapidly as the loadings approached the ultimate stage. Stirrups generally yielded when crossed by the failure crack. In several beams yielding of stirrups occurred only at or immediately after ultimate load. In other beams stirrups yielded at increased rotation of the beam at a load lower than the ultimate load as in the case of A-3-2 and D-3-2. Stirrups did not yield in B-3-2 and B-5-2

though in B-3-4 stirrups exhibited yield strains. In no case did strands yield in the beams failing in the torsion mode. Vertical stirrup legs in the web close to the compression zone recorded tensile strains. Other investigators made a similar observation in prestressed rectangular beams. As T/M ratio reduced, the strand strains increased and the top strands recorded compressive strains. In the pure torsion beams of Series A, the strand strains were of the order of 0.0005. When δ decreased, strain in prestressing strand near the bottom increased for each additional load increments; the increase being dependent on the load ratio δ.

For typical beams failing in a bending mode, the relationship between the transverse load and the bottom strand strain is shown in Fig. 6.4. Except D-3-1 which failed developing its full flexural capacity and torque corresponding to the T/M ratio, where the bottom strands fractured, no other beam developed yield strain in the strands because of the premature failure of the top flange. Though the cracks were very wide the measured induced strains over and above the pre-strain, were of the order of only 0.003 to 0.004 in various beams failing in the bending mode. This is probably due to the larger contribution of torsion to the crack width as compared to that from bending.

6.5 Ratio $M_u/V_u d$

The shear span of 72 in. adopted in the test program shown in Fig. 5.5. was always the same. However, the resulting $M_u/V_u d$ ratios were different for the test beams since the location of the failure section depended on the ratio $T_u/V_u b_w$ or T_u/M_u. From Table 6.1 the

ratio $M_u/V_u d$ for each beam can be computed readily. It ranges from 2.63 to 3.96 for beams at load combination 3, 3.81 to 4.85 for all except one beam of load combination 2, 5.68 to 6.03 for beams at load combination 1, and 5.98 to 6.07 for beams tested in flexure-shear.

6.6 Failure Section

In tests under combined loadings giving rise to a moment gradient, the failure surface assumes importance, as the ultimate flexural moment can be established correctly only if the location of the failure surface is known precisely. Generally a bending mode failure occurs close to the transverse load, in a torsion mode the location of the failure depends on the T/M ratio while in the case of pure torsion it is arbitrary. Because it is impossible to predict the failure surface theoretically and no clearly defined location of the failure surface was observed in the tests, the test results at best are useful to indicate regions of failure surface location. In the bending mode, the failure occurred at a distance of 7 to 10 inches from the centre of the transverse load which is applied through a six inch wide bearing plate. As the flexural shear and moment were reduced relative to torque the failure section moved away from the transverse load. The relationship between load ratio δ and the location of the failure section relative to the transverse load X_u is shown in Fig. 6.5. Beams tested under load combinations 2 and 3, failing in torsion mode, had average X_u differing by about 10 inches. However the difference of X_u for bending and torsion mode failures was about 20 inches. The critical section for beams in pure torsion, not shown in Fig. 6.5, but listed in Table 6.1 varied from about 30

inches to 38 inches. If the strength prediction equations do not have a term involving flexural moment, the value of X_u is not required in estimating the ultimate capacity in torsion mode failures. However, it will be difficult to predict the flexural moment with equal precision. For predicting bending mode failures this location must be known beforehand. However a conservative result can be obtained assuming the critical section at the transverse load.

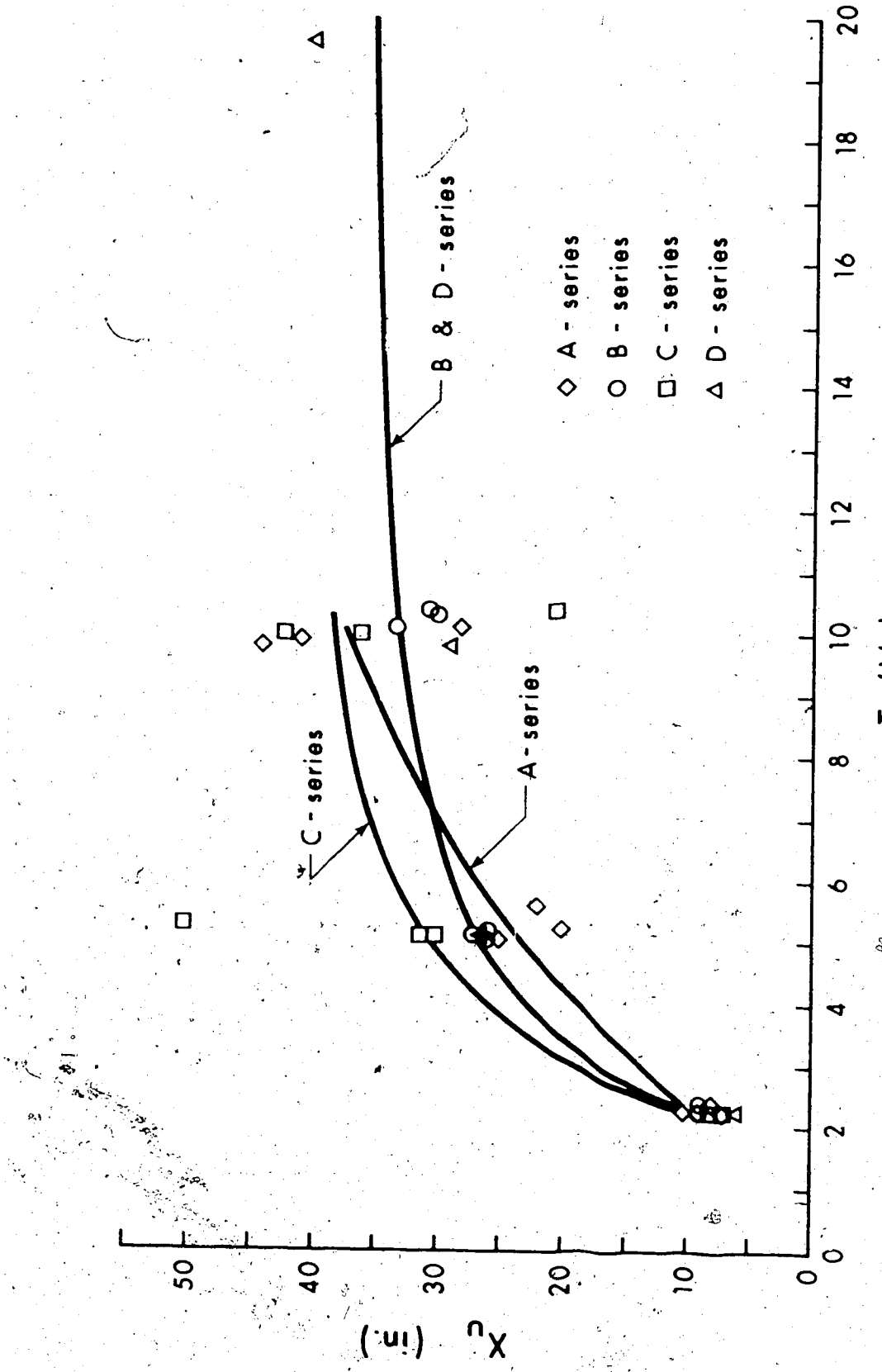

FIG. 6.5 VARIATION OF LOCATION OF FAILURE SURFACE FROM THE TRANSVERSE LOAD

CHAPTER VII

APPLICATION OF THEORETICAL ANALYSES AND DISCUSSION OF TEST RESULTS

7.1 Introduction

In this Chapter, the test results are evaluated, the cracking and ultimate strength theories developed in Chapters III and IV are applied to the test specimens of the present investigation and several others. Comparisons of observed and analytical results are made in Tables 7.1 through 7.7. The interaction of torsion, bending and shear is discussed.

7.2 Cracking Strength

7.2.1 Method 2 (Finite Element Method)

First, the test results of beams of the present investigation are compared with the theoretical cracking strengths obtained by the finite element method of analysis. These strengths together with the maximum principal tensile stresses and deformations are furnished in Table 7.1. For the convenience of discussion beams in which initial cracks occurred on the top face, in the web, and on the bottom face are defined as cracking in Mode 3, Mode 2 and Mode 1 respectively, analogous to the designations of modes of failure of beams. The test beams exhibited all the three modes of initial cracking. Except for one beam, the theory did not over predict the strength of any of the

TABLE 7.1

COMPARISON OF FINITE ELEMENT ANALYSIS WITH TEST RESULTS

Beam No.	P_{cr} (psi)	T_{cr} (in-kip)	P_{cr} (psi)	T_{cr} (Test) (in-kip)	Maximum principal tensile stress at test cracking loads by FEM (psi)	T_{cr} FEM (in-kip)	$\frac{T_{cr}(Test)}{T_{cr}(FEM)}$	Angle of Twist (Rad per in x 10^{-6}) At 70% of test T_{cr} (Test)	At 100% of test T_{cr} FEM)	At 70% of Test T_{cr} (Test) / At 100% of Test T_{cr} FEM)	Flexural Deflection (in x 10^{-3}) At 70% of test T_{cr} (Test)	At 100% of test T_{cr} FEM)	At 70% of test T_{cr} (Test) / At 100% of Test T_{cr} FEM)
A-0-4	4825	-	0	36.00	523	34.63	1.04	142	137	1.06		6.9	-
A-5-4	5480	-	0	41.94	657	41.33	1.16	165	153	1.08		8.3	-
A-4-4	4706	-	0	46.59	687	36.12	1.29	175	168	1.04		6.2	-
A-3-4	4254	-	0	38.64	559	34.50	1.12	143	114	1.25		5.9	-
A-5-3	4372	10.40	5.10	44.21	689	35.37	1.25	100	160	.63	25	32	.78
A-4-3	5140	10.40	5.80	50.26	600	38.38	1.31	175	192	.96	22	34	.59
A-3-3	4460	10.40	5.00	43.34	723	33.60	1.29	130	157	.83	30	30	1.00
A-5-2	4549	5.20	9.00	39.01	685	31.98	1.22	152	141	1.08	43	52	.83
A-4-2	4737	5.75	10.00	46.03	669	32.21	1.15	175	138	1.27	50	45	1.11
A-3-2	4390	5.20	11.00	47.68	861	33.58	1.42	190	172	1.10	65	64	1.02
A-0-1	5383	2.23	13.50	25.04	772	21.59	1.16	65	91	.71	83	71	1.17
A-5-1	4896	2.23	13.50	25.08	737	21.81	1.15	74	90	.82	77	73	.96
A-4-1	4407	2.57	13.00	27.84	743	23.39	1.19	75	100	.75	83	72	1.15
A-3-1	5686	2.23	14.00	25.99	675	24.29	1.07	97	93	1.05	85	71	1.20
A-3-0	--	--	--	--	--	--	--	--	--	--	-	-	-
B-3-4	4932	-	0	53.33	773	43.01	1.24	224	193	1.16		4.3	-
B-5-3	4401	10.40	6.70	58.08	873	40.33	1.44	210	209	1.00	33	39	.85
B-4-3	5135	10.40	7.00	60.68	893	43.65	1.39	209	220	.95	34	39	.87
B-3-3	4731	10.40	6.60	57.21	858	41.16	1.39	245	214	1.14	43	37	1.16
B-5-2	5103	5.20	13.25	57.43	994	39.07	1.47	216	314	.69	78	72	1.08
B-4-2	4431	5.20	13.00	56.35	982	37.07	1.52	197	211	.93	70	68	1.03
B-3-2	4670	5.20	12.50	54.18	952	39.26	1.38	175	203	.86	63	67	.94
B-5-1	4930	2.23	15.00	27.86	602	26.52	1.05	86	105	.81	80	79	1.03
B-4-1	4654	2.23	18.00	33.44	542	25.72	1.30	99	122	.80	100	93	1.08
B-3-1	5279	2.23	16.00	29.72	701	26.77	1.11	101	107	.94	68	62	1.05
B-3-0	--	--	--	--	--	--	--	--	--	--	-	-	-
C-0-4	4237	-	0	41.26	594	35.57	1.16	149	149	1.00		2	
C-5-4	4616	-	0	45.24	681	36.19	1.25	153	169	.91		2	
C-4-4	5132	-	0	45.25	677	38.23	1.19	167	189	.88		2	
C-5-3	4442	10.4	4.80	41.61	727	32.76	1.27	159	150	1.06	32	24	1.33
C-4-3	5337	10.4	5.60	48.55	869	34.68	1.40	157	182	.86	35	29	1.21
C-3-3	5539	10.4	5.70	49.47	880	35.55	1.39	175	185	.95	25	29	.86
C-5-2	4930	5.54	8.50	39.27	793	30.92	1.27	168	147	1.13	58	44	1.27
C-4-2	4676	5.20	10.00	44.75	1000	29.83	1.50	161	168	.96	60	52	1.15
C-3-2	4525	5.20	8.50	36.84	787	28.12	1.31	135	138	.96	44	43	1.16
C-5-1	4734	2.23	10.80	20.07	653	17.92	1.12	45	72	.63	63	56	1.13
C-4-1	5003	2.23	11.00	20.43	697	17.92	1.14	48	74	.64	77	56	1.37
C-3-1	4515	2.23	10.50	19.46	629	17.55	1.11	50	77	.70	65	55	1.18
D-3-4	4879	-	0	45.24	640	38.34	1.18	180	162	1.11		4	
D-3-4A	4407	20.80	2.90	50.29	757	37.53	1.34	191	182	1.05	33	20	1.65
D-3-3	5238	10.40	6.60	57.27	988	37.93	1.51	210	208	1.01	40	37	1.08
D-3-2	4767	5.20	11.50	49.85	1068	32.80	1.52	179	181	.99	67	63	.97
D-3-1	4955	2.23	10.00	15.56	459	19.85	.94	57	67	.85	67	54	1.24
D-3-0	--	--	--	--	--	--	--	--	--	--	-	-	-
						Average	1.26			.94			1.03

TABLE 7.2

COMPARISON OF THEORETICAL AND TEST CRACKING STRENGTHS

Beam No.	$(\frac{T}{Vb})_{cr}$	P_{cr} (kip)	First observed crack: Distance from load (in)	First observed crack: Location on Section	Test T_{cr} (in-kip)	FEM T_{cr} (in-kip)	Plastic[a] theory T_{cr} (in-kip)	Plastic[b] theory T_{cr} (in-kip)	$\frac{T_{cr}(Test)}{T_{cr}(FEM)}$	$\frac{T_{cr}(Test)}{T_{cr}(Plastic^a\ theory)}$	$\frac{T_{cr}(Test)}{T_{cr}(Plastic^b\ theory)}$
A-0-4	∞	0	34	TF	36.02	34.63	34.84	34.84	1.04	1.03	1.03
A-5-4	∞	0	8	TF	47.94	41.33	39.12	39.12	1.16	1.23	1.23
A-4-4	∞	0	14	TF	46.59	36.12	37.30	37.30	1.29	1.25	1.25
A-3-4	∞	0	29	TF	38.64	34.50	35.62	35.62	1.12	1.08	1.08
A-5-3	10.40	5.1	32	W	44.21	35.37	41.22	40.16	1.25	1.07	1.11
A-4-3	10.40	5.8	32	W	50.28	38.38	45.01	44.58	1.31	1.12	1.13
A-3-3	10.40	5.0	28	W	43.34	33.60	39.01	37.21	1.29	1.11	1.16
A-5-2	5.20	9.0	10	W	39.01	31.98	34.93	34.20	1.22	1.12	1.14
A-4-2	5.75	[illegible]	[illegible]	W	38.33	32.21	35.65	34.32	1.19	1.08	1.12
A-3-2	5	[illegible]	[illegible]	W	47.68	33.58	37.98	36.77	1.42	1.26	1.30
A-0-1	[illegible]	[illegible]	[illegible]	BF	25.04	21.59	21.41	19.37	1.16	1.17	1.29
A-5-1	[illegible]	[illegible]	[illegible]	BF	25.08	21.81	21.91	20.35	1.15	1.14	1.23
A-4	[illegible]	[illegible]	[illegible]	BF	27.84	23.39	22.14	22.14	1.19	1.26	1.26
[illegible]	[illegible]	[illegible]	[illegible]	BF	25.99	24.29	22.99	21.76	1.07	1.13	1.19
[illegible]	[illegible]	[illegible]	[illegible]	[illegible]	--	--	--	--	--	--	--
[illegible]	[illegible]	[illegible]	[illegible]	TF/W	53.33	43.01	47.15	47.15	1.24	1.13	1.13
[illegible]	[illegible]	[illegible]	[illegible]	W	58.08	40.33	47.82	46.24	1.44	1.21	1.26
[illegible]	[illegible]	[illegible]	[illegible]	W	60.68	43.65	52.45	51.83	1.39	1.16	1.17
[illegible]	[illegible]	[illegible]	[illegible]	W	57.21	41.16	47.68	46.75	1.39	1.20	1.22
B-	[illegible]	[illegible]	[illegible]	W/BF	57.43	39.07	46.57	43.17	1.47	1.23	1.33
B-	[illegible]	[illegible]	30	W	56.35	37.07	40.93	36.78	1.52	1.38	1.53
B-3-2	5.20	12.5	21	W	54.18	39.24	41.52	39.22	1.38	1.30	1.38
B-5-1	2.23	15.0	10	BF	27.86	26.53	26.24	25.04	1.05	1.06	1.11
B-4-1	2.23	18.0	8	BF	33.44	25.72	24.81	24.25	1.30	1.35	1.38
B-3-1	2.38	16.0	7	BF	29.72	26.77	26.80	26.49	1.11	1.16	1.12
B-3-0	0	--	--	--	--	--	--	--	--	--	--
C-0-4	∞	0	17.5	TF	41.26	35.57	40.95	40.95	1.16	1.01	1.01
C-5-4	∞	0	12	TF	45.24	36.19	42.07	42.07	1.25	1.08	1.08
C-3-4	∞	0	32	TF	45.25	38.03	43.82	43.82	1.19	1.03	1.03
C-5-3	10.4	4.8	34	W	41.61	32.76	38.20	34.59	1.27	1.09	1.20
C-4-3	10.4	5.6	36	W	48.55	34.68	41.13	36.83	1.40	1.18	1.32
C-3-3	10.4	5.7	40	W	49.41	35.55	42.46	37.95	1.39	1.16	1.30
C-5-2	5.54	8.5	30.5	W	39.27	30.92	34.74	29.17	1.27	1.13	1.35
C-4-2	5.20	10.0	17&31	TF to BF	44.75	29.83	33.84	27.96	1.50	1.32	1.60
C-3-2	5.20	8.5	6	BF	36.84	28.12	26.08	26.08	1.31	1.41	1.41
C-5-1	2.23	10.8	11.0	BF	20.07	17.92	16.78	15.75	1.12	1.20	1.27
C-4-1	2.23	11.0	13.75	BF	20.43	17.92	17.24	15.61	1.14	1.19	1.31
C-3-1	2.23	10.5	12.50	BF	19.48	17.55	16.62	15.30	1.11	1.17	1.27
D-3-4	∞	0	--	TF	45.24	38.34	41.08	41.08	1.18	1.10	1.10
D-3-4A	20.8	2.9	40	TF	50.29	37.53	43.21	44.68	1.34	1.16	1.13
D-3-3	10.4	6.6	29	TF/W	57.27	37.93	44.89	42.60	1.51	1.28	1.34
D-3-2	5.2	11.5	43.5/6	W/BF	49.85	32.80	38.69	32.00	1.52	1.29	1.56
D-3-1	2.23	10.0	5.5	BF	18.58	19.85	17.76	17.87	0.94	1.05	1.04
D-3-0	--	--	--	--	--	--	--	--	--	--	--
								Average	1.26	1.17	1.23

TF - Top Face BF - Bottom Face W - Web

[a]Procedure 1 [b]Procedure 2

beams. The beams under pure torsion cracked in Mode 3. In this case, the maximum theoretical principal tensile stresses varied from about 550 psi to 700 psi in all the series. When the flexural moment and shear were predominant, initial cracking occurred in Mode 1. The maximum tensile stresses corresponding to this mode ranged from about 600 psi to 770 psi. The correlation between the predicted and the test strengths is excellent for these beams exhibiting initial cracking in Mode 3 and Mode 1 as is evidenced by the mean of the ratios of test to theoretical strengths of 1.18 and 1.12 in the former and latter modes of cracking.

For Mode 2 cracking which occurred in the thin web, the theory proved to be more conservative than in the other cases. The theoretical maximum principal tensile stresses were in the range of 700 psi to 1100 psi for load combinations 2 and 3. Beams tested at load combination 2 exhibited higher stresses than those at load combination 3. The test strengths are in excess of predicted strengths by 36 percent for load combination 3 and 38 percent for the load combination 2, on the average. However the maximum excess of strength in a few cases was of the order of 40 to 50 percent. This correlation can be considered only fair. Similar trends were also clearly evident in the case of web cracking when the strengths were predicted by an alternate method, that is by Method 1, which will be discussed later. While studying the interaction of torque and shear at cracking, Wyss and Mattock (1971) observed test strengths to the extent of about 50 percent larger than the calculated ones, when the girders cracked

initially in the web. This is not in a way unexpected due to the following explanation. There is a high stress gradient across the thin web of the I section subjected to either pure torsion or combined loadings. It is known that concrete cracks at higher apparent tensile strengths when subjected to higher stress gradients. Further if a plastic distribution of shear stress is assumed, the entire web will be stressed to the same level under pure torsion. Superposition of flexural shear stresses on this torsional shear stress distribution will reduce the tensile stresses on one half of the web to zero if shear stresses due to both forces are equal. Cracking would then occur at higher apparent stresses in a web stressed to the same maximum level as in pure torsion cases or pure shear cases than in a web one half of which is less stressed than the other, as in the case in combined loadings.

7.2.2 Method 2 - Prestressed Rectangular Beams

Several rectangular prestressed beams in the literature were analyzed for cracking strength by the finite element method and the results compared with the experimental values in Tables 7.3 and 7.4. The analysis was applied in each investigation only to representative beams of various loading ratios, eccentricities and levels of prestress for reasons of computer time.

Specimens of the test program of Mukherjee and Warwaruk (1970) exhibited the three modes of cracking. The maximum principal tensile stresses varied from about 500 psi to 1200 psi leaving one beam V205 which behaved differently from its group. In the case of Mode 1 cracking

TABLE 7.3

COMPARISON OF FINITE ELEMENT ANALYSIS WITH TEST RESULTS

Investigator	Beam No.	f'_c (psi)	Effective Prestress (kips)	Eccentricity (in)	f_{TM}	f_{TB}	Maximum principal tensile stress at test cracking loads by FEM (psi)	$\sigma_{cr(test)}$ (in-kips)	$\sigma_{cr(FEM)}$ (in-kips)	$\frac{\sigma_{cr(Test)}}{\sigma_{cr(FEM)}}$	Location of crack (FEM
Mayerjak - Warner (1970)	V22	5260	35.24								Bottom
	V26	5462	36.37				669				Long side
	V27	5018	34.21				635				Bottom
	V02	4464	30.43				1145				Bottom
	V06	5666	38.43				697				Long side
	V07	5005	34.10				1119				Bottom
	V22	5413	46				936				Bottom
	V26	4633	34.37				825				Top
	V27	4778	35.38				861				Bottom
	V102	3986	27.34				645				Bottom
	V105	4218	33.37				693				Long side
	V107	3965	30.38				705				Bottom
	V122	4264	32.38				781				Bottom
	V125	4620	35.44				878				Long side
	V127	4613	34.42				871				Bottom
	V202	5000	36.43				847				Bottom
	V205	5618	44				956				Long side
	V207	5041	41.43				925				Bottom
	V222	5766	40.42				937				Bottom
	V225	5349	42.43				1016				Top
									Average	1.15	
Sangaree and Lin (1970)											Long side
											Bottom
											Bottom
											Bottom
											Bottom
											Bottom
											Bottom
Hendrikson (1968)											Long side
											Bottom
											Bottom
											Bottom
	IV-1-4	5900	56				748				Bottom
	IV-2-4	5900	56				1020				Bottom
	IV-3-4	5900	56				754				Bottom
	IV-4-4	5900	56				621				Bottom
	V-1-4	4480	43.36				548				Long side
	V-2-4	4480	43.36				964				Bottom
	V-3-4	4480	43.36				673				Bottom
	V-4-4	4480	43.36				1147				Bottom
									Average	1.22	
Mirza, Carland and Mattock (1969)	A1	6300	226								Top
	B6	6000	104				538		184.4	.92	Web
	C4	6140	0				539		153.5	.93	Web
									Average	1.00	

TABLE 7.4

COMPARISON OF FINITE ELEMENT ANALYSIS WITH EXPERIMENTAL DEFORMATIONS

Investigator	Beam No.	Angle of Twist (Rad per in x 10^{-6})			Flexural Deflection (in x 10^{-3})		
		At 70% of test T_{cr} (Test)	At 100% of test T_{cr} (FEM)	At 70% of Test T_{cr} (Test) / At 100% of Test T_{cr} (FEM)	At 70% of test T_{cr} (Test)	At 100% of test T_{cr} (FEM)	At 70% of Test T_{cr} (Test) / At 100% of Test T_{cr} (FEM)
Mukherjee - Warwaruk	122	51	55	0.93	70.0	74.1	0.95
	126	88	82	1.07	--	1.8	--
	127	24	28	0.86	100.0	91.3	1.10
	202	79	79	1.00	110.0	103.8	1.06
	206	92	105	0.88	--	1.0	--
	207	27	39	0.77	120.0	121.2	0.99
	222	78	94	0.83	105.0	129.8	0.81
	226	97	103	0.94	--	3.3	--
	227	38	51	0.76	165.0	169.9	0.97
	V102	25	26	0.96	45.0	46	0.98
	V105	69	66	1.05	5.0	15	0.33
	V107	6	11	0.55	40.0	49	0.82
	V122	26	33	0.79	65.0	61.7	1.05
	V125	85	90	0.94	5.0	19.1	0.26
	V127	11	15	0.73	55.0	66.92	0.82
	V202	15	33	0.45	50.0	58.0	0.86
	V205	58	59	0.98	5.0	13.0	0.39
	V207	17	20	0.85	65.0	82.0	0.79
	V222	47	59	0.80	90.0	99.8	0.90
	V225	69	73	0.95	5.0	16.55	0.30

the values of Test T_{cr}/Theoretical T_{cr} varied from 0.96 to 1.36 except for one beam for which it was 1.53 and the mean value was 1.18. The higher test to theoretical ratios occurred in beams having a uniform stress due to prestress. This is probably due to this: two beams one having uniform and the other triangularly eccentric prestress if acted on by a particular bending moment will yield finally triangular and uniform stress over the depth; in the former there is a high stress gradient, while in the latter the stress if uniform. If torsional stresses are superimposed on such triangular and uniform stress distributions, cracking would occur at apparently higher stresses in the beam having a uniform stress due to prestress only and hence higher test strengths.

For beams cracking in Mode 2, the ratio Test T_{cr}/Theoretical T_{cr} was 1.12 disregarding beam V205 as mentioned earlier.

Similarly the strength ratio was 1.45 for beam 226 tested under pure torsion and the theoretical cracking occurred on the top face; but it was reported that the cracking commenced near the upper part of the side face. If the theoretical stress is used according to the test location of the crack on the side, the ratio 1.45 comes closer to unity. The same explanation offered for Mode 1 cracking explains the higher observed strength in Mode 3 cracking of eccentrically prestressed beam 226 subjected to pure torsion. Of the 20 beams of Mukherjee and Warwaruk analyzed herein, 3 beams were subjected to pure torsion, 6 beams to combined bending and torsion, while the remaining had additionally shear force. On the average the strength was con-

servatively predicted within 15 percent of the test strength.

Three rectangular prestressed beams of Gangarao and Zia (1970) subjected to combined bending and torsion, and 16 rectangular prestressed beams of Henry and Zia (1971) were also analysed and the results furnished in Table 7.3. Beams cracking in Mode 1 developed principal tensile stresses ranging from 750 psi to about 1100 psi. These stresses are the maximum stresses given by the finite element analysis and correspond to the location of initial cracking. However the torque-moment ratio used in the cracking analysis by Henry and Zia related to the failure section rather than the first crack section. This as pointed out earlier in Chapter II, may result in computing a cracking strength at a section different from where the crack had actually occurred. If their method is adopted slightly lesser theoretical stresses would occur resulting in better correlation than that reported here. The ratio of observed to theoretical strengths varied from 1.03 to 1.35 and the mean is 1.23. Of these 19 beams only in 3 beams initial cracks occurred on the vertical side at theoretical stresses ranging from 600 psi to 750 psi. Theory predicted the cracking torque 17 percent in excess of the observed torque showing good agreement for Mode 2.

7.2.3 Method 2 - Prestressed I Beams

Three I girders of Wyss et al (1969) under pure torsion were analyzed by this method. The maximum principal tensile stresses in these cases ranged from 536 psi to 677 psi and the ratios of observed to analytical strengths varied from 0.92 to 1.15 indicating very good

correlation.

7.2.4 Method 1

Experimental cracking strengths of the I beams tested in the present program are compared with the analytical results obtained by Method 1 in Table 7.2. In most beams, the centre of the ultimate failure surface and the point of initial cracking were not the same. In some cases they were close to each other. It is not possible to predict precisely either of these locations. In computing the cracking strengths by Method 1, two procedures were adopted. The only difference between these procedures is in fixing the location of the cracking section. If the moment in the test zone is uniform, this difference vanishes.

7.2.4.1 Procedure 1

The V and M ratios corresponding to the test cracking section were used. The values are listed in Table 7.2 and do not include the dead load shear. At this section, on bottom face for Mode 1, on top face for Mode 3, and at both the web-flange junctions and the center of web for Mode 2 the cracking strengths were calculated. The smallest of these values is taken as the cracking load. The average ratios of test to theory are 1.11, 1.21 and 1.18 for Mode 3, Mode 1, and Mode 2 respectively, and the combined average is 1.17. This is a very good correlation. The results are slightly conservative for Mode 2 and Mode 1. Mode 1 cracking is usually associated with modulus of rupture, which is normally more than $6\sqrt{f'_c}$, the tensile strength used in this method. This is probably the reason for lower predictions in Mode 1. The cracking modes predicted by the theory agreed with the

observed cracking modes in virtually all of the test beams.

7.2.4.2 Procedure 2

In this procedure the critical crack is considered to occur on a cross section at a distance equal to half the effective depth of the section from the transverse load measured in the direction of decreasing moment without any regard for the experimental values. Both procedures then would result only in negligible differences in strengths for Mode 1; similar is the case for Mode 2 if the cracking is assumed to commence at the centroid of the web. As initial cracking is assumed to occur anywhere in the web Procedure 2 may yield lower strengths than Procedure 1 in many cases. In the case of web cracking for load combination 2, Procedure 2 more underpredicted the strengths than Procedure 1. This is evident from columns 8, 9, 11 and 12 of Table 7.2. The reason is the variation of bending moment in the test span. If the possibility of web cracking is considered only at the neutral axis as was done by Wyss and Mattock (1971), the theoretical results for Mode 2 presented in Table 7.2 came closer to the observed strengths. The average of ratios of T_{cr} test/T_{cr} calculated is 1.23 for all the beams. This ratio is higher as explained previously than that for Procedure 1.

7.2.5 Deformations

No useful method is available for estimating the post cracking stiffness of prestressed concrete beams. Several investigators observed the initial portion of the torque-twist relationship to be essentially linear up to the commencement of cracking implying elastic

behavior. In this range torsional stiffness was computed using elastic methods and compared to the test stiffness. However differences exist in selecting the experimental stiffness. Henry and Zia (1971) used the torque on the torque-twist curve where the curve deviated from a straight line and the corresponding rotation, Chander et al (1970) correlated the secant modulus of torsional stiffness at 50 percent of the cracking torque to the stiffness derived by the elastic method for prestressed beams subjected to pure torsion. Woodhead and McMullen (1972) used calculated cracking torque but not the test torque which was usually higher and the corresponding experimental angle of twist for prestressed rectangular beams under combined loadings. Johnston and Zia (1971) chose the stiffness of the initial portion of the torque-twist curve, having observed slight nonlinearity beyond 60 to 70 percent of test T_{cr} in the case of hollow prestressed beams. Wyss, Garland and Mattock (1969) took the average slope of the initial linear part of the torque-twist relationship for prestressed I beams under pure torsion. Wyss and Mattock (1971) made comparison of test and theoretical precracking stiffnesses for prestressed I beams under combined loadings with excellent correlation. But the way they defined the test stiffness was not given, presumably it is the average slope of the initial portion of the curve. However it is generally agreed that as the cracking load is approached inelastic deformations do occur, often to a significant extent.

In the present study, the finite element method is used to predict the torsional and flexural deformations. This is an elastic

method but yields as a rule lesser deformations than the exact theory. The theoretical and experimental angles of twist at test cracking loads and 70 percent of test cracking loads, respectively, are compared in Table 7.1 for the I section beams of the present test program. The ratio of test to theoretical angles of twist varied from 0.6 to 1.25; only 5, out of 41 beams exhibited ratios close to these extreme values. On the average this ratio is 0.94 which indicates a very good correlation.

Flexural deflections are also compared at the same torques as the torsional deformations and are listed in Table 7.1. Measured deflections included also those due to prestress. However the deflections obtained from the finite element analysis do not include them. Hence the deflections due to prestress were calculated using the elastic method and added to those obtained by the finite element analysis. On the average the predicted values are within 3 percent of the observed values.

Since for the prestressed concrete beams of Mukherjee and Warwaruk (1970) deformations in the whole range of loading are furnished, they are computed and listed in Table 7.4 at about 70 percent of test cracking strengths under combined loads. When compared with the finite element results, the rotations are conservatively predicted, variations are less than in the case of I beams and except for two beams the correlation in each case is very good.

7.3 Ultimate Strength

At any given load level the test beams were subjected to a constant torque and shear while the bending moment varied in the test zone. As the torque was related to flexural shear and moment by the ratios δ and ψ respectively, once torque was known other forces were obtained. The ultimate strength analysis developed in Chapter IV based on the observed two modes of skew bending failure, is applied to the beams of present investigation and several I beams of other investigations; the results of the former are listed in Table 7.5 together with the governing mode of failure.

7.3.1 Beams Under Pure Torsion

For all the beams tested under pure torsion, though initial cracking occurred in Mode 3, failure took place in Mode 2. Beams A-0-4 and C-0-4 not provided with stirrups failed after one or two increments of load beyond cracking. The cracking strength was 92 to 96 percent of the failure torque. Little ductility was exhibited by these beams. The theory cannot be applied to beams without stirrups. For such beams the cracking strength is taken as the ultimate strength.

The beams were not provided with any longitudinal mild steel. For these beams to develop the torsional capacity corresponding to the volume of the web reinforcement used, the prestressing strands supplied the necessary longitudinal force that would otherwise have been provided by the longitudinal reinforcement. The minimum amount of web reinforcement in the beams was slightly more than the minimum defined by the following equation suggested by Hsu (1968d) for reinforced concrete beams

TABLE 7.5

COMPARISON OF TEST RESULTS WITH THEORY - ULTIMATE TORQUE

Beam	T_u/M_u	T_u/V_u	T_u test (in-kips)	T_u Theory (in-kips)	$\frac{T_u \text{ Test}}{T_u \text{ Theory}}$	Observed mode of failure
A-0-4	"	"	37.33	34.84	1.07	Mode 2
A-5-4	"	"	54.95	41.84	1.31	Mode 2
A-4-4	"	"	56.03	43.29	1.29	Mode 2
A-3-4	"	"	50.64	45.20	1.12	Mode 2
A-5-3	0.849	9.811	50.25	36.93	1.36	Mode 2
A-4-3	0.554	10.153	56.35	42.2	1.34	Mode 2
A-3-3	0.778	9.933	56.37	40.5	1.39	Mode 2
A-5-2	0.261	5.036	46.58	36.6	1.27	Mode 2
A-4-2	0.272	5.626	46.27	39.3	1.18	Mode 2
A-3-2	0.243	5.189	58.51	46.4	1.26	Mode 2
A-0-1	0.085	2.213	36.23	41.80	0.87	Mode 1
A-5-1	0.089	2.218	44.58	44.92	0.99	Mode 1
A-4-1	0.094	2.437	39.90	41.52	0.96	Mode 1
A-3-1	0.087	2.220	43.90	45.83	0.96	Mode 1
A-3-0	0.0	0.0	0.0	0.0	-	No torsion
B-3-4	"	"	61.90	57.39	1.08	Mode 2
B-5-3	0.590	10.400	61.55	44.9	1.37	Mode 2
B-4-3	0.628	10.135	65.88	52.0	1.27	Mode 2
B-3-3	0.590	10.290	65.60	52.5	1.25	Mode 2
B-5-2	0.274	5.153	62.74	46.3	1.36	Mode 2
B-4-2	0.269	5.160	62.75	46.3	1.36	Mode 2
B-3-2	0.291	5.161	65.03	51.6	1.26	Mode 2
B-5-1	0.087	2.274	37.85	44.64	0.85	Mode 1
B-4-1	0.087	2.219	43.65	43.53	1.00	Mode 1
B-3-1	0.092	2.325	43.89	47.04	0.93	Mode 1
B-3-0	0.0	0.0	0.0	0.0	-	No torsion
C-0-4	"	"	44.71	40.[illegible]	1.09	Mode 2
C-5-4	"	"	49.56	37.55	1.32	Mode 2
C-3-4	"	"	56.73	45.52	1.25	Mode 2
C-5-3	0.663	9.960	46.81	35.6	1.31	Mode 2
C-4-3	0.607	9.909	55.49	39.1	1.42	Mode 2
C-3-3	0.542	10.360	56.46	42.6	1.32	Mode 2
C-5-2	0.296	5.328	41.98	35.7	1.17	Mode 2
C-4-2	0.305	5.113	47.68	37.7	1.26	Mode 2
C-3-2	0.297	5.124	46.38	40.0	1.16	Mode 2
C-5-1	0.085	2.213	40.50	40.19	1.01	Mode 1
C-4-1	0.085	2.236	39.58	40.37	0.98	Mode 1
C-3-1	0.086	2.214	39.57	39.74	1.00	Mode 1
C-3-4	"	"	56.57	45.47	1.24	Mode 2
D-3-4A	0.317	19.597	59.77	42.9	1.39	Mode 2
D-3-3	0.607	9.790	62.90	42.9	1.47	Mode 2
D-3-2	0.274	5.120	60.24	39.8	1.51	Mode 2
D-3-1	0.083	2.214	41.78	33.82	1.24	Mode 1
D-3-0	0.0	0.0	0.0	0.0	-	No torsion

Averages

Mode 2, Pure torsion = 1.20

Mode 2, Combined loading = 1.317

Mode 1 = 0.98

$$\frac{A_t}{S} = \frac{125.b.h}{f_{ty}(x_1+y_1)} \qquad (7.1)$$

The test specimens had varying amounts of transverse reinforcement. The reinforcement factor, $x_1 y_1 A_t f_{ty}/S$ ranged from 1.88 to 8.13. This is a rather narrow range. The best way to use a given amount of reinforcement is to have a maximum lever arm. In the thin web of I specimens, the available lever arm between the two legs of the stirrups is only 1.25 inches, about one quarter of that in a 6 inch wide rectangular beam.

The addition of stirrups increased the strength and ductility significantly; the strength increase corresponding to the volume of stirrups used in the beam. Of the three amounts of stirrups used even the smallest resulted in very large ductility. An increase in the level of prestress increased the cracking strength but the post cracking strength was linearly proportional to the web reinforcement factor as suggested by Hsu and Kemp (1969) for prestressed concrete members. The higher observed strengths for beams A-5-4 and A-4-4 than that of A-3-4 which had more transverse reinforcement are due to higher unintended prestress. However the difference between the ultimate and cracking strengths was maximum for beam A-3-4 having the largest amount of web reinforcement of all the three beams. Increase in the amount of web reinforcement resulted in increases of strength but this was realized only at very large rotations where stiffness was almost negligible. It then becomes doubtful whether the increase in the ultimate strength obtained by using more transverse reinforcement is useful. Comparing

D-3-4, C-3-4 and A-3-4, it can be observed that beams of different eccentricities developed the same post cracking strength. In other words these beams differing nominally only in the eccentricity exhibited the same pure torsional strengths.

As the prestress increased, the contribution from the web reinforcement reduced slightly as can be seen from the comparison of B-3-4 with A-3-4, C-3-4 and D-3-4. This means the web steel did not yield and an amount of stirrups smaller than that used in B-3-4 might have rendered the beam under reinforced transversely. The strain gage readings showed that the stirrups yielded. It is however difficult to draw firm conclusions based on the strain gage data, as much depends on the location of the gage relative to the crack.

The theory predicted conservatively the test strengths of beams under pure torsion, failing in Mode 2. The ratios of test to theoretical strengths varied from 1.08 to 1.32 and the average is 1.20. The reasons for the conservatism are discussed in Section 7.3.3.

Slightly better correlation would result by using the modification (equation 2.36) suggested by Wyss et al (1969) to equation (2.35) proposed by Hsu (1967) applicable to concentrically prestressed beams subjected to pure torsion. However it predicted an unconservative result for B-3-4.

7.3.2 Influence of Transverse Shear Force

In the equations derived for the torsion mode of failure, the shear force is present and its effect is to reduce the ultimate strength in combined loadings. This was also noted by Henry and Zia

(1971) in the case of prestressed rectangular beams. As the effect of bending moment is not taken into account for Mode 2, if the magnitude of the transverse shear were to be constant, the torsional strength also would remain constant. If the shear force increases the torsional strength decreases. However it will be clear from the interaction diagrams of test results that small amounts of shear force helped in increasing the test strength in combined loadings. This increase cannot be predicted by the theory.

For Mode 1 failure, the developed equations do not involve shear force and can be applied only to beams which do not develop premature shear failure. None of the specimens tested in the present program failed prematurely in shear.

At cracking, the effect of shear is to increase the tensile stresses on one vertical side and thus reduce the cracking loads. Moderate amounts of bending moment and shear have increased the cracking strength, but further increases of both decreased the strength. This can be observed from the interaction diagrams of cracking presented in Fig. 7.1.

7.3.3 Beams Failing in Mode 2 Under Combined Loading

Beams tested at load combination 3 and 2 generally failed in a torsion mode. The theory assumes that Mode 2 failures are independent of flexural moment. The theoretical predictions for these beams were very conservative under predicting the strengths by 32 percent on the average. Several reasons may be responsible for such low theoretical strengths.

(a) Small amounts of bending moment and shear increased the test strengths in Mode 2. This increase was not reflected in the theory. Similar increases were observed in prestressed rectangular beams by other investigators.

(b) As part of the shear compression forces were resisted by the outstanding flanges on the compression side, assumption of a compression hinge along the web might have resulted in a smaller lever arm of shear compression forces.

(c) More importantly, the strain compatability factor used to obtain the induced strain in the prestressing strands from the yield strain of stirrups most likely underestimated the induced longitudinal strains.

According to the strain compatability factor used the strain in the strands can assume a maximum value of the yield strain of stirrups, i.e. 0.0013, if the crack angle is 45 degrees. As this angle is far less than 45 degrees, the induced strain in the strands is less than 0.0013. However strain measurements on the strands have indicated induced strains above 0.002. Hence the relationship between the yielding and non yielding steels needs to be established more precisely in partially over-reinforced beams such as tested in the present program. The assumption used in the theory regarding the compatability condition is appropriate at cracking only. A more reasonable assumption is warranted but cannot be made at the present time. Until then significant progress can not be made in the skew bending method of analysis for partially over-reinforced beams failing in Mode 2. The theoretical

predictions obtained by the present theory constitute a lower bound solution to strength of beams developing a Mode 2 failure.

Similar conservatism was observed in prestressed rectangular beams using the same compatability of strains. Good correlation was obtained for the prestressed beams tested by Henry and Zia (1971) failing in Mode 2, only when they over estimated the forces in the longitudinal mild steel violating their assumption of compatability of strains between stirrups and the longitudinal steel. They assumed yield force in the longitudinal steel. But according to the compatability conditions the force is far less than that at yield. In analyzing several prestressed rectangular beams in the literature failing in Mode 2, and partially over-reinforced, Woodhead and McMullen (1972) reported test to theoretical strength ratios of 1.30 for majority of beams, more than 1.30 for some, and an average of 1.174.

7.3.4 Beams Failing in Mode 1

Beams of load combination 1 were tested under high bending moment; torque to bending moment ratio equalled approximately the ratio of pure torsional strength to flexure-shear strength in Series A, B and C. These beams failed in Mode 1; but as described in Chapter VI, the failure was premature due to the splitting off of the oustanding flanges. This occurs when the magnitude of torsion is sufficient enough to cause cracking in the top flange which is under compression. In such a case only the web portion of the top flange is effective in resisting the shear-compression forces. However the full width of the top flange can be completely effective in the following two cases:

(a) If the magnitude of torsion is small enough torsional cracking cannot destroy the top flange.

(b) If by the time the initial torsional cracking commences on the top flange, the beam attains its flexural capacity as that in D-3-1.

For simplicity and conservative prediction it is proposed to neglect the outstanding flanges in isolated girders having reinforcement detail similar to that used in the present test program. Instead of full flange width, as only the web portion is considered, the strength of D-3-1 is underestimated giving $T_u$test/$T_u$theory = 1.24. If full flange width is considered this ratio is 1.13. For Mode 1 failures the theory predicted the test strengths closely. The ratios of test to theoretical loads varied from 0.87 to 1.24 with the exception of one beam and the average is 0.98. Beams in Series A, C and B at load combination 1 were expected to fail in an under-reinforced manner in Mode 1 as they were balanced or slightly over-reinforced when transverse load alone was acting. Beams having varying percentages of transverse reinforcement failed nearly at the same load because of reduced effectiveness of the top flange at ultimate.

7.4 Interaction Behavior

7.4.1 General

The net effect of a simultaneous application of torsion, bending and shear on the strength of a member can be expressed by an interaction surface in a three dimensional rectangular coordinate system. Each axis then represents a type of force. Each point on the surface represents the strength of a beam subjected to a certain amount of torsion, bending and shear. It is more convenient to represent the

interaction of forces on two dimensional diagrams. The torsion-bending interaction curve can be obtained by projecting onto the torsion bending plane the intersection of the interaction surface and a plane defined by the loading ratio of torsion and bending. Similarly the interaction curves on the other two planes can be obtained. To construct a three dimensional interaction surface, the interaction curves on three planes must be determined. It is possible to conduct tests and obtain these curves on torsion-bending and bending-shear planes, but it is difficult to get such a curve on the torque-shear plane as shear force cannot be easily simulated without the presence of bending moment in a finite length of a beam.

In defining the pure shear strength V_{uo} Mukherjee and Warwaruk (1970) and Henry and Zia (1971) adopted the equations of ACI 318-63. These equations are usually conservative. Hence a theoretical curve based on these equations may seem too conservative near the shear axis as beams may have test strengths in excess of theoretical predictions of V_{uo}. Other investigators, Ersoy and Ferguson (1968), Mattock (1968), Woodhead and McMullen (1972) defined V_{uo} as the shear strength corresponding to the ultimate flexural capacity. This definition suffers from the disadvantage that V_{uo} depends on the bending moment in that geometry and loading patterns control the strength. Further, it may be unconservative near the shear axis if a premature shear failure occurs. In the present investigation, the latter definition is used in presenting the two dimensional interaction diagrams.

7.4.2 Interaction of Torsion, Bending and Shear at Cracking

The results of interaction between torsion and bending at cracking are presented in Fig. 7.1. It can be observed that the interaction behavior is little affected by the amount of web reinforcement and that except for beams with stirrup spacing at 5 inches in Series A and C, small amounts of bending moment helped in increasing the torsional cracking strength. The reason for the absence of such an increase for A-5-3 and C-5-3 is the smaller prestress for them than that in corresponding beams A-5-4 and C-5-4. The maximum increase was about 12 percent. The cracking torque was greatest when the applied bending moment was equal to the internal moment created by the eccentric prestress. In other words a beam exhibited highest cracking strength when the normal stress due to prestress and bending was uniform in all the series. The torsional strength at cracking did not drop below the pure torsional cracking strength until the coexisting moment was about 60 to 70 percent of bending shear capacity at cracking. As expected increases in level of prestress increased the cracking loads for all load combinations. The beams did not have tension due to prestress alone.

A theoretical cracking curve is plotted for each series in accordance with Procedure 2 of Method 1 cracking analysis. If cracking initiates in the web it is assumed to occur at the centroid of the web. For Mode 3, initial crack is assumed to occur on the face of the top flange at a distance of half the flange width from the edge of the supporting plate of the restraining head, i.e., 8 in. from the center of support.

7.4.3 Interaction of Torsion, Bending and Shear at Ultimate

The non-dimensionalized interaction curves at ultimate between torsion and shear, and torsion and bending are shown in Fig. 7.2 through

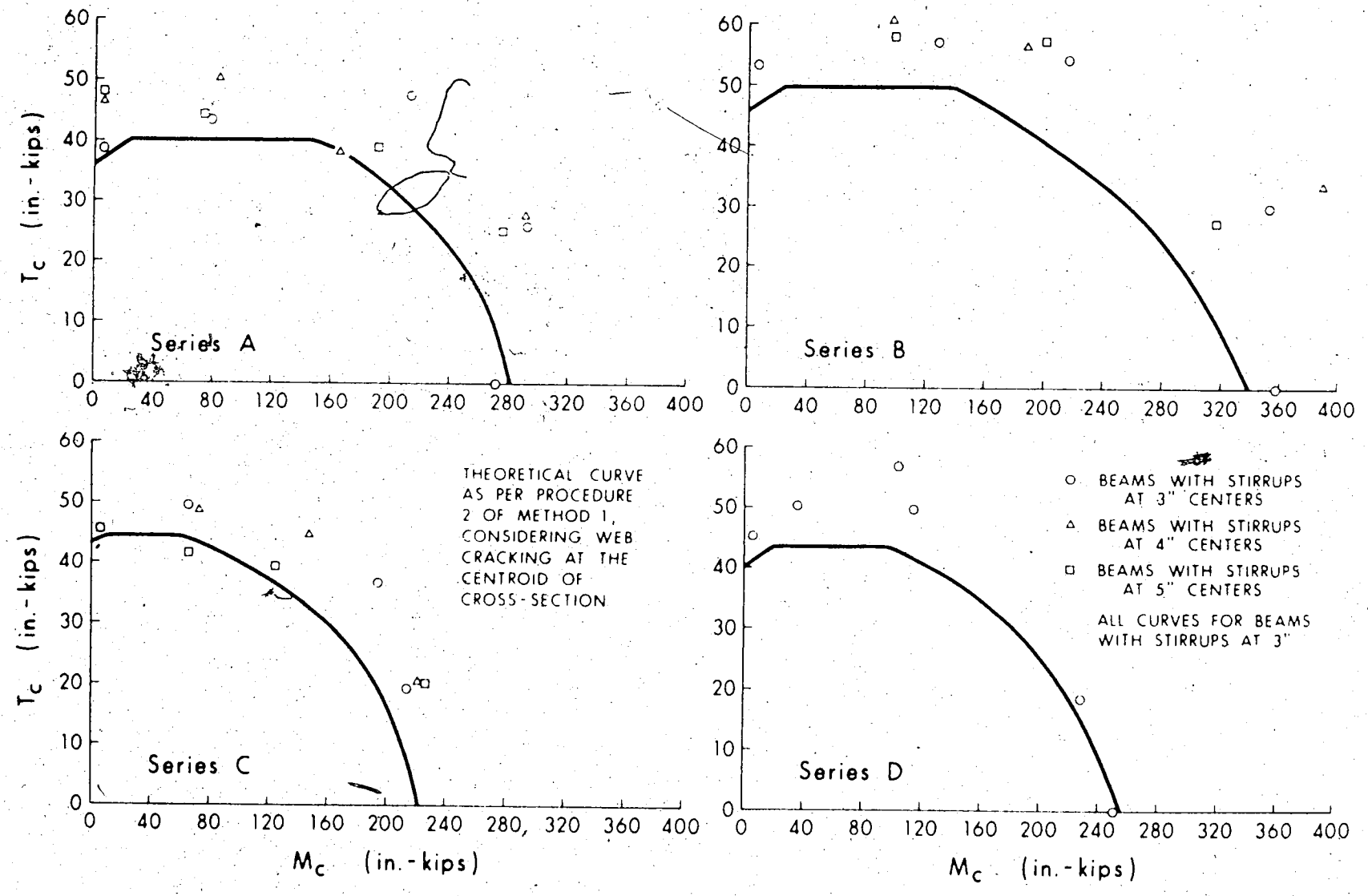

FIG. 7.1 TORQUE-MOMENT INTERACTION DIAGRAMS AT CRACKING

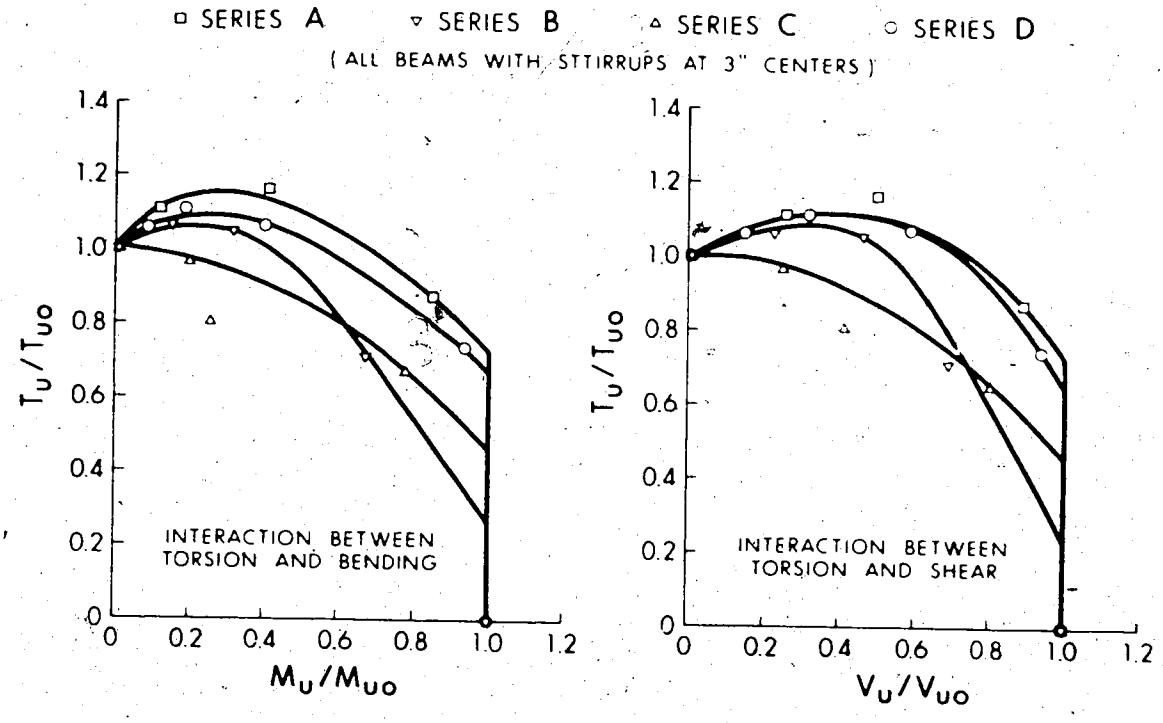

FIG. 7.2 NON-DIMENSIONAL INTERACTION CURVES - TEST RESULTS

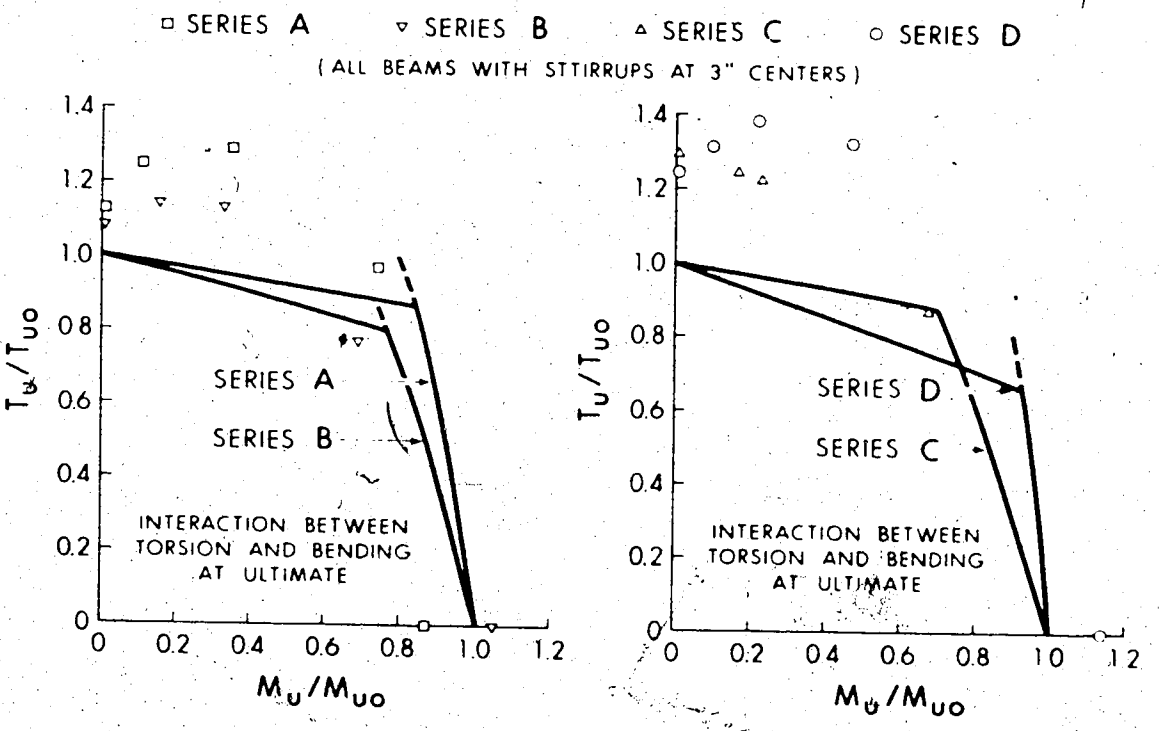

FIG. 7.3 THEORETICAL NON-DIMENSIONAL INTERACTION CURVES AND TEST RESULTS

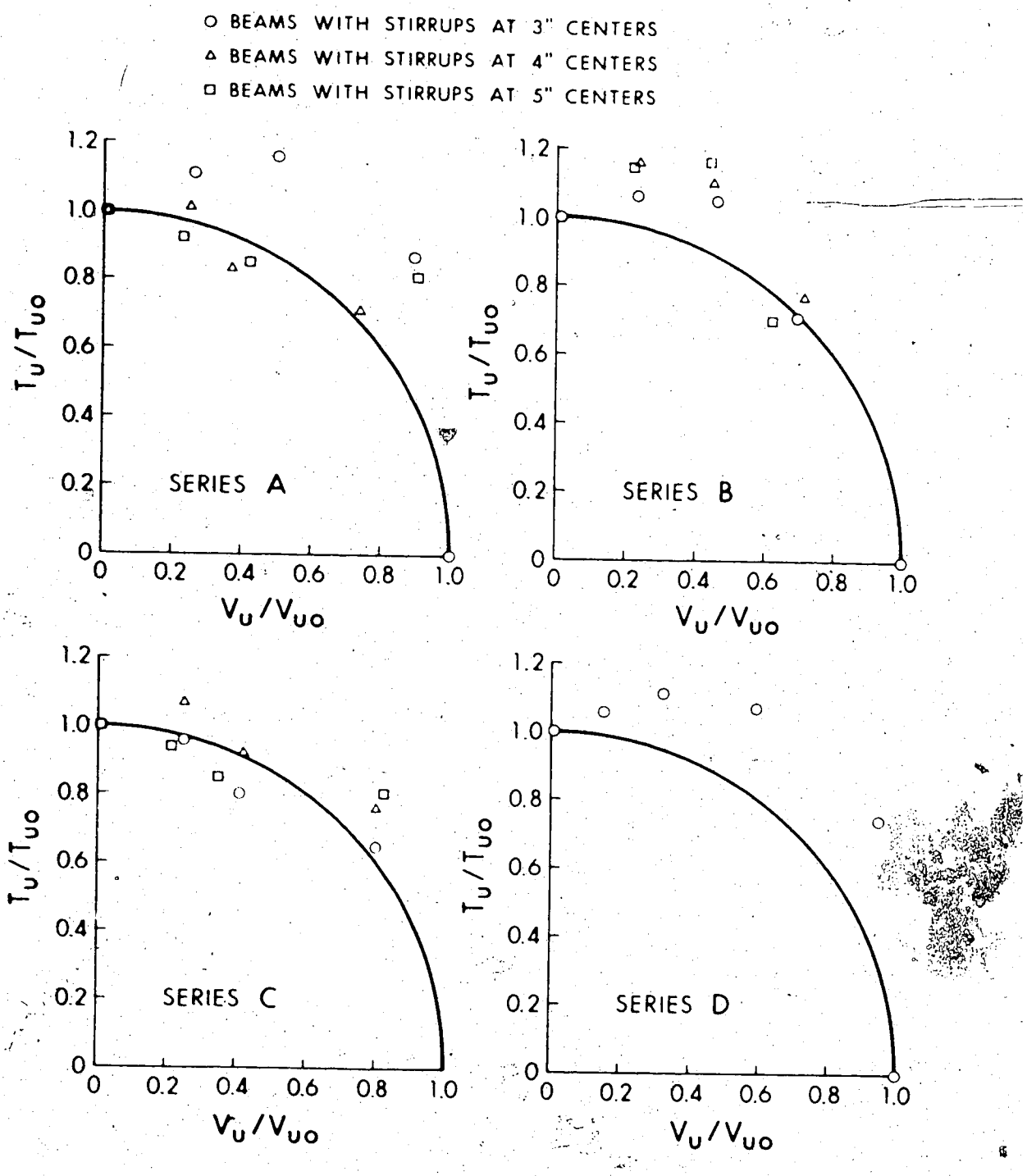

FIG. 7.4 NON-DIMENSIONAL TORSION-SHEAR INTERACTION CURVES - TEST RESULTS

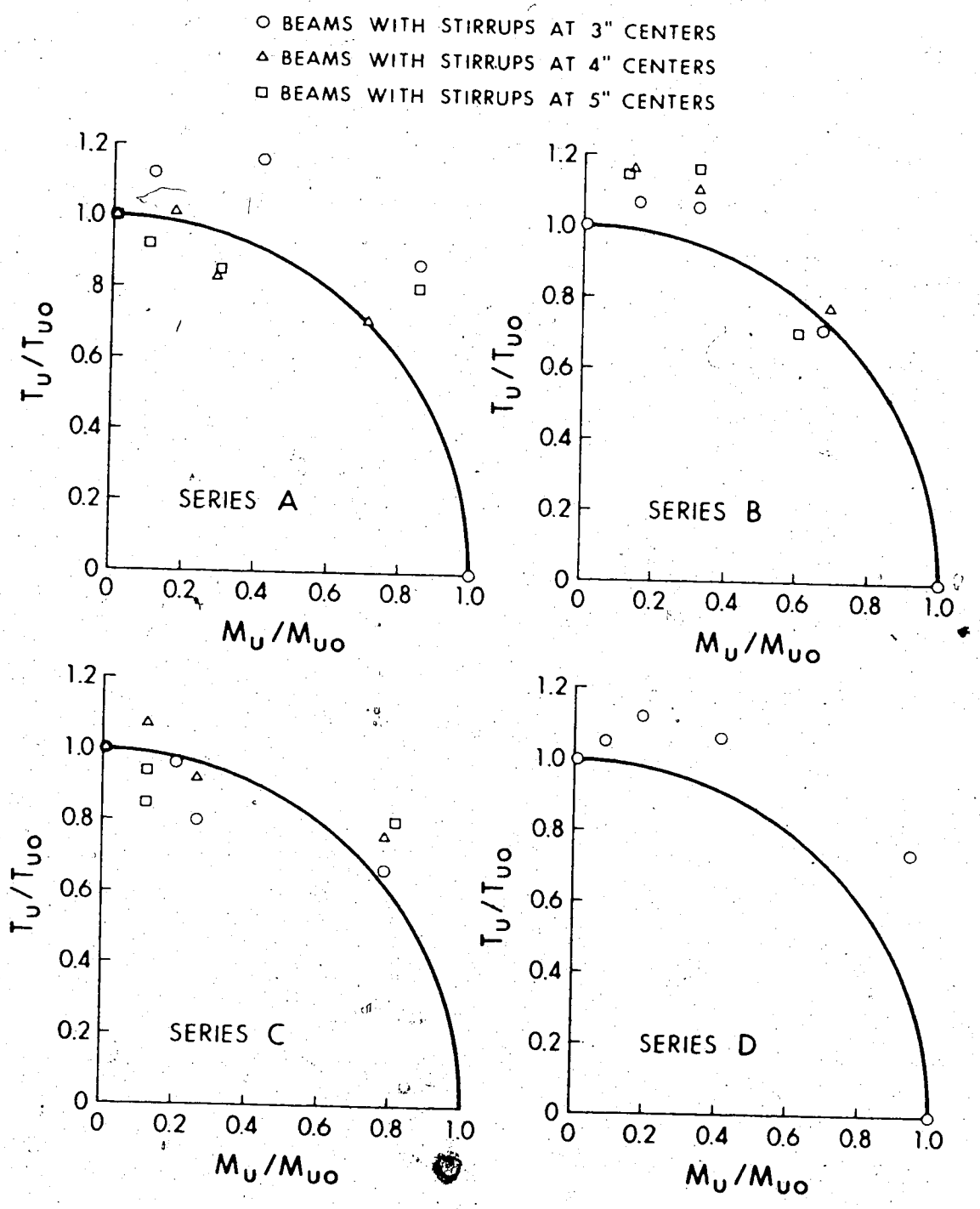

FIG. 7.5 NON-DIMENSIONAL TORSION-BENDING INTERACTION CURVES - TEST RESULTS

7.5. In non-dimensionalizing the forces the shear-flexural capacity of beams in Series C is taken the same as that of Series A. The only difference between these two series is eccentricity of prestress. Flexure-shear tests are made on beams with stirrup spacing at 3 inch centers and it is assumed that the variation of stirrup spacing does not affect the flexure shear strength. Pure torsional tests in Series C beams with stirrup spacing at 4 inches, and in Series B with stirrup spacing at 4 inches and 5 inches were not made. For interaction study, these strengths are obtained from pure torsion tests strengths of the same series with stirrups at different spacing, by adding or subtracting as the case may be, the difference in the contribution of stirrups towards the torsional strength as obtained by theory.

It is evident from Fig. 7.2 that the torsion-shear interaction curves are remarkably similar to the torsion bending curves. This is partly because the control points on the bending and shear axes are obtained by tests, and in flexure-shear tests shear failure did not occur prior to the attainment of flexural capacity whether the beams were under reinforced or over-reinforced flexurally. Examining Fig. 7.2, it becomes evident that with the exception of Series C having the lowest eccentricity, the torque capacity in combined loading increased to a peak value and did not fall below the pure torsional strength until the bending moment was about 40, 55 and 65 percent of the pure flexural strength in Seri B, D and A respectively. This increase was about 6 to 12 percent; beams in Series A with the highest eccentricity showed the highest increase. Regarding the magnitude of increase in the torsional strength these test results differ significantly with the ob-

servations of Bishara (1969) who reported the increases in torsional strength as much as 100 percent in the case of I beams with stirrups under combined loadings. In non dimensionalizing the moments Bishara used theoretical pure torsional strength. The bending strength was reduced only 6 and 15 percent of the pure bending capacity when the applied torque was 75 and 90 percent of the pure torsional strength for Series D and A. For Series B though designed to achieve a square interaction curve this was not obtained due to premature failure of the compression zone. This premature failure was evident in varying degrees in other series. While the gain in torsional strength above pure torsional strength with small amounts of bending and shear was more gradual; the decline in the torsional strength beyond the peak with further increases in other forces was very sharp.

For Series C, all the beams at load combination 3 had 6 to 10 percent less prestress than the corresponding pure torsion beams. This might have been responsible for the absence of gain in the torsional strength above pure torque capacity for the beams at load combination 3.

In Fig. 7.3, the theoretical interaction curves based on the theory are shown. The test strengths represented by points are non-dimensionalized by the theoretical T_{uo} and M_{uo}. The thepretical shear-flexural capacities of the beams A-3-0, B-3-0 and D-3-0 are 684.7, 691.2 and 464.5 in.kips, respectively. These diagrams indicate the close predictions for Mode 1 and conservative predictions for Mode 2.

Beams that failed in Mode 1 have magnitudes of bending moment and torque associated with the corner region away from the coordinate

axes of the nearly rectangular torque-moment interaction diagram. These test results are closely predicted by the theory of Mode 1 and the failure torques are of the same order as those associated with Mode 2 failures. The theoretical torque in Mode 2 in some cases is slightly less than that in Mode 1 as the Mode 2 failures are conservatively predicted by about 20 to 30 percent on the average. Therefore it is necessary to determine at which T/Vb_w ratio Mode 1 changes to Mode 2 failure. This transition occurs at a particular T/Vb_w ratio which must be established from the tests. Sufficient test results are not accumulated here to find the transitional T/Vb_w ratio. However the transition can be reasonably assumed to occur at a T/Vb_w ratio where the predicted bending moment in Mode 1 becomes greater than that in Mode 2.

7.5 Application of Theory to Beams in Literature

The theory presented in Chapter IV was applied to several I section beams reported in the literature. The test and theoretical strengths of specimens failing in Mode 1 and Mode 2 are furnished in Table 7.6 and 7.7 respectively. If data reported in some cases concerning the stress-strain characteristics of strands was inadequate, missing information was obtained from standard stress-strain curves available from the publication by British Ropes Limited, 1967.

The I beams of Gausel (1970), and Wyss and Mattock (1971) exhibiting Mode 1 failure were analyzed and the theory has predicted the test strengths within three percent on the average. T_u test/T_u theory ranged from 0.90 to 1.14. One half of Gausel's beams did not have web reinforcement in the test zone and the other half had. The correlation

TABLE 7.6

COMPARISON OF TEST AND THEORETICAL ULTIMATE MOMENTS FAILING IN BENDING MODE (MODE 1)

Investigator	Beam No.	f'_c (psi)	Prestress force (kips)	Eccentricity (in)	Size and spacing of stirrups in inch	Test Results T_u (in-kips)	Test Results M_u (in-kips)	Theory T_u (in-kips)	Theory M_u (in-kips)	$\frac{T_u \text{ test}}{T_u \text{ theory}}$
Gausel (1970)	9	8236	70.84	2.31	--	42.2	586.08	46.77	650.07	0.90
	10	7483	69.70	2.29	--	55.0	586.08	51.23	548.20	1.07
	11	7810	64.54	2.27	--	--	759.00	--	767.82	--
	12	7653	62.60	2.25	--	52.7	607.20	48.98	563.26	1.08
	13	8747	66.08	2.26	--	59.4	595.32	54.49	544.89	1.09
	14	7923	66.56	2.32	--	52.7	649.44	47.24	581.06	1.12
	15	7455	67.92	2.32	--	65.3	541.75	64.90	538.69	1.01
	16	7085	67.36	2.29	--	65.3	541.75	65.85	546.58	0.99
	9W	7384	70.84	2.31	#2 @ 6.3	42.2	651.20	43.50	669.93	0.97
	10W	6887	69.70	2.29	#2 @ 6.3	66.4	586.10	60.66	535.59	1.09
	11W	7597	64.54	2.27	#2 @ 4.49	52.7	759.00	46.43	668.83	1.14
	12W	7795	62.60	2.25	#2 @ 4.49	71.2	607.00	64.13	547.06	1.11
	13W	8335	66.08	2.26	#2 @ 2.88	80.7	595.30	72.33	533.76	1.12
	14W	8094	66.56	2.32	#2 @ 2.88	75.9	514.00	78.27	529.82	0.97
	15W	6943	67.92	2.32	#2 @ 2.97	84.0	541.80	82.04	529.16	1.02
	16W	6659	67.36	2.29	#2 @ 2.97	75.9	476.70	84.44	530.31	0.90
									Average	1.04
Wyss and Mattock (1971)	B2	7100	217.4	4.86	#4 @ 9	0	6500.4	0	6000.4	--
	B3	5950	220.2	4.88	#4 @ 9	368.8	4108.8	353.3	3921.1	1.04
	B4	7350	224.5	5.05	#4 @ 9	393.5	4257.6	386.6	4178.6	1.02
	B5	7300	230.9	5.01	#4 @ 9	392.8	4520.4	385.9	4436.0	1.02
	B6	7050	224.0	4.97	#4 @ 9	385.1	4345.2	400.1	4521.3	0.96
	B8	6650	223.2	4.96	#4 @ 6	427.7	4206.0	412.8	3983.6	1.04
	B9	6740	217.6	4.93	#4 @ 6	450.0	4232.4	434.8	4091.8	1.03
	B10	7050	219.8	4.93	#4 @ 6	430.3	4232.4	446.4	4390.7	0.96
	B11	7300	218.1	4.94	--	343.4	3819.6	347.8	3861.1	0.99
									Average	1.01

TABLE 7.7

COMPARISON OF TEST AND THEORETICAL ULTIMATE MOMENTS FAILING IN TORSION MODE (MODE 2)

Investigator	Beam No	f'_c (psi)	Prestress force (kips)	Eccentricity (in)	Size and spacing of stirrups in inch	Test Results T_u (in-kips)	Test Results V_u (kips)	Theory T_u (in-kips)	Theory V_u (kips)	$\frac{T_u \text{ Test}}{T_u \text{ Theory}}$
Wyss,	A2	6120	226	4.9	15	318	0	365.6	0	0.87
Garland	A3	6000	226	4.9	8	391	0	436.7	0	0.90
and	A4	6000	226	4.9	5	430	0	530.2	0	0.81
Mattock	B2	5800	104	5.0	15	219	0	232	0	0.94
	B3	6100	104	5.0	8	296	0	287.5	0	1.03
	B4	6100	104	5.0	5	320	0	363	0	0.88
	C3	6180	0	0	8	254	0	185	0	1.37
	C4	6180	0	0	5	367	0	346.5	0	1.06
									Average	0.98

with the test strengths has been equally good in both cases.

Wyss and Mattock reported the outstanding flanges split away from the girders at ultimate. Because the horizontal legs of the stirrups were separate bars and did not have the full development length their contribution to the strength is neglected. However it can be noted that in Mode 1, the number of horizontal legs of the stirrups intersected by a failure crack is usually one or two and in the girders of Wyss et al none because of the higher inclination of the crack to the axis of the beam and the narrow web. Even if the intersected horizontal legs are assumed to yield and their strength contribution taken into account, the difference in strength is only of the order of 1 to 3 percent. In their case there is no contribution from the horizontal legs. For the reasons stated in Section 7.3.4, the outstanding flange parts were neglected in analyzing Gausel's beams.

Several full scale I girders, prestressed and non prestressed, tested under pure torsion by Wyss, Garland and Mattock (1969) were also analysed. These beams failed in Mode 2. T_u test/T_u theory varied from 0.81 to 1.37 for prestressed and reinforced girders. On the average the theory over predicted the strength by only 2 percent.

CHAPTER VIII

SUMMARY AND CONCLUSIONS

8.1 Summary

This investigation was devoted to the study of the behavior of prestressed concrete I section beams loaded in combined torsion, bending and shear. The experimental phase of this study consisted of tests on 44 eccentrically prestressed I beams to evaluate the effect of eccentricity and level of prestress, varying combinations of torsion, bending and shear and various amounts of transverse reinforcement on the behavior and strength of these beams. The analytical phase of the study included strength predictions at cracking and ultimate of prestressed concrete I beams. Test results were discussed, and theory was applied to the beams of the present investigation and that of others.

The following conclusions are drawn, based on the findings of the tests reported here.

8.2 Conclusions

1. Prestressed concrete I beams subjected to torsion, bending, and shear can develop initial cracks either on the top face, on the web, or on the bottom face. The location of the initial crack depends on the relative dimensions of the cross-section, on the magnitude and eccentricity of prestress, and on the relati amounts of torsion, bending and shear.

2. An increase in prestress causes corresponding increase in the cracking torque of prestressed I beams; initiation of cracking appears to be governed more by the total prestress rather than stress at a point.

3. Moderate amounts of bending moment increase the torsional cracking strength. This is greatest when the applied bending moment is equal to the internal moment created by the eccentric prestress. Bending moment along with the corresponding shear in excess of an optimum amount results in rapid reduction of the torsional cracking strength.

4. Prior to cracking the initial torsional stifness is nearly independent of the amount of transverse reinforcement, and the magnitudes of torsion, bending and shear. However the secant torsional stiffness at cracking is higher for the beams loaded at a very low T/M ratio than for beams loaded a a high T/M ratio. Flexural stiffness of the uncracked section is unaffected by the presence of torsion.

5. The three dimensional finite element analysis developed here using hexahedrons predicts conservatively the cracking strength of prestressed and reinforced concrete beams subjected to combined loadings. This method of analysis is more conservative for the case of web cracking in I beams than that for cracking at other locations on the cross-section. The theory estimates the test strength within 26 percent, on the average. The torsional and flexural stiffnesses at 70 percent of the test cracking strength can be satisfactorily estimated. This analysis has reinforced the possibility of neglecting the intermediate principal tensile stress in formulating the failure criteria of concrete for slender beams.

6. Assuming full plastic distribution of torsional shear stress and elastic distribution of stresses due to other forces, and using the principal stress failure criteria coupled with the tensile strength of concrete which is estimated equal to the splitting tensile strength, the

cracking strengths are conservatively predicted. This method also, like the finite element method, proves to be more conservative for the case of web cracking than that for cracking at other locations on the cross-section. The case of the web cracking is more closely predicted if the initial crack is assumed to occur at the centroid of the cross-section. The theory conservatively estimates the test strength within 17 percent, on the average.

7. Similar to reinforced and prestressed concrete rectangular beams, prestressed I beams can fail in skew bending either in a bending mode (Mode 1) or a torsion mode (Mode 2). The bending mode of failure is characterized by the formation of a compression hinge in the top flange joined by an approximately continuous tensile crack on the other three sides. The torsion mode (Mode 2) is recognized by a nearly continuous tensile crack on the two flange faces and on one side of the web. Based on the type of crack patterns observed, it is concluded that the location of the compression hinge is close to one face of the web rather than along the sides of the flanges. This location is in line with the findings of Wyss, Garland and Mattock (1969) and in contradiction with that suggested by Gvozdev et al (1968) and by Woodhead and McMullen (1972).

8. The failure mode need not be the same as the initial cracking mode; for example as in the case for beams of this investigation subjected to pure torsion.

9. Isolated I beams with web reinforcement such as those tested in the present investigation in which the compression zone is not provided with any anchored binding reinforcement may fail in an over-reinforced

manner, even though such I beams are under-reinforced in pure torsion and in pure bending. The reason for such behavior resulting in premature failure and lesser strength is the reduced effectiveness of the compressed flange resisting the shear-compression forces because the outstanding flange splits off due to torsionally induced cracking. However, it can be expected that such a premature failure can be avoided by providing confining reinforcement in the compression flange.

10. The configuration of the web reinforcement used in the present investigation can adequately resist torsion. The vertical legs should continue across the full width of the flange. It is not necessary to use closed rectangular stirrups as a web reinforcement.

11. The addition of web reinforcement increases the strength and ductility of beams under pure torsion and under combined loadings.

12. The minimum amount of web reinforcement used in this investigation corresponds approximately to that suggested by Hsu (1968d) for reinforced concrete rectangular beams with similar width and depth dimension of the stirrup. This minimum is sufficient to enable the beam under pure torsion or combined loadings to fail at loads in excess of cracking loads.

13. The ultimate strength of prestressed I beams subjected to combined loadings can now be predicted by the theory presented in Chapter IV which is based on a skew bending failure mechanism taking into account strain compatibility. The bending mode analysis presented here takes into account the splitting off of the outstanding compression flange due to torsional cracking and the resulting premature failure by neglecting

the flange tips. If the amount of torsion applied is small such a premature failure may not occur and the full flange width can be considered effective. For such cases if the outstanding flanges are neglected, the analysis yields conservative results. The agreement between the test and theoretical results is good (Tu test/Tu theory = 0.98) for bending mode failures.

The torsion mode analysis can be applied only to beams reinforced longitudinally and transversely and it predicts the test strength conservatively; the prediction of strength is reasonably good (Tu test/Tu theory = 1.20) for beams under pure torsion, but rather conservative for combined loadings (Tu test/Tu theory = 1.32).

14. Until a more accurate assumption concerning strain compatibility conditions of reinforcement is established, significant progress cannot be made in the skew bending method of analysis for partially over-reinforced beams failing in Mode 2.

15. The post cracking torsional and flexural stiffnesses depend primarily on the loading ratio and also on the amount of reinforcement and eccentricity of prestress.

16. In web reinforced beams as long as the web reinforcement is sufficient to prevent failure at cracking, the torsional and the flexural ductilities do not vary significantly as the web reinforcement is varied.

17. Torsional and flexural ductilities depend mainly on the loading ratios. Rotation capacity at ultimate reduces as the T/M ratio decreases or level of prestress increases.

REFERENCES

American Concrete Institute, 1963. Building code requirements for reinforced concrete. ACI 318-63, Detroit, Michigan.

American Concrete Institute, 1971. Building code requirements for reinforced concrete. ACI 318-71, Detroit, Michigan.

Anderson, P., 1937. Rectangular concrete sections under torsion. Proceedings American Concrete Institute 34:1-11.

Arockiasamy, M., 1964. Torsional strength of reinforced concrete members. The Indian Concrete Journal (India) 38 (11), 421-430.

Bach, C., 1911. Elastizitat und Festigkeit. Springer-Verlag, Berlin.

Barton, T.G., and Kirk, D.W., 1973. Concrete T-beams subject to combined loading. Journal of the Structural Division ASCE 99 (ST4): 687-700.

Behera, U., Rajagopalan, K.S., and Ferguson, P.M., 1970a. Reinforcement for torque in Spandrel L-beams. Journal of the Structural Division ASCE 96(ST2): 371-380.

Behera, U., Ferguson, P.M., 1970b. Torsion, shear, and bendirg on stirruped L-beams. Journal of the Structural Division ASCE 96 (ST7): 1271-1286.

Bishara, A., 1969. Prestressed concrete beams under combined torsion, bending, and shear. Journal of the American Concrete Institute 66 (7): 525-538.

Birkeland, C.J., Hamilton, M.E., and Mattock, A.H., 1967. Strength of reinforced concrete beams without web reinforcement in combined torsion, shear and bending. The Trend in Engineering 19(4): 8-12, University of Washington, Seattle.

Bradburn, J.H., 1968. An investigation of combined bending and torsion in rectangular reinforced concrete members. Ph.D. Thesis, Department of Civil Engineering, North Carolina State University at Raleigh.

Bresler, B., and Pister, K., 1958. Strength of concrete under combined stresses. Journal of the American Concrete Institute 30(3): 321-345.

Chander, H., Kemp, E.L., and Wilhelm, W.J., 1970. Prestressed concrete rectangular members subjected to pure torsion. Civil Engineering Studies Report No. 2007, West Virginia University, Morgantown, West Virginia.

Clough, R.W., 1969. Comparison of three dimensional finite elements. Proc. of Symposium on Application of Finite Element Methods in Civil Engineering, ASCE: 1-26, Nashville.

Cowan, H.J., 1950. An elastic theory for the torsional strength of rectangular reinforced concrete beams. Magazine of Concrete Research. 2(4): 3-8.

Cowan, H.J., Armstrong, S., 1955. Experiments on the strength of reinforced and prestressed concrete beams and of concrete-encased steel joists in combined bending and torsion. Magazine of Concrete Research 7 (19): 3-20.

Collins, M.P., Walsh, P.F., Archer, F.E., and Hall, A.S., 1968. Reinforced concrete in torsion. Uniciv. Report No. R-31, University of New South Wales, Sydney.

Collins, M.P., 1969. The normal moment yield criterion applied to beams in flexure-torsion. International Conference on Shear, Torsion, and Bond in Reinforced and Prestressed Concrete, Coimbattore, India.

Collins, M.P., and Lampert, P., 1971. Designing for torsion. Structural Concrete Symposium, Department of Civil Engineering, University of Toronto. 38-79.

Desayi, P., and Krishanan, S., Equation for the stress-strain curve of concrete. Journal of the American Concrete Institute. 61 (3):345-350.

Ltqren, L., 1972. Reinforced concrete beams loaded in combined torsion, bending and shear. Publication 71:3, Division of Concrete Structures, Chalmers University of Technology, Göteborg.

Ersoy, U., and Ferguson, P.M., 1968. Concrete beams subjected to combined torsion and shear - experimental trends. SP No. 18. Torsion of Structural Concrete. American Concrete Institute, Detroit, Michigan.

Evans, Paul R., Kemp, E.L., and Wilhelm, W.J., 1970. The behavior of T- and L-shaped plain and reinforced concrete beams loaded in torsion. Civil Engineering Studies Report No. 2006, West Virginia University, Morgantown, West Virginia.

Evans, R.H., and Khalil, M.G.A., 1970. The behavior and strength of prestressed concrete and rectangular beams subjected to combined bending and torsion. The Structural Engineer 48(2): 59-73.

Farmer, L.E., and Ferguson, P.M., 1967. T-beams under combined bending, shear, and torsion. Journal of the American Concrete Institute 64 (11): 757-766.

Gangarao, H.V.S., and Zia, P., 1970. Rectangular prestressed concrete beams under combined bending and torsion. Department of Civil Engineering, North Carolina State University at Raleigh.

Gaušel, E., 1970. Ultimate strength of prestressed I-beams under combined torsion, bending, and shear. An ACI Summary Paper title No. 67-42. Journal of the American Concrete Institute 67 (9): 675-678.

Gardner, R.P.M., 1960. The behavior of prestressed concrete I-beams under combined bending and torsion. T.R. No. 329. Cement and Concrete Association, London, England.

Gesund, H., and Boston, L.A., 1964. Ultimate strength in combined bending and torsion of concrete beams containing only longitudinal reinforcement. Journal of the American Concrete Institute 61(11): 1453-1471.

Gesund, H., Schuette, F.J., Buchanan, G.R., and Gray, G.A., 1964. Ultimate strength in combined bending and torsion of concrete beams containing both longitudinal and transverse reinforcement. Journal of the American Concrete Institute. 61: 1509-1522.

Goode, C.D., and Helmy, M.A., 1968. Ultimate strength of reinforced concrete beams in combined bending and torsion. SP-18: 357-377. Torsion of Structural Concrete. American Concrete Institute, Detroit, Michigan.

Gopalakrishnayya, A.V., 1973. Analysis of cracking of earth dams. Ph.D. Thesis, Department of Civil Engineering, University of Alberta, Edmonton.

Gvozdev, A.A., Lessig, N.N., and Rulle, L.K., 1968. Research on reinforced concrete beams under combined bending and torsion in the Soviet Union. SP-18: 307-336. Torsion of Structural Concrete. American Concrete Institute, Detroit, Michigan.

Henry, R.L., and Zia, P., 1971. Behavior of rectangular prestressed concrete beams under combined torsion, bending and shear. Department of Civil Engineering, North Carolina State University at Raleigh.

Hsu, T.T.C., 1967. Private communication to members of ACI Committee 438, Torsion, Oct. 17, 1967.

Hsu, T.T.C., 1968a. Torsion of structural concrete-plain concrete rectangular sections. SP No. 18. Torsion of Structural Concrete. American Concrete Institute, Detroit, Michigan.

Hsu, T.T.C., 1968b. Torsion of structural concrete - a summary on pure torsion. SP No. 18. Torsion of Structural Concrete. American Concrete Institute, Detroit, Michigan.

Hsu, T.T.C., 1968c. Torsion of structural concrete - uniformly prestressed rectangular members without web reinforcement. Journal of Prestressed Concrete Institute 13 (2): 34-44.

Hsu, T.T.C., 1968d. Ultimate torque of reinforced rectangular beams. Journal of the Structural Division ASCE 94 (ST2): 485-510.

Hsu, T.T.C., 1968e. Behavior of reinforced concrete rectangular members. SP No. 18. Torsion of Structural Concrete. American Concrete Institute, Detroit, Michigan.

Hsu, T.T.C., and Kemp, E.L., 1969. Background and practical application of tentative design criteria for torsion. Journal of the American Concrete Institute 66 (1): 12-23.

Humphreys, R., 1957. Torsional properties of prestressed concrete. The Structural Engineer 35 (6): 213-224

Johnston, D.W., and Zia, P., 1971. Hollow prestressed concrete beams under combined torsion, bending, and shear. Department of Civil Engineering, North Carolina State University at Raleigh.

Kemp, E.L., Sozen, M.A., and Siess, C.P., 1961. Torsion in reinforced concrete. Structural Research Series No. 226, Department of Civil Engineering, University of Illinois, Urbana, Illinois.

Kirk, D.W., and Lash, S.D., 1971. T beams subject to combined bending and torsion. Journal of the American Concrete Institute 68 (2): 150-159.

Kirk, D.W., and Loveland, N.C., 1972. Unsymmetrically reinforced T-beams subject to combined bending and torsion. Journal of the American Concrete Institute 69 (8): 492-499.

Klus, J.P., 1968. Ultimate strength of reinforced concrete beams in combined torsion and shear. Journal of the American Concrete Institute 65 (3): 210-225.

Kupfer, H., Hilsdorf, H.K., and Rusch, H., 1969. Behavior of concrete under biaxial stresses. Journal of the American Concrete Institute 66(8): 656-666.

Kuyt, B., 1971. A theoretical investigation of ultimate torque as calculated by the Truss theory and by the Russian equilibrium method. Magazine of Concrete Research 23 (77): 155-160.

Kuyt, B., 1972. A method for ultimate strength design of rectangular reinforced concrete beams in combined torsion, bending and shear. Magazine of Concrete Research 23 (78): 15-24.

Lampert, P., and Thurlimann, B., 1968. Torsionversuche on stahlbeton-balken. Bericht Nr. 6506-2, Institute fur Baustatik, ETH Zurich.

Lampert, P., and Thurlimann, B., 1969. Torsions-Biege-Versuche on Stahlebetonbalken. Bericht Nr. 6506-3, Institut fur Baustatik, ETH Zurich.

Lampert, P., 1971. Torsion and bending in reinforced and prestressed concrete members. Proceedings of the Institution of Civil Engineers, Vol. 50: 487-505.

Lampert, P., Luchinger, P., and Thurlimann, B., 1971. Torsionversuche an stahl-und spannbetonbalken, Bericht Nr. 6506-4, Institut fur Baustatik, ETH Zurich.

Lampert, P., and Collins, M.P., 1972. Torsion, bending and confusion - An attempt to establish the facts. Journal of the American Concrete Institute 69(8): 500-504.

Leonhardt, F., 1970. Shear and torsion in prestressed concrete. Lecture, Session IV, VI FIP Congress, Prague, Czechoslovakia.

Lessig, N.N., 1958. Theoretical and experimental investigation of reinforced concrete elements subjected to combined bending and torsion. Theory of Design and Construction of Reinforced Concrete Structures. PP. 73-84. Moscow, Russia.

Lessig, N.N., 1959. Determination of the load-bearing capacity of reinforced concrete elements with rectangular cross section subjected to flexure and torsion. Trudy No. 5: 5-28. Concrete and Reinforced Concrete Institute, Moscow, Russia.

Liao, H., and Ferguson, P.M., 1969. Combined torsion in reinforced concrete I-beams with stirrups. Journal of the American Concrete Institute 66 (12): 986-993.

Marshall, W.T., and Tembe, N.R., 1941. Experiments on plain and reinforced concrete in torsion. The Structural Engineer 19 (11): 177-191.

Marshall, W.T., 1944. The torsional resistance of plastic materials with special reference to concrete. Concrete and Constructional Engineering 39: 83-88.

McGee, W.D., and Zia, P., 1973. Prestressed concrete members under torsion, shear and bending. Department of Civil Engineering, North Carolina State University at Raleigh.

McHenry, D., and Karni, J., 1958. Strength of concrete under combined tensile and compressive stresses. Journal of the American Concrete Institute 29 (10): 829-839.

McMullen, A.E., and Warwaruk, J., 1967. The torsional strength of rectangular reinforced concrete beams subjected to combined loading. Report No. 2. Department of Civil Engineering, University of Alberta, Edmonton.

Mitchell, D., Lampert, P., and Collins, M.P., 1971. The effects of stirrup spacing and longitudinal restraint on the behavior of reinforced concrete beams subjected to torsion. Publication 71-22, Department of Civil Engineering, University of Toronto, Toronto.

Miyamoto, T., 1927. Torsional strength of reinforced concrete. Concrete and Constructional Engineering, London 22: 637.

Mukherjee, P.R., and Kemp, E.L., 1967. Ultimate torsional strength of plain, prestressed, and reinforced concrete members of rectangular cross section. Civil Engineering Studies No. 2003. Department of Civil Engineering, West Virginia.

Mukherjee, P., and Warwaruk, J., 1970. Prestressed concrete beams with web reinforcement under combined loading. Structural Engineering Report No. 24, University of Alberta, Edmonton.

Nadai, A., 1931. Plasticity. McGraw Hill Book Company, Inc., New York.

Nylander, H., 1945. Vridning och vridningsinspänning vid betongkonstruktioner (Torsion and Torsional Restraint by Concrete Structures). Bulletin No. 3, Statens Committee für Byggnadsforskning, Stockholm, Sweden.

Prandtl, L., 1903. Zur torsion von prismatichen staben. Physikalische Zeitschreift 4: 758-770.

Pandit, G.S., and Warwaruk, J., 1968. Reinforced concrete beams in combined bending and torsion. SP No. 18. Torsion of Structural Concrete. American Concrete Institute, Detroit, Michigan.

Pandit, G.S., 1970. Discussion of "Prestressed concrete beams under combined torsion, bending, and shear". Journal of the American Concrete Institute. 67 (1): 61-63.

Rajagopalan, K.S., Behera, U., and Ferguson, P.M., 1971. Partially over-reinforced beams under pure torsion. Journal of the American Concrete Institute 68 (10): 740-747.

Rajagopalan, K.S., Behera, U., and Ferguson, P.M., 1972. Total interaction method for torsion design. Journal of the Structural Division ASCE 98 (ST9): 2097-2117.

Ramakrishnan, V., and Jayaraman, V., 1968. Combined bending and torsional strength of reinforced concrete T-beams without web reinforcement. The Indian Concrete Journal, India. 42 (3): 120-125.

Rao, D.L.N., and Warwaruk, J., 1973. Discussion of "Unsymmetrically reinforced T-beams subject to combined bending and torsion". Journal of the American Concrete Institute 70 (2): 153.

Rausch, E., 1929. Berechnungdes Eisenbetons gegen Verdrehung, Julius Springer, Berlin.

Reeves, J.S., 1962. Prestressed concrete tee beams under combined bending and torsion. T.R. No. 364. Cement and Concrete Association, London, England.

Saint Venant, B. de 1856. Memoires de l'acdemie des' sciences de savants et rongers. Paris. 14: 233-560.

Seth, B.R., 1958. Non-homogeneous yield conditions. I.U.T.A.M. Symposium on non-homogeneity in elasticity and plasticity, Warsaw.

Turner, L., and Davies, V.C., 1934. Plain and reinforced concrete in torsion, with particular reference to reinforced concrete beams. Selected Engineering Papers No. 165. The Institute of Civil Engineers, London, England.

Victor, D.J., and Ferguson, P.M., 1968a. Reinforced concrete T-beams without stirrups under combined moment and torsion. Journal of American Concrete Institute 65 (1): 29-36.

Victor, D.J., and Ferguson, P.M., 1968b. Beams under distributed load creating moment, shear, and torsion. Journal of the American Concrete Institute 65 (4): 295-309.

Wilson, E.L., 1966. Analysis of plane stress structures. Computing Program Series, University of California, Berkeley, California.

Wilson, E.L., 1970. User's manual of SAP. Berkeley, California.

Woodhead, H.R., and McMullen, A.E., 1972. A study of prestressed concrete under combined loading. Research Report No. CE 72-43, University of Calgary, Calgary.

Wyss, A.N., Garland, J.B., and Mattock, A.H., 1969. A study of the behavior of I-section prestressed concrete girders subject to torsion. Structures and Mechanics Report SM 9-1, University of Washington, Seattle.

Wyss, A.N., and Mattock, A.H., 1971. A study of I section prestressed concrete girders subject to torsion, shear, and bending. Structures and Mechanics Report SM 71-1, University of Washington, Seattle.

Yudin, V.K., 1962. Determination of the load-bearing capacity of reinforced concrete elements of rectangular cross-section under combined torsion and bending. Beton i zhelezobeton 6: 265-268.

Zia, P., 1960. Torsional strength of prestressed concrete members. Ph.D. thesis, Department of Civil Engineering, University of Florida, Gainsville.

Zia, P., 1961. Torsional strength of prestressed concrete members. Journal of the American Concrete Institute 57 (10): 1337-1359.

Zia, P., 1970. What do we know about torsion in concrete members. Journal of the Structural Division ASCE 96 (ST6): 1185-1199.

APPENDIX A

A.1 Torque-Twist and Load-Deflection Curves

Torque versus angle of twist and load versus deflection curves for beams tested in the experimental phase of the program are presented in Fig. A1 through A20. Each figure contains curves for several beams and for clarity the origin of each curve is offset by a fixed magnitude. Torque-twist and load-deflection curves for each beam represent the entire range of loading. In some cases the curves during the last increment of loading are shown as broken lines since measurements could not be available. In the load-deflection curves of a few beams, the last point on the curve represents the twisting of the beam without any increment in bending load.

A.2 Typical Failure Crack Patterns

Sketches of typical failure crack patterns for the beams in the form of developed surfaces are shown in Fig. A21 through A32. The location of the transverse load is shown by cross hatching on the top face of beam; this serves to identify the location of the failure surface relative to the transverse load.

A.3 Photographs of Beams

The photographs of the beams indicating the development of the crack patterns during the test are shown in Plate A.1 through Plate A.7 . For each beam views of the sourth and north faces on which shear stresses due to torsion and shear are respectively additive and subtractive are presented.

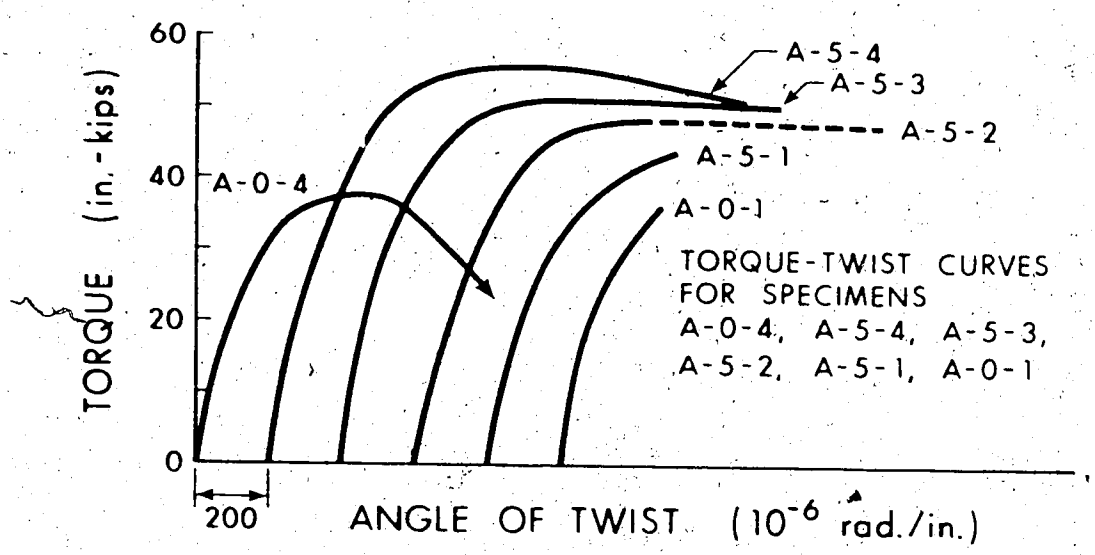

FIG. A.1 TORQUE-TWIST CURVES FOR SERIES - A BEAMS

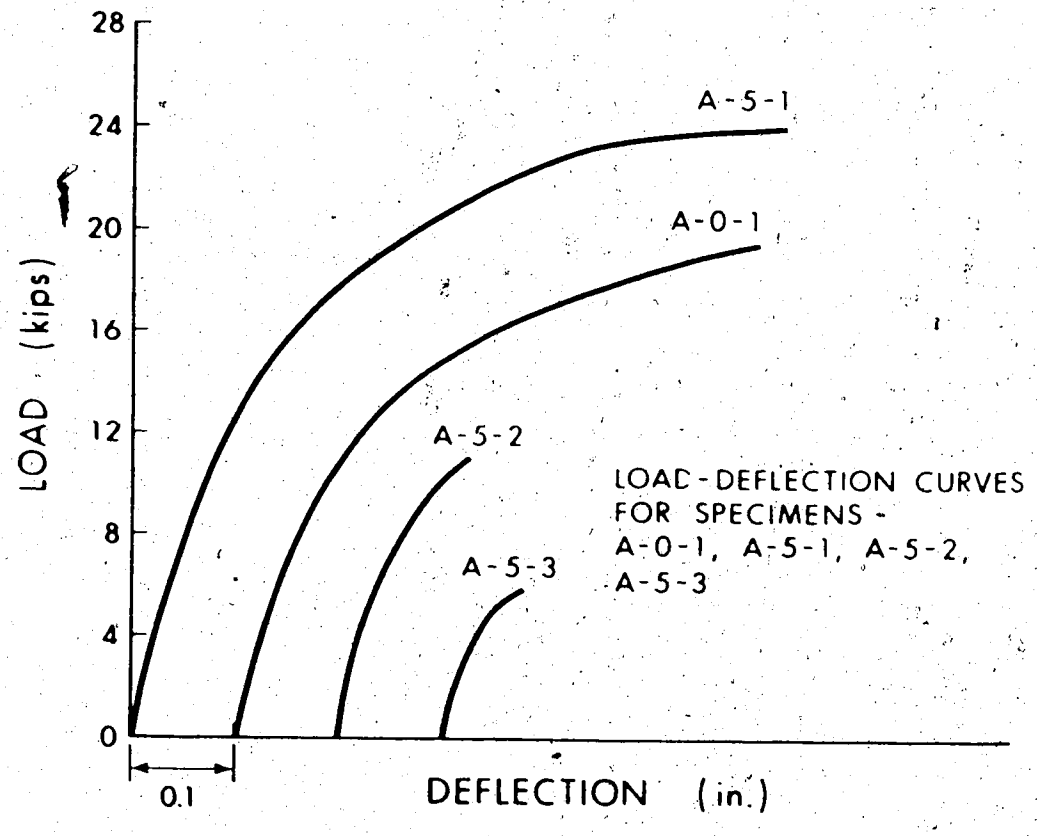

FIG. A.2 LOAD-DEFLECTION CURVES FOR SERIES - A BEAMS

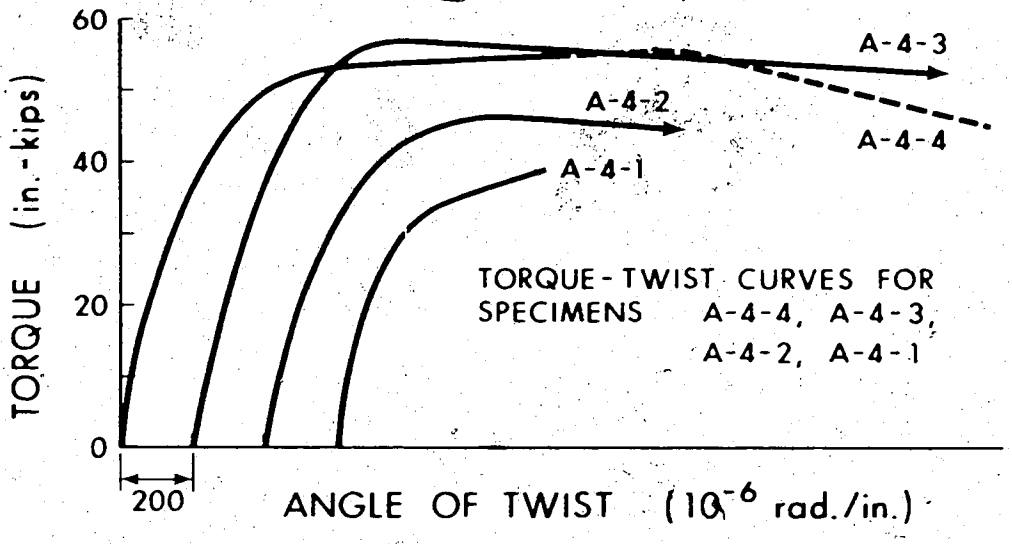

FIG. A.3 TORQUE-TWIST CURVES FOR SERIES - A BEAMS

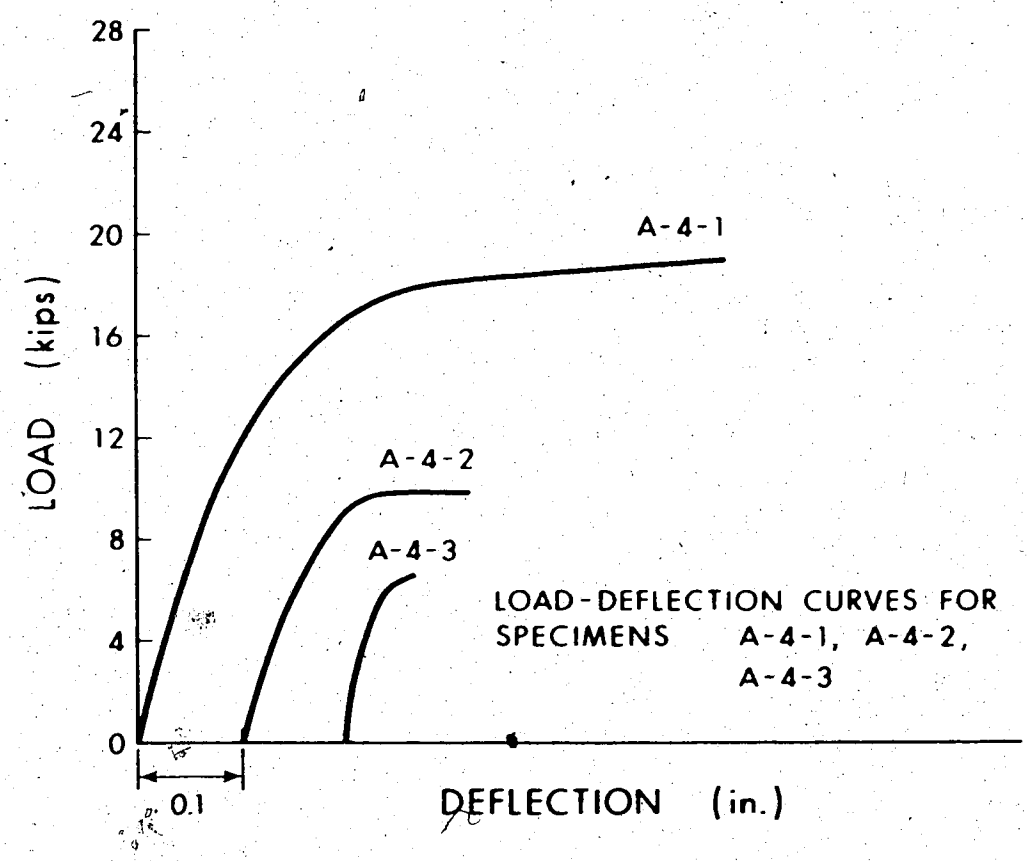

FIG. A.4 LOAD-DEFLECTION CURVES FOR SERIES - A BEAMS

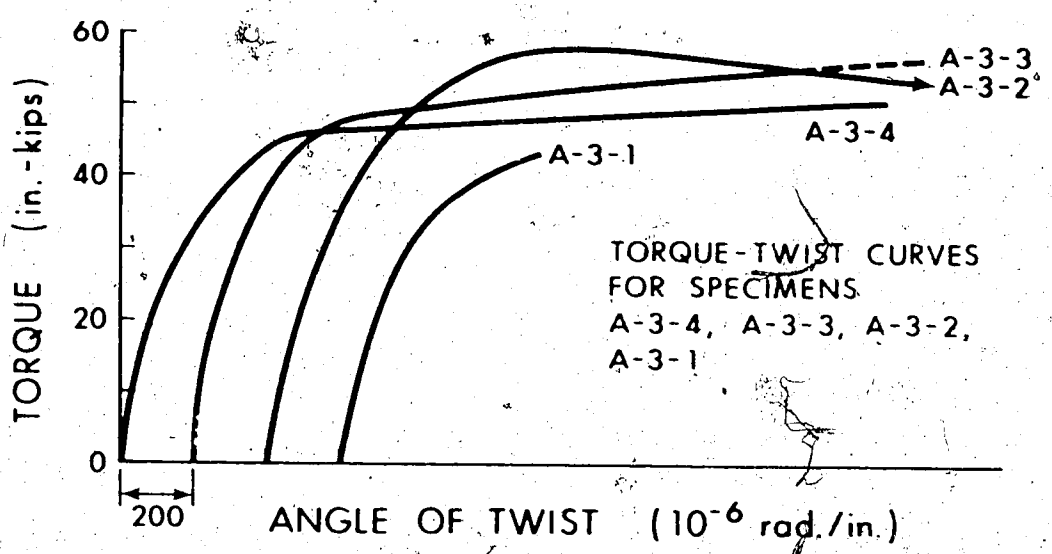

FIG. A.5 TORQUE-TWIST CURVES FOR SERIES - A BEAMS

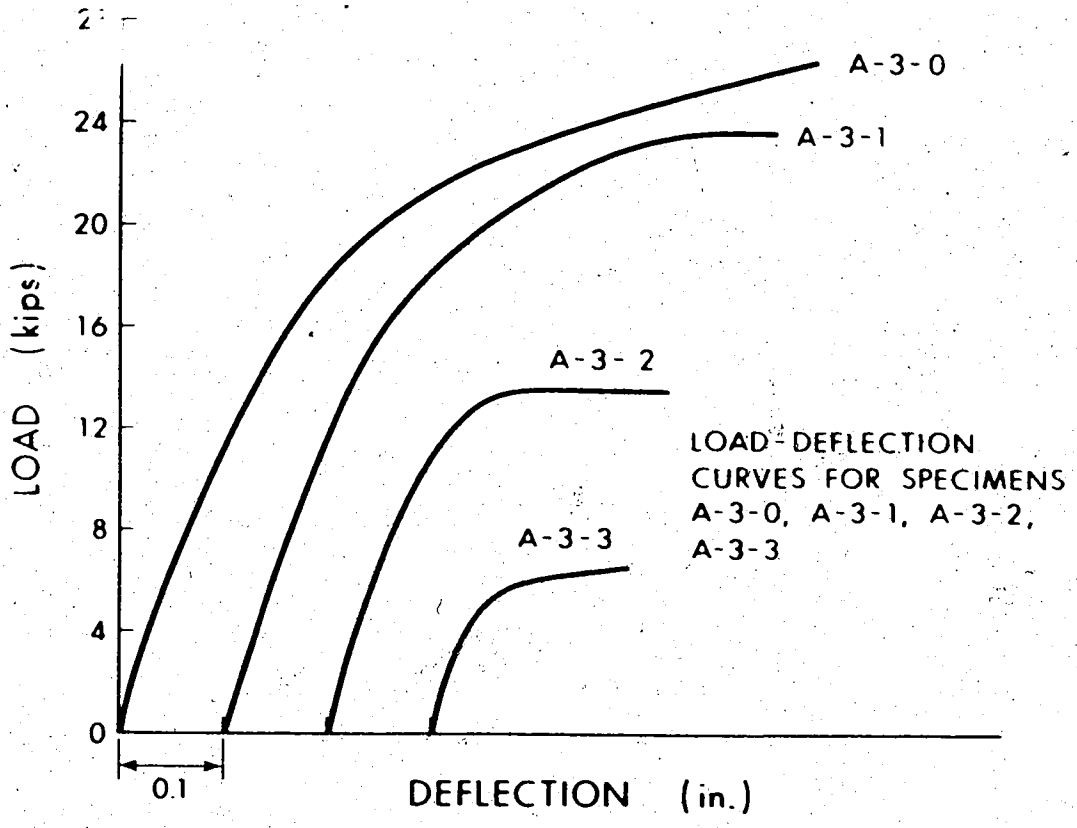

FIG. A.6 LOAD-DEFLECTION CURVES FOR SERIES - A BEAMS

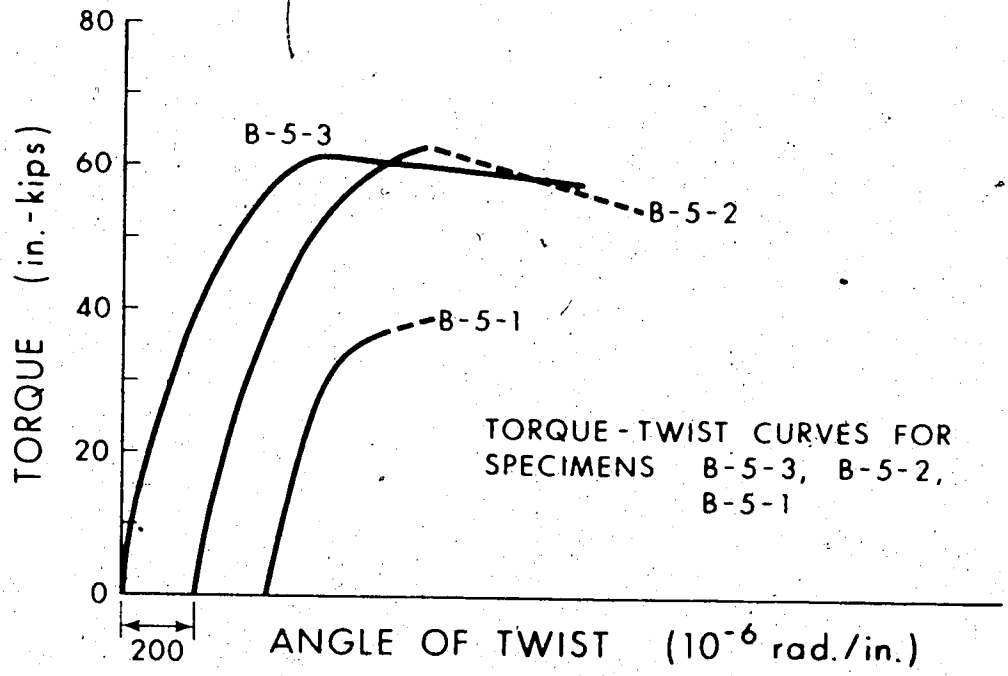

FIG. A.7 TORQUE-TWIST CURVES FOR SERIES - B BEAMS

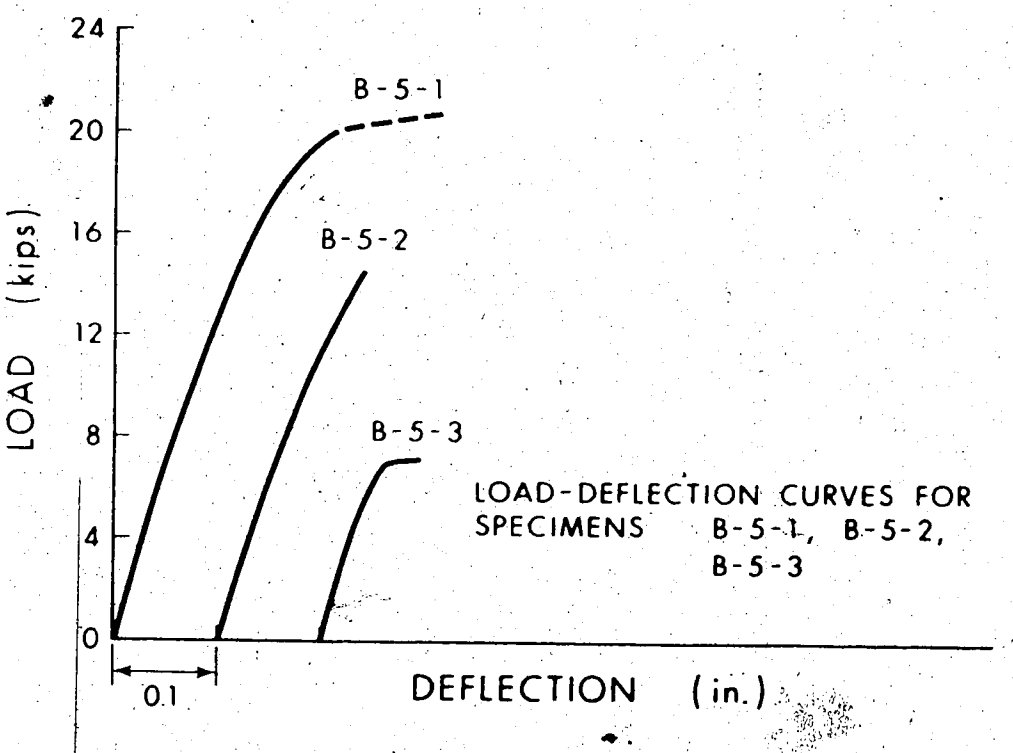

FIG. A.8 LOAD-DEFLECTION CURVES FOR SERIES - B BEAMS

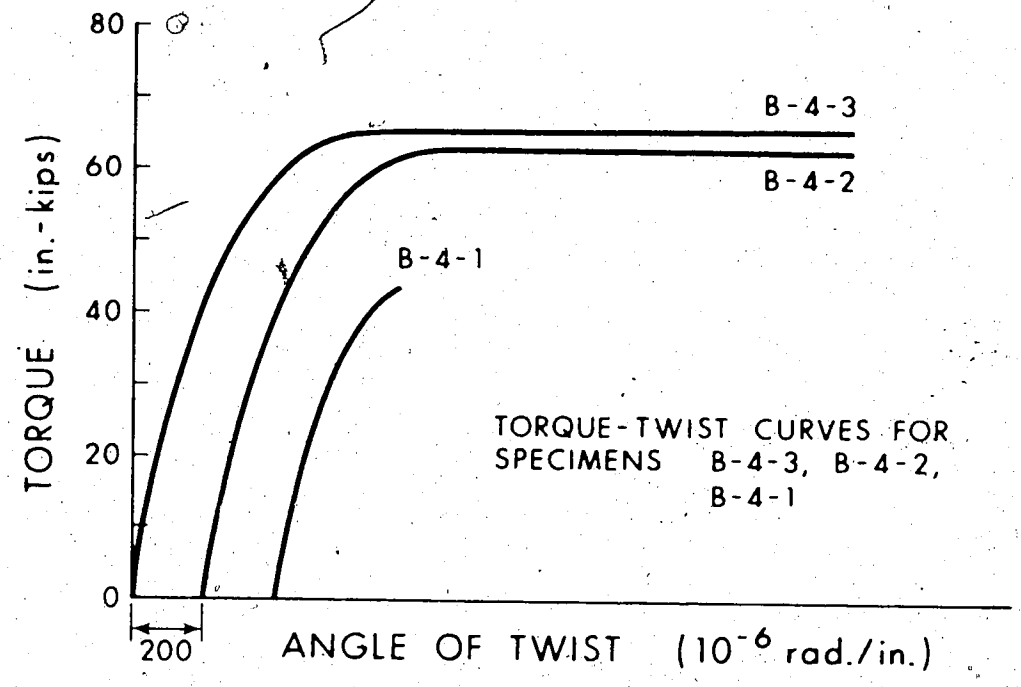

FIG. A.9 TORQUE-TWIST CURVES FOR SERIES - B BEAMS

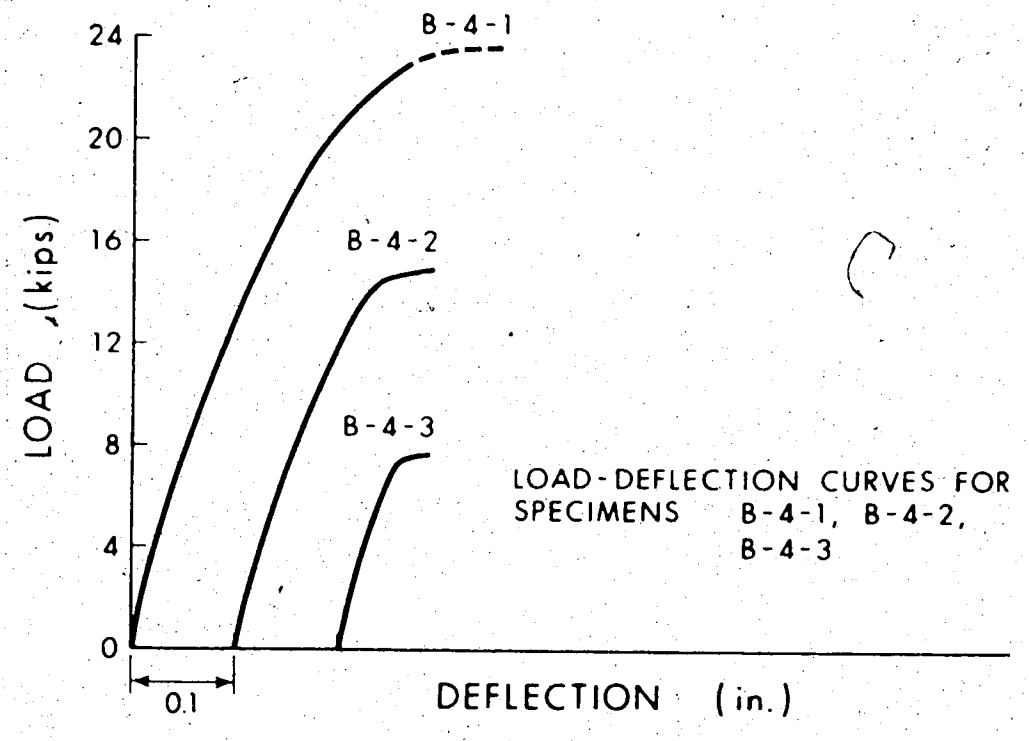

FIG. A.10 LOAD-DEFLECTION CURVES FOR SERIES - B BEAMS

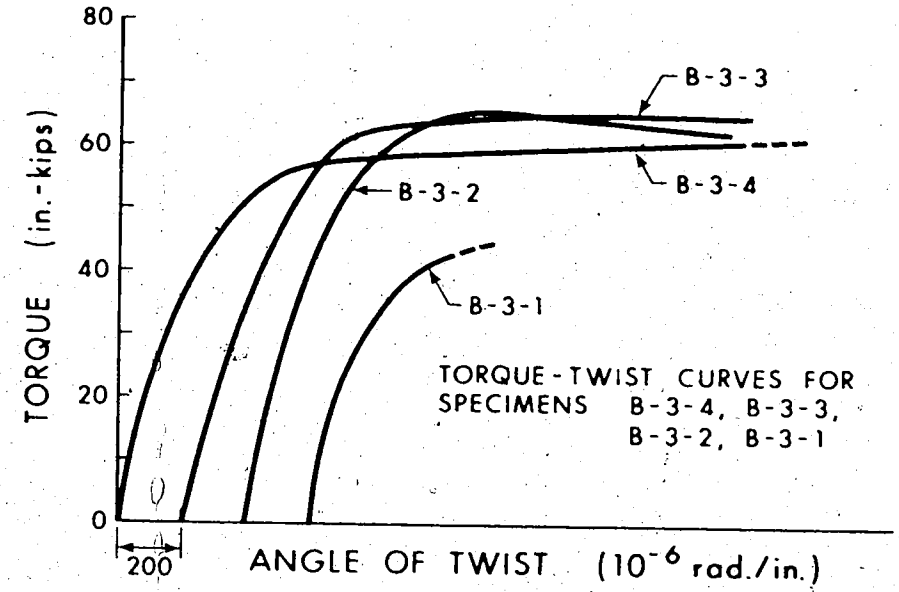

FIG. A.11 TORQUE-TWIST CURVES FOR SERIES - B BEAMS

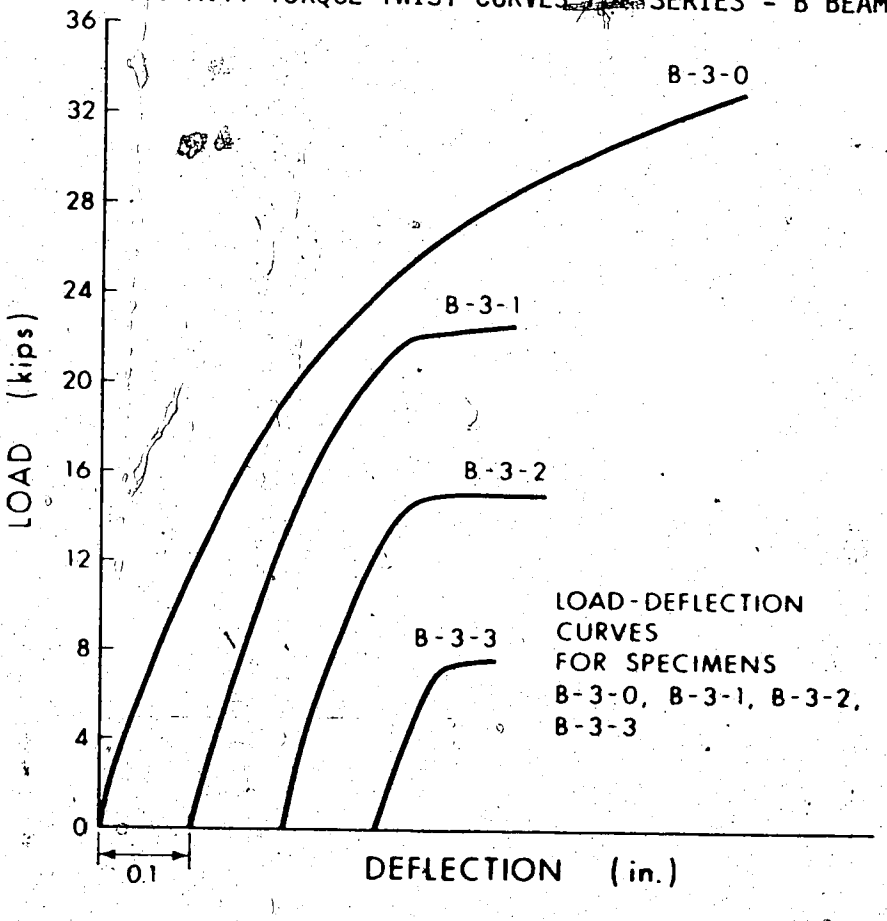

FIG. A.12 LOAD-DEFLECTION CURVES FOR SERIES - B BEAMS

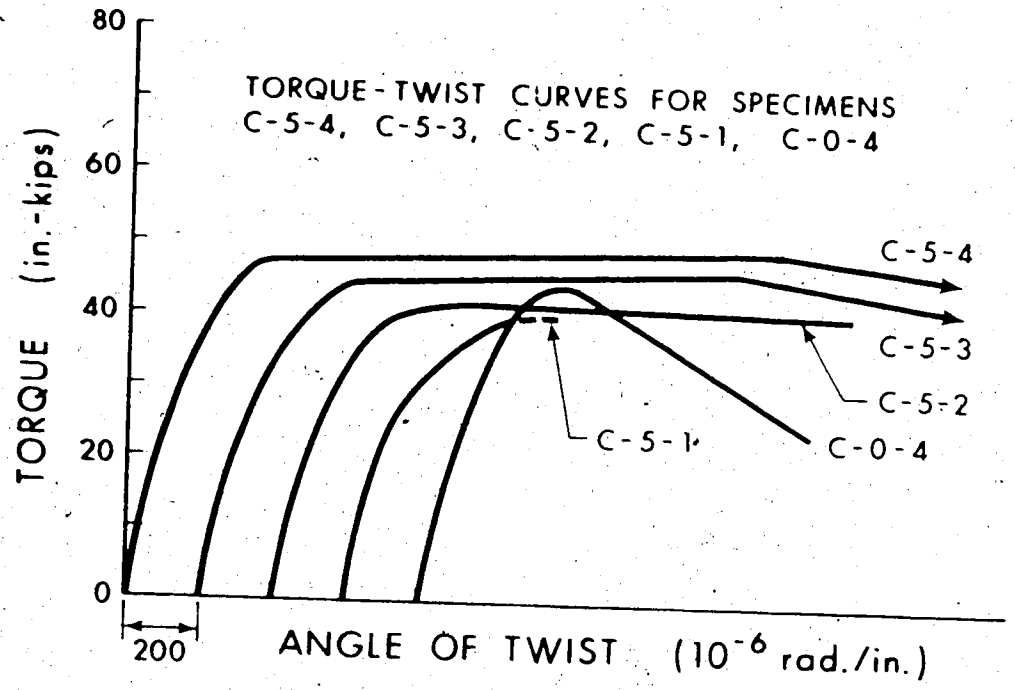

FIG. A.13 TORQUE-TWIST CURVES FOR SERIES - C BEAMS

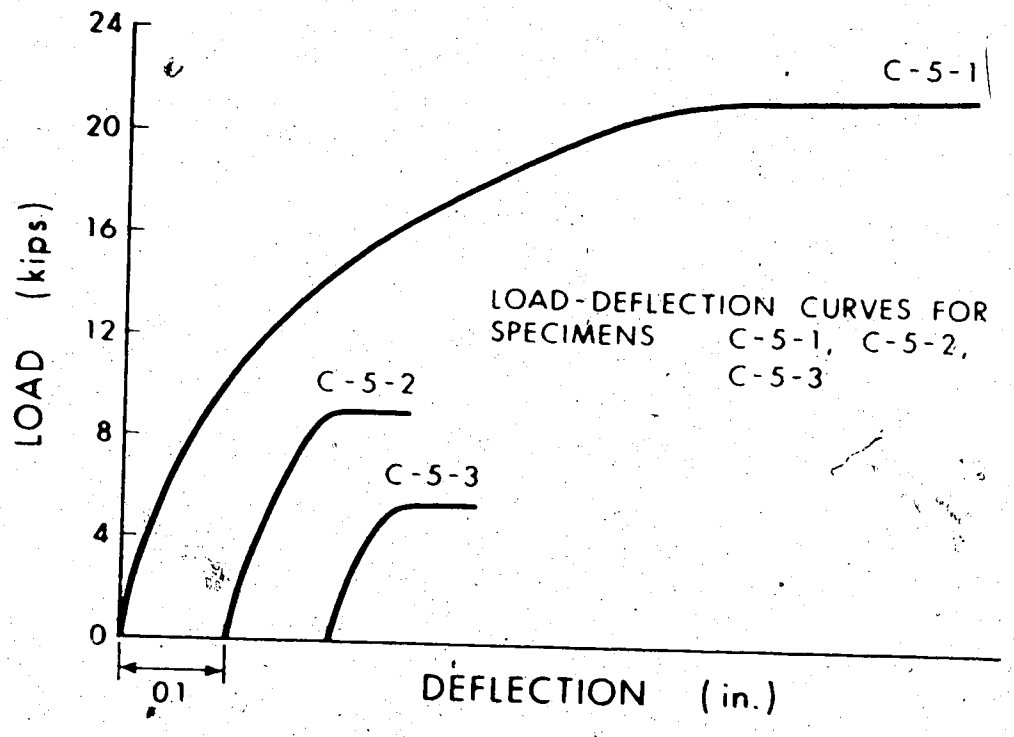

FIG. A.14 LOAD-DEFLECTION CURVES FOR SERIES - C BEAMS

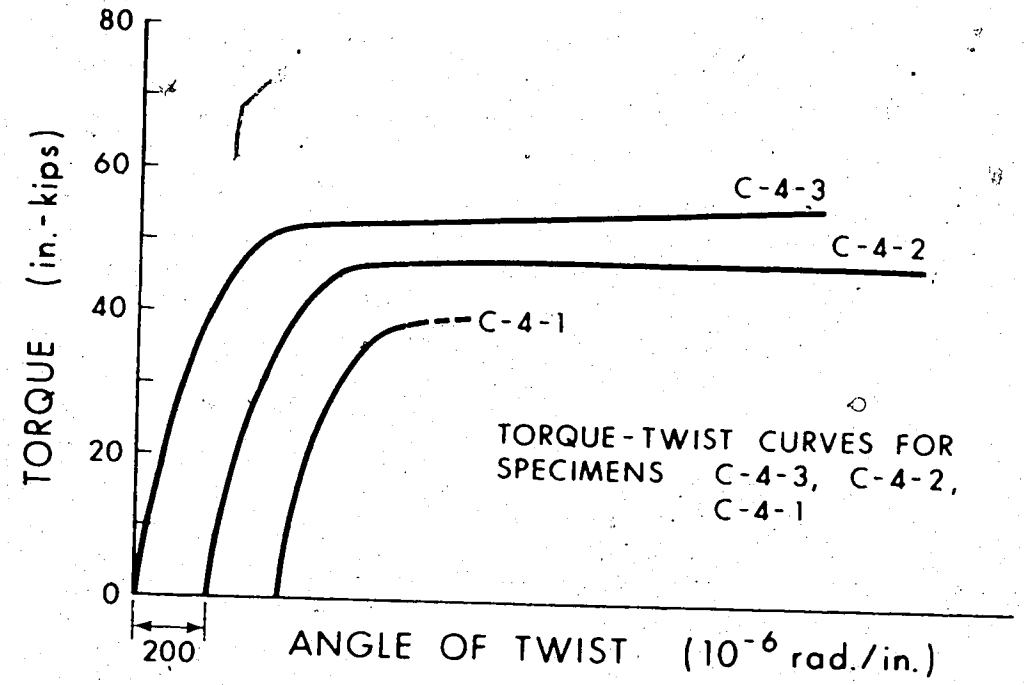

FIG. A.15 TORQUE-TWIST CURVES FOR SERIES - C BEAMS

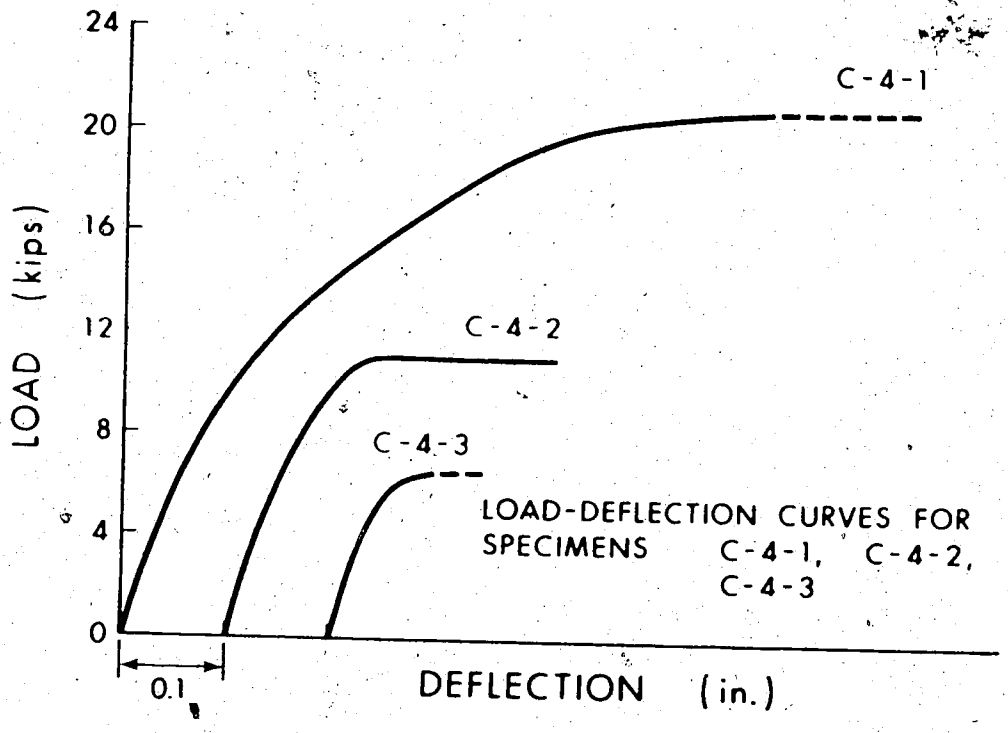

FIG. A.16 LOAD-DEFLECTION CURVES FOR SERIES - C BEAMS

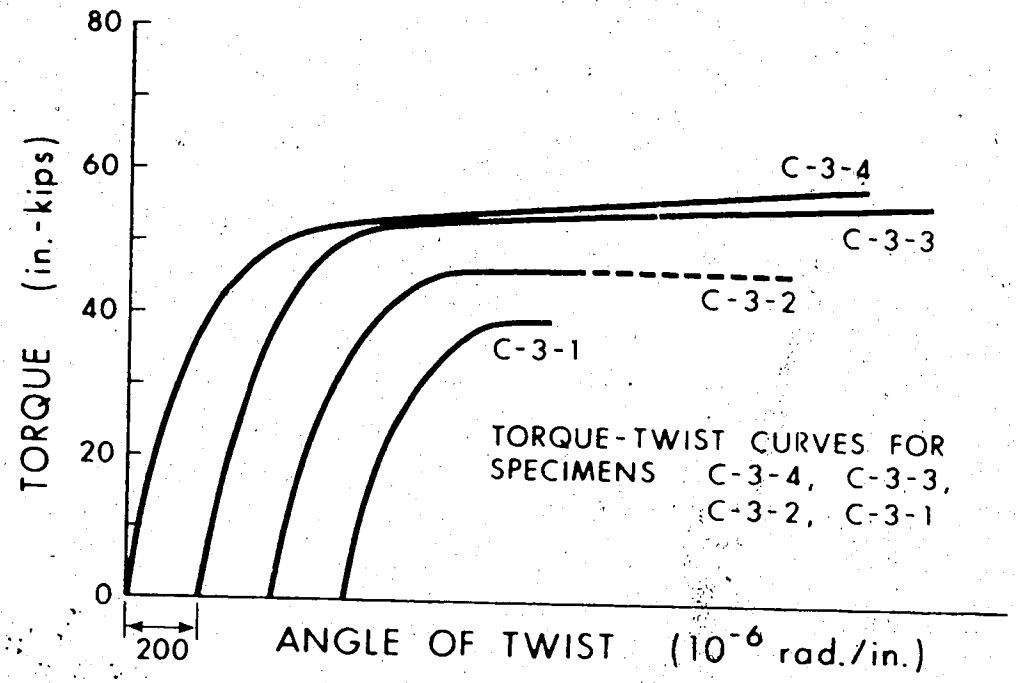

FIG. A.17 TORQUE-TWIST CURVES FOR SERIES - C BEAMS

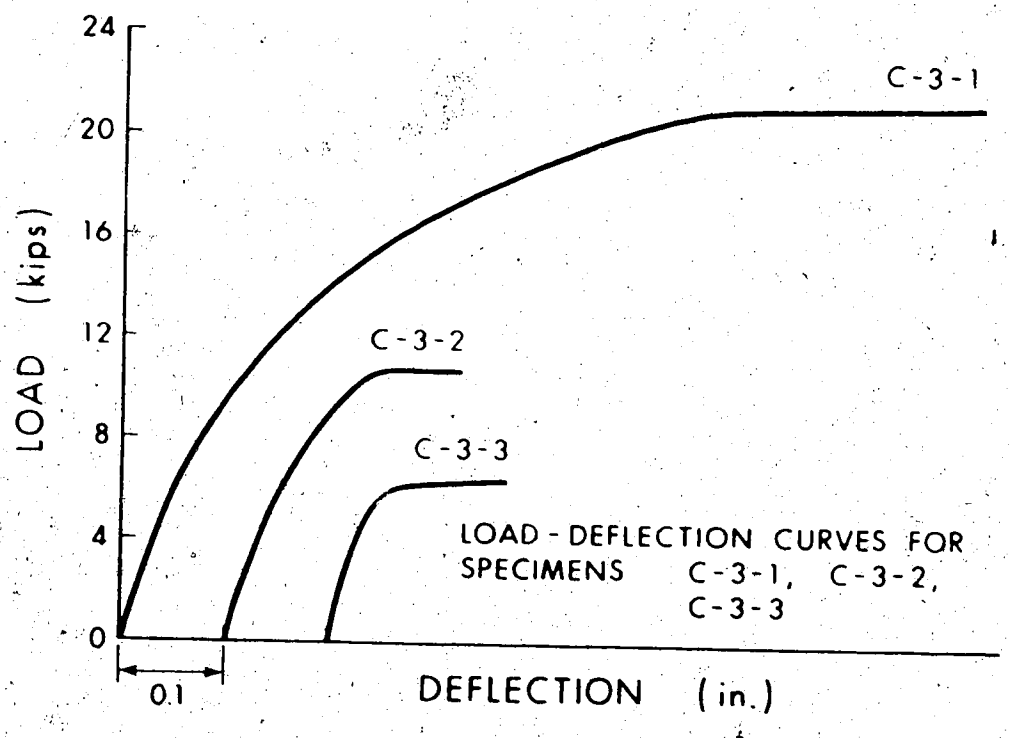

FIG. A.18 LOAD-DEFLECTION CURVES FOR SERIES - C Beams

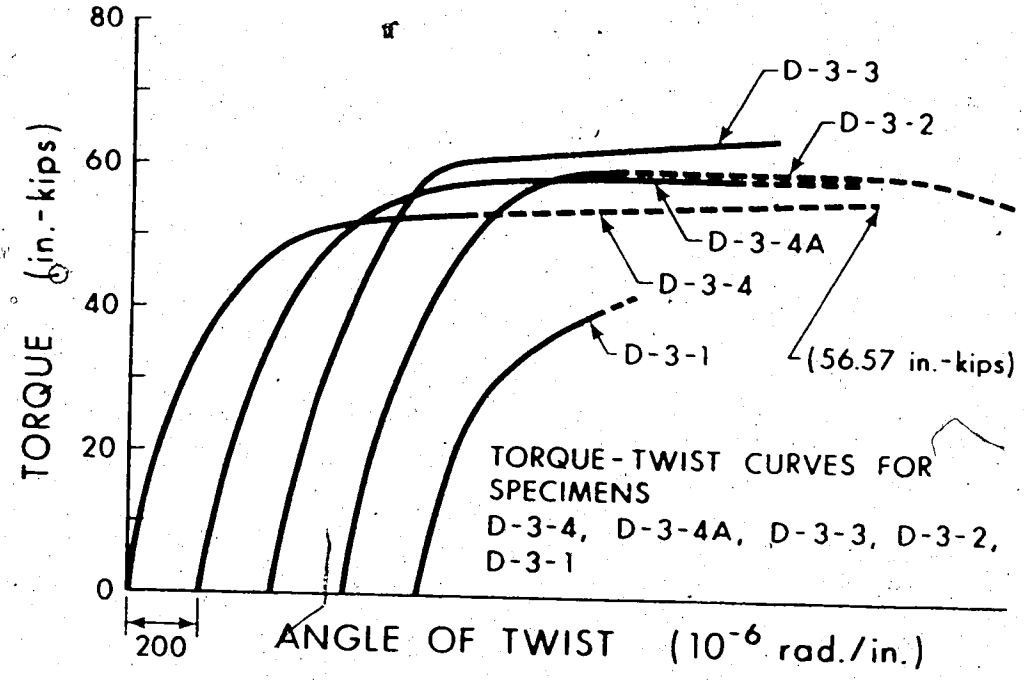

FIG. A.19 TORQUE-TWIST CURVES FOR SERIES - D BEAMS

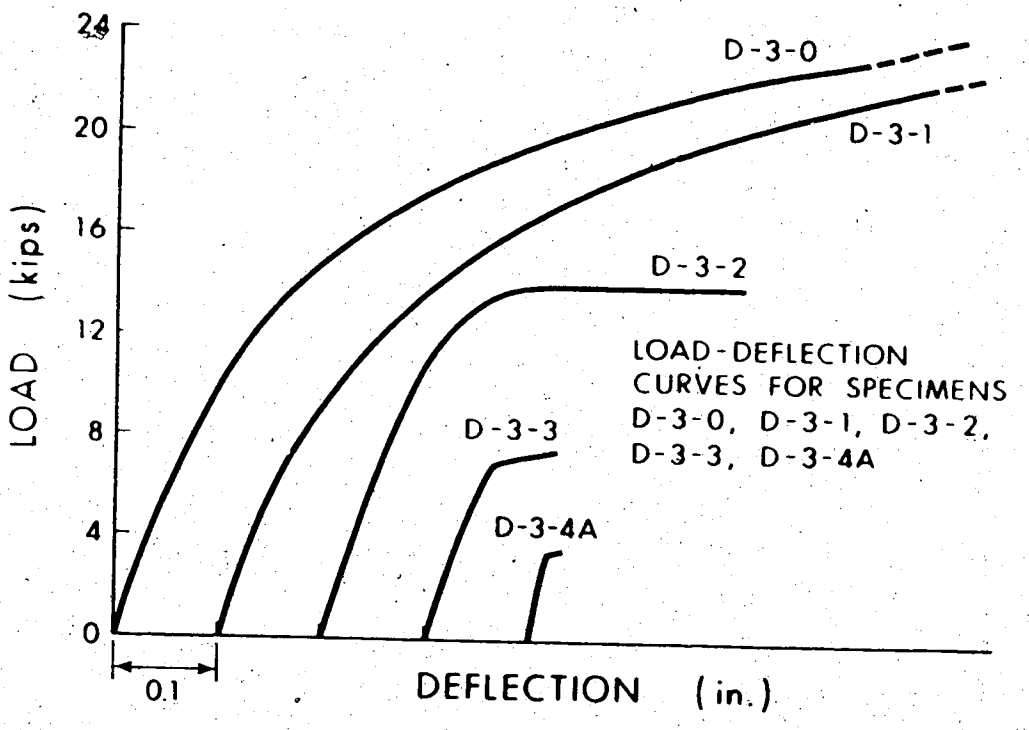

FIG. A.20 LOAD-DEFLECTION CURVES FOR SERIES - D BEAMS

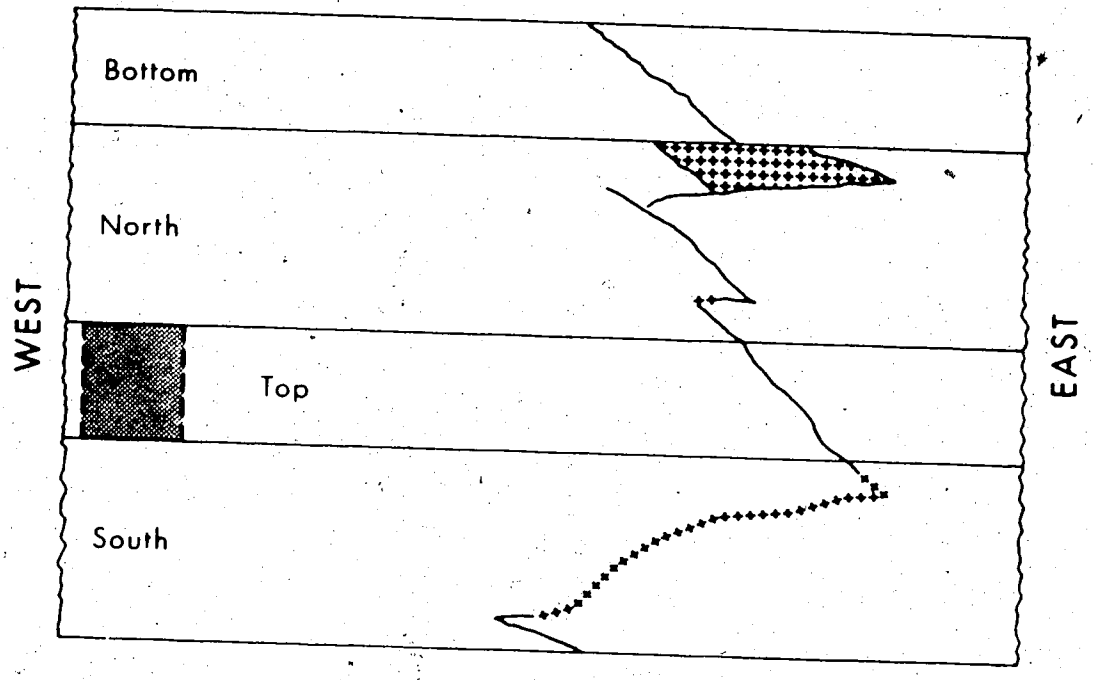

BEAM A-4-4

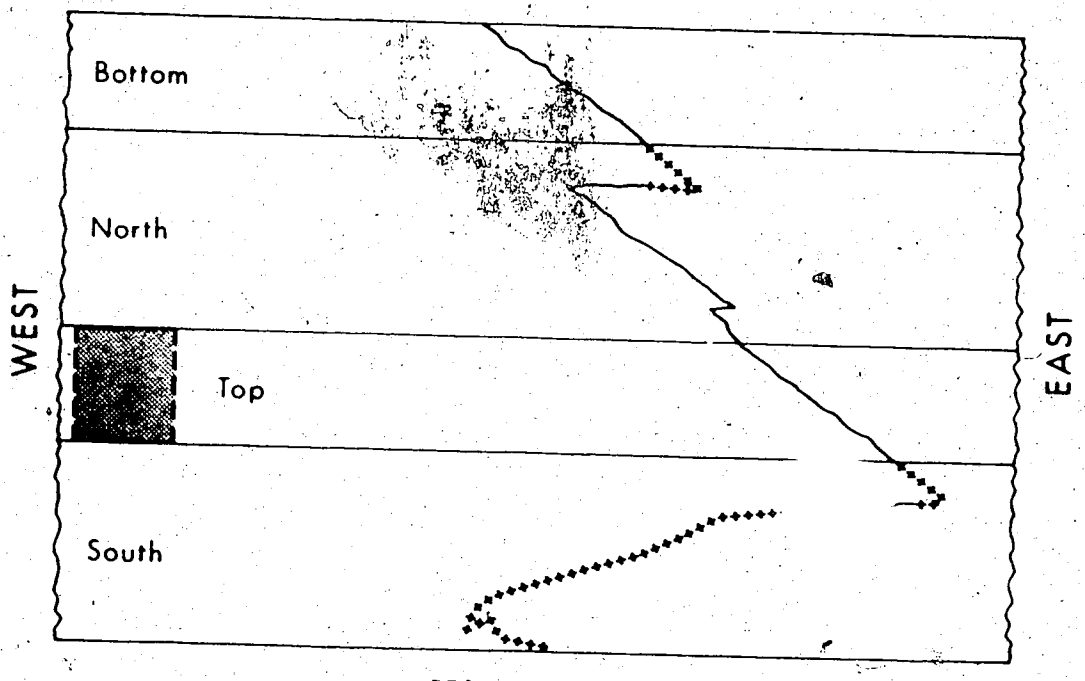

BEAM B-3-4

FIG. A.21 CRACK PATTERN FOR BEAMS A-4-4 AND B-3-4

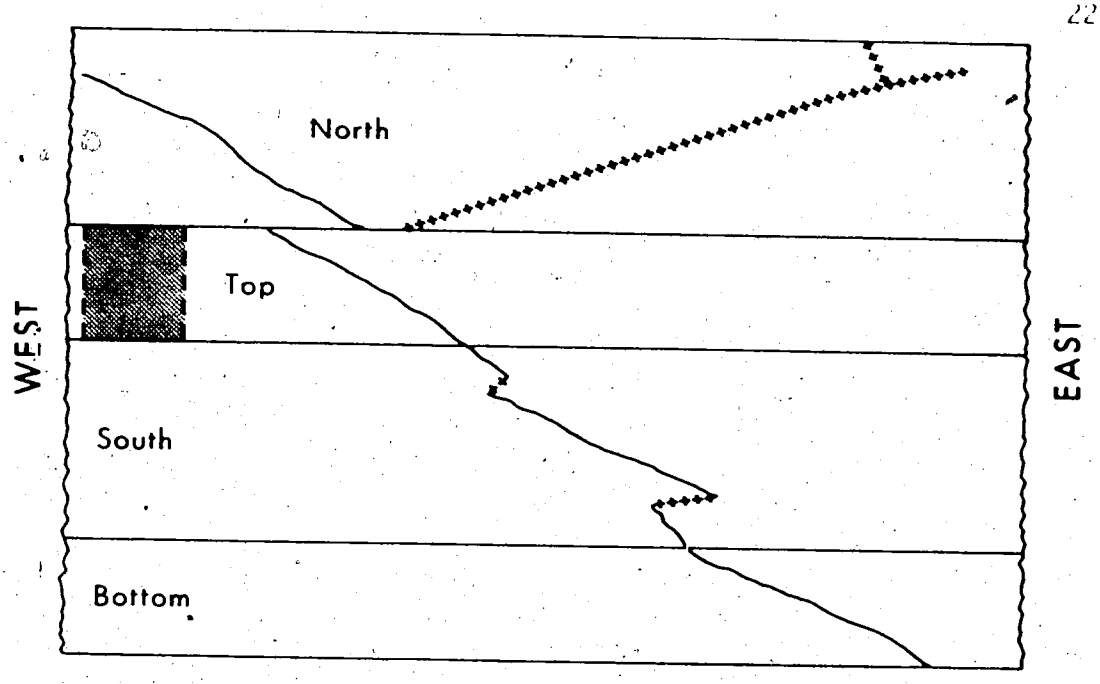

BEAM C-0-4

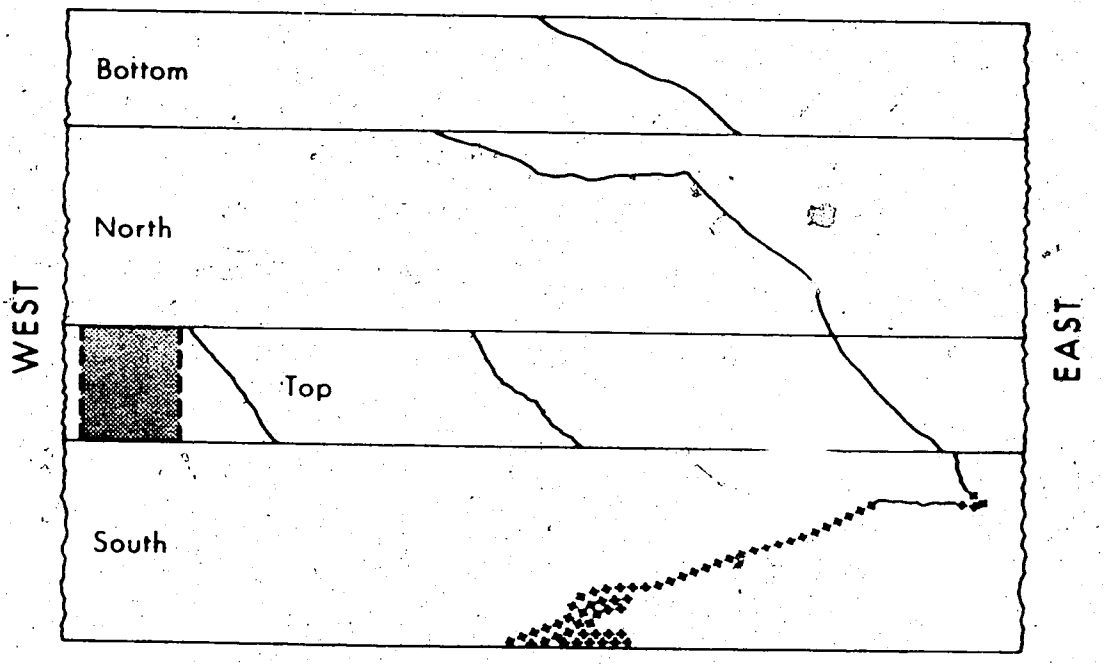

BEAM D-3-4

FIG. A.22 CRACK PATTERN FOR BEAMS C-0-4 AND D-3-4

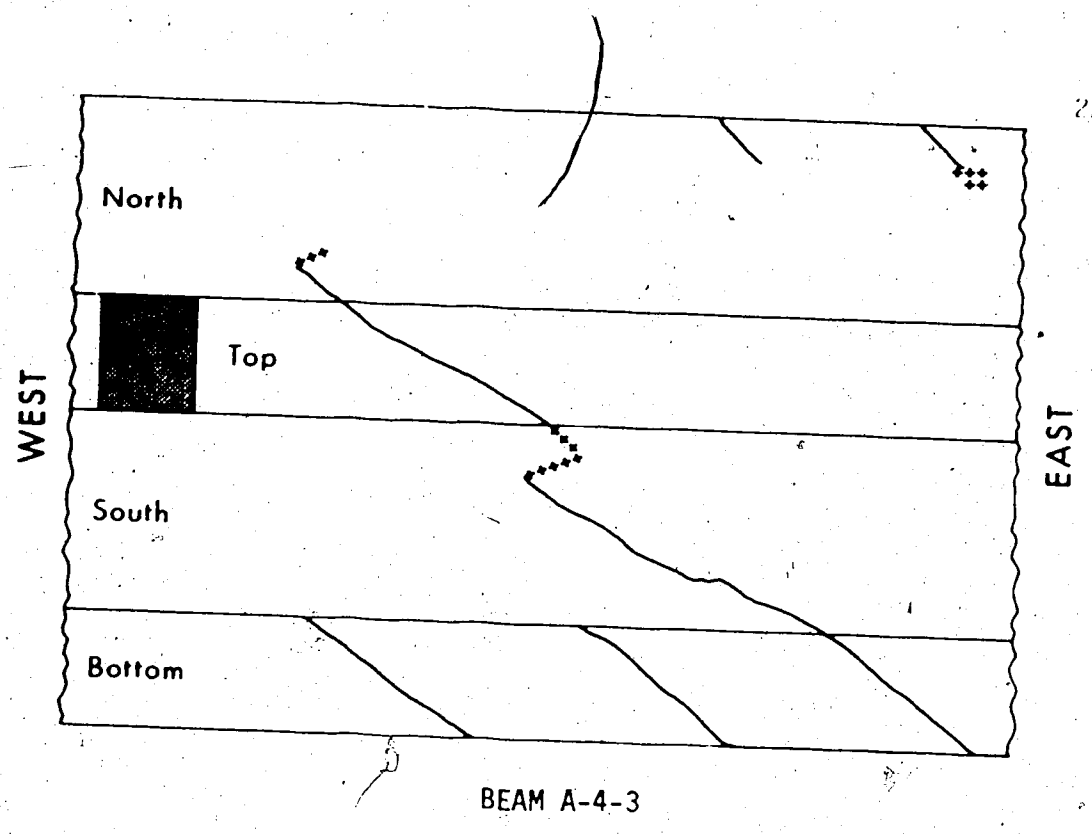

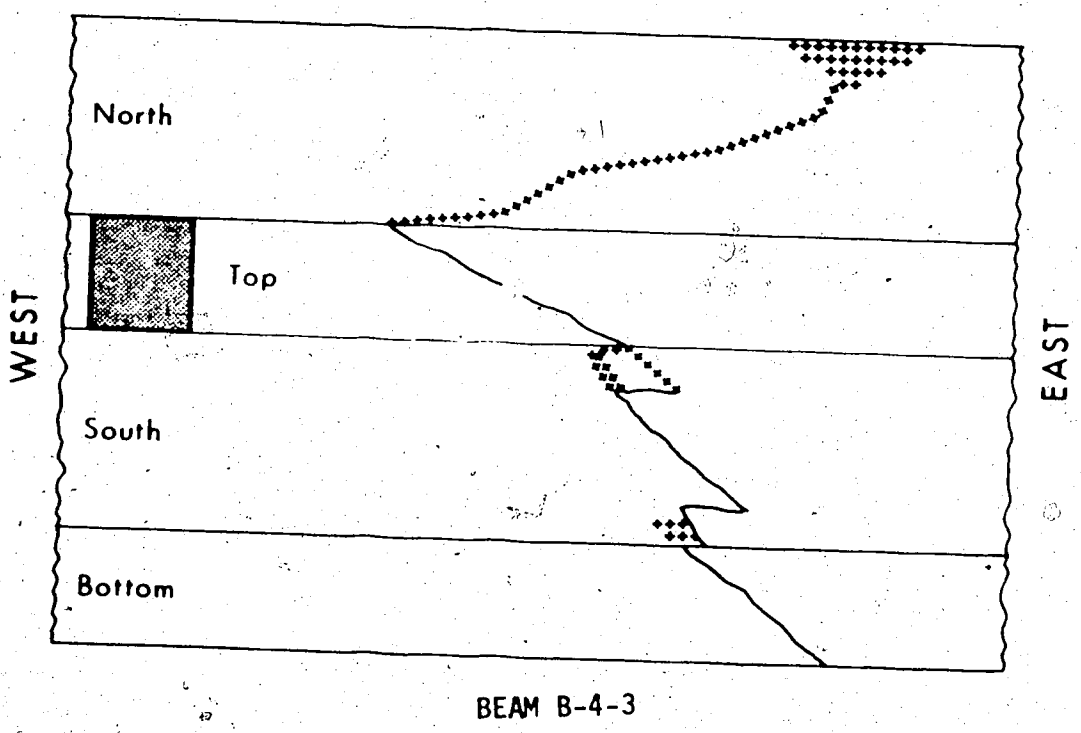

FIG. A.23 CRACK PATTERN FOR BEAMS A-4-3 AND B-4-3

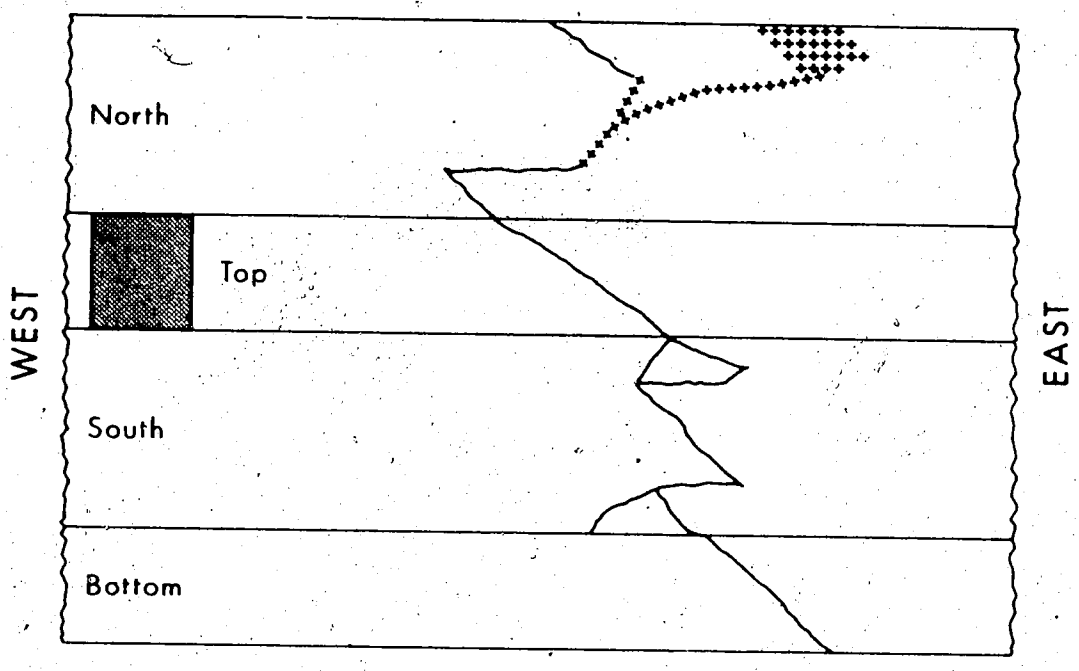

BEAM D-3-3

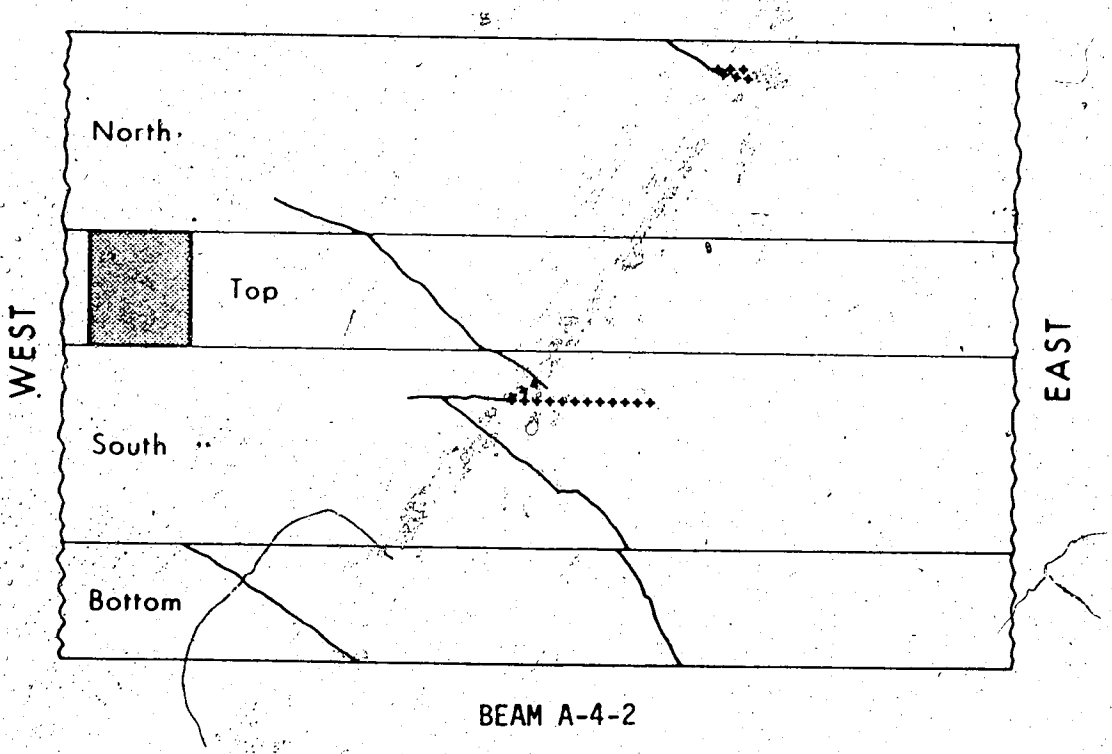

BEAM A-4-2

FIG. A.24 CRACK PATTERN FOR BEAMS D-3-3 AND A-4-2

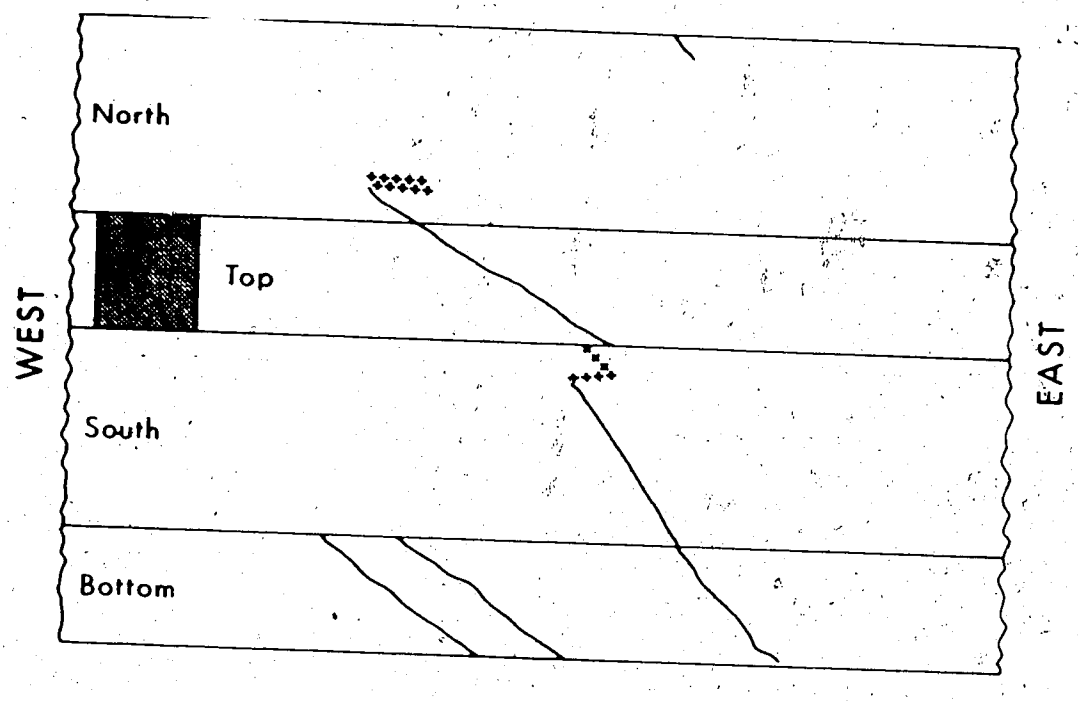

BEAM B-3-2

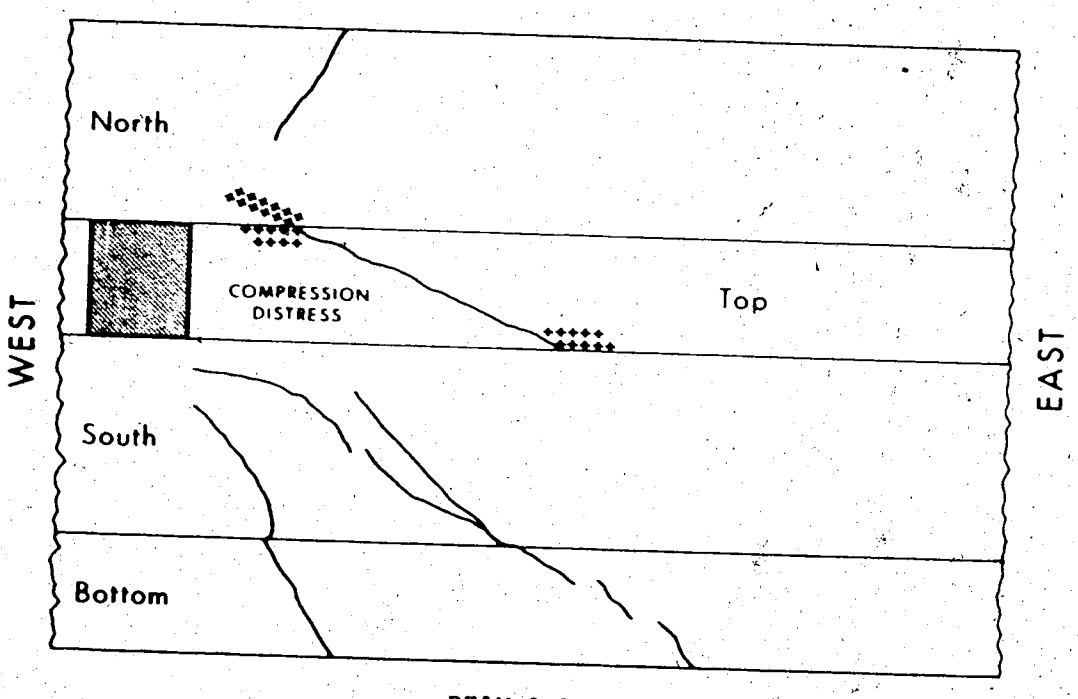

BEAM A-5-1

FIG. A.25 CRACK PATTERN FOR BEAMS B-3-2 AND A-5-1

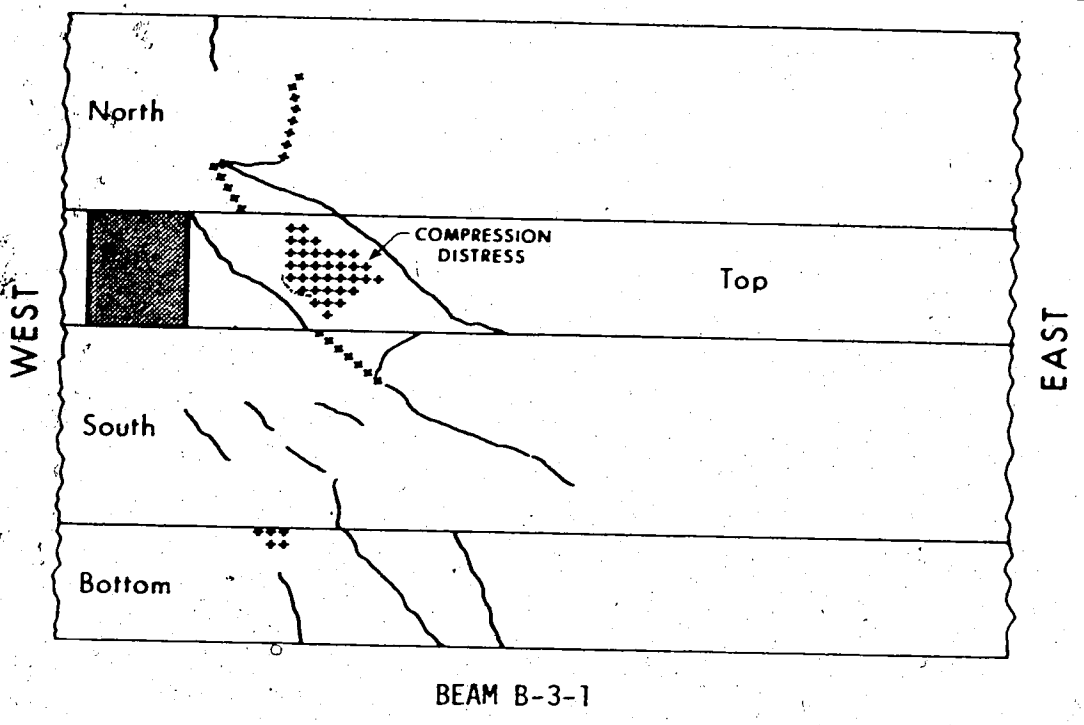

BEAM B-3-1

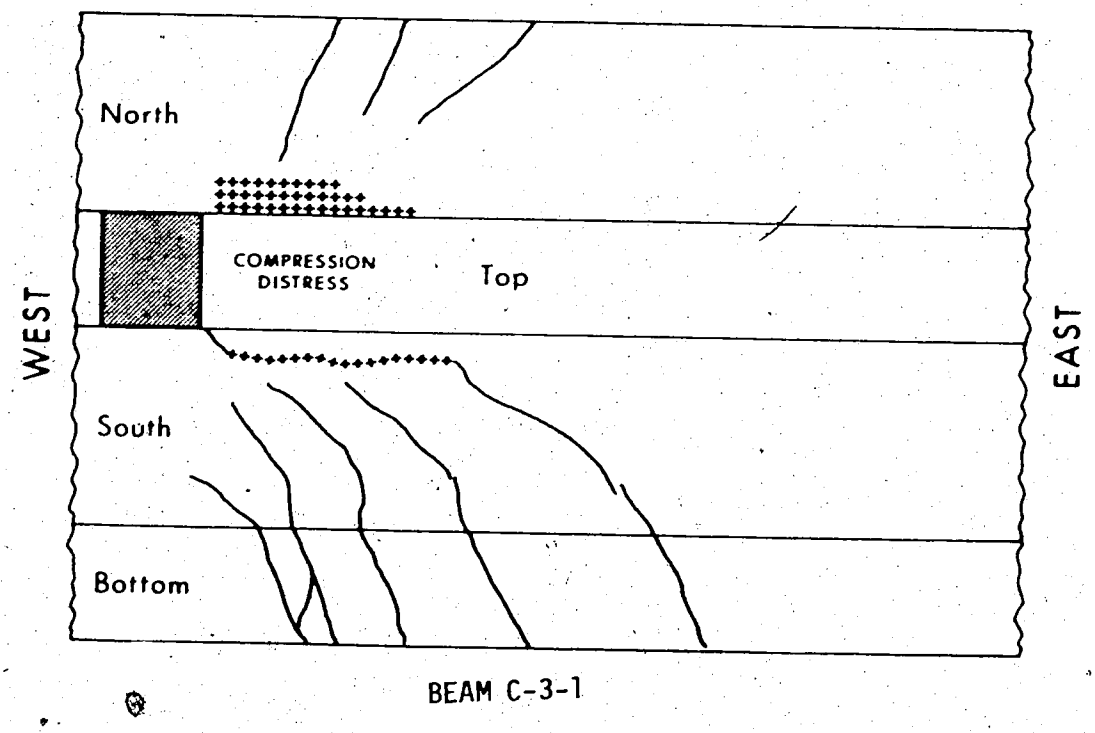

BEAM C-3-1

FIG. A.26 CRACK PATTERN FOR BEAMS B-3-1 AND C-3-1

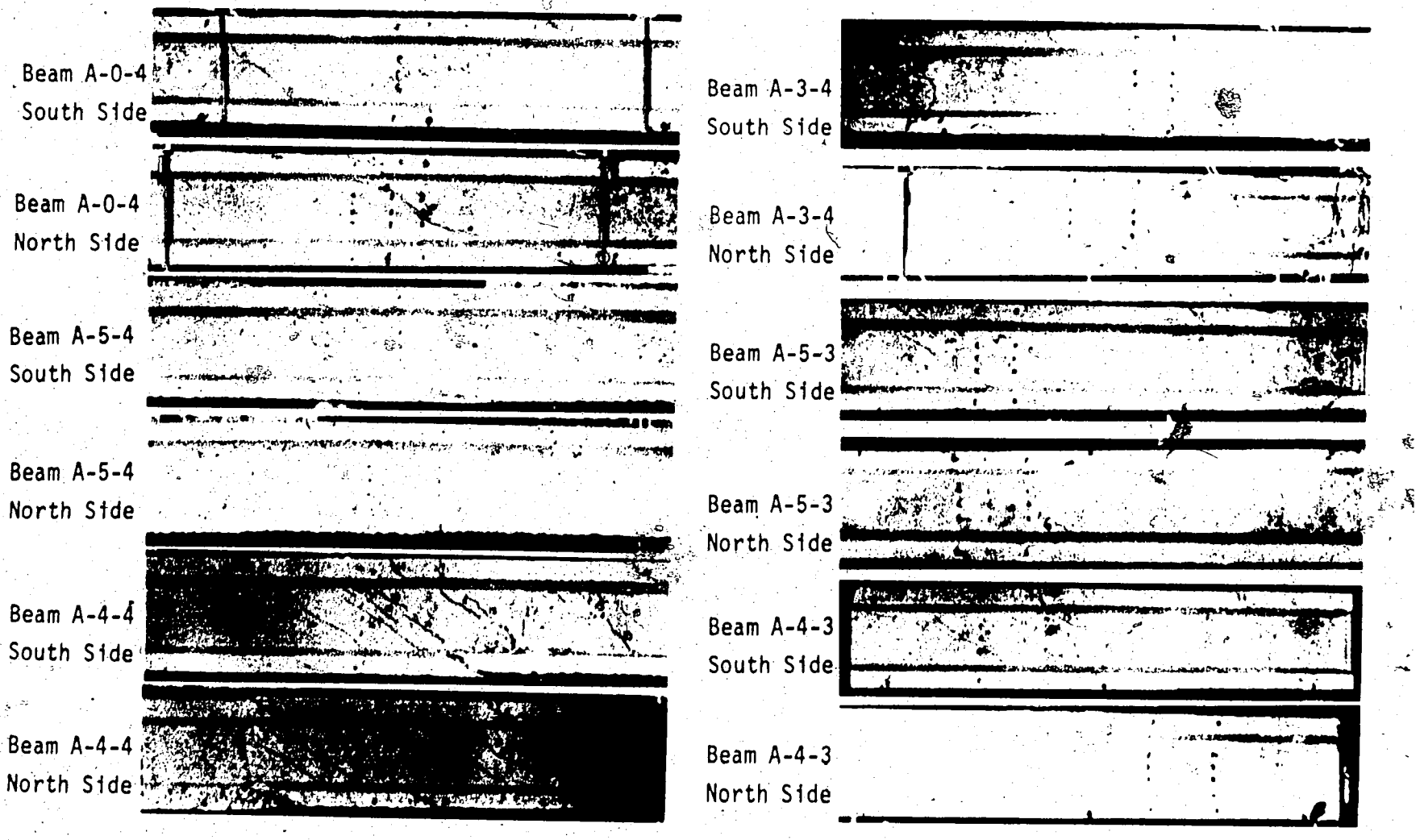

PLATE A.1 APPEARANCE OF BEAMS AFTER TEST

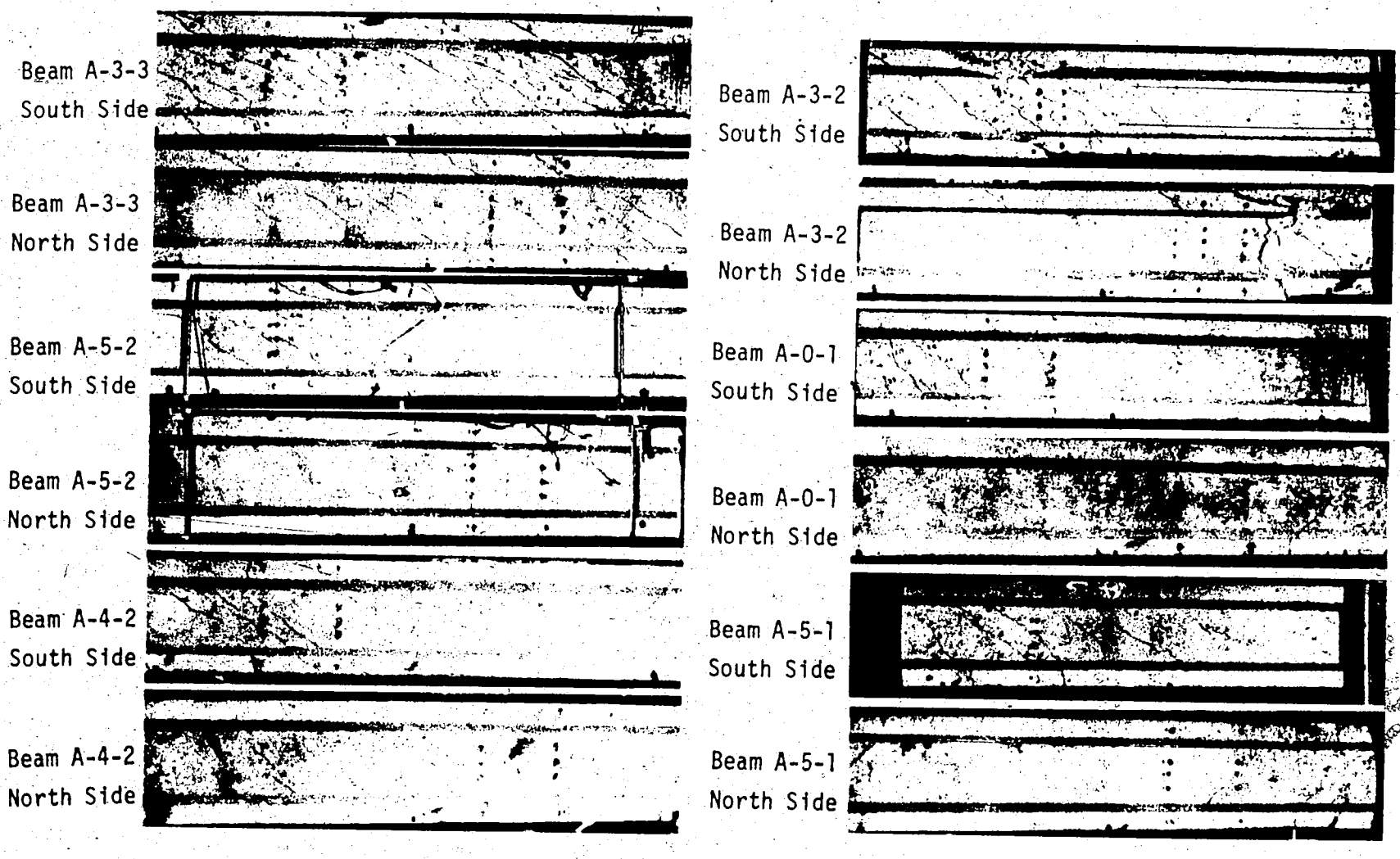

PLATE A.2 APPEARANCE OF BEAMS AFTER TEST

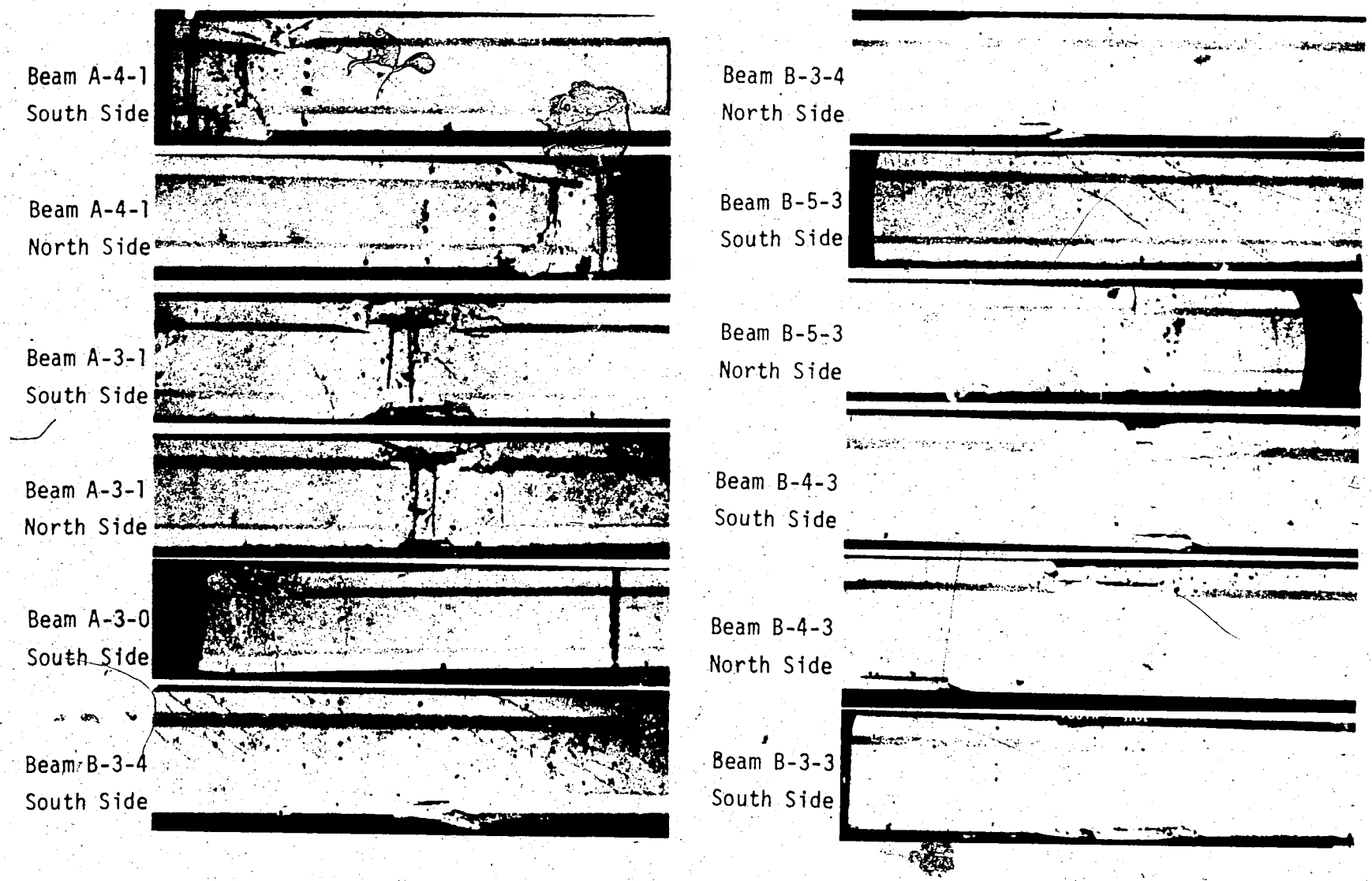

PLATE A.3 APPEARANCE OF BEAMS AFTER TEST

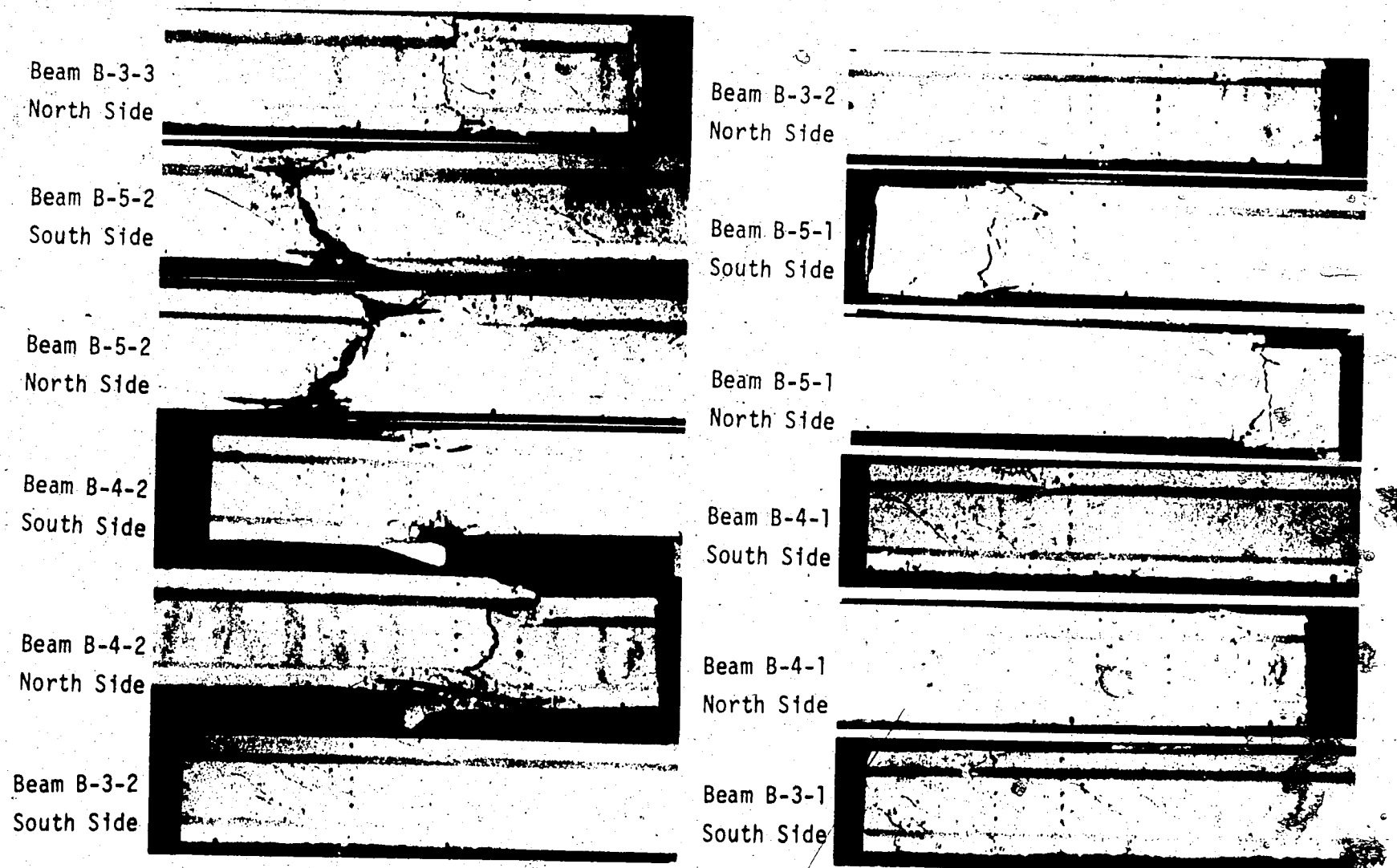

PLATE A.4 APPEARANCE OF BEAMS AFTER TEST

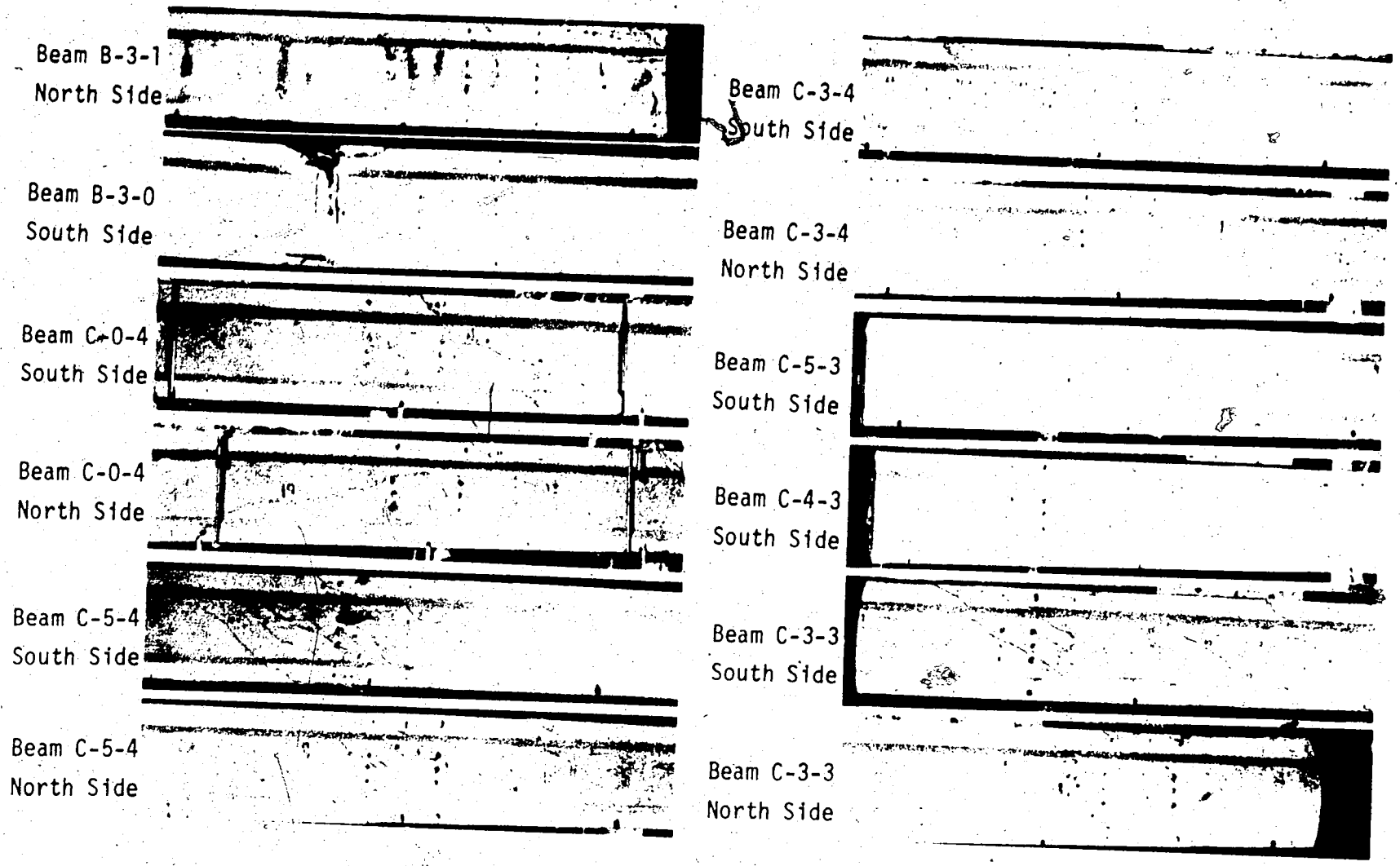

PLATE A.5 APPEARANCE OF BEAMS AFTER TEST

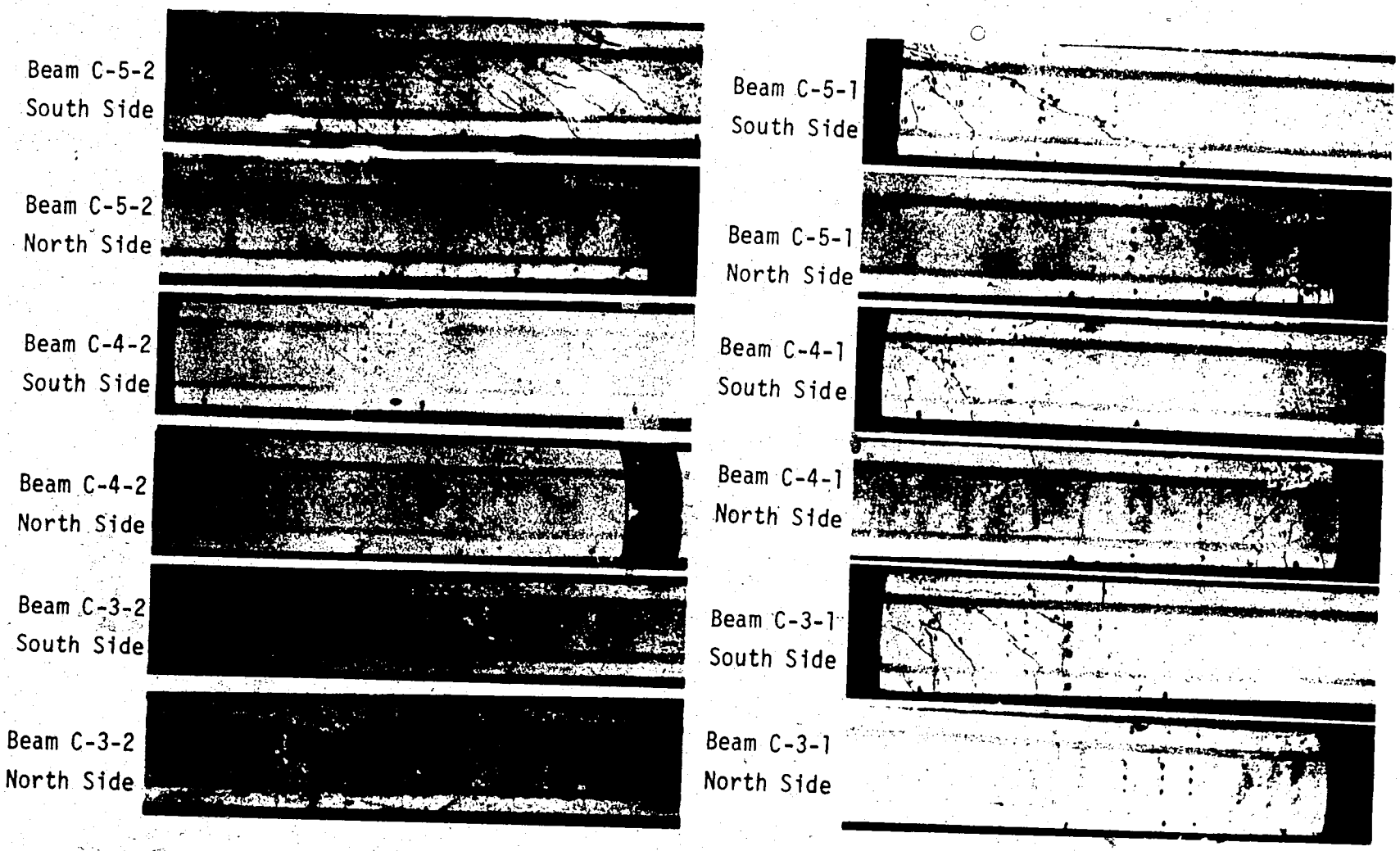

PLATE A.6 APPEARANCE OF BEAMS AFTER TEST

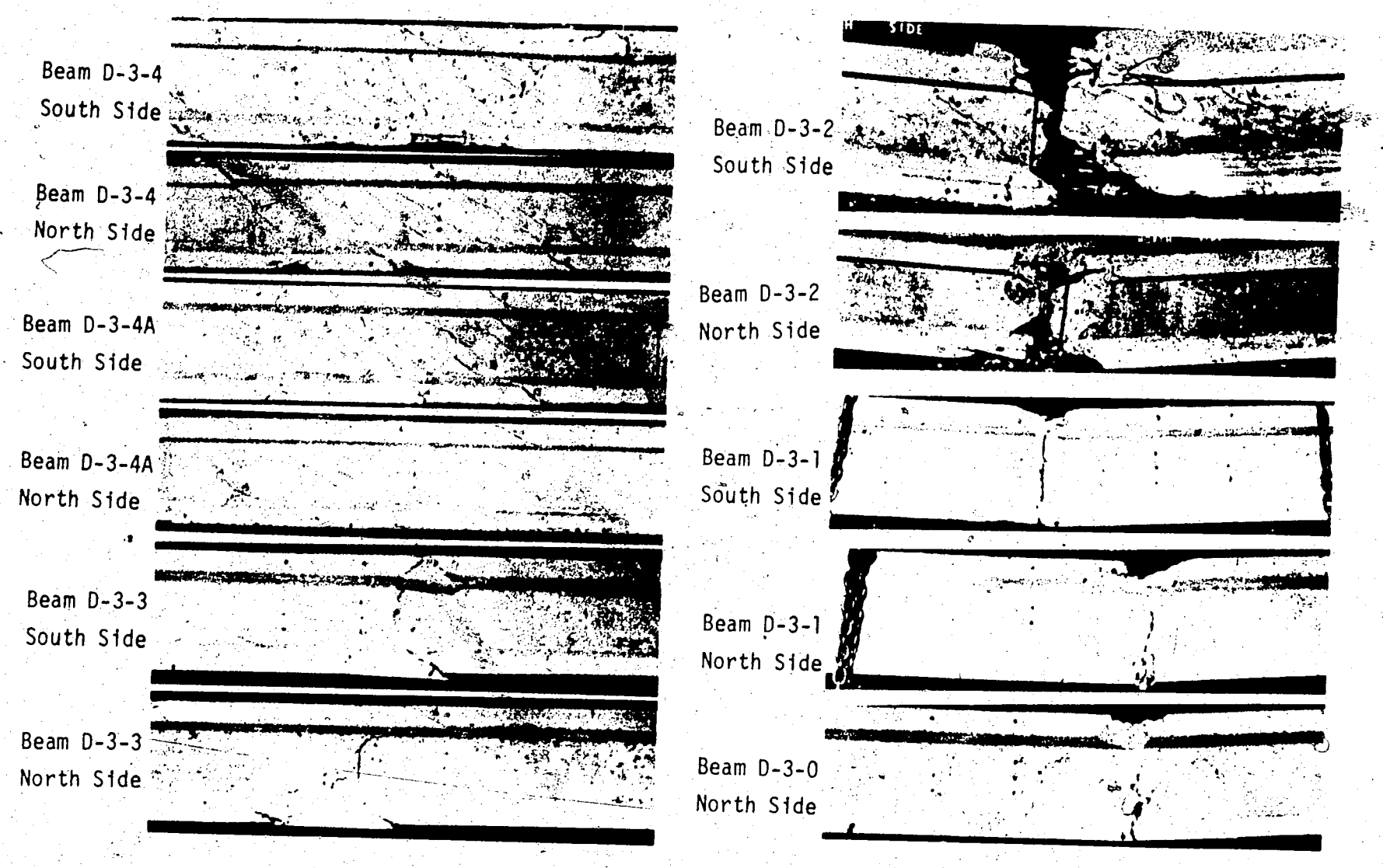

PLATE A.7 APPEARANCE OF BEAMS AFTER TEST

APPENDIX B

THREE DIMENSIONAL FINITE ELEMENT ANALYSIS

B.1 General

This computer program relates to a three dimensional finite elemert analysis for predicting the cracking strength of concrete beams subject to combined loadings. A general description of the program, formulation of element stiffness, and a listing are given below.

B.2 Usage and Limitations

The program was written in the Fortran IV Language for the IBM 360-67 installation operating under MTS at the University of Alberta, Edmonton. It is hardware dependent and will provide a solution for problems that do not exceed the following size.

Number of elements	560
Number of nodes	950
Number of materials	1

The limits can be easily extended by changing the Dimension statements provided the material used is the same. Even small three dimensional problems require large storage and computation time. In such problems, the system stiffness matrix requires most of the share of the total storage. Economy in the storage of the stiffness matrix can be achieved recognizing its banded nature and symmetry. Further economy can be effected by generating the stiffness elements in blocks and transferring the data to auxiliary storage keeping only two blocks in core for current

computations. In the present program, only two fixed size square blocks are in core, each block having a size of one-half band width. This method hence requires only (2 half band width (half band width + 1)) words of in-core storage. Thus there is only a limit on the half band width, and the total number of equations that can be solved is unlimited. Using this program a problem having a one-half band width up to 300 can be solved by the IBM 360-67 computer with a usable memory of 1024 k. However with large systems of equations round-off starts to play an important role. A clear remedy is to do the computations in double precision. But this roughly doubles the core storage requirement. Above all there is a limit on the time of computation, one would not like to exceed. Hence it is recommended that the band width be limited to 200, with a maximum number of equations.

B.3 Salient Features

A two dimensional finite element program with a block solver for solving equations, developed by Wilson (1966), and an equation solver coded by Gopalakrishnaiah (1973), formed the basis in the development of this program. An eight node hexahedron is used in this program for the three dimensional cracking analysis of reinforced and prestressed concrete beams. The same elelent is specialized for a triangular prism.

B.3.1 Improvement of Bending Performance

Before use is made of any element in an analysis it is desirable to test its performance in structural idealizations made of beam type structures. Clough (1969) has shown that eight noded hexahedra cannot adequately represent plate bending mechanism though its performance is

good in short deep beams. However, based on comparison of several elements he recommended an eight node element for analysis of general elastic solids. Gopalakrishnayya (1973) used eight node hexahedra in the analysis of the cracking of earth dams. His formulation, although not meant for bending problems, has poor bending characteristics for beams of usual proportions even at an aspect ratio of about 2.5.

Hence as suggested by Wilson (1966), the general hexahedron element is modified here to improve its bending behavior. The modification consists of the addition of extra degrees of freedom, within the element. This causes a violation of inter-element displacement compatibility. The generalized displacements associated with the extra degrees of freedom within the element are eliminated at the element level after the element stiffness is formed by static condensation. The resulting hexahedron has significantly improved bending characteristics.

B.3.2 Data Transfer in Solver

The structure stiffness matrix is generated in blocks and solved in blocks, keeping only two consecutive blocks at any time in the core; economizing the requirement of core storage. This process requires transfer of data from sequential disc files to core and vice-versa. An efficient method of data transfer between core and disc files using certain system oriented subroutines and appropriate equivalent statements resulting in considerable savings in the cost of computation has been available (Soil Mechanics report number 20, University of Alberta, 1973) and is used in the program.

B.3.3 Element Stiffness Formulation

The stiffness is the same for elements of same size and orientation provided the material is same, wherever they occur in the model. Further economy in computation time is achieved by formulating the element stiffness only once for a group of identical elements and storing it in a sequential disc file for subsequent use by an identical element.

B.3.4 Solution of Different Load Vectors

If more than one loading condition is to be solved economically it is not necessary to invert the stiffness matrix for every load vector. Hence, the reduced matrix is stored in a temporary sequential disc file and used every time for reducing the new load vector. This facilitates solution of several problems with inversion made only once.

B.4 Description of Subroutines

The computer program uses eleven subroutines with the main program. Further, it requires the following system-oriented subroutines in connection with data transfer between core and auxiliary storage.

RCALL, SETDSN, ADROF, WRITE, READ, NOTE, POINT

Additionally, another system subroutine TIME computes and prints the CPU time. The details of these system subroutines can be obtained from the MTS system manuals. A brief description and purpose of each of the eleven subroutines used, follows. Figure B.1 shows the order of calling the subroutines.

MAIN PROGRAM

The main program calls subroutine THREED. The dimensions of certain arrays depending on the one-half band width and size of the

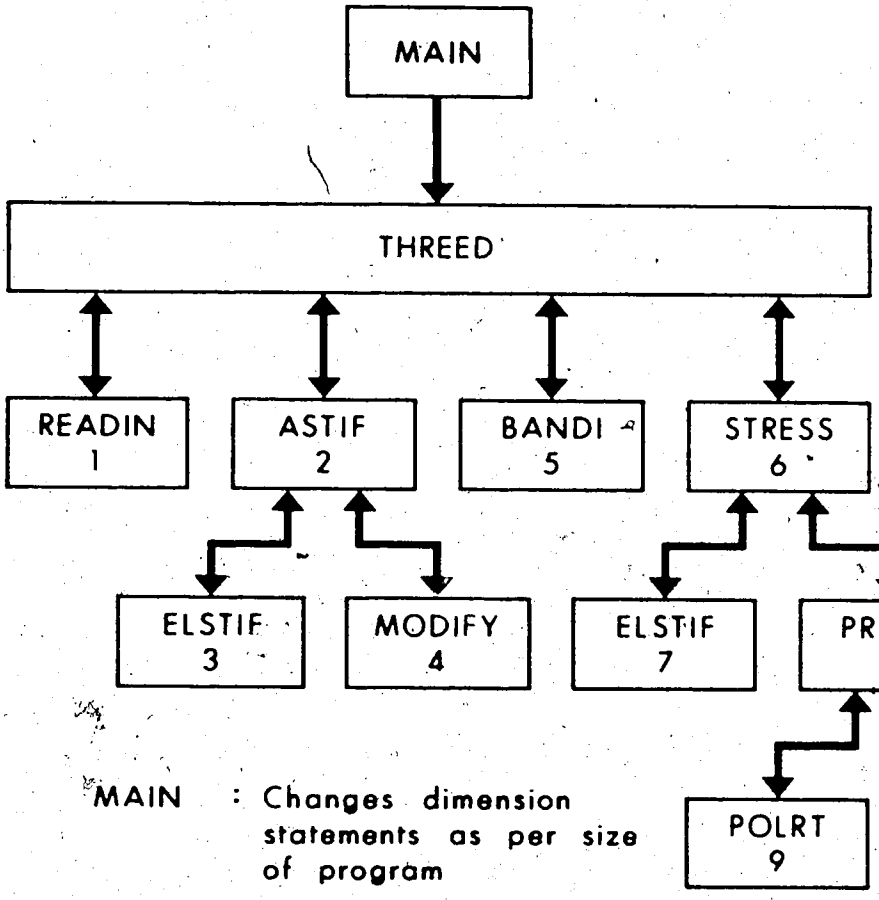

MAIN : Changes dimension statements as per size of program

THREED : Calls all subroutines

1 READIN : Reads and outputs nodal, element, material data

2 ASTIF : Forms system stiffness

3 ELSTIF : Assembles element stiffness

4 MODIFY : Modifies displacement boundary conditions

5 BANDI : Solves equations

6 STRESS : Prints stresses

7 ELSTIF : Computes stresses

8 PRINCI : Calls POLRT and EIGEN

9 POLRT : Computes principal stresses

10 EIGEN : Computes principal stress directions

Note : Numbers represent the order of execution of subroutines

FIG. B.1 ORDER OF CALLING SUBROUTINES

problem are supplied to other subroutines.

THREED

This subroutine calls all the other subroutines, computes modulus matrix and the coefficients necessary for numerical integration. It further reads load vectors for each problem, if more than one loading condition is studied.

READIN

This subroutine reads the nodal data, element data, material properties and the first loading condition. It computes the one-half band width. READIN incorporates a data generating facility not only across the cross section but also along the length if needed; only a minimum amount of information, is then needed as input to specify the problem topology and geometrics.

ASTIF

This subroutine assembles the load vector and the system stiffness matrix after obtaining element stiffness from subroutine ELSTIF. The assembly is through a direct stiffness approach. Element stiffness contributions are directly added to the structure stiffness by using a simple labelling technique in blocks of fixed size (half band width) x (half band width + 1). Subroutine MODIFY, called for each node, implements the displacement boundary conditions in blocks. As the blocks are formed, they are stored in a temporary sequential disc file (file number 2). At the time of formation and subsequent solution of the stiffness equations, only two consecutive blocks are needed in the core at any time. Hence storing of other blocks in auxiliary storage, not needed for the current computation saves core space, allowing the solution of larger problems.

ELSTIF

This subroutine formulates the element stiffness matrix and stores it in a temporary sequential disc file (file Number 3). The ASTIF subroutine reads element stiffness from this disc file. The subroutine is skipped if it has already formed once the stiffness of an element having the same size and orientation. It further calculates the element and nodal stresses and strains when called by subroutine STRESS.

MODIFY

This subroutine modifies the stiffness matrix and the load vector in accordance with the displacement boundary conditions.

BANDI

This subroutine solves in single precision, the modified stiffness matrix equations in blocks, by the method of direct Gauss elimination. For reduction, or back substitution, only two consecutive blocks of the stiffness matrix are required in the core. Blocks are transferred from disc files to core and vice-versa when required. For reduction, the structure stiffness matrix is obtained from file Number 2 as formed in ASTIF. The reduced equations used for back substitution are stored in file Number 1.

If more than one load condition is to be solved, it is not necessary to invert the matrix each time. The same reduced matrix available in file Number 1 is stored once for all the load conditions in file Number 2 where, previously unreduced stiffness elements were available. For solving each new loading condition the reduced matrix is read from file Number 2, computations using the new load vector are completed and the equations are then stored in file Number 1. Back

substitution is carried on from file Number 1 as before.

STRESS

The subroutine computes stresses and strains by calling subroutine ELSTIF. It also calls subroutine PRINCI for calculating principal stresses and their directions.

PRINCI

This subroutine calls subroutines POLRT and EIGEN for the computation of principal stresses and their directions.

POLRT

This is a subroutine of the IBM SS package and calculates the principal stresses, by reading element and nodal stresses computed in ELSTIF.

EIGEN

This is another subroutine from the IBM SS package and computes the principal stress directions.

B.5 Changes Necessary in the Main Program Before Execution

The dimension declaration of certain arrays in the program is to be in accordance with the one-half band width and number of equations of the problem to be solved. This can be accomplished in the main program without recourse to the rest of the program once these dimension values are known exactly. Because of a flexibility provided, the program can be terminated after the generation and output of the geometry of the problem, number of equations, and one-half band width. This allows to check the input data and gives the values of the one-half band width and number of equations. To execute up to this stage, some arbitrary values can be assigned to the one-half band width, number of equations, and

program run. Once the exact values are known, dimension and equivalent statements are set accordingly in the main program and execution is allowed to continue until the end. The statements requiring a change in the main program are detailed below:

MBI = Half band width (MBAND)

NLD = MBAND X Number of blocks

DIMENSION B(NLD), A(MBAND, 2 X MBAND), BL(MBAND), BR(MBAND), AL(MBAND X MBAND), AR(MBAND X MBAND)

EQUIVALENCE (B(1), BL(1)), (B(MBAND+1), BR(1)), (A(1,1), AL(1)), (A(1,MBAND+1), AR(1))

B.6 Gauss Quadrature, Load Conditions, and Output

The computer program permits the use of both a hexahedron or a triangular prism which is specialized from the hexahedran. Two point Gauss quadrature is used in the integration of the element stiffness matrix. In the case of a triangular prism, as it is formed by combining two pairs of nodes of hexahedron, to avoid quantities allowing to tend to infinity, stresses and strains are computed very close to the nodes but not exactly at the nodes.

The program provides for the solution of any number of load conditions with the inversion of stiffness matrix accomplished only once. Nodal code value - 1 is to be specified for the nodes where forces are specified for different load conditions. By supplying unit weight of the material, the self weight of the beam can be taken into account.

The output from the program consists of a reprint of all the input data, nodal displacements, and element and average nodal stresses

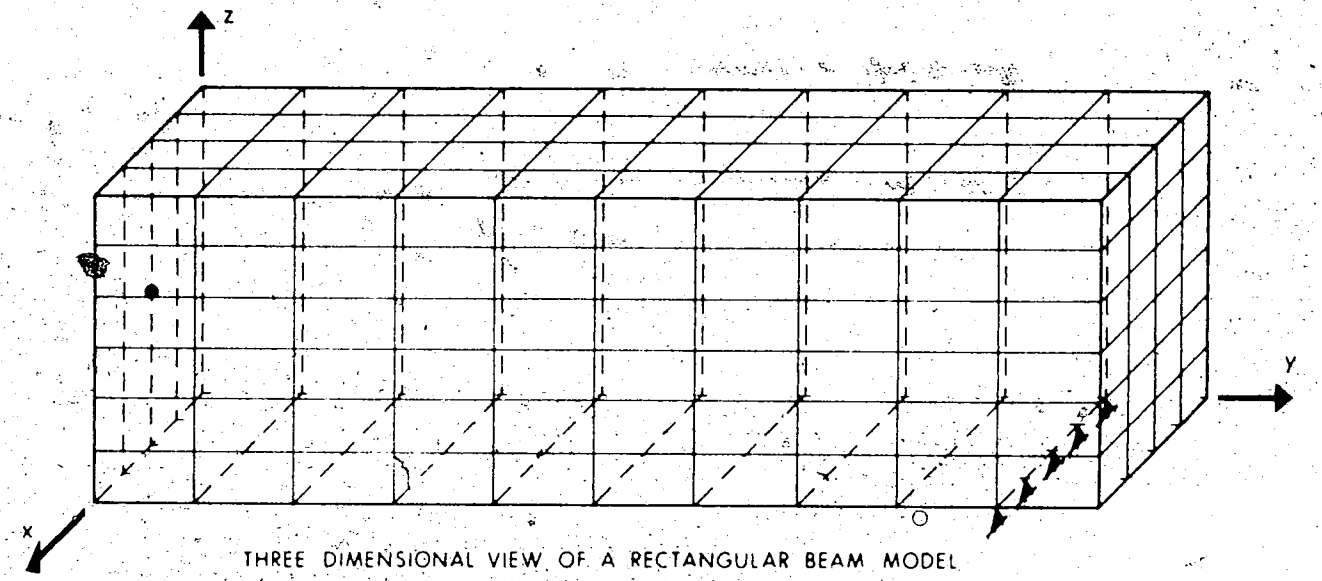

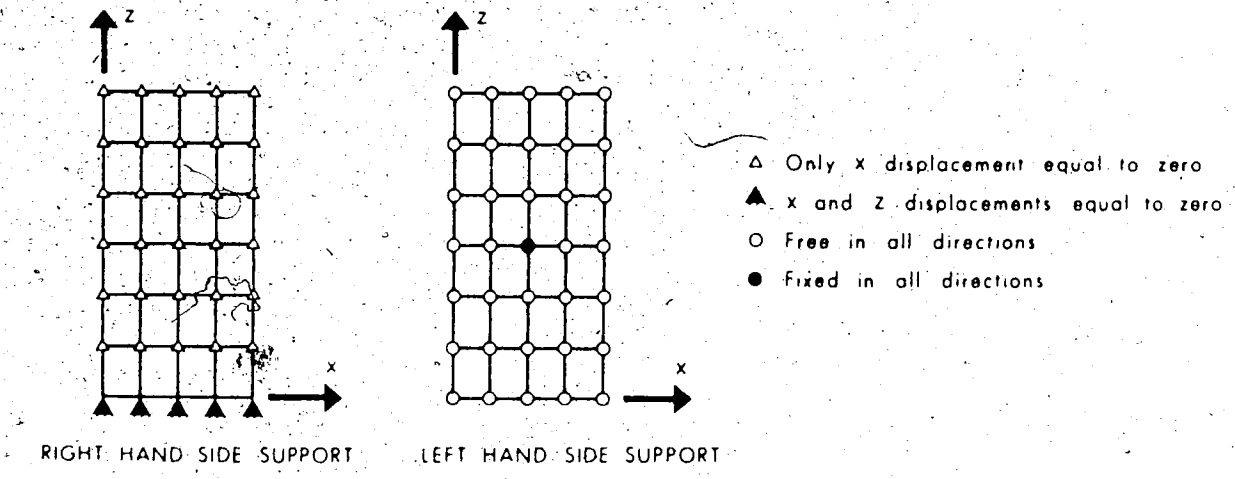

FIG. B.2 IDEALIZATION OF RECTANGULAR BEAM INTO FINITE ELEMENTS OF HEXAHEDRA

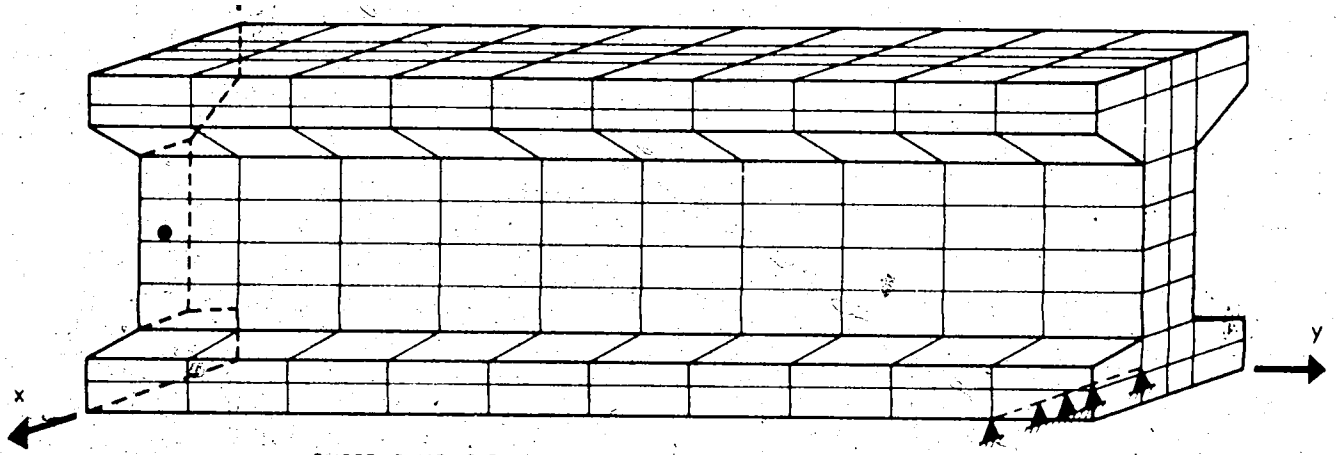

THREE DIMENSIONAL VIEW OF AN I BEAM MODEL

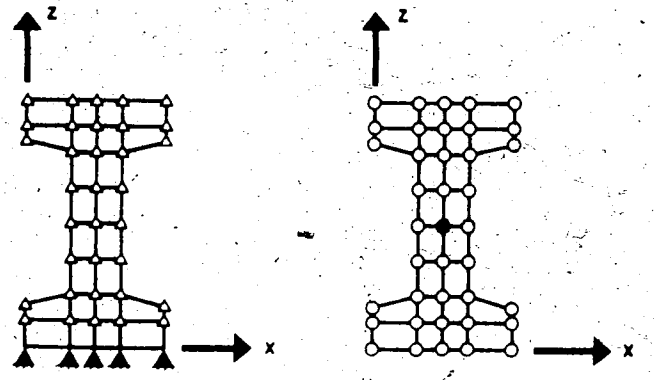

RIGHT HAND SIDE SUPPORT LEFT HAND SIDE SUPPORT

△ Only x displacement equal to zero
▲ x and z displacements equal to zero
O Free in all directions
● Fixed in all directions

FIG. B.3 IDEALIZATION OF I BEAM INTO FINITE ELEMENTS OF HEXAHEDRA

and strains. It also includes element maximum shear stress, principal stresses and strains and their directions at the centre, on the required faces, and at each node.

B.7 Estimation of Computation Time

It is advantageous to estimate in advance the time required for the solution of a problem. The computation time essentially consists of amounts of time required for the calculation of element stiffness, assembly of structure stiffness, solution of equilibrium equations and computation of stresses and strains. Once the number of elements, nodes and one-half band width of a model are known, the computation time can be reasonably evaluated.

Time required for one element stiffness formulation is approximately 2.5 seconds. As stiffness is not formed for identical elements, the total time for stiffness formulation may be obtained by multiplying the number of groups of dissimilar elements by 2.5 seconds. Time required for stress calculation can be arrived at by multiplying the number of nodes by about 0.5 seconds. Based on the solution of several problems of different sizes (different one-half band widths), it has been possible to draw a relationship between the average computation time required for the solution of equations in one block and the one-half band width. This relationship is furnished in Fig. B.4. As the solution time for a given number of equations and band width depends on the number of displacement boundary conditions implemented, the time predicted by means of Fig.B.4 is approximate in a situation different from the ones used to plot the curve in this figure. Total solution time of equations may be approximated as the product of the number of blocks and the time required

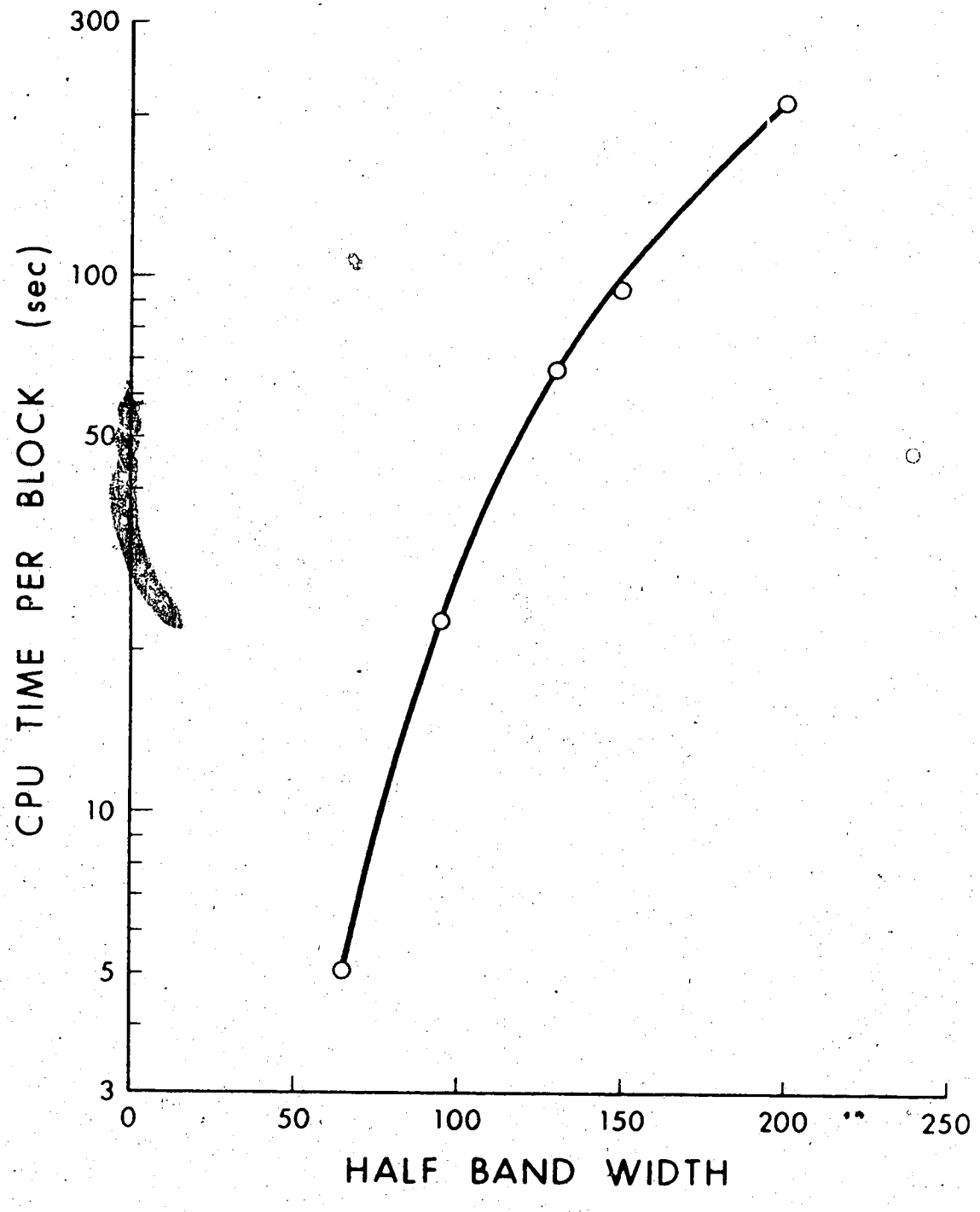

FIG. B.4 APPROXIMATE CPU TIME FOR THE SOLUTION OF EACH BLOCK OF EQUATIONS

for one block as obtained from Fig. B.4.

B.8 Code for Nodes

Each node is assigned a code consisting of a two digit number to represent its boundary displacement condition. The codes used to identify various boundary displacement conditions are detailed below:

Code	X force or displacement	Y force or displacement	Z force or displacement.
00	X-force	Y-force	Z-force
01	X-force	Y-force	Z-displacement
02	X-force	Y-displacement	Z-force
03	X-displacement	Y-force	Z-force
04	X-displacement	Y-force	Z-displacement
10	X-displacement	Y-displacement	Z-force
11	X-force	Y-displacement	Z-displacement
12	X-displacement	Y-displacement	Z-displacement

B.9 Code for Face of an Element

Each element is provided with a code consisting of a two digit number to identify the faces on whose centres stresses are to be computed. A maximum of two faces can be specified. Each digit of the code represents a face.

Code	Faces
0	Centre of element
1	X-coordinate positive face
2	Y-coordinate positive face
3	X-coordinate negative face
4	Y-coordinate negative face
5	Z-coordinate negative face
6	Z-coordinate positive face

B.10 Nodal and Element Data Generation

Automatic data generation within the program reduces the amount of data to be input. Nodal data is to be fed in ascending order. If a certain series of nodes are equally spaced in a straight line and have their numbers in increasing order, intermediate nodes can be automatically generated with their nodal code and nodal displacements or loads equal to zero, by supplying only the two nodes at the beginning and end of that part.

For example as shown in Fig. B.5 9 to 13 are equally spaced in the Z-direction, and nodes 13 to 16 in both the x and z-directions. Each extent is a straight line. All nodes from 9 to 16 can be generated by giving information only for nodes 9, 13 and 16. If any intermediate nodes 10, 11, 12, 14, or 15 have nodal codes or displacements or forces different from zero, they can be taken care of individually at a later stage. Nodes 24 to 30 cannot be generated in one sequence and have to be read individually.

The elements can be read in at random one by one, however,

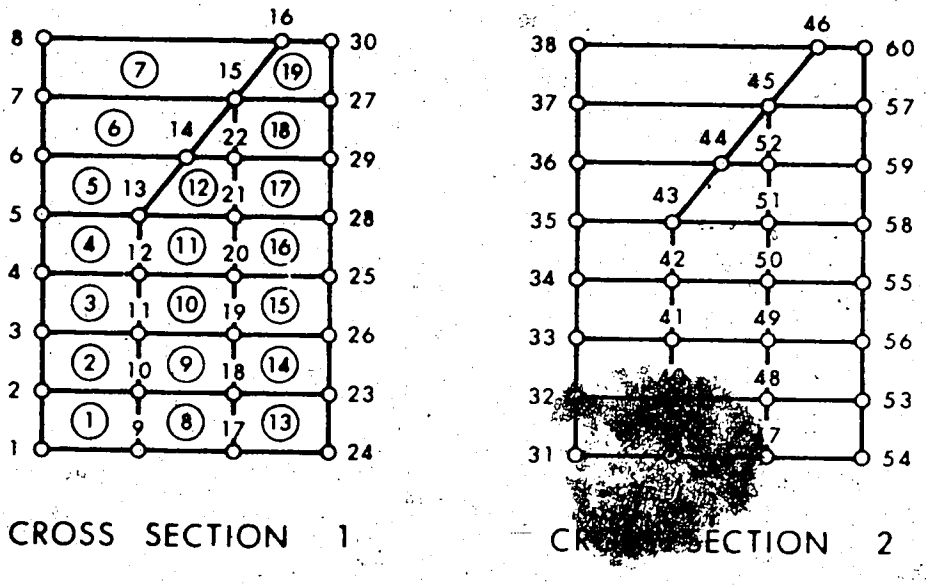

Note : Element numbers are circled

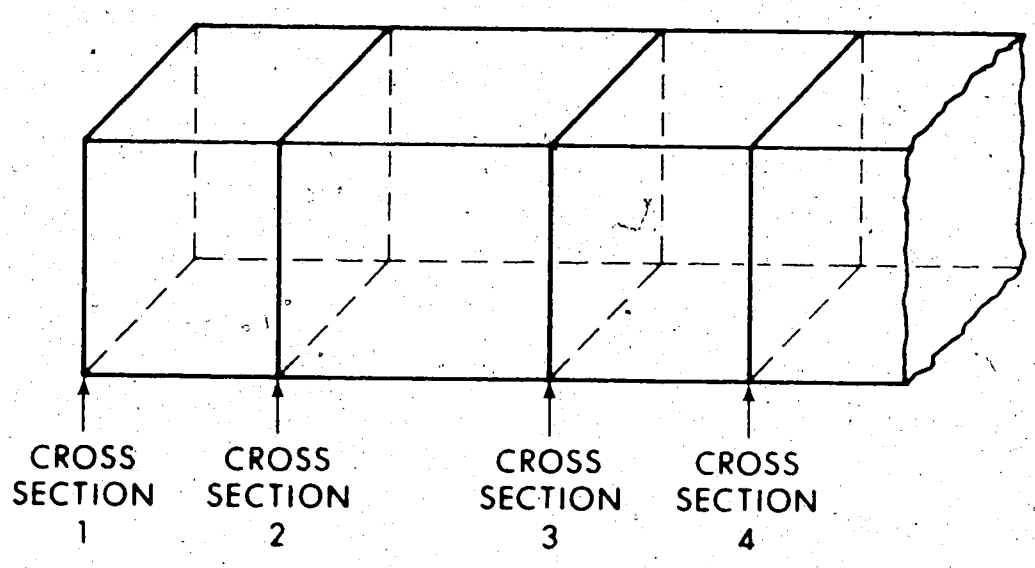

FIG. B.5 A GENERAL LAYOUT OF ELEMENTS AND NODES

it is preferable to do it in order. If a group of consecutive elements have their numbers and their corresponding nodal numbers in increasing order, the element data of all the elements in the group can be generated by the computer by feeding in only the final element. All the elements created in one extent assume the same material number, element code, element size code, and element face code, as the first element of the group. If any elements, in the process of automatic generation assume any of these code values different from their actual codes, the proper values can be fed in individually. The variable "NUMTIE" represents the total number of groups of elements in the model each group being fed in one extent. If all the elements are input individually NUMTIE will equal the total number of elements in the model. Again, referring to Fig. B.5, elements 1 to 7 can be generated by giving only the data of element Number 1. All the elements 2 to 7 have the same material number, element code, element size code, and element face code as element Number 1. However, elements 13 to 19 have to be read in individually as the nodes from 54 to 60 are not in increasing order.

If the nodes are spaced in the same way across all the cross sections, and if the element properties are the same throughout the length as of the elements enclosed by the first and second cross sections, then by providing the nodal and element data of first cross section alone, the properties of the whole beam can be generated. This facility reduces the input data to approximately five percent of the total required if the beam is modelled using 20 tiers of elements along its length.

B.11 Size and Creation of Disc Files

A total of three temporary sequential disc files of sufficient size are to be created for the execution of the program. Two files, one for storing the structure stiffness matrix (file Number 2), the other for storing reduced stiffness matrix (file Number 1), are needed. The third file (file Number 3), stores the element stiffness matrix, and HMUL5, a matrix generated in connection with static condensation. The size of a file can be expressed in terms of the number of tracks required. Each track of the file corresponds to about 7000 bytes. The number of tracks needed for the first and second files are given

$$\text{Number of tracks} = \frac{\text{(Number of blocks) x}}{\text{(half band width)(half band width + 1)}} \left(\frac{4}{7000}\right)$$

The number of tracks for file Number 3 can be calculated as follows:

$$\text{Number of tracks} = (24 \times 24 + 9 \times 24) \begin{bmatrix}\text{Number of}\\ \text{groups of}\\ \text{dissimilar}\\ \text{elements}\end{bmatrix} \left(\frac{4}{7000}\right)$$

The following control cards are necessary for the creation of the files:

```
$CREATE Ø - T Ø TYPE = SEQ Ø SIZE = nT
$CREATE Ø - TEMP2Ø TYPE = SEQ Ø SIZE = nT
$CREATE Ø - T1 Ø TYPE = SEQ Ø SIZE = nT
$RUN Ø - LOAD # Ø 1 = - T Ø 2 = - TEMP2Ø 3 = - T1
```

where "n" represents the number of tracks.

B.12 Variables Associated with Size of Problem

The arrays whose dimensions depend on the size of problem, in terms of number of elements, number of nodes, and number of element

size code, are given below. These dimensions as declared in the program need not be changed if the following limits are not exceeded:

Number nodes	= 950
Number of elements	= 560
Number of element size code	= 100

In case they are exceeded, the common or dimension statements of the arrays are to be accordingly specified. Further, statement 24 in subroutine ASTIF is to be changed in accordance with the maximum element size code.

Variable	Description	Minimum Size
KODEL	code assigned for each element to identify as hexahedron or triangular prism	(NUMEL)
KELLS	code for specifying the faces of each element over which stresses are required	(NUMEL)
KOST	code for size of each element for formulating the element stiffness matrix	(NUMEL)
KODE	code for each node to identify its boundary displacement condition	(NUMNP)
KOUNT	counter used for averaging nodal stresses and strains	(NUMNP)
LCHECK	variable used to determine whether element stiffness is to be formed or already has been done	(as many as the number of groups of dissimilar elements)
MB1	one-half band width	
MAT	material number alloted for each element	(NUMEL)

NLD	number of blocks x one-half band width	
NP	vector of eight nodes stored in order of each element	(8, NUMEL)
SIGPC	vector of element principal stresses, strains, and maximum shear at the centre of an element	(NUMEL,7)
SIGP1	vector of element principal stresses, strains, and maximum shear at the centre of face 1	(NUMEL,7)
SIGP2	vector of element principal stresses, strains, and maximum shear at the centre of face 2	(NUMEL,7)
SIGA	nodal stress vector	(NUMNP,6)
STNODE	nodal strain vector	(NUMNP,3)
U	force or displacement at each node in the direction of x-coordinate	(number of blocks X MBAND/3)
V	force or displacement at each node in the direction of y-coordinate	(number of blocks X MBAND/3)
W	force or displacement at each node in the direction of z-coordinate	(number of blocks X MBAND/3)
WEIGHT	weight at each of the 8 nodes of an element	(as many as number of groups of dissimilar elements)
X	x-coordinate of a node	(NUMNP)
Y	y-coordinate of a node	(NUMNP)
Z	z-coordinate of a node	(NUMNP)

B.13 Input Data Format

General Data

1. Read: HED, NUMNP, NUMEL, NUMAT, NUMTIE, NUTRPR, NLODC (18A4/6I6) - two cards

HED	= Heading
NUMNP	= Number of nodal points
NUMEL	= Number of elements
NUMAT	= Number of materials
NUMTIE	= Number of series of hexahedra in the model If each element is read in separately, this will be equal to the total number of elements. (NUMEL)
NUTRPR	= Number of triangular prisms in the model
NLODC	= Number of total load conditions

2. Read: E, PR, RO (F12.0, F6.3, F7.3) - one card

E	= Modulus of elasticity
PR	= Poissons ratio
RO	= Unit weight (If RO is non zero, the self weight of the material is included in the negative z-direction

3. Read: NRSEPA (I4) - one card If equal to zero, only the nodal and element data on the first cross section will be read and the information for the rest of the model will automatically be generated. If equal to non zero, nodal and element data has to be read at every cross section along the length of the model.

NRSEPA	= This variable is used to determine how data is going to be read.

4. Read: NREP, NSUMN, NS1 (3I4) - one card If NRSEPA ≠ 0, this read statement is skipped

NREP = less than the number of nodal sections along length of model

NSUMN = Number of nodes in the cross sections

NS1 = Number of elements in one tier along the length

Nodal Data

5. Read: N, KODE(N), X(N), Y(N), Z(N), U(N), V(N), W(N), (2I3, 6F5.0)

Number of cards depends on the problem and one of the two ways nodal data is fed. One card for each node.

N = Nodal number

KODE(N) = Nodal kode (Refer Sec. B.8)

X(N) = x-coordinate of node

Y(N) = y-coordinate of node

Z(N) = z-coordinate of node

U(N) = force or displacement at node in the x-coordinate direction

V(N) = force or displacement at node in the y-coordinate direction

W(N) = force or displacement at node in the z-coordinate direction

If NRSEPA = 0, nodes on one cross section are generated by the execution of Read 5. If NRSEPA ≠ 0, by this all the nodes of the model are generated.

6. Read: YIN (F5.0), As many cards as NREP

YIN = y-coordinate of the nodal cross section along the length, starting from the second cross section

If NRSEPA = 0, execution of Read 6, generates all the nodes of the beam model.

7. Read: NKOCH1 (I4) - one card

If NKOCH1 = 0, earlier nodal code generation does not require a change. And Read 8 and 9 are skipped.

8. Read: NKOCH2 (I4) - As many cards as NKOCH1

NKOCH2 = one less than the number of nodes where nodal code is to be changed in one extent

9. Read: N, KODE(N) (2I4) - As many cards as NKOCH1.

N = node number

KODE(N) = nodal code

Element Data

10. Read: NUMEE (I4) - As many cards as NUMTIE

NUMEE = one less than the number of hexahedra in each series

If NUMEE = 0, only one element will be read

11. Read: M, NP(1,M), NP(2,M), NP(3,M), NP(4,M), NP(5,M), NP(6,M) NP(7,M), NP(8,M), MAT(M), KODEL(M) KOST(M), KELLS(M), (13I5) - As many cards as NUMTIE.

M = element number

NP(I,M) = nodal numbers at the eight corners of an element in counter clockwise direction

MAT(M) = material number

KODEL(M) = type of element. If equal to zero, hexahedron. If equal to one, for triangular prism

KOST(M) = code for the size and orientation of an element

Elements having same size and orientation have same code for size, for purposes of calculation of element stiffness.

KELLS(M) = Element face code. Two digit number, each digit identifying a particular face on the centre of which stresses are to be computed (refer Sec. B.9).

12. Read: M, NP(I,M), MAT(M), KODEL(M), KOST(M), KELLS(M), (13I5),

As many cards as NUTRPR

If NUTRPR = 0 as given in Read 1, then Read 12 is skipped.

13. Read: NELFC (I4) - one card

If NELFC = 0, Read 14 is skipped.

NELFC = number of elements if any having face code different from what is generated earlier

14. Read: M, KELLS(M), (2I4) - As many cards as NELFC.

M = element number

KELLS(M) = face code of element

15. Read: NELF (I4) - one card

NELF = number of elements if any having element code size different from what is generated earlier

16. Read: M, KOST(M), (2I4) - As many cards as NELF

M = element number

KOST(M) = element size code

If NRSEPA ≠ 0, data of elements is generated by the time Read 16 is executed, if NRSEPA = 0, element data on the first cross section only is read.

17. Read: KADD (I4) - as many as (NREP-1)

KADD = A number to be added to each of the tiers of elements along the length, to specify the element size code.

If all the tiers along the length of beam have the same length in the y-direction, then KADD for all the tiers is equal to zero.

First Load Condition

18. Read: NOCHNO (I4) - one card

NOCHNO	= number of nodes where nodal forces are to be assigned

19. Read: N, KODE(N), U(N), V(N), W(N) (2I4, 3F6.0) - as many cards as NOCHNO

N	= node number
KODE(N)	= nodal code
U(N)	= x-force at node
V(N)	= y-force at node
W(N)	= z-force at node

20. Read: NPARA (I4) - one card

NPARA	= If > 0 execution terminates after the generation of nodal and element data, semi band width and number of equations. If NPARA = 0 solution is continued.

Other Load Conditions

21. Read: NCHNO (I4) - one card. As many times as number of load conditions - 1.

NCHNO	= number of nodes where nodal forces are to be assigned for the particular load condition

22. Read: N,KODE(N),U(N), V(N), W(N), (2I4, 3F6.0) - As many cards as NCHNO. As many times as number of (load conditions - 1).

N	= node number
KODE(N)	= nodal code (-1)
U(N)	= x-force at node
V(N)	= y-force at node
W(N)	= z-force at node

B.14 Element Stiffness of Isoparametric Hexahedron

An eight-node hexahedron is used for the three dimensional cracking analysis of reinforced and prestressed concrete beams, in this investigation. It is based on the element developed by Irons and Zienkiewich. The element performance in bending is greatly improved by the addition of incompatible deformations as suggested by E.L. Wilson (1970).

An arbitrary hexahedron is shown in Fig. B.6. The nodes of the element can be described by the three axes (x,y,z) constituting an orthogonal right handed system. This is referred to as the Global Coordinate System. A local coordinate system (also designated as natural coordinates) (ξ,η,ζ) is adopted, in which, for this element, each pair of opposite faces have values of +1 and -1 on an axis. Thus in local coordinates the solid is a cube while it may be a distorted and warped six-faced solid in space. The local coordinate system generalizes and simplifies the formulation. It further facilitates the integration necessary to obtain the element stiffness.

The local coordinates are related to global coordinates by a set of linear interpolation functions.

$$\begin{Bmatrix} X \\ Y \\ Z \end{Bmatrix} = \left[\begin{array}{ccc|ccc|ccc|ccc} P & 0 & 0 & & & & & & & & & \\ 0 & P & 0 & & & & & & & & & \\ 0 & 0 & P & & & & & & & & & \end{array}\right] \begin{Bmatrix} \bar{X} \\ \bar{Y} \\ \bar{Z} \end{Bmatrix} \qquad (B.1)$$

where $P = \langle P_1\ P_2\ P_3\ P_4\ P_5\ P_6\ P_7\ P_8 \rangle$

P_1, P_2, P_3 etc. are interpolation functions

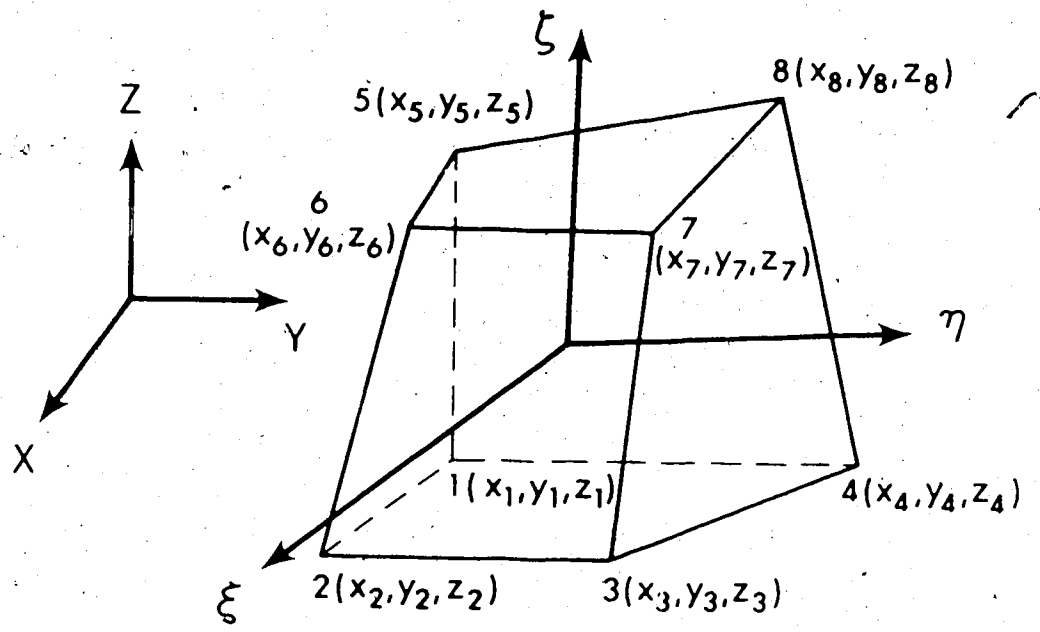

(a) GLOBAL COORDINATES

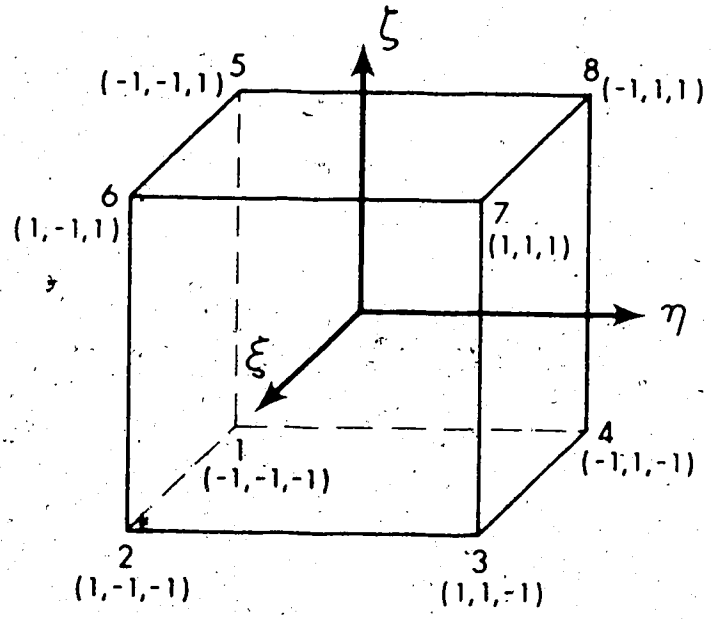

(b) LOCAL COORDINATES

FIG. B.6 THREE DIMENSIONAL COORDINATE SYSTEMS

$$P_1 = \frac{1}{8}(1-\xi)(1-\eta)(1-\zeta)$$

$$P_2 = \frac{1}{8}(1+\xi)(1-\eta)(1-\zeta)$$

$$P_3 = \frac{1}{8}(1+\xi)(1+\eta)(1-\zeta)$$

$$P_4 = \frac{1}{8}(1-\xi)(1+\eta)(1-\zeta)$$

$$P_5 = \frac{1}{8}(1-\xi)(1-\eta)(1+\zeta)$$

$$P_6 = \frac{1}{8}(1+\xi)(1-\eta)(1+\zeta)$$

$$P_7 = \frac{1}{8}(1+\xi)(1+\eta)(1+\zeta)$$

$$P_3 = \frac{1}{8}(1-\xi)(1+\eta)(1+\zeta)$$

$$\bar{X}^T = \langle x_1\ x_2\ x_3\ x_4\ x_5\ x_6\ x_7\ x_8 \rangle$$

$$\bar{Y}^T = \langle y_1\ y_2\ y_3\ y_4\ y_5\ y_6\ y_7\ y_8 \rangle$$

$$\bar{Z}^T = \langle z_1\ z_2\ z_3\ z_4\ z_5\ z_6\ z_7\ z_8 \rangle$$

x_1, y_1, z_1, etc. are coordinates of nodes in Global System.
The interpolation functions are in terms of local coordinates of the element.

In an isoparametric element the same interpolation functions are used to describe the geometry and the displacements of the element.

Accordingly the relationship between the nodal displacement vectors and the element displacements may be written, assuming displacements in the element vary linearly between the nodes.

$$\begin{Bmatrix} u \\ v \\ w \end{Bmatrix} = \left| \begin{matrix} P & 0 & 0 \\ 0 & P & 0 \\ 0 & 0 & P \end{matrix} \right| \begin{Bmatrix} \bar{u} \\ \bar{v} \\ \bar{w} \end{Bmatrix} \tag{B.2}$$

where $\bar{u}^T = \langle u_1\ u_2\ u_3\ u_4\ u_5\ u_6\ u_7\ u_8 \rangle$

$\bar{v}^T = \langle v_1\ v_2\ v_3\ v_4\ v_5\ v_6\ v_7\ v_8 \rangle$

$\bar{w}^T = \langle w_1\ w_2\ w_3\ w_4\ w_5\ w_6\ w_7\ w_8 \rangle$

$\bar{u}$, $\bar{v}$, $\bar{w}$ are nodal displacement vectors.

To improve the bending characteristics of the element, the displacements within the element are assumed to be of the following form:

$$\begin{Bmatrix} u \\ v \\ w \end{Bmatrix} = \left| \begin{matrix} P & P_m & 0 & 0 & 0 & 0 \\ 0 & 0 & P & P_m & 0 & 0 \\ 0 & 0 & 0 & 0 & P & P_m \end{matrix} \right| \begin{Bmatrix} \bar{u} \\ \bar{u}_m \\ \bar{v} \\ \bar{v}_m \\ \bar{w} \\ \bar{w}_m \end{Bmatrix} \tag{B.3}$$

where $P_m = \langle P_9\ P_{10}\ P_{11} \rangle$

$$P_9 = (1-\xi^2)$$

$$\{\varepsilon\} = [B]\{r_m\} \qquad \text{(B.4b)}$$

$\{r_m\}$ is the nodal displacement vector including displacement amplitudes associated with extra degrees of freedom

$[B]$ is the strain-displacement matrix

As the displacements U, V, W are not expressed directly in terms of global coordinates x, y, z the chain rule of differentiation has to be adopted. The chain rule in matrix form is expressed as:

$$\begin{Bmatrix} \frac{\partial}{\partial \xi} \\ \frac{\partial}{\partial \eta} \\ \cdot \\ \frac{\partial}{\partial \zeta} \end{Bmatrix} = \begin{vmatrix} \frac{\partial x}{\partial \xi} & \frac{\partial y}{\partial \xi} & \frac{\partial z}{\partial \xi} \\ \frac{\partial x}{\partial \eta} & \frac{\partial y}{\partial \eta} & \frac{\partial z}{\partial \eta} \\ \frac{\partial x}{\partial \zeta} & \frac{\partial y}{\partial \zeta} & \frac{\partial z}{\partial \zeta} \end{vmatrix} \begin{Bmatrix} \frac{\partial}{\partial x} \\ \frac{\partial}{\partial y} \\ \frac{\partial}{\partial z} \end{Bmatrix} \qquad \text{(B.5)}$$

$$= [J] \begin{Bmatrix} \frac{\partial}{\partial x} \\ \frac{\partial}{\partial y} \\ \frac{\partial}{\partial z} \end{Bmatrix} \qquad \text{(B.5a)}$$

where [J] is called the Jacobian matrix.

By multiplying both sides of equation (B.5) by $[J^{-1}]$

$$\begin{Bmatrix} \frac{\partial}{\partial x} \\ \frac{\partial}{\partial y} \\ \frac{\partial}{\partial z} \end{Bmatrix} = [J^{-1}] \begin{Bmatrix} \frac{\partial}{\partial \xi} \\ \frac{\partial}{\partial \eta} \\ \frac{\partial}{\partial \zeta} \end{Bmatrix} \tag{B.6}$$

By equation (B.6) the derivatives of displacements U, V, W with respect to global coordinates can be expressed in terms of natural coordinate derivatives of the displacements.

From the principle of minimum potential energy the stiffness matrix may be expressed as:

$$K = \int_V B^T C B \, dV \tag{B.7}$$

where the matrix [C] is the stress-strain relationship for an elastic solid of isotropic material.

$$C = \frac{E}{(1+\nu)(1-2\nu)} \begin{vmatrix} 1-\nu & \nu & \nu & 0 & 0 & 0 \\ \nu & (1-\nu) & \nu & 0 & 0 & 0 \\ \nu & \nu & (1-\nu) & 0 & 0 & 0 \\ 0 & 0 & 0 & \frac{1-2\nu}{2} & 0 & 0 \\ 0 & 0 & 0 & 0 & \frac{1-2\nu}{2} & 0 \\ 0 & 0 & 0 & 0 & 0 & \frac{1-2\nu}{2} \end{vmatrix} \tag{B.8}$$

Thus once the matrices [B] and [C] are known, the element stiffness can be formulated. As the matrix (B) is expressed in natural co-

ordinates the integration is to be carried out in the same coordinates.

$$K = \int^{1}\int^{1}\int^{1} B^{T}CB \, dV \qquad (B.9)$$

using the relationship $dV = dxdydz = |J| \, d\xi \, d\eta \, d\zeta$.

As it is impossible to perform the integration explicitly in equation (B.9), numerical integration is employed. In carrying out numerical integration by Gauss quadrature the matrices [J], [B], and the argument in equation (B.9) are evaluated at specific set of values of coordinates ξ, η, ζ. The number of integration points required in Gauss quadrature to achieve satisfactory results depends on shape of the element and finess of the mesh. In this investigation two point quadrature formula is employed. It is programmed to obtain the matrix product $B^{T}CB$ detJ for each of the integration points and they are appropriately combined to form 33 X 33 element stiffness matrix. The number of integration on points required depends on the shape of the element and on the finess of the mesh.

B.15 Static Condensation

The force-displacement relationship of the element may be expressed as

$$[F_m] = [K][r_m] \qquad (B.10a)$$

$$\begin{Bmatrix} F_x \\ F \\ F_z \\ F_{xm} \\ F_{ym} \\ F_{zm} \end{Bmatrix}_{33X1} = \begin{vmatrix} K_{aa} & K_{ab} \\ K_{ba} & K_{bb} \end{vmatrix}_{33X33} \begin{Bmatrix} \bar{U} \\ \bar{V} \\ \bar{W} \\ \bar{U}_m \\ \bar{V}_m \\ \bar{W}_m \end{Bmatrix}_{33X1} \qquad \text{(B.10b)}$$

where F_{xm}, F_{ym}, F_{zm} are the external forces associated with the generalized displacements $\bar{U}_m$, $\bar{V}_m$, $\bar{W}_m$. Since there are no external forces associated with the displacements $\bar{U}_m$, $\bar{V}_m$, $\bar{W}_m$, they may be expressed in terms of the eight corner nodal displacements. From equation (B.10b), it can be shown

$$\begin{Bmatrix} \bar{U}_m \\ \bar{V}_m \\ \bar{W}_m \end{Bmatrix} = - [K_{bb}^{-1}][K_{ba}] \begin{Bmatrix} \bar{U} \\ \bar{V} \\ \bar{W} \end{Bmatrix} \qquad \text{(B.11)}$$

Now the nodal forces and the displacements are related as follows:

$$\begin{Bmatrix} F_x \\ {}_{1-8} \\ F_y \\ {}_{1-8} \\ F_z \\ {}_{1-8} \end{Bmatrix} = [k_{aa} - k_{ab}\, k_{bb}^{-1} k_{ba}] \begin{Bmatrix} \bar{U} \\ \bar{V} \\ \bar{W} \end{Bmatrix} \qquad \text{(B.12)}$$

The final element stiffness matrix is 24X24 in size.

B.16 Evaluation of Stress

The stresses at any point are given by:

$$[\sigma] = [C][\varepsilon] = [C][B][r_m] \tag{B.13a}$$

If [B] is partitioned.

$$[\sigma] = [C][B_a \; B_b] \begin{Bmatrix} \bar{U} \\ \bar{V} \\ \bar{W} \\ \bar{U}_m \\ \bar{V}_m \\ \bar{W}_m \end{Bmatrix} \tag{B.13b}$$

The stress may be expressed in terms of Conner displacements

$$[\sigma] = [C][B^*][r]$$

where $$[B^*] = [B_a - B_b K_{bb}^{-1} K_{ba}]$$

The generalized displacements $\{\bar{U}_m, \bar{V}_m, \bar{W}_m\}$ calculated at the time of element stiffness formulation, are saved and used for the evaluation stresses.

B.17 Theoretical Cracking Load

The stress components for the three coordinate planes and the principal stresses are related by the following equation.

$$S^3 - (\sigma_x+\sigma_y+\sigma_z)\, S^2 + (\sigma_x\sigma_y+\sigma_y\sigma_z+\sigma_x\sigma_z-\tau_{yz}^2 - \tau_{xz}^2-\tau_{xy}^2)\, S - (\sigma_x\sigma_y\sigma_z+2\tau_{yz}\tau_{xz}\tau_{xy}-\sigma_x\tau_{yz}^2 - \sigma_y\tau_{xz}^2-\sigma_z\tau_{xy}^2) = 0 \qquad (B.14)$$

where σ_x, σ_y, σ_z, τ_{xy}, τ_{yz}, τ_{xy} are the six stress components, in the presen case these yield the stress distribution at cracking load with the effect of prestress eliminated making use of principle of superposition after the analysis is run.

S = Principal tensile stress

If the load is increased in a proportion f, the stresses also increase in the same proportion assuming the linear elasticity.

Equation (B.14) may be written as:

$$S^3 - (\sigma_x+\sigma_y+\sigma_z)fS^2 + (\sigma_x\sigma_y+\sigma_y\sigma_z+\sigma_x\sigma_z - \tau_{yz}^2-\tau_{xz}^2-\tau_{xy}^2)f^2S - (\sigma_x\sigma_y\sigma_z+2\tau_{yz}\tau_{xz}\tau_{xy} - \sigma_x\tau_{yz}^2-\sigma_y\tau_{xz}^2-\sigma_z\tau_{xy}^2)f^3 = 0 \qquad (B.15)$$

where f = load factor and also stress factor. If prestress P is to be superimposed on this stress distribution it adds to the component σ_y which is the stress in the longitudinal direction.

$$S^3 - f(\sigma_x+\sigma_y+\sigma_z)\, S^2 - PS^2 + (\sigma_x\sigma_y+\sigma_y\sigma_z+\sigma_x\sigma_z - \tau_{yz}^2-\tau_{xz}^2-\tau_{xy}^2)\, f^2S + (\sigma_x+\sigma_z)\, f^2SP - (\sigma_x\sigma_y\sigma_z+2\tau_{yz}\tau_{zx}\tau_{xy}-\sigma_x\tau_{yz}^2 - \sigma_y\tau_{xz}^2-\sigma_z\tau_{xy}^2)\, f^3 - (\sigma_x\sigma_z-\tau_{xz}^2)\, Pf^2 = 0 \qquad (B.16)$$

From this equation for the given values of the stress components, prestress and a maximum principal tensile stress equal to the tensile strength of concrete, the factor f can be obtained. This factor gives the proportion in which the applied load associated with the stress components σ_x, σ_y etc is to be increased or decreased to yield a principal tensile stress equivalent to the tensile strength of concrete at a given prestress, and hence the theoretical load.

```
HIS  FORTRAN IV G COMPILER (O/S REL 21.6)          MAIN
C
C     CRACKING ANALYSIS OF CONCRETE BEAMS SUBJECT TO COMBINED LOADINGS
C
C
C     THE PROGRAM CONSISTS OF FINITE ELEMENT ANALYSIS USING
C     ISOPARAMETRIC EIGHT NODED HEXAHEDRA WITH TWENTY FOUR DEGREES
C     OF FREEDOM
C
C
C*****************************************************************
C     MAIN PROGRAM
C*****************************************************************
C
C     THE MAIN PROGRAM ALLOWS TO CHANGE THE DIMENSION AND EQUIVALENCE
C     STATEMENTS IN ACCORDANCE WITH THE SIZE OF THE PROBLEM
C
0001          DIMENSION B(2500),A(150,300),BL(150),BR(150),AL(22500),AP(22500),
             1D(2500)
0002          EQUIVALENCE (B(1),BL(1)),(B(151),BR(1)),(A(1,1),AL(1)),(A(1,151),
             1AP(1))
0003          NB1=150
0004          NB2=2*NB1
0005          LA=NB1**2
0006          LA2=LA
0007          NLD=2500
0008          CALL THREED(B,A,BL,BR,AL,AP,NB1,NB2,LA,LA2,NLD,D)
0009          STOP
0010          END
```

```
HTS  FORTRAN IV G COMPILER (O/S REL 21.6)          THREED
0001          SUBROUTINE THREED(AP,STIF,APL,APR,STIFL,STIFR,NB1,NB2,LA,LA2,NLD,D
             1)
C
C     THE SUBROUTINE COMPUTES MODULUS MATRIX. READS EXTERNAL LOADS IF
C     MORE THAN ONE LOADING CONDITION IS TO BE SOLVED
C
0002          COMMON X(950),Y(950),Z(950),U(980),V(980),W(980),NODE(980)
0003          COMMON STNODE(950,3),KOUNT(950),SIGA(950,6)
0004          COMMON MAT(560),MP(8,560),MOST(560),KFILS(560),SIGPC(560,7),
             1SIGP1(560,7),SIGP2(560,7),KODEL(560)
0005          COMMON ELDISP(24)
0006          COMMON KSHIFT,NUMBLK,MPROP,NLODC,E,PP,PO,LCHECK(100)
0007          COMMON ETA(50),SI(50),ZETA(50),EMM(6,6),BM(6,33),ESTM(24,33),
             1PSTEP(33,33),PE(33),M,NEQ,NBAND,ELM(24),WEIGHT(96),NUMNP,NUMEL,
             2NUMAT
0008          DIMENSION AP(NB2),STIF(NB1,NB2),APL(NB1),APR(NB1),STIFL(LA2),
             1STIFR(LA),D(NLD)
0009          DIMENSION ESTIF(24,24),HMUL1(9,24),ESTIFL(576),HMUL5L(216),
             1INFO(4),INDEX1(100),HMULS(24,9)
0010          EQUIVALENCE (HMULS(1,1),HMUL5L(1)),(ESTIF(1,1),ESTIFL(1))
0011          INTEGER CPTIM,SCP(20)
0012          CALL TIME (0)
0013          EXTERNAL GETFD
0014          INTEGER ADROF,FDUB,FDUB1
0015          CALL RCALL(GETFD,2,0,ADROF('-T '),1,FDUB,6100)
0016          CALL SETDSW(1,'-T ',FDUB,6100)
0017          CALL RCALL(GETFD,2,0,ADROF('-T1 '),1,FDUB1,6100)
0018          CALL SETDSW(1,'-T1 ',FDUB1,6100)
0019          GO TO 101
0020      100 WRITE(6,600)
0021      600 FORMAT('FILE ERROR')
0022          STOP
0023      101 CONTINUE
0024     1500 NPROB=1
0025          CALL READIN(AP,STIF,APL,APR,STIFL,STIFR,NB1,NB2,LA,LA2,NLD,D)
0026          CALL TIME(1,1)
C     IF NPARA IS GREATER THAN 0 EXECUTION IS TERMINATED AFTER
C     GENERATION OF NODAL AND ELEMENT DATA
C*************************READ STATEMENT*****************************22
0027          READ(5,320)NPARA
0028          IF(NPARA.GT.0)GO TO 350
0029          WRITE(6,903)NPROB
0030          DO 500 I=1,5,4
0031          SI(I)=-1.
0032          SI(I+1)=1.
0033          SI(I+2)=1.
0034          SI(I+3)=-1.
0035          SI(I+16)=-.999
0036          SI(I+17)=.999
0037          SI(I+18)=.999
0038      500 SI(I+19)=-.999
0039          DO 501 I=1,7,8
0040          J1=I+1
0041          DO 502 K=I,J1
0042          ETA(K)=-1.
```

```
MTS   FORTRAN IV G COMPILER (O/S REL 21.6)              THREED

              ETA(K+2)=1.
              ETA(K+16)=-.999
      502     ETA(K+18)=.999
      501     CONTINUE
              DO 503 I=1,4
              ZETA(I)=-1.
              ZETA(I+4)=1.
              ZETA(I+16)=-.999
      503     ZETA(I+20)=.999
              ZETA(25)=0.0
              ETA(25)=0.0
              SI(25)=0.0
              DO 200 I=26,31
              SI(I)=0.0
              ETA(I)=0.0
              ZETA(I)=0.0
      200     CONTINUE
              SI(26)=1.0
              SI(28)=-1.0
              ETA(27)=1.0
              ETA(29)=-1.0
              ZETA(30)=-1.0
              ZETA(31)=1.0
      C       TWO POINT FORMULA
              T1=-0.57735027
              T2=-(T1)
              DO 13 I=9,12
              SI(I)=T1
      13      SI(I+4)=T2
              DO 11 I=9,13,4
              ETA(I)=T1
              ETA(I+1)=T1
              ETA(I+2)=T2
      11      ETA(I+3)=T2
              DO 12 I=9,15,2
              ZETA(I)=T1
      12      ZETA(I+1)=T2
              EMM1=E*(1.-PR)/((1.+PR)*(1.-2.*PR))
              EMM2=PR/(1.-PR)
              EMM3=(1.-2.*PR)/(2.*(1.-PR))
              INITIALISATION OF MODULUS MATRIX
              DO 14 I=1,6
              DO 14 J=1,6
      14      EMM(I,J)=0.0
              EMM(1,1)=EMM1
              EMM(2,2)=EMM1
              EMM(3,3)=EMM1
              EMM(4,4)=EMM1*EMM3
              EMM(5,5)=EMM1*EMM3
              EMM(6,6)=EMM1*EMM3
              EMM(1,2)=EMM1*EMM2
              EMM(1,3)=EMM1*EMM2
              EMM(2,1)=EMM(1,2)
              EMM(3,1)=EMM(1,3)
              EMM(2,3)=EMM1*EMM2
```

```
MTS   FORTRAN IV G COMPILER (O/S REL 21.6)              THREED

              EMM(3,2)=EMM(2,3)
              WRITE(6,7)
              WRITE(6,6)((EMM(I,J),J=1,6),I=1,6)
              CALL TIME(1,1)
              CALL ASTIF(AP,STIF,API,APS,STIFL,STIFS,MB1,MB2,LA,LA2,NLD,D,
             1     FDUB1,FSTIF,HMULS,FSTIFL,HMULSL,INPC,INDEX1)
              CALL TIME(1,1)
              GO TO 910
      800     NPROB=NPROB+1
              WRITE(6,903)NPROB
      C*************************READ STATEMENT**********************************23
              READ(5,120)NOCHNO
              WRITE(6,904)NOCHNO
              DO 900 I=1,NOCHNO
      C*************************READ STATEMENT**********************************24
              READ(5,901)N,KODE(N),U(N),V(N),W(N)
      900     WRITE(6,107)N,KODE(N),X(N),Y(N),Z(N),U(N),V(N),W(N)
              CALL TIME(1,1)
      910     CALL BAND1(AP,STIF,API,APS,STIFL,STIFS,MB1,MB2,LA,LA2,NLD,D,
             1FDUB)
              CALL TIME(1,1)
              CALL STRESS (AP,STIF,API,APS,STIFL,STIFS,MB1,MB2,LA,LA2,NLD,D,
             1     FDUB1,FSTIF,HMULS,FSTIFL,HMULSL,INPC,INDEX1)
              CALL TIME(1,1)
              IF(NPROB.NE.NLOD)GO TO 800
      110     WRITE(6,1600)(D(N),N=1,NSS)
      150     RETURN
      1600    FORMAT(10E12.5)
      1500    FORMAT(6F12.5)
      6       FORMAT(1X,6F12.5)
      7       FORMAT(///1X,'MODULUS MATRIX')
      920     FORMAT(2F8.3)
      410     FORMAT(6E12.5)
      120     FORMAT(I4)
      903     FORMAT('1',10X,'LOADING NUMBER ',I6//)
      904     FORMAT(10X,'NUMBER OF NODES WHERE LOADS ARE CHANGED',I6//)
      901     FORMAT(2I4,3F8.3)
      107     FORMAT('1',10X,'NODAL POINT INP[illegible]','NODE  KODE        XCOORD
             1YCOORD     ZCOORD     XFORCE          YFORCE          ZFORCE'//)
      1[illegible] FORMAT(I4,I6,6F1[illegible])
              END
```

```
MTS  FORTRAN IV G COMPILER (O/S REL 21.6)          READIN

0001            SUBROUTINE READIN(AP,STIF,APL,APP,STIFL,STIFP,MB1,MB2,LA,LA2,WLD,
               1D)
                C
                C     THE SUBROUTINE READS AND PRINTS DATA CONCERNING NODES,ELEMENTS
                C     MATERIAL PROPERTIES. AUTOMATICALLY GENERATES ELEMENT AND NODAL
                C     DATA BOTH CROSS SECTIONWISE AND LENGTHWISE IF REQUIRED. READS AND
                C     PRINTS LOADS FOR THE FIRST LOADING CONDITION AFTER COMPUTING BAND
                C     WIDTH
                C
0002                  COMMON X(950),Y(950),Z(950),U(980),V(980),W(980),KODE(980)
0003                  COMMON STNODE(950,3),KOUNT(950),SIGA(950,6)
0004                  COMMON MAT(560),NP(8,560),KOST(560),RELLS(560),SIGPC(560,7),
               1SIGP1(560,7),SIGP2(560,7),KODEL(560)
0005                  COMMON ELDISP(24)
0006                  COMMON KSHIFT,NUMBLK,NPROB,NLODC,E,PR,RO,LCHPCE(100)
0007                  COMMON ETA(50),SI(50),ZETA(50),EPP(6,6),EM(6,33),KSTH(6,33),
               1ESTEP(33,33),PE(33),M,NEQ,NBAND,LR(24),WEIGHT(90),NUMNP,NUMEL,
               2NUMAT
0008                  DIMENSION AP(MB2),STIF(MB1,MB2),APL(MB1),APP(MB1),STIFL(LA2),
               1STIFP(LA),D(WLD)
0009                  DIMENSION HED(18)
                C     READ GENERAL INFORMATION
               C**********READ STATEMENT**********1
0010                  READ(5,100)HED,NUMNP,NUMEL,NUMAT,NUMTIE,NUTEPP,NLODC
0011                  WRITE(6,101)HED,NUMNP,NUMEL,NUMAT,NUMTIE,NUTEPP,NLODC
                C
                C     READ AND WRITE MATERIAL PROPERTIES
                C
0012                  WRITE(6,102)
               C**********READ STATEMENT**********2
0013                  READ(5,55)E,PR,RO
0014                  WRITE(6,103)E,PR,RO
               C**********READ STATEMENT********3
0015                  READ(6,112)NRSEPA
0016                  IF(NRSEPA.GT.0)GO TO 63
               C**********READ STATEMENT********4
0017                  READ(5,503)NREP,NSUMR,NS1
0018                  WRITE(6,503)NREP,NSUMR,NS1
                C     READ AND WRITE NODAL DATA AND GENERATE INTERMEDIATE NODAL DATA
                C
0019               63 CONTINUE
0020                  WRITE(6,105)
0021                  L=1
               C**********READ STATEMENT**********5
0022                  READ(5,106)N,KODE(N),X(N),Y(N),Z(N),U(N),V(N),W(N)
0023                  GO TO 40
0024               20 READ(5,106)N,KODE(N),X(N),Y(N),Z(N),U(N),V(N),W(N)
0025                  DN=N-L
0026                  DX=(X(N)-X(L))/DN
0027                  DY=(Y(N)-Y(L))/DN
0028                  DZ=(Z(N)-Z(L))/DN
0029               25 L=L+1
0030                  IF(N-L)50,40,30
0031               30 X(L)=X(L-1)+DX
0032                  Y(L)=Y(L-1)+DY
```

```
MTS  FORTRAN IV G COMPILER (O/S REL 21.6)          READIN

0033                  Z(L)=Z(L-1)+DZ
0034                  KODE(L)=0
0035                  U(L)=0
0036                  V(L)=0
0037                  W(L)=0
0038                  GO TO 25
0039               40 CONTINUE
0040                  IF(NRSEPA.GT.0)GO TO 61
0041                  IF(NSUMR-N)50,60,20
0042               61 IF(NUMNP-N)50,60,20
                C
0043               50 WRITE(6,108)N
0044                  CALL EXIT
0045               60 CONTINUE
0046                  IF(NRSEPA.GT.0)GO TO 62
0047                  NODTR=NSUMR
0048                  DO 500 NA=1,NREP
               C**********READ STATEMENT**********
0049                  READ(5,501)TIN
0050                  DO 502 N=1,NSUMR
0051                  NODTR=NODTR+1
0052                  KODE(NODTR)=KODE(N)
0053                  X(NODTR)=X(N)
0054                  Y(NODTR)=Y(N)+TIN
0055                  Z(NODTR)=Z(N)
0056                  U(NODTR)=U(N)
0057                  V(NODTR)=V(N)
0058                  W(NODTR)=W(N)
0059              502 CONTINUE
0060              500 CONTINUE
0061               62 CONTINUE
                C     ASSIGN PROPER KODE FOR NODES GENERATED EARLIER WITH KODE(N)=0
                C     NKOCH1=0 MEANS EARLIER NODAL KODE GENERATION IS O.K
                C     OTHERWISE IT GIVES THE NUMBER OF STRETCHES WHERE KODE REQUIRES
                C     CHANGE
               C**********READ STATEMENT**********7
0062                  READ(5,112)NKOCH1
0063                  IF(NKOCH1.EQ.0)GO TO 45
0064                  DO 46 I=1,NKOCH1
                C     NKOCH2 IS ONE LESS THAN THE NUMBER OF POINTS FOR WHICH KODE IS TO
                C     BE CHANGED AT ASTRETCH
               C**********READ STATEMENT**********8
0065                  READ(5,112)NKOCH2
               C**********READ STATEMENT**********9
0066                  READ(5,110)N,KODE(N)
0067                  IF(NKOCH2.EQ.0)GO TO 46
0068                  DO 47 J=1,NKOCH2
0069                  N=N+1
0070                  KODE(N)=KODE(N-1)
0071               47 CONTINUE
0072               46 CONTINUE
                C     NUMTIE IS THE NUMBER OF STRETCHES OF HEXAHEDRA TO BE READ
                C     NUMEE IS THE NUMBER OF HEXAHEDRA IN EACH STRETCH
0073               45 WRITE(6,107)(N,KODE(N),X(N),Y(N),Z(N),U(N),V(N),W(N),N=1,NUMNP)
                C     READ AND WRITE ELEMENT DATA AND GENERATE INTERMEDIATE HEXAHEDRA
```

```
MTS  FORTRAN IV G COMPILER (O/S-PFL 21.6)          PRICE

C      AND TRIANGULAR PRISMS IF ANY
0074          WRITE(6,109)
0075          DO 70 MO=1,NUMTIE
C*************************READ STATEMENT*****************************1
0076          READ(5,112)NWEEE
0077          WRITE(6,112)NWEEE
C*************************READ STATEMENT*****************************11
0078          READ(5,113)M,(NP(II,M),II=1,M),MAT(M),RODEL(M),ROST(M),RELLS(M)
0079          WRITE(6,117)M,(NP(II,M),II=1,M),MAT(M),RODEL(M),ROST(M),RELLS(M)
0080          IF(NUMEE.EQ.0)GO TO 70
0081          DO 72 II=1,NUMEE
0082          M=M+1
0083          MAT(M)=MAT(M-1)
0084          RODEL(M)=RODEL(M-1)
0085          ROST(M)=ROST(M-1)
0086          RELLS(M)=RELLS(M-1)
0087          NP(1,M)=NP(1,M-1)+1
0088          NP(2,M)=NP(2,M-1)+1
0089          NP(3,M)=NP(3,M-1)+1
0090          NP(4,M)=NP(4,M-1)+1
0091          NP(5,M)=NP(5,M-1)+1
0092          NP(6,M)=NP(6,M-1)+1
0093          NP(7,M)=NP(7,M-1)+1
0094          NP(8,M)=NP(8,M-1)+1
0095          WRITE(6,117)M,(NP(II,M),II=1,M),MAT(M),RODEL(M),ROST(M),RELLS(M)
0096       72 CONTINUE
0097       70 CONTINUE
0098          IF(NUTRPR.EQ.0)GO TO 76
C         READ TRIANGULAR PRISMS INDIVIDUALLY
0099          DO 75 I=1,NUTRPR
C*************************READ STATMENT*****************************1
0100          READ(5,113)M,(NP(II,M),II=1,8),MAT(M),RODEL(M),ROST(M),RELLS(M)
0101          WRITE(6,117)M,(NP(II,M),II=1,8),MAT(M),RODEL(M),ROST(M),RELLS(M)
0102       74 CONTINUE
0103       76 CONTINUE
0104          IF(NUMAT.EQ.1)GO TO 77
C         ASSIGN PROPTR MAT(M) IF DIFFERENT FROM PREVIOUS VALUE FOR THE ELEMENTS
C         RODIEL=NUMBER OF ELEMENTS HAVING MATERIAL DIFFERENT FROM THAT
C         OF THOSE AT THE ENDS OF THAT STRETCH
C*************************READ STATMENT*****************************11
0105          READ (5,112)NODIEL
0106          DO 78 I=1,NODIEL
C*************************READ STATEMENT*****************************1
0107       78 READ(5,110)M,MAT(M)
0108       77 CONTINUE
C*************************READ STATEMENT*****************************15
0109          READ(5,300)NELPC
0110          IF(NELPC.EQ.0)GO TO 150
0111          WRITE(6,155)
0112          DO 151 I=1,NELPC
C*************************READ STATEMENT*****************************16
0113          READ(5,110)M,RELLS(M)
0116       151 WRITE(6,156)M,RELLS(M)
0115       150 CONTINUE
C*************************READ STATEMENT*****************************17
```

```
MTS  FORTRAN IV G COMPILER (O/S PFL 21.6)          READIN

0116          READ(5,112)NELP
0117          IF(NELP.EQ.0)GO TO 700
0118          WRITE(6,701)
0119          DO 702 I=1,NELP
C*************************READ STATEMENT*****************************1
0120          READ(5,110)M,ROST(M)
0121       702 WRITE(6,156)M,ROST(M)
0122       700 CONTINUE
0123          IF(NRSEPA.GT.0)GO TO 65
0124          NREP1=NREP-1
0125          NS=NS1
0126          NSUM1=0
0127          DO 512 MA1=1,NREP1
0128          NSUM1=NSUM1+NSUMM
C*************************READ STATEMENT*****************************1
0129          READ(5,112)KACD
0130          DO 515 M=1,NS1
0131          NS=NS+1
0132          MAT(NS)=MAT(M)
0133          RODEL(NS)=RODEL(M)
0134          RELLS(NS)=RELLS(M)
0135          ROST(NS)=ROST(M)+KACC
0136          NP(1,NS)=NP(1,M)+NSUM1
0137          NP(2,NS)=NP(2,M)+NSUM1
0138          NP(3,NS)=NP(3,M)+NSUM1
0139          NP(4,NS)=NP(4,M)+NSUM1
0140          NP(5,NS)=NP(5,M)+NSUM1
0141          NP(6,NS)=NP(6,M)+NSUM1
0142          NP(7,NS)=NP(7,M)+NSUM1
0143          NP(8,NS)=NP(8,M)+NSUM1
0144       515 CONTINUE
0145       512 CONTINUE
0146          DO 520 M=1,NUMEL
0147          WRITE(6,117)M,(NP(II,M),II=1,8),MAT(M),RODEL(M),ROST(M),RELLS(M)
0148       520 CONTINUE
0149       65 CONTINUE
C         DETERMINATION OF BAND WIDTH AND NUMBER OF EQUATIONS
0150          I=0
0151          DO 40 M=1,NUMEL
0152          DO 40 J=1,7
0153          II=I+1
0154          DO 40 J =II,M
0155          K=IABS(NP(1,M)-NP(J,M))
0156          IF(K.GT.I)I=K
0157       40 CONTINUE
0158          MBAND=I*(I+1)
0159          NE=I*NUMNOD
0160          WRITE(6,114)MBAND,NE
0161       600 CONTINUE
0162          IF(MBAND.LE.1000)GO TO 11
0163          WRITE(6,115)
0164          CALL EXIT
0165       90 WRITE(6,111)
0166          CONTINUE
C*************************READ STATEMENT*****************************20
```

```
MTS  FORTRAN IV G COMPILER (0/S REL 21.6)          READIN

0167            READ(5,300)NOCHNO
0168            WRITE(6,904)NOCHNO
0169            DO 900 I=1,NOCHNO
          C*********************READ STATEMENT*********************************21
0170            READ(5,901)N,KODE(N),U(N),V(N),W(N)
0171        900 WRITE(6,107)N,KODE(N),X(N),Y(N),Z(N),U(N),V(N),W(N)
0172            RETURN
0173        501 FORMAT(F5.0)
0174        503 FORMAT(3I4)
0175        904 FORMAT(10X,'NUMBER OF NODES WHERE LOADS ARE CHANGED=',I6//)
0176        903 FORMAT(///,10X,'LOADING NUMBER=',I6//)
0177        100 FORMAT(I4)
0178        301 FORMAT(I4,F8.2)
0179        302 FORMAT(4I4,3F6.3)
0180        701 FORMAT(///3X,'ELEMENT',2X,'ELE SIZE NODE', [illegible])
0181        303 FORMAT(////
                11H ,      26H  SUPPORT NODE  NUMBER   = ,I6/
                21H ,      26H  BENDING LOAD           = ,E14.6/)
0182        104 FORMAT(//
                11H ,   ,  26HDEFLECTION MEASURED AT   = ,I6/)
0183        105 FORMAT(//
                11H ,      26H NODE CONCERNING TORQUE = ,I6/
                21H ,      26H NODE CONCERNING TORQUE = ,I6/
                31H ,      26H NODE CONCERNING TORQUE = ,I6/
                41H ,      26H NODE CONCERNING TORQUE = ,I6/
                51H ,      26H BEAM WIDTH             = ,E14.6/
                61H ,      26H TORQUE                 = ,E14.6)
0184        116 FORMAT(  'READIN COMPLETED'///)
0185        155 FORMAT(///3X,'ELEMENT NO','ELE FACE NODE',//)
0186        156 FORMAT(4X,I4,6X,I4)
0187        100 FORMAT(18A4/6I6)
0188        101 FORMAT(1H1,10X,18A4,////
                11H ,      26H  NUMBER OF NODAL POINTS= ,I6/
                21H ,      26H  NUMBER OF ELEMENTS    = ,I6/
                31H ,      26H  NUMBER OF MATERIAL    = ,I6/
                41H ,      26H  NUMBER OF TIPA USED   = ,I6/
                51H ,      26H  NUMBER OF PRISMS USED = ,I6/
                61H ,      26H  NO. OF LOAD CONDITIONS= ,I6/)
0189        103 FORMAT(F12.0,10X,F6.3,8X,F12.8)
0190        102 FORMAT(///3X,'MODULUS E',5X,'POISSONS RATIO',5X,'UNIT WEIGHT',//)
0191        104 FORMAT('1',10X,'NODAL POINT INPUT'//,'NODE  [illegible]        XCORD
               1YCOORD     ZCOORD     XFORCE          YFORCE          ZFORCE'//)
0192        106 FORMAT(1H ,I5,F17.0,F15.3,F17.3)
0193        901 FORMAT(2I4,3F6.3)
0194         [illegible] FORMAT(F12.0,F[illegible],F7.3)
0195        106 FORMAT(2I5,6F5.3)
0196        107 FORMAT(I4,I6,6F12.4)
0197        108 FORMAT(1H0,20H ERROR IN NODAL DATA NODE= ,I4)
0198        109 FORMAT('1',10X,'ELEMENT DATA'///,
               1'ELEM    N1    N2    N3    N4    N5    N6    N7    N8   MAT.NUM.     ELE ROD
               2F.      ELE SIZE NODE.       ELE FACE [illegible]'///)
0199        110 FORMAT(2I4)
0200        112 FORMAT(I4)
0201        113 FORMAT(11I5)
0202        114 FORMAT(///10X,'BAND WIDTH              =',I6/
               110X,'NUMBER OF EQUATIONS=',I6)
0203        115 FORMAT(///10X,33H PROBLEM [illegible] SPECIFIED [illegible], [illegible])
0204        117 FORMAT(1015,10X,I5,10X,I5,10X,I5)
0205            END
```

```
MTS  FORTRAN IV G [illegible] (0/S REL 21.6)          ELSTIF

0001            SUBROUTINE ELSTIF(AP,STIF,APL,APR,STIFL,STIFR,MB1,MB2,LA,LA2,
               1NID,D,KOP,EDUB1,FSTU[illegible],HMUL[illegible],ESTIFL,HMULSL,INFO,INDEX1,
               2SIGPLC,SIGEL1,SIGEL2,ESTRNC,ESTRN1,ESTRN2)
          C
          C     THE SUBROUTINE ASSEMBLES ELEMENT STIFFNESS AND STORES IN D[illegible]
          C     COMPUTES NODAL AND ELEMENT STRESSES AFTER NODAL DISPLACEMENTS    ARE
          C     KNOWN
          C
0002            COMMON X(950),Y(950),Z(950),U(980),V(980),W(980),KODE(980)
0003            COMMON STNODE(950,3),KOUNT(950),SIGA(950,6)
0004            COMMON MAT(560),NP(8,560),KOST(560),KEIL(560),SIGPC(560,7),
               1SIGP1(560,7),SIGP2(560,7),KOIEL(560)
0005            COMMON ELDISP(24)
0006            COMMON ESHIFT,NUMELX,NPROB,NLODC,E,PR,RO,ICHECK(100)
0007            COMMON ETA(50),SI(50),ZETA([illegible]),EMM(6,[illegible]),IM(6,33),ESTM(6,33),
               1ESTIFF([illegible],33),PF(33),M,NEQ,MBAND,LM(24),WEIGHT(96),NUMNP,NUMEL,
               2NUMAT
0008            DIMENSION AP(MB2),STIF(MB1,MB2),APL(MB1),APR(MB1),STIFL(LA2),
               1STIFR(LA),D(NID)
0009            DIMENSION ESTIF(24,24),HMUL1(9,24) ,ESTIFL(576),HMULSL(216),
               1INFO(4),INDEX1(100),HMUL[illegible](24,9)
0010            DIMENSION CKBB(9,9),GKAB(24,9),CKBA(9,24),HMUL1(9,24),HMUL[illegible](24,24
               1),F(9,9)
0011            DIMENSION SIGEL[illegible](6),SIGEL1(6),SIGEL2(6),ESTRNC(6),ESTRN1(6),
               1ESTRN2(6)
0012            INTEGER*2 LEN
0013            INTEGER EDUB1
0014            IF(KOP.EQ.1)GO TO 4000
0015            NAME=KOST(M)
0016            INFO(1)=INDEX1(NAME)
0017            CALL POINT(EDUB1,INFO,1)
0018            CALL READ(ESTIFL(1),LEN,0,LT,EDUB1,6550)
0019            CALL READ(HMULSL(1),LEN,0,LT,EDUB1,6550)
0020            WRITE(6,[illegible])LEN,M,HMULSL(1),HMULSL(2),HMULSL(3),HMULSL(4)
0021       4000 CONTINUE
0022            L1=NP(1,M)
0023            L2=NP(2,M)
0024            L3=NP(3,M)
0025            L4=NP(4,M)
0026            L5=NP(5,M)
0027            L6=NP(6,M)
0028            L7=NP(7,M)
0029            L8=NP(8,M)
0030            DO 200 I=1,33
0031            DO 200 J=1,33
0032        200 ESTIF(I,J)=0.0
0033            VOL=0.0
0034            IF(KOP.EQ.2) GO TO [illegible]
0035            DO 11 NN=1,8,[illegible]
0036            L=NN1
0037            GO TO 700
0038        [illegible] IF(KODE(M).EQ.1) GO TO [illegible]
0039            DO [illegible] NN2=1,8
0040            L=NN2
0041            [illegible] TO 700
```

MTS FORTRAN IV G COMPILER (OS REL 21.6) ELSTIF

```
0042      760 IF (770.NBJ+17,
0043          L=NB3
0044          GO TO 700
0045      300 KELLS1=KELLS(M)/10
0046          KELLS2=KELLS(M)-KELLS1*10
0047          IF(KELLS1.EQ.0)GO TO 301
0048          IF(KELLS1.EQ.1)L=26
0049          IF(KELLS1.EQ.2)L=27
0050          IF(KELLS1.EQ.3)L=28
0051          IF(KELLS1.EQ.4)L=29
0052          IF(KELLS1.EQ.5)L=30
0053          IF(KELLS1.EQ.6)L=31
0054          GO TO 700
0055      301 IF(KELLS2.EQ.0)GO TO
0056          IF(KELLS2.EQ.1)L=26
0057          IF(KELLS2.EQ.2)L=27
0058          IF(KELLS2.EQ.3)L=28
0059          IF(KELLS2.EQ.4)L=29
0060          IF(KELLS2.EQ.5)L=30
0061          IF(KELLS2.EQ.6)L=31
0062          GO TO 700
0063      10. L=25
0064      700 AL1=-(1.-ETA(L))*(1.-ZETA(L))*(1./8.)
0065          AL2=-AL1
0066          AL3=(1.+ETA(L))*(1.-ZETA(L))*(1./8.)
0067          AL4=-AL3
0068          AL5=-(1.-ETA(L))*(1.+ZETA(L))*(1./8.)
0069          AL6=-AL5
0070          AL7=(1.+ETA(L))*(1.+ZETA(L))*(1./8.)
0071          AL8=-AL7
0072          AL9=-2.*SI(L)
0073          BL1=-(1.-SI(L))*(1.-ZETA(L))*(1./8.)
0074          BL2=-(1.+SI(L))*(1.-ZETA(L))*(1./8.)
0075          BL3=-BL2
0076          BL4=-BL1
0077          BL5=-(1.-SI(L))*(1.+ZETA(L))*(1./8.)
0078          BL6=-(1.+SI(L))*(1.+ZETA(L))*(1./8.)
0079          BL7=-BL6
0080          BL8=-BL5
0081          BL9=-2.*ETA(L)
0082          CL1=-(1.-SI(L))*(1.-ETA(L))*(1./8.)
0083          CL2=-(1.+SI(L))*(1.-ETA(L))*(1./8.)
0084          CL3=-(1.+SI(L))*(1.+ETA(L))*(1./8.)
0085          CL4=-(1.-SI(L))*(1.+ETA(L))*(1./8.)
0086          CL5=-CL1
0087          CL6=-CL2
0088          CL7=-CL3
0089          CL8=-CL4
0090          CL9=-2.*ZETA(L)
C         FORMATION OF JACOBIAN MATRIX.  J.
0091          EJ31=X(L1)*CL1+X(L2)*CL2+X(L3)*CL3+X(L4)*CL4+X(L5)*CL5+X(L6)*CL6
         1+X(L7)*CL7+X(L8)*CL8
0092          EJ32=Y(L1)*CL1+Y(L2)*CL2+Y(L3)*CL3+Y(L4)*CL4+Y(L5)*CL5+Y(L6)*CL6
         1+Y(L7)*CL7+Y(L8)*CL8
0093          EJ33=Z(L1)*CL1+Z(L2)*CL2+Z(L3)*CL3+Z(L4)*CL4+Z(L5)*CL5+Z(L6)*CL6
```

MTS FORTRAN IV G COMPILER (OS REL 21.6) ELSTIF

```
         1+Z(L7)*CL7+Z(L8)*CL8
0094          EJ21=X(L1)*BL1+X(L2)*BL2+X(L3)*BL3+X(L4)*BL4+X(L5)*BL5+X(L6)*BL6
         1+X(L7)*BL7+X(L8)*BL8
0095          EJ22=Y(L1)*BL1+Y(L2)*BL2+Y(L3)*BL3+Y(L4)*BL4+Y(L5)*BL5+Y(L6)*BL6
         1+Y(L7)*BL7+Y(L8)*BL8
0096          EJ23=Z(L1)*BL1+Z(L2)*BL2+Z(L3)*BL3+Z(L4)*BL4+Z(L5)*BL5+Z(L6)*BL6
         1+Z(L7)*BL7+Z(L8)*BL8
0097          EJ11=X(L1)*AL1+X(L2)*AL2+X(L3)*AL3+X(L4)*AL4+X(L5)*AL5+X(L6)*AL6
         1+X(L7)*AL7+X(L8)*AL8
0098          EJ12=Y(L1)*AL1+Y(L2)*AL2+Y(L3)*AL3+Y(L4)*AL4+Y(L5)*AL5+Y(L6)*AL6
         1+Y(L7)*AL7+Y(L8)*AL8
0099          EJ13=Z(L1)*AL1+Z(L2)*AL2+Z(L3)*AL3+Z(L4)*AL4+Z(L5)*AL5+Z(L6)*AL6
         1+Z(L7)*AL7+Z(L8)*AL8
0100          DETERJ=EJ11*(EJ22*EJ33-EJ32*EJ23)-EJ12*(EJ21*EJ33-EJ23*EJ31)+
         1EJ13*(EJ21*EJ32-EJ22*EJ31)
0101          A11=(EJ22*EJ33-EJ32*EJ23)*(1./DETERJ)
0102          A21=-(EJ21*EJ33-EJ23*EJ31)*(1./DETERJ)
0103          A31=(EJ21*EJ32-EJ22*EJ31)*(1./DETERJ)
0104          A12=-(EJ12*EJ33-EJ13*EJ32)*(1./DETERJ)
0105          A22=(EJ11*EJ33-EJ13*EJ31)*(1./DETERJ)
0106          A32=-(EJ11*EJ32-EJ12*EJ31)*(1./DETERJ)
0107          A13=(EJ12*EJ23-EJ13*EJ22)*(1./DETERJ)
0108          A23=-(EJ11*EJ23-EJ13*EJ21)*(1./DETERJ)
0109          A33=(EJ11*EJ22-EJ12*EJ21)*(1./DETERJ)
0110          PF(1)=A11*AL1+A12*BL1+A13*CL1
0111          PF(2)=A21*AL1+A22*BL1+A23*CL1
0112          PF(3)=A31*AL1+A32*BL1+A33*CL1
0113          PF(4)=A11*AL2+A12*BL2+A13*CL2
0114          PF(5)=A21*AL2+A22*BL2+A23*CL2
0115          PF(6)=A31*AL2+A32*BL2+A33*CL2
0116          PF(7)=A11*AL3+A12*BL3+A13*CL3
0117          PF(8)=A21*AL3+A22*BL3+A23*CL3
0118          PF(9)=A31*AL3+A32*BL3+A33*CL3
0119          PF(10)=A11*AL4+A12*BL4+A13*CL4
0120          PF(11)=A21*AL4+A22*BL4+A23*CL4
0121          PF(12)=A31*AL4+A32*BL4+A33*CL4
0122          PF(13)=A11*AL5+A12*BL5+A13*CL5
0123          PF(14)=A21*AL5+A22*BL5+A23*CL5
0124          PF(15)=A31*AL5+A32*BL5+A33*CL5
0125          PF(16)=A11*AL6+A12*BL6+A13*CL6
0126          PF(17)=A21*AL6+A22*BL6+A23*CL6
0127          PF(18)=A31*AL6+A32*BL6+A33*
0128          PF(19)=A11*AL7+A12*BL7+A13*
0129          PF(20)=A21*AL7+A22*BL7+A23*
0130          PF(21)=A31*AL7+A32*BL7+A33*CL7
0131          PF(22)=A11*AL8+A12*BL8+A13*CL8
0132          PF(23)=A21*AL8+A22*BL8+A23*CL8
0133          PF(24)=A31*AL8+A32*BL8+A33*CL8
0134          PF(25)=A11*AL9
0135          PF(26)=A21*AL9
0136          PF(27)=A31*AL9
0137          PF(28)=A12*BL9
0138          PF(29)=A22*BL9
0139          PF(30)=A32*BL9
0140          PF(31)=A13*CL9
```

```
0141                PF(32)=A21*CL9
0142                PF(33)=A31*CL9
                C       FORMATION OF B MATRIX
                C       INITIALISATION OF B MATRIX
0143                DO 14 I=1,6
0144                DO 14 J=1,33
0145             14 BM(I,J)=0.0
0146                DO 15 J=1,31,3
0147                BM(1,J)=PE(J)
0148                BM(4,J)=PE(J+1)
0149             15 BM(6,J)=PE(J+2)
0150                DO 16 J=2,32,3
0151                BM(2,J)=PE(J)
0152                BM(4,J)=PE(J-1)
0153             16 BM(5,J)=PE(J+1)
0154                DO 17 J=3,33,3
0155                BM(3,J)=PE(J)
0156                BM(5,J)=PE(J-1)
0157             17 BM(6,J)=PE(J-2)
0158                IF(KOP.EQ.2)GO TO 120
                C       FORMATION OF ELEMENT STRESS MATRIX
                C       INITIALISATION OF ELEMENT STRESS MATRIX
0159                DO 19 I=1,6
0160                DO 19 J=1,33
0161                ESTM(I,J)=0.0
0162                DO 19 N=1,6
0163             19 ESTM(I,J)=ESTM(I,J)+EMM(I,N)*BM(N,J)
0164                IF(KOP.EQ.1)GO TO 2*
0165            120 CONTINUE
0166                DO 68 I=1,6
0167                DO 68 J=1,24
0168                HMUL3(I,J)=0.0
0169                DO 68 N=1,9
0170             68 HMUL3(I,J)=HMUL3(I,J)+SM(I,(N+24))*HMDSP(J,N)
0171                DO 69 I=1,6
0172                DO 69 J=1,24
0173             69 BM(I,J)=BM(I,J)-HMUL3(I,J)
0174                DO 121 I=1,6
0175                DO 121 J=1,24
0176                ESTM(I,J)=0.0
0177                DO 121 N=1,6
0178            121 ESTM(I,J)=ESTM(I,J)+EMM(I,N)*BM(N,J)
0179                IF(L.LT.
0180                IF(L.EQ.2
0181                IF(KFILS(
0182                IF(KFILS(M)
0183                IF(L.NE.25)GO TO 304
0184            *** DO 830 I=1,6
0185                SIGELC(I)=0.0
0186                DO 830 J=1,24
0187            830 SIGELC(I)=SIGELC(I)+ESTM(I,J)*ELDISP(J)
0188                DO 840 I=1,6
0189                ESTMC(I)=0.
0190                DO 840 J=1,24
0191            840 ESTMC(I)=ESTMC(I)+ESTM (I)*BM(I,J)*ELDISP(J)
```

```
0194                ESTMC(I)=ESTMC(I)*1000.
0195                IF(KFILS(M).EQ.0)KELL(M)=-KELL(M)
0196            *** CONTINUE
0197                GO TO 900
0198             40 CONTINUE
0199                DO 1506 I=1,6
0200                SIGEL2(I)=0.0
0201                DO 1503 J=1,24
0202             1503 SIGEL2(I)=SIGEL2(I)+ESTM(I,J)*ELDISP(J)
0203            1504 CONTINUE
0204            1505 CONTINUE
0205                DO 1507 I=1,6
0206                ESTMC(I)=0.0
0207                DO 1508 J=1,24
0208            1508 ESTMC(I)=ESTMC(I)+BM(I,J)*ELDISP(J)
0209             1507 CONTINUE
0210                KELL(M)=-KELL(M)
0211                GO TO 301
0212            1304 CONTINUE
0213                DO 1500 I=1,6
0214                SIGEL1(I)=0.0
0215                DO 1501 J=1,24
0216                SIGEL1(I)=SIGEL1(I)+ESTM(I,J)*ELDISP(J)
0217            1502 CONTINUE
0218            1500 CONTINUE
0219                DO 1505 I=1,6
0220                ESTMC1(I)=0.0
0221                DO 1506 J=1,24
0222            1506 ESTMC1(I)=ESTMC1(I)+BM(I,J)*ELDISP(J)
0223                ESTMC1(I)=ESTMC1(I)*1000.
0224            1505 CONTINUE
0225                GO TO 302
0226             920 IF(KOSEL(M).EQ.0)GO TO 940
0227                M=NP(5-16,M)
0228                KOUNT(M)=KOUNT(M)+1
0229                DO 950 I=1,6
0230                DO 950 J=1,24
0231             950 SIGA(M,I)=SIGA(M,I)+ESTM(I,J)*ELDISP(J)
0232                DO 960 I=1,3
0233                DO 960 J=1,24
0234             960 STNODE(M,I)=STNODE(M,I)+BM(I,J)*ELDISP(J)
0235             940 CONTINUE
0236                GO TO 400
0237            9400 M=NP(I,M)
0238                KOUNT(M)=KOUNT(M)+1
0239                DO 920 I=1,6
0240                DO 920 J=1,24
0241             920 SIGA(M,I)=SIGA(M,I)+ESTM(I,J)*ELDISP(J)
0242                DO 930 I=1,3
0243                DO 930 J=1,24
0244             930 STNODE(M,I)=STNODE(M,I)+BM(I,J)*ELDISP(J)
0245             940 CONTINUE
0246                GO TO 300
                    FORMATION OF ELEMENT STIFFNESS MATRIX
```

```
PTS  FORTRAN IV G COMPILER (O/S REL 21.8)          ESSIF

0286          25 DO 20 I=1,33
0287             DO 20 J=1,33
0288             DO 20 M=1,6
0289          20 ESTEF(I,J)=ESTFF(I,J)+BM(M,I)*FSTM(M,J)*DETERD
0290             VOL=VOL*DETERJ
0291             WEIG=VOL*80/8.
0292             LAX=HOST(M)
0293             WEIGHT(LAX)=WEIG
0294          33 CONTINUE
0295             DO 40 I=1,9
0296             DO 60 J=1,9
0297             CBBB(I,J)=ESTFF((I+24),(J+24))
0298          60 CONTINUE
0299             DO 61 I=1,24
0300             DO 61 J=1,9
0301             CBAB(I,J)=ESTFF(I,(J+24))
0302          61 CONTINUE
0303             DO 62 I=1,9
0304             DO 62 J=1,24
0305             CBBA(I,J)=ESTFF((I+24),J)
0306          62 CONTINUE
C            INVERSION OF MATRIX CBBB
0307             M=9
0308             DO 6 I=1,M
0309             DO 7 J=1,M
0310             IF(I-J)6,8,6
0311           8 P(I,J)=1.0
0312             GO TO 7
0313           6 P(I,J)=0.0
0314           7 CONTINUE
0315           4 CONTINUE
C            DIVIDE PIVOT ROW BY ITS MAIN DIAGONAL ELEMENT
0316             DO 65 K=1,M
0317             DIV=CBBB(K,K)
0318             DO 38 J=1,M
0319             CBBB(K,J)=CBBB(K,J)/DIV
0320          38 P(K,J)=P(K,J)/DIV
C            REPLACE EACH ROW BY LINEAR COMBINATION WITH PIVOT ROW
0321             DO 43 I=1,M
0322             AMULT=CBBB(I,K)
0323             IF(I-K)39,43,39
0324          39 DO 42 J=1,M
0325             CBBB(I,J)=CBBB(I,J)-AMULT*CBBB(K,J)
0326          42 P(I,J)=P(I,J)-AMULT*P(K,J)
0327          43 CONTINUE
0328          65 CONTINUE
0329             DO 63 I=1,9
0330             DO 63 J=1,24
0331             HMUL1(I,J)=0.0
0332             DO 63 M=1,9
0333          63 HMUL1(I,J)=HMUL1(I,J)+P(I,M)*CBBA(M,J)
0334             DO 68 I=1,24
0335             DO 68 J=1,24
0336             HMUL2(I,J)=0.0
0337             DO 68 M=1,9
```

```
PTS  FORTRAN IV G COMPILER (O/S REL 21.8)          ESSIF

0338          64 HMUL2(I,J)=HMUL2(I,J)+CBAB(I,M)*HMUL1(M,J)
0339             DO 65 I=1,24
0340             DO 65 J=1,24
0341          65 ESTIF(I,J)=ESTEF(I,J)-HMUL2(I,J)
0342             DO 220 J=1,9
0343             DO 221 I=1,24
0344             HMUL5(I,J)=HMUL1(J,I)
0345          221 CONTINUE
0346          220 CONTINUE
0347             NSTRES=NOST(M)
0348             CALL NOTE(FOUR1,INFO)
0349             INDEX1(NSTRES)=INFO(2)
0350             LEN=5760*8
0351             CALL WRITE(ESTIFL(1),LEN,,1,FOUR1,ERR)
0352             GO TO 551
0353          600 WRITE(6,600)
0354             STOP
0355          551 CONTINUE
0356             WRITE(6,552)LEN,M,ESTIFL(1),ESTIFL(2),ESTIFL(575),ESTIFL(576)
0357             LEN=216*8
0358             CALL WRITE(HMULSL(1),LEN,0,1,FOUR1,ERR)
0359             WRITE(6,552)LEN,M,HMULSL(1),HMULSL(2),HMULSL(3),HMULSL(4)
0360          900 CONTINUE
0361             RETURN
0362         1002 FORMAT(1X,5I10)
0363         1600 FORMAT(1X,I10)
0364         1601 FORMAT(1X,8I8)
0365          402 FORMAT(1X,10E12.6)
0366          553 FORMAT(1X,I4,8F12.5)
0367          600 FORMAT( 'ERROR FILE IN FESTIF')
0368          552 FORMAT(1X,2I8,8F12.5)
0369          110 FORMAT(2X,E12.5)
0370           23 FORMAT(E12.5)
0371           22 FORMAT(1X,2I4,E12.4)
0372            5 FORMAT(1X,2E14.8)
0373         3000 FORMAT(3I3)
0374            1 FORMAT(20F3.1)
0375            3 FORMAT(F7.1,F9.2)
0376             END
```

```
MTS  FORTRAN IV G COMPILER (O/S REL 21.7)          ASTIF

0001          SUBROUTINE ASTIF(AP,STIF,APL,APF,STIFL,STIFR,MB1,MB2,IA,IAL,
             1NLD,D,     PDUB1,ESTIF,HMULS,ESTIFL,HMULSL,INFO,INDEX1)
C
C
C         THE SUBROUTINE FORMS SYSTEM STIFFNESS IN BLOCKS
C
0002          COMMON X(950),Y(950),Z(950),U(980),V(980),W(980),KODE(980)
0003          COMMON STWORF(950,3),KOUNT(950),SIGA(950,6)
0004          COMMON MAT(560),MP(8,560),KOST(560),KFLLS(560),SIGPC(560,7),
             1SIGP1(560,7),SIGP2(560,7),KODEL(560)
0005          COMMON ELDISP(24)
0006          COMMON KSHIFT,NUMBLK,NPROB,NLODC,E,PR,BO,LCHECK(100)
0007          COMMON ETA(50),SI(50),ZETA(50),EMM(6,6),EM(6,3),ESTM(6,3),
             1ESTIF(33,33),PE(33),M,NEQ,MBAND,LM(24),WEIGHT(90),NUMNP,NUMEL,
             2NUMAT
0008          DIMENSION AP(MB2),STIF(MB1,MB2),APL(MB1),APF(MB1),STIFL(LA2),
             1STIFR(LA),D(NLD)
0009          DIMENSION ESTIF(24,24),HMUL1(9,24),ESTIFL(576),HMULSL(216),
             1INFO(8),INDEX1(100),HMULS(24,9)
0010          DIMENSION SIGELC(6),SIGEL1(6),SIGEL2(6),ESTRNC(6),ESTRN1(6),
             1ESTRN2(6)
0011          INTEGER*2 LEN
0012          MBYTES=MBAND*MBAND*8
0013          AMUNREC=FLOAT(MBYTES)/32000
0014          NUMREC=MBYTES/32000
0015          IF((AMUNREC-NUMREC).GT.0.0) NUMREC=NUMREC+1
0016      600 FORMAT('FILE ERROR IN ASTIF')
C         DEFINING BLOCKS AND INITIALISATION OF AP VECTOR ELEMENTS OF
C         STIFFNESS MATRIX STIF(J,I) OF 2MBAND*MBAND
0017          REWIND 2
0018          MB=MBAND/3
0019          ND=3*MB
0020          NEQ=2*ND
0021          NUMBLK=0
0022          DO 10 I=1,NEQ
0023          AP(I)=0.0
0024          DO 10 J=1,ND
0025       10 STIF(J,I)=0.0
0026          DO 107 I=1,100
0027      107 LCHECK(I)=1
C         FORM STIFFNESS MATRIX IN BLOCKS
0028       20 NUMBLK=NUMBLK+1
0029          MB=MB*(NUMBLK+1)
0030          MM=MM-MB
0031          MI=MM-MB+1
0032          WRITE(6,1)NUMBLK,MI,MB
0033          KSHIFT=3*MI-3
0034          DO 100 M=1,NUMEL
0035          IF(MAT(M))100,100,101
0036      101 DO 103 I=1,8
0037          IF(MP(I,M)-MI)103,104,104
0038      104 IF(MP(I,M)-MB)105,105,103
0039      103 CONTINUE
0040          GO TO 100
0041      105 LCH=KOST(M)
0042          IF(LCHECK(LCH).LT.1)GO TO 106

MTS  FORTRAN IV G COMPILER (O/S REL 21.7)          ASTIF

0043          CALL FSTIF(AP,STIF,APL,APF,STIFL,STIFR,MB1,MB2,IA,IAL,NDOF,D,
             1PDUB1,ESTIF,HMULS,ESTIFL,HMULSL,INFO,INDEX1,
             2SIGELC,SIGEL1,SIGEL2,ESTRNC,ESTRN1,ESTRN2)
0044          LCHECK(LCH)=-1
0045      106 MAT(M)=-MAT(M)
0046          NSTRES=KOST(M)
0047          INFO(1)=INDEX1(NSTRES)
0048          CALL POINT(PDUB1,INFO,1)
0049          CALL READ(ESTIFL(1),LEN,0,LZ,PDUB1,6550)
0050          WRITE(6,552)LEN,M,ESTIFL(1),ESTIFL(2),ESTIFL(575),ESTIFL(576)
0051          GO TO 501
0052      550 WRITE(6,606)
0053          STOP
0054      501 CONTINUE
0055          CALL READ(HMULSL(1),LEN,0,LZ,PDUB1,6550)
0056          WRITE(6,552)LEN,M,HMULSL(1),HMULSL(2),HMULSL(3),HMULSL(4)
C         ASSEMBLE ELEMENT STIFFNESS MATRIX ELEMENTS IN TO TOTAL STIFFNESS
C         MATRIX
0057          DO 35 I=1,8
0058          I2=I*I
0059          LM(I2)=3*MB(I,M)
0060          LM(I2-1)=LM(I2)-1
0061       35 LM(I2-2)=LM(I2)-2
0062          DO 200 I=1,24
0063          II=LM(I)-KSHIFT
0064          DO 200 J=1,24
0065          JJ=LM(J)-II+1-KSHIFT
0066          IF(JJ.LE.0)GO TO 200
0067          STIF(JJ,II)=STIF(JJ,II)+ESTIF(J,I)
0068      200 CONTINUE
C         ADD GRAVITY LOADS IN TO LOAD VECTOR AP
0069          DO 36 I=1,24,3
0070          II=LM(I)-KSHIFT
0071       36 AP(II)=AP(II)-WEIGHT(LCH)
0072      100 CONTINUE
0073          WRITE(6,700)
0074          WRITE(6,701)(M,MAT(M),M=1,NUMEL)
C         ADD NODAL LOADS IN TO AP VECTOR
0075          DO 400 M=ML,MM
0076          M3=3*M-KSHIFT
0077          AP(M2)=AP(M2)+W(M)
0078          AP(M2-1)=AP(M2-1)+V(M)
0079      400 AP(M2-2)=AP(M2-2)+U(M)
C         MODIFY STIFFNESS AND LOAD VECTOR FOR DISPLACEMENT BOUNDARY
C         CONDITION
0080          DO 420 M=ML,MM
0081          IF(M-NUMNP)430,430,420
0082      430 M3=3*M-KSHIFT
0083          IF(KODE(M)-10)450,440,440
0084      440 IF(KODE(M)-11)420,450,450
0085      450 CALL MODIFY (AP,STIF,APL,APF,STIFL,STIFR,MB1,MB2,IA,IAL,NDOF,D,M,
             1)
0086          GO TO 420
0087      445 IF(KODE(M)-12)446,410,420
0088      446 I2=M2-2
```

```
      CALL MODIFY (AP,STIF,APL,APR,STIFL,STIFR,MR1,MR,,IA,IA,,N,C,L,II,N
     1)
      GO TO 820
  800 IF=N2-1
      CALL MODIFY (AP,STIF,APL,APR,STIFL,STIFR,MR1,MR,,IA,LA,,NLD,D,IF,N
     1)
      GO TO 820
  820 II=N2-2
      CALL MODIFY (AP,STIF,APL,APR,STIFL,STIFR,MR1,MR,,IA,IA,,NLD,C,II,N
     1)
      CALL MODIFY (AP,STIF,APL,APR,STIFL,STIFR,MR1,MR2,LA,LA,,NLD,C,N,,N
     1)
      GO TO 820
  840 II=N2-2
      IF=N2-1
      CALL MODIFY (AP,STIF,APL,APR,STIFL,STIFR,MR1,MR2,IA,IA,,NLD,D,II,N
     1)
      CALL MODIFY (AP,STIF,APL,APR,STIFL,STIFR,MR1,MR,,IA,LA,,NLD,C,IF,N
     1)
      GO TO 820
  870 IF(KODE(N).EQ.12) GO TO [illegible]
      IF=N2-1
      CALL MODIFY (AP,STIF,APL,APR,STIFL,STIFR,MR1,MR,,IA,LA,,NLD,D,IF,N
     1)
      CALL MODIFY (AP,STIF,APL,APR,STIFL,STIFR,MR1,MR,,IA,IA,,NLD,D,N2,N
     1)
      GO TO 820
  810 II=N2-2
      IF=N2-1
      CALL MODIFY (AP,STIF,APL,APR,STIFL,STIFR,MR1,MR,,IA,IA,,NLD,D,II,N
     1)
      CALL MODIFY (AP,STIF,APL,APR,STIFL,STIFR,MR1,MR,,IA,IA,,NLD,D,IF,N
     1)
      CALL MODIFY (AP,STIF,APL,APR,STIFL,STIFR,MR1,MR,,IA,IA,,NLD,D,N2,N
     1)
  820 CONTINUE
      DO 750 N=N1,NN
      N2=3*N-KSHIFT
      IF(KODE(N).LT.0)GO TO 2000
      D(3*N)=AP(N2)
      D(3*N-1)=AP(N2-1)
      D(3*N-2)=AP(N2-2)
      GO TO 750
 2000 D(3*N)=AP(N2)-W(N)
      D(3*N-1)=AP(N2-1)-V(N)
      D(3*N-2)=AP(N2-2)-U(N)
  750 CONTINUE
      WRITE(6,3000)NL,NN,NUMBLK,KSHIFT
C     WRITE BLOCK OF EQUATIONS ON DISK AND SHIFT UP THE NEXT LOWER
C     BLOCK
C     FOR KODE THE FOLLOWING IS SPECIFIED.
C     ALL FORCES***1=Z DISP***2=Y DISP***[illegible] DISP***[illegible] Y&Z [illegible]
C     1[illegible] X&Y DISP***11= Y&Z DISP*** 12=ALL DISP****
      IFN=12000
      LL=1
      DO 800 I=1,NUMBER
      IF(L.EQ.NUMBER)LIN=NRTTT-((NUMBER-1)*12000)
      CALL WRITE (STIFL(II),LIN,[illegible],[illegible])
      WRITE(6,700)II,LIN,STIFL(II)
      II=LL+8000
      GO TO 800
  801 WRITE(6,600)
      STOP
  800 CONTINUE
      LIN=NBAND*N
      CALL WRITE (APL,LIN,[illegible])
      WRITE(6,700)NBAND,LIN,APL(1)
  700 FORMAT(2I10,F20.7)
      DO 860 I=1,NC
      K=I+ND
      AP(I)=AP(K)
      AP(K)=0.0
      DO 860 J=1,NC
      STIF(J,I)=STIF(J,K)
  860 STIF(J,K)=0.0
C     CHECK FOR THE LAST BLOCK
      IF(NN-NUMND)20,870,870
  870 CONTINUE
  871 RETURN
  [illegible] FORMAT(1X,I8,4E12.5)
  [illegible] FORMAT(1X,10E12.4)
      1 FORMAT(/12X,'BLOCK NUMBER=',I5/12X,'LOWEST NODE NUMBER IN BLOCK=',
     2I5/12X,'HIGHEST NODE NUMBER IN BLOCK=',I5/)
  101 FORMAT(/1I5)
  [illegible] FORMAT(/1X,'ELEMENT STIFFNESS MATRIX FORMED FOR THE ELEMENTS WITH
     1-VE MAT(N) FOR THE FOLLOWING',/)
 3000 FORMAT(4I4)
 [illegible] FORMAT([illegible],I10)
      END
```

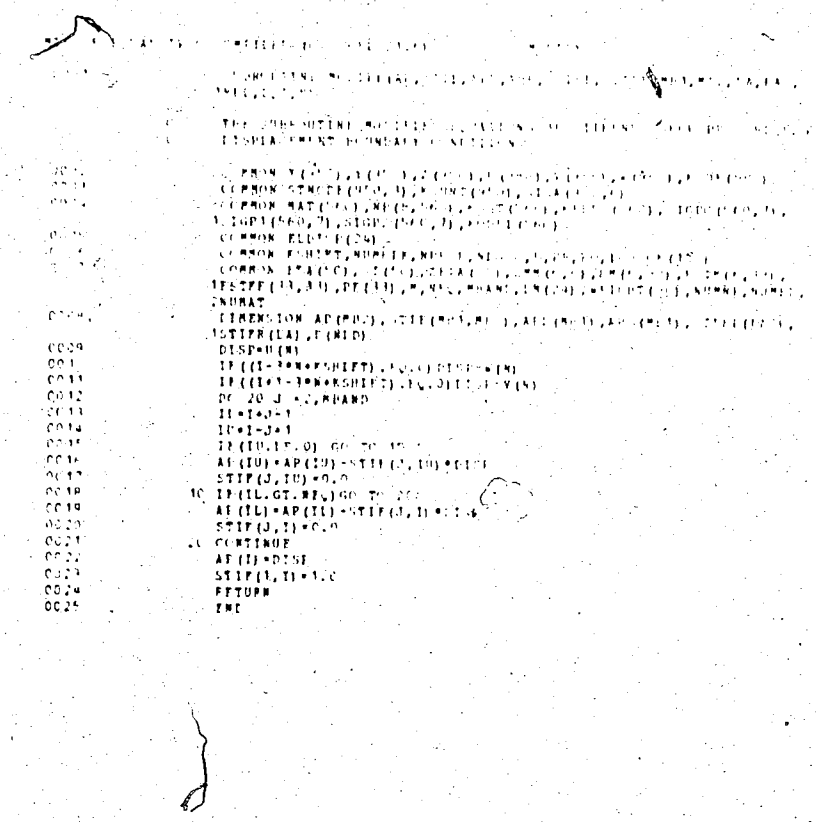

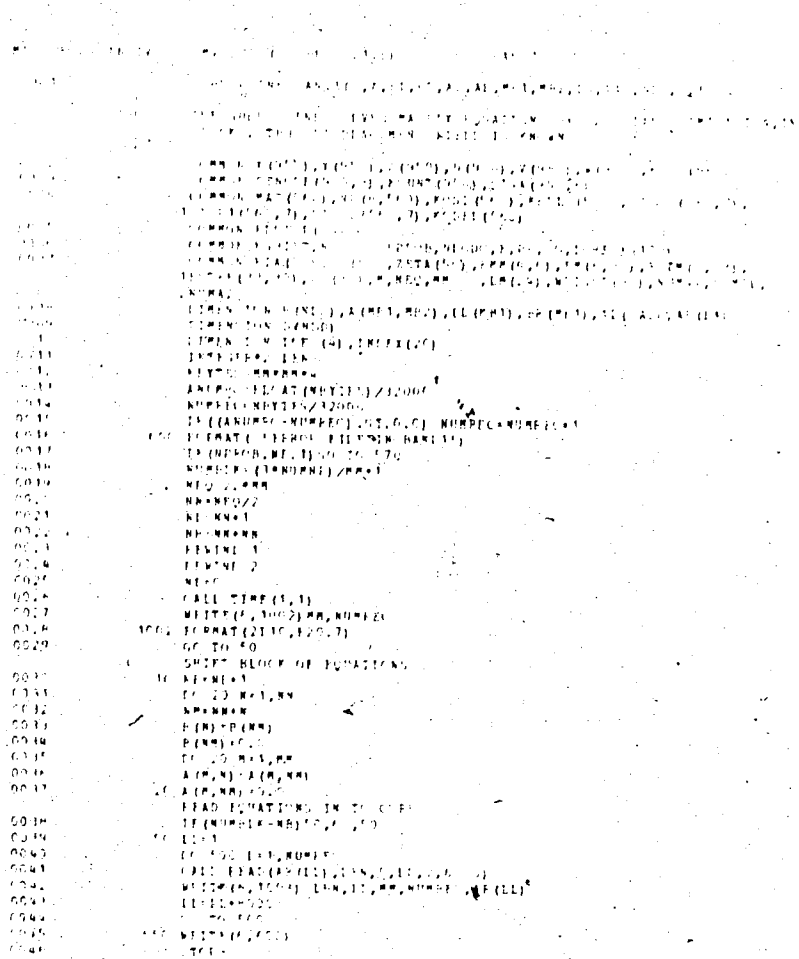

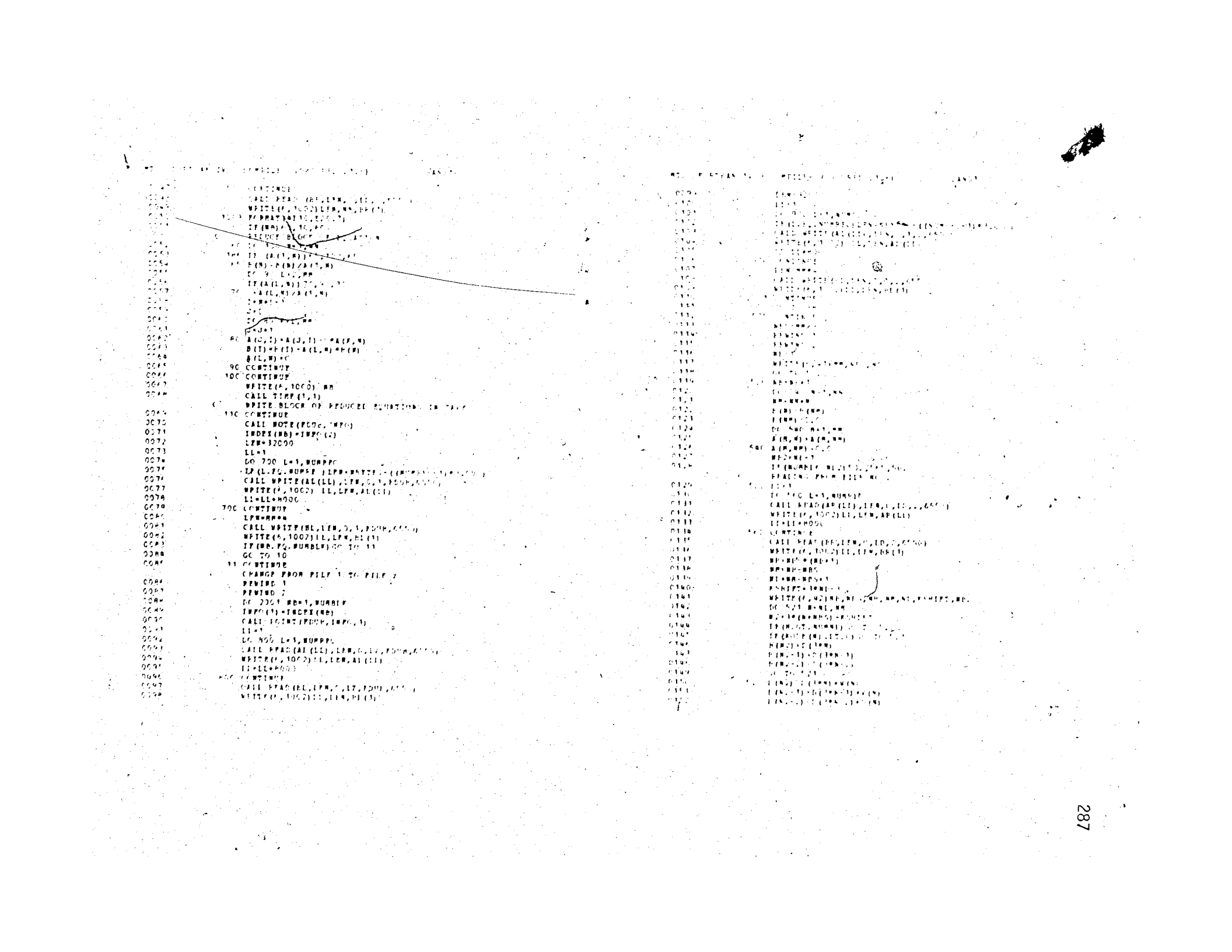

MTS FORTRAN IV G COMPILER (0/S REL 21.8) MAIN

```
              GO TO 521
          520 B(N2)=0.0
              B(N2-1)=0.0
              B(N2-2)=0.0
          521 WRITE(6,93)B(N2),B(N2-1),B(N2-2),B(3*N),B(3*N-1),B(3*N-2),W(N),
             1V(N),U(N),M,N2,NL,NM,NF
              WRITE(6,525)NH,NM,NL,FSHIFT,NB
              IF(NB.EQ.1)GO TO 520
          565 DO 999 N=1,NM
              IF(A(1,N))998,999,998
          998 BN=B(N)
              B(N)=BN/A(1,N)
              DO 999 L=2,NM
              I=N+L-1
              B(I)=B(I)-A(L,N)*BN
          999 CONTINUE
        C     WRITE IN FILE NO 1 THE REDUCED EQUATIONS
              NB1=NB-1
              WRITE(6,45)NB1
              CALL NOTE(FDUB,INFO)
              INDEX(NB1)=INFO(2)
              LEN=32000
              LL=1
              DO 901 L=1,NUMREC
              IF(L.EQ.NUMREC)LEN=NBYTES-((NUMREC-1)*32000)
              CALL WRITE(AL(LL),LEN,0,1,FDUB,&550)
              WRITE(6,1002) LL,LEN,AL(LL)
              LL=LL+8000
          901 CONTINUE
              LEN=NM*8
              CALL WRITE(BL,LEN,0,1,FDUB,&550)
              WRITE(6,1002)LL,LEN,BL(1)
              WRITE(6,45)NB1
              IF(NB1.EQ.NUMBLK)GO TO 560
              GO TO 520
          560 CONTINUE
        C     BACK SUBSTITUTION FROM FILE NO 1
              NB=NUMBLK
          150 CONTINUE
              INFO(1)=INDEX(NB)
              CALL POINT(FDUB,INFO,1)
              LL=1
              DO 801 L=1,NUMREC
              CALL READ(AL(LL),LEN,0,LZ,FDUB,&550)
              WRITE(6,1002)LL,LEN,AL(LL)
              LL=LL+8000
          801 CONTINUE
              CALL READ(BL,LEN,0,LZ,FDUB,&550)
              WRITE(6,1002)LL,LEN,BL(1)
              DO 140 M=1,NM
              N=NM+1-M
              DO 130 K=2,NM
              L=N+K-1
          130 B(N)=B(N)-A(K,N)*B(L)
              NP=N+NN
```

MTS FORTRAN IV G COMPILER (0/S REL 21.8) MAIN

```
              B(NP)=B(N)
          140 A(NP,NM)=B(N)
              WRITE(6,1001) NB
              CALL TIME(1,1)
              NB=NB-1
              IF(NB)150,160,150
        C     STORE UNKNOWNS IN B ARRAY
          160 K=0
              NUMEQ=3*NUMNP
              DO 180 NB=1,NUMBLK
              DO 180 N=1,NN
              NP=N+NN
              K=K+1
              IF(K.GT.NUMEQ) GO TO 190
          180 B(K)=A(NB,NM)
          190 CONTINUE
              WRITE(6,300)
              DO 30 N=1,NUMNP
           30 WRITE(6,315)N,B(3*N-2),B(3*N-1),B(3*N)
          151 RETURN
          300 FORMAT('1',10X,'NODAL DISPLACEMENT'///,'NODE        X DISPL
             1Y DISPL                Z DISPL'//)
          315 FORMAT(I4,3E15.5)
         1000 FORMAT(//10X,'EQUATIONS REDUCED IN BLOCK NUMBER',I5//)
         1001 FORMAT(//10X,'BACK SUBSTITUTION COMPLETED IN BLOCK NUMBER',I5//)
          525 FORMAT(5I4)
           41 FORMAT(1X,3I6)
           42 FORMAT(1X,7I6)
           43 FORMAT(1X,9E12.5,5I4)
           44 FORMAT(1X,3I6,2E5.4)
           45 FORMAT(1X,I6)
              END
```

283

```
0001           SUBROUTINE PRINT(AP,STIF,AEL,AEE,STIFL,STIFR,MB1,MB2,LA,LA2,NLD,
              *    FOUR1,ESTIF,MMUL1,ESTIFL,MMUL5,INFO,INDEX1)
        C
        C      THE SUBROUTINE PRINTS ELEMENT,NODAL STRESSES AND PRINCIPAL
        C      STRESSES AND THEIR DIRECTIONS
        C
0002           COMMON X(950),Y(950),Z(950),D(480),V(480),W(480),FOIE(960)
0003           COMMON STNODE(950,3),NCOUNT(950),SIGA(950,6)
0004           COMMON MAT(560),NP(8,560),FOUT(560),KELLS(560),SIGC(560,7),
              1SIGP1(560,7),SIGP2(560,7),FOIEI(560)
0005           COMMON ELDISP(24)
0006           COMMON NSHIFT,NUMBER,NPROB,NLOCK,P,PP,RO,LCHECK(10)
0007           COMMON ETA(50),SI(50),ZETA(50),EMM(6,6),BM(6,11),ESTR(6,11),
              1ESTEF(33,33),PF(33),N,NEQ,MBAND,IM(24),WEIGHT(90),NUMNP,NUMEL,
              2NUMAT
0008           COMMON/AREA1/NGETS,NSUPP,ETHICO,NNDM(20),TIC,DHTTM,NWIDTH,
              1ICFOUT,NOTOQ1,NOTOQ2,NOTOQ3,NOTOQ4
0009           DIMENSION AP(MB2),STIF(MB1,MB2),AEL(MB1),APP(MB1),STIFL(LA2),
              1STIFR(LA),D(NLD)
0010           DIMENSION ESTIF(24,24),MMUL1(9,24) ,ESTIFL(576),MMUL5L(216),
              1INFO(8),INDEX1(100),MMUL5(24,9)
0011           DIMENSION SIGELC(6),SIGEL1(6),SIGEL2(6),ESTRNC(6),ESTRN1(6),
              1ESTRN2(6),SIGP(8),DLN(6)
0012           INTEGER*2 LIN
0013           INTEGER FOUR1
        C      INITIALISES COUNT OF ELEMENTS ADJOINING NODAL POINT N.
        C      AVERAGE NODAL POINT STRESSES SIGA ARE INITIALISED.
0014           SIG1C=0.0
0015           SIG2C=0.0
0016           SIG3C=0.0
0017           SIG1CS=0.0
0018           SIG2CS=0.0
0019           SIG12=0.0
0020           SIG22=0.0
0021           SIG32=0.0
0022           SIG12S=0.0
0023           SIG22S=0.0
0024           SIG11=0.0
0025           SIG21=0.0
0026           SIG31=0.0
0027           SIG11S=0.0
0028           SIG21S=0.0
0029           M1C=0
0030           M2C=0
0031           M3C=0
0032           M1CS=0
0033           M2CS=0
0034           M12=0
0035           M22=0
0036           M32=0
0037           M12S=0
0038           M22S=0
0039           M11=0
0040           M21=0
0041           M31=0
```



```
0042           M11S=0
0043           M21S=0
0044           DO 5 N=1,NUMNP
0045           NCOUNT(N)=0
0046           DO 5 J=1,6
0047         5 SIGA(N,J)=0.0
0048           DO 6 N=1,NUMNP
0049           DO 6 J=1,3
0050         6 STNODE(N,J)=0.0
0051           WRITE(6,500)
0052           DO 10 M=1,NUMEL
        C      COMPUTE ELEMENT [illegible]
0053           DO 15 I=1,8
0054           I2=3*I
0055           IMI2=3*NP(I,M)
0056           ELDISP(I2)=AP(IMI2)
0057           ELDISP(I2-1)=AP(IMI2-1)
0058        15 ELDISP(I2-2)=AP(IMI2-2)
        C      COMPUTE ELEMENT STRESSES AT CENTRE OF ELEMENT
0059           MAT(M)=IABS(MAT(M))
0060           CALL ELSTIF(AP,STIF,AEL,AEE,STIFL,STIFR,MB1,MB2,LA,LA2,NLD,D,2,
              1FOUR1,ESTIF,MMUL1,ESTIFL,MMUL5L,INFO,INDEX1,
              2SIGELC,SIGEL1,SIGEL2,ESTRNC,ESTRN1,ESTRN2)
0061           WRITE(6,1102)M,(SIGELC(I),I=1,6),(ESTRNC(I),I=1,3),KELLS(M)
0062           CALL PRINCI   (1,SIGELC,SIGP)
0063           DO 200 I=1,4
0064       200 SIGPC(M,I)=SIGP(I)
0065           IF(SIGPC(M,1).LT.SIG1C) GO TO 110
0066           SIG1C=SIGPC(M,1)
0067           M1C=M
0068       110 IF(SIGPC(M,1).GT.SIG2C) GO TO 102
0069           SIG2C=SIGPC(M,1)
0070           M2C=M
0071       102 IF(SIGPC(M,4).LT.SIG3C) GO TO 1405
0072           SIG3C=SIGPC(M,4)
0073           M3C=M
0074      1405 CONTINUE
0075           CALL PRINCI   (2,ESTRNC,SIGP)
0076           DO 1402 I=1,3
0077           J=I+4
0078      1402 SIGPC(M,J)=SIGP(I)
0079           IF(SIGPC(M,5).LT.SIG1CS)GO TO 1403
0080           SIG1CS=SIGPC(M,5)
0081           M1CS=M
0082      1403 IF(SIGPC(M,7).GT.SIG2CS)GO TO 1404
0083           SIG2CS=SIGPC(M,7)
0084           M2CS=M
0085      1404 CONTINUE
0086           IF(KELLS(M).[illegible]
0087           WRITE(6,1102)M,([illegible](I),I=1,6),([illegible](I),I=1,3),KELLS(M)
0088           CALL PRINCI   (1,SIGEL1,SIGP)
0089           DO 1420 I=1,4
0090      1420 SIGP1(M,I)=SIGP(I)
0091           IF(SIGP1(M,1).LT.SIG11) GO TO 1421
0092           SIG11=SIGP1(M,1)
```

```
      [illegible]
 1421 IF(SIGP1(M,3).[illegible])GO TO [illegible]
      SIG21=SIGP1(M,3)
      M21=M
 14[illegible] IF(SIGP1(M,4).LT.SIG31)GO TO 14[illegible]
      SIG31=SIGP1(M,4)
      M31=M
 1423 CONTINUE
      CALL PRINCI    (2,ESTRN1,SIGP)
      DO 1430 I=1,3
      J=I+4
 1430 SIGP1(M,J)=SIGP(I)
      IF(SIGP1(M,5).LT.SIG11S)GO TO 1431
      SIG11S=SIGP1(M,5)
      M11S=M
 1431 IF(SIGP1(M,7).GT.SIG21S)GO TO 1432
      SIG21S=SIGP1(M,7)
      M21S=M
 1432 CONTINUE
      IF(KELLS(M).LT.7)GO TO 1400
      WRITE(6,1102)M,(SIGEL2(I),I=1,6),(ESTRN2(I),I=1,3),KELLS(M)
      CALL PRINCI    (1,SIGEL2,SIGP)
      DO 1410 I=1,4
 1410 SIGP2(M,I)=SIGP(I)
      IF(SIGP2(M,1).LT.SIG12)GO TO 1411
      SIG12=SIGP2(M,1)
      M12=M
 1411 IF(SIGP2(M,3).GT.SIG22)GO TO 1412
      SIG22=SIGP2(M,3)
      M22=M
 1412 IF(SIGP2(M,4).LT.SIG32)GO TO 1413
      SIG32=SIGP2(M,4)
      M32=M
 1413 CONTINUE
      CALL PRINCI    (2,ESTRN2,SIGP)
      DO 1414 I=1,3
      J=I+4
 1414 SIGP2(M,J)=SIGP(I)
      IF(SIGP2(M,5).LT.SIG12S)GO TO 1415
      SIG12S=SIGP2(M,5)
      M12S=M
 1415 IF(SIGP2(M,7).GT.SIG22S)GO TO 1416
      SIG22S=SIGP2(M,7)
      M22S=M
 1416 CONTINUE
 1400 CONTINUE
   10 CONTINUE
      WRITE(6,1001)
      WRITE(6,1480)
      WRITE(6,1002)(M,(SIGPC(M,I),I=1,7),M=1,NUMEL)
      WRITE(6,1000)SIG1C,M1C,SIG2C,M2C,SIG3C,M3C
      WRITE(6,1001)
      WRITE(6,1460)
      DO 1450 M=1,NUMEL
      IF(KELLS(M).GT.7)WRITE(6,1002)M,(SIGP1(M,I),I=1,7)
```



```
 14[illegible] CONTINUE
      WRITE(6,100[illegible])[illegible]
      WRITE(6,1001)
      WRITE(6,1470)
      DO 1440 M=1,NUMEL
      IF(KELLS(M).GT.7)WRITE(6,1002)M,(SIGP2(M,I),I=1,7)
 1440 CONTINUE
      WRITE(6,1000)SIG12,M12,SIG22,M22,SIG32,M32
C     AVERAGE NODAL STRESSES AND STRAINS
      DO 1600 N=1,NUMNP
      VANI=KOUNT(N)
      IF(VANI.EQ.0.0)GO TO 1600
      DO 1601 I=1,6
      SIGA(N,I)=SIGA(N,I)/VANI
 1601 CONTINUE
 1600 CONTINUE
      DO 1602 N=1,NUMNP
      SUP=KOUNT(N)
      IF(SUP.EQ.0.0)GO TO 1602
      DO 1603 I=1,3
      STNODE(N,I)=STNODE(N,I)/SUP
 1603 CONTINUE
 1602 CONTINUE
      WRITE(6,1604)
      DO 1606 N=1,NUMNP
 1606 WRITE(6,1605) N,SIGA(N,1),SIGA(N,2),SIGA(N,3),SIGA(N,4),SIGA(N,5),
     1SIGA(N,6),STNODE(N,1),STNODE(N,2),STNODE(N,3)
      WRITE(6,4001)
      DO 4000 N=1,NUMNP
      DO 4010 I=1,6
      DLN(I)=SIGA(N,I)
 4010 CONTINUE
      CALL PRINCI(1,DLN,SIGP)
      WRITE(6,4002)N,(SIGP(I),I=1,4)
 4000 CONTINUE
      REWIND 3
      RETURN
 4002 FORMAT(I4,4F12.5)
 1460 FORMAT(///3X,'ELEMENT PRINCIPAL STRESSES AND STRAINS ON FACE 1',/)
 1470 FORMAT(///3X,'ELEMENT PRINCIPAL STRESSES AND STRAINS ON FACE 2',/)
 1480 FORMAT(///3X,'ELE PRINCIPAL STRESSES & STRAINS AT CENTRE OF ELE',/
     1)
 1102 FORMAT(1X,I4,9E12.5,9X,I2)
   50 FORMAT('1',10X,'ELEMENT STRESSES'///,'ELEM     SIGMA X     SIGMA Y
     1     SIGMA Z     SIGMA XY     SIGMA YZ     SIGMA ZX     STRAIN XX     ST
     2RAIN YY     STRAIN ZZ     ELE PAGE'//)
 1604 FORMAT('1',10X,'AVERAGE NODAL STRESSES'///,'NODE     SIGMA X     SIGMA
     1 Y     SIGMA Z     SIGMA XY     SIGMA YZ     SIGMA ZX     STRAIN X
     2STRAIN Y     STRAIN Z'///)
 1605 FORMAT(I4,9E12.5)
 1002 FORMAT(I4,7E12.5)
 1001 FORMAT('1',10X,'PRINCIPAL [illegible]'///,'ELEM     SIGMA [illegible]     SIGMA
     1     SIGMA 3     MAX SHEAR     STRAIN 1     STRAIN 2     STRAIN 3'//)
 1000 FORMAT(///,
     1'THE MAXIMUM PRINCIPAL STRESSES [illegible],TOP AND [illegible] IN ELEM,I[illegible]
```

```
FORTRAN IV [illegible]

      2X,'MINIMUM PRINCIPAL [illegible] ',E15.6,' [illegible] IN PSIM,I2/
      2X,'MAXIMUM SHEAR [illegible] ',E15.6,' [illegible] IN PSIM,I2/)
 [illegible] FORMAT(I3)
 [illegible] FORMAT([illegible],//,[illegible] SIGMA [illegible]
     [illegible] SIGMA [illegible] MAX [illegible])
 [illegible] FORMAT(7X,I4,[illegible],E16.6,[illegible])
 [illegible] FORMAT(I4,F8.2)
 [illegible] FORMAT(8I4,[illegible])
 [illegible] FORMAT([illegible],F16.6,5X,F16.6)
 [illegible] FORMAT(1X,[illegible])
      END
```

```
FORTRAN IV [illegible]

      [illegible] PRINCIPAL [illegible]
      DIMENSION [illegible]
      DIMENSION [illegible]
      IF(IDEN.[illegible]) GO TO [illegible]
      FAC1=1.
      FAC2=[illegible]
      GO TO [illegible]
  [illegible] FAC1=[illegible]
      FAC2=0.25
  [illegible] CONTINUE
      S1=Q(1)+Q(2)+Q(3)
      S2=Q(1)*Q(2)+Q(2)*Q(3)+Q(3)*Q(1)-FAC1*(Q(4)**2+Q(5)**2+Q(6)**2)
      S3=Q(1)*Q(2)*Q(3)+FAC2*Q(4)*Q(5)*Q(6)-FAC1*(Q(1)*Q(5)**2+Q(2)*
     1Q(6)**2+Q(3)*(Q(4)**2))
      ICOF(1)=-S3
      ICOF(2)=S2
      ICOF(3)=-S1
      ICOF(4)=1.
      CALL POLRT(XCOF,COF,3,SIGP,ROOTI,IER)
C     PRINCIPAL STRESSES ARRANGED IN DESCENDING ORDER
      DO 300 I=1,2
      JJ=3-I
      DO 310 J=1,JJ
      IF(SIGP(J).GT.SIGP(J+1)) GO TO 320
      GO TO 310
  320 X2=SIGP(J)
      X1=SIGP(J+1)
      SIGP(J+1)=X2
      SIGP(J)=X1
  310 CONTINUE
  300 CONTINUE
C     MAXIMUM SHEAR STRESS
      SIGP(4)=(SIGP(1)-SIGP(3))/2.
      IF(IDEN.EQ.2)GO TO 900
      A(1)=Q(1)-SIGP(1)
      A(2)=Q(4)
      A(3)=Q(2)-SIGP(1)
      A(4)=Q(6)
      A(5)=Q(5)
      A(6)=Q(3)-SIGP(1)
      CALL EIGEN (A,R,3,[illegible])
      DO 25 NIL=1,9
      DIR(NIL)=ARCOS(R(NIL))*180./3.[illegible]
   25 CONTINUE
      WRITE(6,[illegible]) (DIR(NIL),NIL=1,9)
  900 RETURN
  [illegible] FORMAT(3F8.4)
  [illegible] FORMAT(6F8.4)
  [illegible] FORMAT(2X,9F[illegible])
  [illegible] FORMAT([illegible])
      END
```

```
IBM  FORTRAN IV G COMPILER (O/S REL 21.7)          POLRT

0001            SUBROUTINE POLRT(XCOF,COF,M,ROOTR,ROOTI,IER)
                C
                C     THE SUBROUTINE COMPUTES PRINCIPAL ZEROS
                C
0002            DIMENSION XCOF(1),COF(1),ROOTR(1),ROOTI(1)
0003            DOUBLE PRECISION XO,YO,X,Y,XPR,YPR,UX,UY,V,TT,XT,U,XT2,YT2,SUMSQ,
               1 DX,DY,TEMP,ALPHA
0004            IPIT=0
0005            N=M
0006            IER=0
0007            IF(XCOF(N+1)) 10,25,10
0008          10 IF(N) 15,15,32
                C       SET ERROR CODE TO 1
0009          15 IER=1
0010          20 RETURN
                C       SET ERROR CODE TO 4
0011          25 IER=4
0012             GO TO 20
                C       SET ERROR CODE TO 2
0013          30 IER=2
0014             GO TO 20
0015          32 IF(N-36) 35,35,30
0016          35 NX=N
0017             NXX=N+1
0018             N2=1
0019             KJ1 = N+1
0020             DO 40 L=1,KJ1
0021             MT=KJ1-L+1
0022          40 COF(MT)=XCOF(L)
                C       SET INITIAL VALUES
0023          45 XO=.00500101
0024             YO=0.01000101
                C       ZERO INITIAL VALUE COUNTER
0025             IN=0
0026          50 X=XO
                C       INCREMENT INITIAL VALUES AND COUNTER
0027             XO=-10.0*YO
0028             YO=-10.0*X
                C       SET X AND Y TO CURRENT VALUE
0029             X=XO
0030             Y=YO
0031             IN=IN+1
0032             GO TO 59
0033          55 IPIT=1
0034             XPR=X
0035             YPR=Y
                C       EVALUATE POLYNOMIAL AND DERIVATIVES
0036          59 ICT=0
0037          60 UX=0.0
0038             UY=0.0
0039             V =0.0
0040             TT=0.0
0041             XT=1.0
0042             U=COF(N+1)
0043             IF(U) 65,130,65

IBM  FORTRAN IV G COMPILER (O/S REL 21.7)          POLRT

0044          65 DO 70 I=1,N
0045             L=N-I+1
0046             TEMP=COF(L)
0047             XT2=X*XT-Y*YT
0048             YT2=X*YT+Y*XT
0049             U=U+TEMP*XT2
0050             V=V+TEMP*YT2
0051             FI=I
0052             UX=UX+FI*XT*TEMP
0053             UY=UY-FI*YT*TEMP
0054             XT=XT2
0055          70 YT=YT2
0056             SUMSQ=UX*UX+UY*UY
0057             IF(SUMSQ) 75,110,75
0058          75 DX=(V*UY-U*UX)/SUMSQ
0059             X=X+DX
0060             DY=-(U*UY+V*UX)/SUMSQ
0061             Y=Y+DY
0062          78 IF(DABS(DY)+DABS(DX)-1.0D-10) 100,80,80
                C       STEP ITERATION COUNTER
0063          80 ICT=ICT+1
0064             IF(ICT-500) 85,85,90
0065          85 IF(IPIT) 100,90,100
0066          90 IF(IN-5) 50,95,95
                C       SET ERROR CODE TO 3
0067          95 IER=3
0068             GO TO 20
0069         100 DO 105 L=1,NXX
0070             MT=KJ1-L+1
0071             TEMP=XCOF(MT)
0072             XCOF(MT)=COF(L)
0073         105 COF(L)=TEMP
0074             ITEMP=N
0075             N=NX
0076             NX=ITEMP
0077             IF(IPIT) 120,55,120
0078         110 IF(IPIT) 115,60,115
0079         115 X=XPR
0080             Y=YPR
0081         120 IPIT=0
0082         122 IF(DABS(Y)-1.0D-6*DABS(X)) 135,125,145
0083         125 ALPHA=X+X
0084             SUMSQ=X*X+Y*Y
0085             N=N-2
0086             GO TO 140
0087         130 X=0.0
0088             NX=NX-1
0089             NXX=NXX-1
0090         135 Y=0.0
0091             SUMSQ=0.0
0092             ALPHA=X
0093             N=N-1
0094         140 COF(2)=COF(2)+ALPHA*COF(1)
0095         145 DO 150 L=2,N
0096         150 COF(L+1)=COF(L+1)+ALPHA*COF(L)-SUMSQ*COF(L-1)
```

```
MTS  FORTRAN IV G COMPILER (C/S REL 21.6)          PLOT

 0097          155 RCOY
 0098              R
 0099              M2=E
 0100              IF(SUMSQ) 160,165,160
 0101          160 T=-T
 0102              SUMSQ=0.
 0103              GO TO 155
 0104          165 IF(M) 20,20,40
 0105              END
```



```
MTS  FORTRAN IV G COMPILER (C/S REL 21.6)          EIGEN

 0001              SUBROUTINE EIGEN(A,R,N,MV)
             C
             C     THE SUBROUTINE COMPUTE  PRINCIPAL STRESS DIRECTIONS
             C
 0002              DIMENSION A(1),R(1)
 0003            5 RANGE=1.0E-6
 0004              IF(MV-1) 10,25,10
 0005           10 IQ=-N
 0006              DO 20 J=1,N
 0007              IQ=IQ+N
 0008              DO 20 I=1,N
 0009              IJ=IQ+I
 0010              R(IJ)=0.0
 0011              IF(I-J) 20,15,20
 0012           15 R(IJ)=1.0
 0013           20 CONTINUE
             C        COMPUTE INITIAL AND FINAL NORMS (ANORM AND ANORMX)
 0014           25 ANORM=0.0
 0015              DO 35 I=1,N
 0016              DO 35 J=I,N
 0017              IF(I-J) 30,35,30
 0018           30 IA=I+(J*J-J)/2
 0019              ANORM=ANORM+A(IA)*A(IA)
 0020           35 CONTINUE
 0021              IF(ANORM) 165,165,40
 0022           40 ANORM=1.414*SQRT(ANORM)
 0023              ANRMX=ANORM*RANGE/FLOAT(N)
             C        INITIALIZE INDICATORS AND COMPUTE THRESHOLD, THR
 0024              IND=0
 0025              THR=ANORM
 0026           45 THR=THR/FLOAT(N)
 0027           50 L=1
 0028           55 M=L+1
             C        COMPUTE SIN AND COS
 0029           60 MQ=(M*M-M)/2
 0030              LQ=(L*L-L)/2
 0031              LM=L+MQ
 0032           62 IF( ABS(A(LM))-THR) 130,65,65
 0033           65 IND=1
 0034              LL=L+LQ
 0035              MM=M+MQ
 0036              X=0.5*(A(LL)-A(MM))
 0037           68 Y=-A(LM)/ SQRT(A(LM)*A(LM)+X*X)
 0038              IF(X) 70,75,75
 0039           70 Y=-Y
 0040           75 SINX=Y/ SQRT(2.0*(1.0+( SQRT(1.0-Y*Y))))
 0041              SINX2=SINX*SINX
 0042           78 COSX= SQRT(1.0-SINX2)
 0043              COSX2=COSX*COSX
 0044              SINCS =SINX*COSX
             C        ROTATE L AND M COLUMNS
 0045              ILQ=N*(L-1)
 0046              IMQ=N*(M-1)
 0047              DO 125 I=1,N
 0048              IQ=(I*I-I)/2
```

```
OS  FORTRAN IV G COMPILER (O/S REL 21.7)                EIGEN
0049            IF(I-L) 90,115,90
0050         80 IF(I-M) 85,115,90
0051         85 IM=I+MQ
0052            GO TO 95
0053         90 IM=M+IQ
0054         95 IF(I-L) 100,105,105
0055        100 IL=I+LQ
0056            GO TO 110
0057        105 IL=L+IQ
0058        110 X=A(IL)*COSX-A(IM)*SINX
0059            A(IM)=A(IL)*SINX+A(IM)*COSX
0060            A(IL)=X
0061        115 IF(MV-1) 120,125,120
0062        120 ILP=ILQ+I
0063            IMP=IMQ+I
0064            X=R(ILP)*COSX-R(IMP)*SINX
0065            R(IMP)=R(ILP)*SINX+R(IMP)*COSX
0066            R(ILP)=X
0067        125 CONTINUE
0068            X=2.0*A(LM)*SINCS
0069            Y=A(LL)*COSX2+A(MM)*SINX2-X
0070            X=A(LL)*SINX2+A(MM)*COSX2+X
0071            A(LM)=(A(LL)-A(MM))*SINCS+A(LM)*(COSX2-SINX2)
0072            A(LL)=Y
0073            A(MM)=X
C               TESTS FOR COMPLETION
C               TEST FOR M = LAST COLUMN
0074        130 IF(M-N) 135,140,135
0075        135 M=M+1
0076            GO TO 60
C               TEST FOR L = SECOND FROM LAST COLUMN
0077        140 IF(L-(N-1)) 145,150,145
0078        145 L=L+1
0079            GO TO 55
0080        150 IF(IND-1) 160,155,160
0081        155 IND=0
0082            GO TO 50
C               COMPARE THRESHOLD WITH FINAL NORM
0083        160 IF(TNR-ANORM) 165,165,85
C               SORT EIGENVALUES AND EIGENVECTORS
0084        165 IQ=-N
0085            DO 185 I=1,N
0086            IQ=IQ+N
0087            LL=I*(I-1)/2
0088            JM=N*(I-2)
0089            DO 185 J=I,N
0090            JQ=JQ+N
0091            MM=J*(J-J)/2
0092            IF(A(LL)-A(MM)) 170,185,185
0093        170 X=A(LL)
0094            A(LL)=A(MM)
0095            A(MM)=X
0096            IF(MV-1) 175,185,175
0097        175 DO 180 R=1,N
0098            ILP=IQ+R
```

```
OS  FORTRAN IV G COMPILER (O/S REL 21.7)                EIGEN
0099            IMP=JQ+R
0100            X=R(ILR)
0101            R(ILR)=R(IMP)
0102        180 R(IMP)=X
0103        185 CONTINUE
0104            RETURN
0105            END
```